A theoretical and experimental, model system investigation of core Ionisation phenomena, for polymers

Harrison, Alan

UNIVERSITY OF DURHAM

A thesis entitled

"A Theoretical and Experimental, Model System Investigation of Core Ionisation Phenomena, for Polymers"

submitted by

ALAN HARRISON. B.Sc.

A candidate for the degree of Doctor of Philosophy

Graduate Society

September 1981

To my parents, and Judith

"..... We are perhaps not far removed from the time when we shall be able to submit the bulk of chemical phenomena to calculation".

Joseph Louis Gay-Lussac

Memoires de la Société d'Arcueil

2,207(1808)

ACKNOWLEDGEMENTS

I wish to extend my warmest thanks to my supervisor, Professor D.T. Clark for introducing me to the experimental and theoretical aspects of E.S.C.A.

His unfailing enthusiasm for this field is fortunately coupled with a passion for sport which has kept me both mentally and physically alert over an enjoyable three years.

Thanks are also due to my contemporary and friend, Pete Stephenson, whose goals were also fortunately not all of a chemical nature, but whose experimental skill has often produced results which were thankfully consistent with my own. Over the past year, it has been both beneficial and a pleasure to work with Bill Brennan, himself a theorist in Chemistry (and soccer), and in my first year in Durham I was fortunate to be able to draw upon the vast experience of Dr. Alan Dilks to whom I am sincerely grateful. Brief visits to the laboratory by Professor A. Sgamellotti and Dr. F. Tarantelli from Perugia have proved most instructive and I wish to offer my thanks to them, and all those other colleagues whose presence in the laboratory over the past three years have made my stay here such an enjoyable one.

Gratitude is also expressed to the Science Research Council for the provision of a research grant and computing facilities via the Rhel Workstation and to the University of Durham for research and computing facilities at Numac. In connection with the above the assistance of Dr. M.F. Guest (Daresbury Laboratory) and Dr. A.M. Lamont (Numac) are gratefully acknowledged.

Finally, I would like to thank Mrs. Elizabeth Nevins for her considerable skills in assisting with the many diagrams presented in this thesis, and Mrs. Marion Wilson for her great patience and skill in typing this (often illegible) manuscript.

MEMORANDUM

The work described in this thesis was carried out in the University of Durham between October 1978 and September 1981. The work has not been submitted for any other degree, and is the original work of the author except where acknowledged by reference. Parts of this thesis have been the subject of the following publications:

1. D.T. Clark and A. Harrison, "A non-empirical LCAO MO SCF and experimental investigation on the core-ionised states of acetylacetone and some of its enol tautomers". J. Electron Spectrosc. Rel. Phenom, 23, 39 (1981).

2. D.T. Clark and A. Harrison, "E.S.C.A. Applied to Polymers XXXI. A Theoretical Investigation of Molecular Core Binding and Relaxation Energies in a Series of Prototype Systems for Nitrogen and Oxygen Functionalities in Polymers", J.Polym.Sci.Polym.Chem. Ed. in press (1981).

3. D.T. Clark and A. Harrison, "A Theoretical Investigation of the Ground and Core Hole States of the Secondary Butyl Cation". Chem.Phys.Lett. in press (1981).

4. D.T. Clark and A. Harrison, "A Non-Empirical LCAO MO SCF Investigation of the Ground and Core Ionised States of Tetrahedrane and Cyclobutadiene". Chem.Phys. in press (1981).

5. D.T. Clark and A. Harrison, "A Theoretical Investigation of the Ground and Core Hole States of the Cyclopentyl Cation". Chem.Phys.Lett. to be submitted.

6. D.T. Clark and A. Harrison, "A Non-Empirical LCAO MO SCF Investigation of the Ground and Core Ionised States of 2,5-Cyclohexadiene-1,4-dione and 3,5-Cyclohexadiene-1,2-dione". J.Electron Spectrosc. Rel.Phenom. to be submitted.

ABSTRACT

The photoemission of electrons from molecules upon their irradiation by X-rays forms the basis of E.S.C.A. (XPS) spectroscopy. The electrons remaining in the molecule experience an effective increase in nuclear charge accompanying photoionisation, and undergo a "relaxation" process. The energy associated with this (the relaxation energy) affects not only the intensity and shape of the experimentally determined peak, but also its position (or binding energy) to a significant extent and gives rise to accompanying lower kinetic energy, satellite structure.

By means of well-established quantum mechanical methods, it is possible to calculate theoretically the binding energies and relaxation energies for core electron photoionisation, and the transition energies and intensities of accompanying shake-up satellites.

A series of C,H,N,O, containing molecules has been investigated encompassing a wide range of functionalities of interest to the polymer chemist. Trends in binding energies as a function of electronic environment are established and their dependence upon changes in relaxation effects is noted. The manner in which weak interactions of the ground state are enhanced on going to the core hole state manifold is demonstrated in a determination of the classical or non-classical nature of carbocations of current interest and in a study of hydrogen bonding in 1,3 dicarbonyl systems. Shifts in binding energy are found to be highly characteristic of a given structural type and in the case of the latter this is also manifest in the accompanying satellite structure.

Finally, the importance of such structure is emphasised in studies relating to the isomeric hydrocarbons and benzoquinones, where the factors determining shifts in binding energy are so short range in nature as to render them negligible.

CONTENTS

CHAPTER ONE

MOLECULAR ORBITAL THEORY

1.1 Introduction

This Chapter contains a brief survey of some fundamental concepts and relationships needed for the theory of electronic structure of many-electron systems. with special emphasis on Molecular Orbital (MO) theory. The appropriate forms of both the Hamiltonian operator and the wavefunction are developed and then solution of the Schrödinger equation is discussed within the Hartree-Fock formalism. The inadequacies of this method are discussed and mention is made of correlation and relativistic effects. Finally, a brief description of the computational procedures and special features of the programs used is included.

A vast body of literature is available, covering this whole area and several texts have been used in this discussion.[1-10]

1.2 An Introductory Survey of Quantum Mechanics

1.2.1 The Schrödinger Equation

The electronic structure and properties of any molecule. in any of its available stationary states, may be determined in principle by solution of the time-independent Schrödinger equation. For a system of n electrons in a potential field of N nuclei this is of the form:

$$\hat{H}\psi(r,R) = E\psi(r,R) \qquad (1.1)$$

where $\hat{H}$ is the Hamiltonian operator (total energy operator)

E is the total energy of the system;

and $\psi(r,R)$ is the wavefunction depending upon both the electronic coordinates r and nuclear coordinates R, such that $\psi^*\psi$ is the probability density function for the electron distribution in a 4n dimensional 'space'.

For such a system comprising of N nuclei, with charges $Z_\mu e$ and masses M_μ (μ= 1,2, ... N), and n electrons, with charges -e and masses M_e, the Hamiltonian operator is of the form:

$$\hat{H} = \sum_{\mu=1}^{N} \frac{-h^2}{8\pi^2 M_\mu} \nabla^2_\mu + \sum_{i=1}^{n} \frac{-h^2}{8\pi^2 M_e} \nabla^2_i - \sum_{i=1}^{n} \sum_{\mu=1}^{N} \frac{Z_\mu e^2}{\kappa_o r_{i\mu}} + \sum_{\mu=1}^{N} \sum_{\nu>\mu}^{N} \frac{Z_\mu Z_\nu e^2}{\kappa_o r_{\mu\nu}} + \sum_{i=1}^{n} \sum_{j>i}^{n} \frac{e^2}{\kappa_o r_{ij}} \qquad (1.2)$$

where h is Planck's constant;

∇^2 is the Laplacian operator $\frac{\delta^2}{\delta_{xi}^2} + \frac{\delta^2}{\delta_{yi}^2} + \frac{\delta^2}{\delta_{zi}^2}$;

κ_o ($=4\pi\varepsilon_o$) where ε_o is the permittivity of free space

and r is the distance between two particles in the system with i and j referring to the electrons, and μ and ν the nuclei.

It is convenient to express the equation in a more simplified form by the introduction of atomic units. Thus, the rest mass of the electron, M_e, $h/2\pi$, e and κ_o are set equal to unity. Clearly, the eigenvalues resulting from the solution of the Schrodinger equation in this form will also be in terms of atomic units. The total energy E will be in "hartrees" (E_o) where $E_o = \frac{e^2}{a_o \kappa_o}$ and a_o ($= \frac{\bar{h}^2}{M_e^2} \kappa_o$) is the atomic unit of length, the "bohr".

The energy computed in hartrees is defined for a single particle:

$$1 \text{ hartree particle}^{-1} = 27.2107 \text{eV particle}^{-1}.$$

For an Avagadro number of particles, in CGS or SI units this value becomes:

$$1 \text{ hartree particle}^{-1} \quad 627.5 \text{kcal mol}^{-1} \quad 2625.5 \text{ kJ mol}^{-1}.$$

The Hamiltonian therefore reduces to the expression:

$$\hat{H} = -\frac{1}{2} \sum_{\mu=1}^{N} \frac{1}{M_\mu} \nabla^2_\mu - \frac{1}{2} \sum_{i=1}^{n} \nabla_i^2 - \sum_{i=1}^{n} \sum_{\mu=1}^{N} \frac{Z_\mu}{r_{i\mu}}$$

$$+ \sum_{\mu=1}^{N} \sum_{\nu>\mu}^{N} \frac{Z_\mu Z_\nu}{r_{\mu\nu}} + \sum_{i=1}^{n} \sum_{j>i}^{n} \frac{1}{r_{ij}} \qquad (1.3)$$

The first and second terms in the operator relate to the kinetic energy of the nuclei and electrons respectively, whilst the remaining three potential energy terms, in order of appearance, are the nucleus-electron attraction and the nuclear-nuclear and electron-electron, repulsion expressions.

Solution of equation (1.1) may be simplified by the introduction of certain assumptions and approximations. Thus if the Born-Oppenheimer[11] approximation is introduced then the wavefunction is effectively separated into two parts:

$$\psi(r,R) = \psi_R(r) \quad \theta(R) \qquad (1.4)$$

This assumption is equivalent to the physical idea that electrons can instantaneously adjust their motion to any change in motion of the nuclei. $\psi_R(r)$ is therefore an electronic wavefunction for fixed nuclear positions whilst $\theta(R)$ is the nuclear wave function. The validity of this

assumption relies upon the function $\psi_R(r)$ having a parametric dependence upon the nuclear coordinates.[12] Also, only that part of the Hamiltonian operator which is dependent upon the position, and not the momenta of the nuclei is considered. The kinetic energy operator due to the nuclei ($\hat{T}_R$) is therefore neglected, where:

$$\hat{T}_R = -\frac{1}{2} \sum_{\mu=1}^{N} \frac{1}{M_\mu} \nabla^2_\mu \qquad (1.5)$$

The electronic Hamiltonian operator is therefore of the form:

$$\hat{H}_e = -\frac{1}{2} \sum_{i=1}^{n} \nabla^2_i - \sum_{i=1}^{n} \sum_{\mu=1}^{N} \frac{Z_\mu}{r_{i\mu}} + \sum_{\mu=1}^{N} \sum_{\nu>\mu}^{N} \frac{Z_\mu Z_\nu}{r_{\mu\nu}} + \sum_{i=1}^{n} \sum_{j>i}^{n} \frac{1}{r_{ij}} \qquad (1.6)$$

Denoting $\hat{h}$ as the sum of the mono-electronic operators and $\hat{V}$ as the potential-energy operator for the repulsion terms, the electronic Hamiltonian may be re-written as:

$$\hat{H}_e = \hat{h} + \hat{V} \qquad (1.7)$$

The operator $(\hat{h} + \hat{V})$ is assumed to satisfy the Schrödinger equation:

$$(\hat{h} + \hat{V}) \quad \psi_R(r) = E(R) \quad \psi_R(r) \qquad (1.8)$$

E(R) is the total energy of the system within the fixed-nuclei approximation and is equal to the electronic energy of the n electrons moving in the field provided by the N, fixed-coordinate, nuclei PLUS their mutual repulsion energy. Plotting E(R) as a function of the nuclear coordinates will lead to a potential-energy surface in the general case, or

more specifically, for diatomic molecules, the potential-energy curve, if the Born-Oppenheimer approximation is a valid one.

That the solution of (1.1) may be treated as a purely electronic problem is evident in the large ratio between the electronic and nuclear masses, however in the specific case of the Jahn-Teller effect,[13] a property generally considered to be electronic in nature, the motion of the nuclei has a profound effect.

The Schrödinger equation describing the nuclei therefore has the form:

$$(\hat{T}_R + E(R))\ \theta(R) = E_N\ \theta(R) \qquad (1.9)$$

Clearly the total energy E is the sum of the electronic energy evaluated at the equilibrium configuration plus the nuclear energy:

$$E_{total} = E(R_o) + E_N \qquad (1.10)$$

A second assumption made in formulating expression (1.2) is that terms representing interactions between particles other than those of purely electrostatic origin, such as electron spin-orbit interactions and electron-nuclear spin coupling, have been neglected. The omission of magnetic terms from $\hat{H}$ is deliberate since magnetic effects are on a very much smaller energy scale than electrostatic effects. Using (1.2) therefore determines the electronic distribution by means of the non-relativistic, spin-free, electrostatic Hamiltonian $\hat{H}$. A brief discussion of the magnitudes of the relativistic corrections to this model will be presented in a subsequent section.

Attention will now be drawn towards determining the form of the electronic wave function $\psi_R(r)$. Although the electronic wavefunction does not take into account electron spin, for many-electron systems it is necessary to include spin in the electronic wave function in order to satisfy the Pauli principle which in turn ensures that only valid forms of the electronic wave function are considered in accordance with the restrictions imposed by the indistinguishability of the electrons. The non-relativistic theory of electron spin based upon the general theory of angular momentum determines that associated with each electron is a spin variable ($M_S = \pm \frac{1}{2}$). The two possible spin functions for an electron i are written as $\alpha(i)$, where $M_S = \frac{1}{2}$ and $\beta(i)$, where $M_S = -\frac{1}{2}$.

In this representation,

$$\begin{aligned} \alpha(\tfrac{1}{2}) &= 1, \quad \alpha(-\tfrac{1}{2}) = 0 \\ \beta(\tfrac{1}{2}) &= 0, \quad \beta(-\tfrac{1}{2}) = 1 \end{aligned} \tag{1.11}$$

and clearly, the spin functions are orthonormal:

$$\begin{aligned} \int \alpha(i)^* \ \alpha(i) \ dM_S &= 1 \\ \int \alpha(i)^* \ \beta(i) \ dM_S &= 0 \end{aligned} \tag{1.12}$$

The Pauli principle requires that the total wave function be antisymmetric under the simultaneous interchange of coordinates r_i of any two electrons and this is made possible by the ability to express r_i in terms of both space and spin variables. Thus, where $\hat{P}$ is an operator producing an arbitrary permutation among the electronic space and spin variables r_i, and p is the parity of the permutation - the number of pair transpositions to which the permutation is equivalent, then:

$$\hat{P}\psi_R(r_1, r_2, \ldots r_i \ldots r_n) = (-1)^p \psi_R(r_1, r_2, \ldots r_i \ldots r_n) \quad (1.13)$$

is a constraint which must be satisfied by any trial wave function if a valid solution to the electronic wave equation is to be found.

There are two distinct methods which enable this difficulty to be overcome. The first is to construct all possible spin functions for an n-electron system, investigate their transformations under permutations and consider only those solutions of equation (1.1) which when combined with the known spin functions produce a total wave function which is anti-symmetric under permutations. A good account of this method is given by Kotani *et al.*[14]

The method considered here will be that due to Slater, in which the spatial and spin dependence of the wave functions are combined from the beginning of the calculation despite the absence of electron spin in the Schrödinger equation.

Inspection of the form of the molecular-electronic Hamiltonian (1.6) demonstrates that the analytical problem presented by the solution of the Schrodinger equation is a partial differential equation in 3n dimensions. Due to the electron-electron repulsion term in the operator, there can be no further reduction into equations of smaller dimension. For one-electron systems, where of course, no electron repulsion terms exist solution of the three-dimensional equation is possible by analytical methods but it is clear that an "exact" solution of the Schrödinger equation for molecules is not possible. However if the electron-electron repulsion operator could be neglected then a simpler equation would result.

$$H_e' \psi_R'(r) = \hat{h} \psi_R'(r) = E' \psi_R'(r) \qquad (1.14)$$

where the prime indicates this simplification.

Clearly, since e-e repulsion terms are neglected, there is an equation of this type for each of the n electrons.

$$\hat{h}(i) \phi_j(i) = \varepsilon_j \phi_j(i) \qquad (1.15)$$

where $\phi_j(i)$ and ε_j are the eigenfunctions and eigenvalues of $\hat{h}(i)$ respectively.

Then:

$$\psi_R'(r) = \phi_1(1) \phi_2(2) \ldots \phi_k(n) \qquad (1.16)$$

and

$$E' = \varepsilon_{j1} + \varepsilon_{j2} + \ldots \varepsilon_{jn} \qquad (1.17)$$

In these expressions, the functions $\phi_j(i)$ are orbitals, in the sense that "an orbital is a solution of any real or model single-electron Schrödinger equation". The electronic spatial variables r_i are abbreviated by i. The fact that the true molecular electronic Hamiltonian does contain the terms $\sum_{i=1}^{n} \sum_{j>i}^{n} \frac{1}{r_{ij}}$ means that $\psi_R'(r)$ is not the true molecular electronic wave function. However the idea of a one-electron function (the orbital approximation) is conceptually simple, and it is useful to consider products of one-electron functions in determining how close it is possible to approach the exact functions. Thus, if it is possible to partition the n-electron Hamiltonian into n separate one-electron Hamiltonians then an appropriate solution of the full Schrödinger equation is given by a linear combination of the products of the orbitals defined by the one-electron wave equation.

The many electron wavefunctions may be constructed as products of one-electron, spin orbitals, which in turn are the combination of both the spatial coordinates and spin-function α or β of each electron:

$$\psi(1.2. \ldots n) = \psi_1(1) \quad \psi_2(2) \ldots \psi_n(n) \tag{1.18}$$

and

$$\psi_j(i) = \begin{matrix} \phi_j(i) & \alpha(i) \\ \phi_j(i) & \beta(i) \end{matrix} \tag{1.19}$$

where both the prime and subscript R have been dropped, since it is now understood that ψ is a non-exact electronic wave function within the fixed nuclei approximation, and i is the abbreviation for both space and spin variables associated with each electron.

Since the electrons are indistinguishable, there are n! permutations of equation (1.18) which are also solutions to the wave equation. A solution, as previously noted, is only physically meaningful if it satisfies the Pauli principle, and therefore introducing the antisymmetrising operator $\hat{A}$ to the simple product of spin orbitals, transforms them into the corresponding Slater determinant.

$$\hat{A} = \frac{1}{\sqrt{n!}} \sum_{p}^{n!} \hat{P} \tag{1.20}$$

where $\hat{P}$ is as defined in (1.13).

$$\psi(1,2 \ldots n) = \frac{1}{\sqrt{n!}} \sum_{p}^{n!} \hat{P}\psi_1(1) \; \psi_2(2) \ldots \psi_n(n) \tag{1.21}$$

$$\psi(1\ 2, \ldots n) = \frac{1}{\sqrt{n!}} \begin{vmatrix} \psi_1(1) & \ldots\ldots & \psi_n(1) \\ \vdots & & \vdots \\ \psi_1(n) & \ldots\ldots & \psi_n(n) \end{vmatrix} \tag{1.22}$$

The factor $\frac{1}{\sqrt{n!}}$ ensures that the determinant is normalised, providing that the spin-orbitals $\psi_i(i)$ form an orthonormal set. Clearly, each $\psi_i(i)$ may be expressed in terms of its space and spin functions (1.14) in the above determinant and this is generally abbreviated by writing only the diagonal elements, the normalisation factor being understood:

$$\psi(1,2 \ldots n) = |\phi_1(1)\alpha(1)\phi_1(2)\beta(2) \ldots \phi_n(n-1)\alpha(n-1)\phi_n(n)\beta(n)| \quad (1.23)$$

$$= |\phi_1\overline{\phi}_1 \ldots \phi_n\overline{\phi}_n| \quad (1.24)$$

where α spin is understood and β spin is denoted by the bar, $\overline{\ }$.

It is clear that the Pauli exclusion principle is now satisfied - by the properties of determinants.

1.2.2 The Variation Principle

The variation principle[15] is based upon the fact that the energy for any normalised approximate wave function ψ is the expectation value of the Hamiltonian operator:

$$E = \int \psi^* \hat{H} \psi \, d\tau \quad (1.25)$$

and will lie above the true energy of the molecular system under consideration.

Before considering the application of the variation method, the properties of the wave function should be re-iterated, in that it must be continuous, single-valued, and possess an integrable square (to satisfy the normalisation condition).

$$\int \psi^* \psi \, d\tau = 1 \tag{1.26}$$

Because of the Hermitian symmetry of the operator $\hat{H}$. it can be shown that eigen functions associated with different eigen values of the same system are orthogonal.

$$\int \psi_\kappa^* \psi_\lambda \, d\tau = \delta_{\kappa\lambda} = \begin{cases} 1 & \kappa = \lambda \\ 0 & \kappa \neq \lambda \end{cases} \tag{1.27}$$

where $\delta_{\kappa\lambda}$ is termed the Kronecker delta.

From the wave equation, the following may be derived,

$$\int \psi^* \hat{H} \psi d\tau = E \int \psi^* \psi \, d\tau \tag{1.28}$$

or $$E = \frac{\int \psi^* \hat{H} \psi \, d\tau}{\int \psi^* \psi \, d\tau}$$

In accordance with the variation principle, if ψ is replaced by some approximate function $\tilde{\psi}$ then the associated energy $\tilde{E}$ will be a higher valued, approximation to the true energy solution of the Schrodinger equation:

$$\tilde{E} = \frac{\int \tilde{\psi}^* \hat{H} \tilde{\psi} \, d\tau}{\int \tilde{\psi}^* \tilde{\psi} \, d\tau} > E \tag{1.29}$$

In the transformed Schrodinger equation, the variational solution is obtained by minimising the value of an "integrated expression"; the solution is the best possible solution of the model type in the mean; however the differential form has point by point solutions. It must therefore be expected that molecular properties dependent upon the value of $\tilde{\psi}$ at particular points in space, e.g. spin hyperfine coupling constants, will not be well described. whilst those dependent upon various integrations of $\tilde{\psi}$ should be well reproduced.

The variation method provides a technique for the computation of the approximate, orbital model wave function:

$$\psi = \sum_{\kappa=1}^{n} D_\kappa \quad \Phi_\kappa \qquad (1.30)$$

where

$$\Phi_\kappa = |\psi_1(1)\ \psi_2(2)\ \ldots\ \psi_n(n)|$$

and

$$\psi_j(i) = \phi_j(i)\,\alpha(i) \quad \text{or} \quad \phi_j(i)\,\beta(i)$$

The tilde (above ψ) has been dropped since only approximate wave functions are to be considered.

Expression (1.30) is substituted into the variational expression (1.29) which is then minimised with respect to the coefficients D_κ and any parameters contained in the definition of the spatial orbitals $\phi_j(i)$.

The full optimisation of expression (1.30) is termed the Multi-Configuration Self-Consistent Method, and in practice is complex and time consuming for many-electron systems. The most widely used approach is the Molecular Orbital model in which only a single term is retained from expression (1.30) ($D_1=1$, $D_i=0$, $i>1$). All of the computational effort is thrown into choosing the best possible orbitals in this single configuration. Alternatively, the Valence-Bond method fixes the orbitals $\phi_j(i)$ and optimises the coefficients D_i of an essentially multi-configuration wave function. Both the Hartree - Fock and Valence bond methods are special cases of the Generalised Valence Bond (GVB) approach.

In this method every orbital is allowed to be different

and singly occupied, no orthogonality conditions are placed on the orbitals each orbital is solved self consistently in the field due to other orbitals, and the wave function ensures that the total wavefunction possesses the proper spin symmetry. Goddard, using this method, has examined the results of *ab initio* calculations of reaction coordinates and noted the dependence of the activation energy upon certain phase relationships between the orbitals of both reactants and products. This forms the basis for the Orbital Phase Continuity Principle.[16]

The computation of optimum linear expansion coefficients, D_i of (1.30), when functions Φ are not optimised. is particularly easy to formulate in general.

Therefore if

$$\psi = \sum_{\kappa} D_{\kappa} \Phi_{\kappa}$$

then substitution into (1.29) gives:

$$\tilde{E} = \frac{\sum_{ij} D_i D_j H_{ij}}{\sum_{ij} D_i D_j S_{ij}} \qquad (1.31)$$

where

$$H_{ij} = \int \Phi_i \hat{H} \Phi_j \, d\tau \qquad (1.32)$$

and

$$S_{ij} = \int \Phi_i \Phi_j \, d\tau \qquad (1.33)$$

Rearranging (1.31) gives:

$$\sum_i D_i D_j S_{ij} \tilde{E} = \sum_i D_i D_j H_{ij} \qquad (j=1,2,\ldots)$$

Forming $\frac{\delta E}{\delta D_j}$ for each value of j and equating each partial derivative to zero ensures a minimum in (1.31).

Collecting the resulting equations in matrix form gives:

$$(\underline{H} - \tilde{E}\,\underline{S})\,\underline{D} = \underline{0} \qquad (1.34)$$

or $\underline{H}\,\underline{D} = \tilde{E}\,\underline{S}\,\underline{D}$

where $\underline{H}$ and $\underline{S}$ are the matrices whose elements are defined by (1.32) and (1.33) respectively, and $\underline{D}$ is a column vector of the coefficients D_i. Choosing a set of orthogonal functions Φ, reduces (1.34) to the matrix analogue of the Schrödinger Equation:

$$\underline{H}\,\underline{D} = \tilde{E}\,\underline{D} \qquad (1.35)$$

since $\underline{S} = \underline{1}$.

Eigen vector ($\underline{D}$) and eigenvalue ($\tilde{E}$) problems of this form find their solutions in diagonalisation of the matrix ($\underline{H}$). Thus the variational calculation associated with the Valence-Bond method reduces to a single matrix diagonalisation.

1.3 The Self Consistent-Field Method

The most frequent application of the variation principle is to the calculation of Self Consistent Field (SCF) wave functions. For a given geometry of a particular molecule in a closed shell state, any number of different Slater determinants may be used as approximate wave functions. However, there is only one Hartree-Fock determinant, namely that for which the orbitals ϕ_i in (1.24) have been varied to give the lowest possible energy. By minimising the energy resulting from the single determinantal wave function, a set of complicated integrodifferential equations result, the Hartree-Fock (HF) equations.

Only for one-electron systems such as the hydrogen atom can the HF equations be solved in closed form. However, they have been solved to a high degree of accuracy by numerical integration in the cases of atoms. For molecules, each molecular orbital (M.O.) is constructed from a number of basis functions. usually centred on the various nuclei and referred to as atomic orbitals (AO) (due to their one centre forms), although they are not necessarily the orbitals used for an isolated atom. This is usually referred to as the "linear combination of atomic-orbitals" (LCAO) approximation.

Clearly, only approximate solutions may be ootained in molecular calculations since it is never possible to include a mathematically complete set of basis functions, but the SCF energy and wavefunction will approach the HF results, as the set is expanded. The MO method will therefore determine the best possible (lowest energy) single-configuration solution of the Schrödinger equation, within a finite basis set, termed the Self Consistent-Field (SCF) wave function.

1.3.1 The Hartree Fock (HF) Equations

Given the usual non-relativistic Hamiltonian,

$$\hat{H} = \sum_{\mu=1}^{2n} \hat{h}_{\mu} + \sum_{\mu=1}^{(2n-1)} \sum_{\nu>\mu}^{2n} \frac{1}{r_{\mu\nu}} \qquad (1.36)$$

(neglecting the nuclear repulsion term, which for the system, within the fixed nuclei approximation. will be constant) for a system of 2n electrons a general expression may be derived for the total energy of the closed shell configuration in which n spatial orbitals are doubly occupied.

$\hat{h}_\mu$ is a monoelectronic operator describing the interaction of the μ^{th} electron with the κ nuclei and the expectation value of this operator represents the associated independent particle energy. Analogous to equation 1.6, this operator takes the form

$$\hat{h}_\mu = -\frac{1}{2} \nabla^2_\mu - \sum_{\kappa=1}^{N} \frac{Z_\kappa}{r_{\mu\kappa}} \qquad (1.37)$$

Where ψ_o is a determinant of spin-orbitals, whose spatial components are the orthonormal molecular orbitals ϕ_i constructed as a linear combination of atomic orbitals. n_i then the electronic energy is given as:

$$E = \langle \psi_o | \sum_\mu \hat{h}_\mu + \sum_{\mu=1}^{(2n-1)} \sum_{\nu>\mu}^{2n} \frac{1}{r_{\mu\nu}} | \psi_o \rangle \qquad (1.38)$$

where $\langle \psi_o |\hat{H}| \psi_o \rangle \equiv \int \psi_o^* \hat{H} \psi_o \, d\tau$, introducing the bra-ket notation of Dirac, and

$$\psi_o(1,2, \ldots 2n) = |\psi_1(1)\psi_2(2) \ldots \psi_{2n}(2n)| = | \phi_1\overline{\phi}_1\phi_2\overline{\phi}_2 \ldots \phi_n\overline{\phi}_n |$$

when $\psi_\mu(\mu) = \phi_i(\mu)\ \alpha(\mu)$ and $\phi_{(\mu+1)}(\mu+1) = \phi_i(\mu+1)\ \beta(\mu+1)$.

After integrating over the spin coordinates, the monoelectronic portion becomes:

$$2 \sum_{i=1}^{n} \langle \phi_i(\mu) |\hat{h}_\mu| \phi_i(\mu) \rangle \equiv 2 \sum_{i=1}^{n} h_{ii}^{\phi} \qquad (1.39)$$

where the superscript ϕ indicates that the matrix representatives are over the molecular orbital basis. For identity permutations of the two-electron integrals,

$$\sum_{\mu=1}^{(2n-1)} \sum_{\nu>\mu}^{2n} \psi_\mu(\mu)\psi_\nu(\nu) \left| \frac{1}{r_{\mu\nu}} \right| \psi_\mu(\mu)\psi_\nu(\nu) \rangle \qquad (1.40)$$

Whenever μ is odd and $\nu = \mu + 1$ then

$$\psi_{\mu}(\mu) = \phi_i(\mu)\ \alpha(\mu) \text{ and } \psi_{\nu}(\nu) = \phi_i(\nu)\ \beta(\nu) \tag{1.41}$$

Integrating over spin gives:

$$\sum_{i=1}^{n} \langle \phi_i(\mu)\ \phi_i(\nu)\ \frac{1}{r_{\mu\nu}}\ \phi_i(\mu)\ \phi_i(\nu) \rangle = \sum_{i=1}^{n} J_{ii}\ \phi \tag{1.42}$$

Where J_{ii} is a coulombic integral, defined generally as:

$$J_{ij} = \langle \phi_i(\mu)\ \phi_j(\nu) |\ \frac{1}{r_{\mu\nu}}\ |\ \phi_i(\mu)\ \phi_j(\nu) \rangle \tag{1.43}$$

Such an integral represents the energy due to electrostatic repulsion between a pair of electrons having charge distributions $|\phi_i(\mu)|^2$ and $|\phi_j(\nu)|^2$, respectively.

For all other values of $\mu<\nu$ there are four ways in which the coulombic integral J_{ij} from (1.40) can be obtained:

i.e. $$\psi_{\mu}(\mu) = \begin{cases} \phi_i(\mu)\,\alpha(\mu) \\ \phi_i(\mu)\,\beta(\mu) \end{cases}$$

either one of which may be associated with

$$\psi_{\nu}(\nu) = \begin{cases} \phi_j(\nu)\,\alpha(\nu) \\ \phi_j(\nu)\,\beta(\nu) \end{cases}$$

Identity permutations then lead to a two-electron contribution of

$$\sum_{i=1}^{n} J_{ii}\phi + 4 \sum_{i=1}^{(n-1)} \sum_{j>i}^{n} J_{ij}\phi \tag{1.44}$$

In the case of two-electron permutations (odd parity) then

$$- \sum_{\mu}^{(2n-1)} \sum_{\nu>\mu}^{2n} \langle \psi_{\mu}(\mu)\ \psi_{\nu}(\nu) |\ \frac{1}{r_{\mu\nu}}\ | \psi_{\nu}(\mu)\ \psi_{\mu}(\nu) \tag{1.45}$$

When μ is odd and $\nu = \mu + 1$, zero integrals result due to spin orthogonality. For other values of $\mu<\nu$ the forms of the integrals are:

$$\langle \phi_i(\mu)\ \phi_j(\nu) \left| \frac{1}{r_{\mu\nu}} \right| \phi_j(\mu)\ \phi_i(\nu) \rangle = K_{ij} \qquad (1.46)$$

and these are termed exchange integrals. Unlike the coulombic integrals, the exchange integrals have no simple classical interpretation since they arise solely as a consequence of the non-classical antisymmetry principle. Of the four $\mu<\nu$ combinations leading to a particular K_{ij}, only two (those involving only one type of spin function) lead to non-zero integrals for two-electron permutations. Thus the total contribution due to two-electron permutations is:

$$2 \sum_{i=1}^{n-1} \sum_{j>i}^{n} K_{ij}^{\phi} \qquad (1.47)$$

The total electronic energy can now be written as a summation over the n spatial orbitals, thus

$$E = 2 \sum_{i=1}^{n} h_{ii}^{\phi} + \sum_{i=1}^{n} J_{ii}^{\phi} + 2 \sum_{i=1}^{(n-1)} \sum_{j>i}^{n} (2 J_{ij}^{\phi} - K_{ij}^{\phi})$$

$$= 2 \sum_{i=1}^{n} h_{ii}^{\phi} + \sum_{ij}^{n} (2 J_{ij}^{\phi} - K_{ij}^{\phi}) \qquad (1.48)$$

Equation (1.48) is valid only for electronic systems with closed shell configurations in which the total wave function is approximated as a single determinant of doubly occupied spatial orbitals. For other configurations a different expression is required and in a later section this treatment will be extended to open shell configurations.

Using the variation method, the object is now to determine the best single determinantal wave function which leads to a minimum value of the energy (1.48) subject to the restriction that the orbitals are orthonormal.

Introducing Lagrangian multipliers (λ_{ij})

$$E = 2\sum_{i=1}^{n} h_{ii}^{\phi} + \sum_{i,j}^{n} (2J_{ij}^{\phi} - K_{ij}^{\phi}) - 2\sum_{i,j}^{n} \lambda_{ij} (\langle \phi_i | \phi_j \rangle - \delta_{ij}) \tag{1.49}$$

where $\delta_{ij} = 1, \; i = j$

$\delta_{ij} = 0, \; i \neq j$

For E to have a minimum value, it must be invariant to an infinitessimally small change in the molecular orbitals ϕ_i.

Defining the Coulomb and Exchange operators by:

$$\begin{aligned} \hat{J}_i(\mu)\,\phi_j(\mu) &= \langle \phi_i(\nu) \left| \frac{1}{r_{\mu\nu}} \right| \phi_i(\nu) \rangle \phi_j(\mu) \\ \hat{K}_i(\mu)\,\phi_j(\mu) &= \langle \phi_i(\nu) \left| \frac{1}{r_{\mu\nu}} \right| \phi_j(\nu) \rangle \phi_j(\mu) \end{aligned} \tag{1.50}$$

then the integrals in (1.49) may be written

$$\begin{aligned} J_{ij}^{\phi} &= \langle \phi_i(\mu) | \hat{J}_j(\mu) | \phi_i(\mu) \rangle = \langle \phi_j(\nu) | \hat{J}_i(\nu) | \phi_j(\nu) \rangle \\ K_{ij}^{\phi} &= \langle \phi_i(\mu) | \hat{K}_j(\mu) | \phi_i(\mu) \rangle = \langle \phi_j(\nu) | \hat{K}_i(\nu) | \phi_j(\nu) \rangle \end{aligned} \tag{1.51}$$

The first order variation in E is:

$$\delta E = 2\sum_{i=1}^{n} (\langle \delta\phi_i | \hat{h}_\mu | \phi_i \rangle + \langle \phi_i | \hat{h}_\mu | \delta\phi_i \rangle)$$

$$+ \sum_{i,j}^{n} (\langle \delta\phi_i | 2\hat{J}_j - \hat{K}_j | \phi_i \rangle + \langle \phi_i | 2\hat{J}_j - \hat{K}_j | \delta\phi_i \rangle)$$

$$+ \sum_{i,j}^{n} \left(\langle \delta\phi_j \mid 2\hat{J}_i - \hat{K}_i \mid \phi_j \rangle + \langle \phi_j \mid 2\hat{J}_i - \hat{K}_i \mid \delta\phi_j \rangle \right)$$

$$- 2 \sum_{i,j}^{n} \left(\lambda_{ij} \langle \delta\phi_i \mid \phi_j \rangle + \lambda_{ij} \langle \phi_i \mid \delta\phi_j \rangle \right) \qquad (1.52)$$

$\hat{h}_\mu$ is the mono-electronic part of the atomic Hamiltonian operator. The first and second double summations are symmetric in their indices and lead to the same final sums. Thus,

$$\delta E = 2 \sum_{i}^{n} \left[\langle \delta\phi_i \mid \hat{h}_\mu + \sum_{j}^{n} (2\hat{J}_j - \hat{K}_j) \mid \phi_i \rangle \right]$$

$$+ 2 \sum_{i}^{n} \left[\langle \phi_i \mid \hat{h}_\mu + \sum_{j}^{n} (2\hat{J}_j - \hat{K}_j) \mid \delta\phi_i \rangle \right] \qquad (1.53)$$

$$- 2 \sum_{i,j}^{n} \left(\lambda_{ij} \langle \delta\phi_i \mid \phi_j \rangle + \lambda_{ij} \langle \phi_i \mid \delta\phi_j \rangle \right)$$

Since $\hat{h}_\mu$, $\hat{J}_j$ and $\hat{K}_j$ are hermitian, the first and second summations are the adjoints of each other. Also,

$$\sum_{i,j}^{n} \lambda_{ij} \langle \phi_i \mid \delta\phi_j \rangle = \sum_{i,j}^{n} \lambda_{ji} \langle \delta\phi_i \mid \phi_j \rangle^* \qquad (1.54)$$

Therefore (1.53) becomes:

$$\delta E = 2 \sum_{i}^{n} \left[\langle \delta\phi_i \mid \hat{h}_\mu + \sum_{j}^{n} (2\hat{J}_j - \hat{K}_j) \mid \phi_i \rangle - \sum_{j}^{n} \lambda_{ij} \langle \delta\phi_i \mid \phi_j \rangle \right]$$

$$+ 2 \sum_{i}^{n} \left[\langle \delta\phi_i \mid \hat{h}_\mu + \sum_{j}^{n} (2\hat{J}_j - K_j) \mid \phi_i \rangle^* - \sum_{j}^{n} \lambda_{ji} \langle \delta\phi_i \mid \phi_j \rangle^* \right]$$

$$(1.55)$$

When $\delta E = 0$

$$\left[\hat{h}_\mu + \sum_j^n (2\hat{J}_j - \hat{K}_j) \right] \phi_i = \sum_j^n \phi_j \lambda_{ij} \qquad (1.56)$$

and

$$\left[\hat{h}_\mu + \sum_j^n (2\hat{J}_j - \hat{K}_j) \right] \phi_i^* = \sum_j^n \phi_j^* \lambda_{ji} \qquad (1.57)$$

Taking the complex conjugate of (1.57) and subtracting from (1.56) gives:

$$\sum_j^n \phi_j (\lambda_{ij} - \lambda_{ji}^*) = 0 \qquad (1.58)$$

and since the orbitals ϕ_j are linearly independent, then $\lambda_{ij} = \lambda_{ji}^*$

The equations (1.56) and (1.57) are complex conjugates of one another and are termed the Hartree-Fock (HF) equations originally proposed simultaneously and independently by Fock[17] and by Slater[18], though the present derivation is a modification of that given by Roothaan[19]. The λ_{ij} are eigenvalues of the molecular orbitals ϕ_i and where the Fock operator is defined by

$$\hat{F} = \hat{h}_\mu + \sum_j^n (2\hat{J}_j - \hat{K}_j) \qquad (1.59)$$

then the HF equations may be written in the form

$$\hat{F}\phi_i = \phi_i \lambda_i \qquad (1.60)$$

Clearly these are expressed in terms of the molecular orbitals ϕ_i, which in themselves may each be expressed in terms of a linear combination of atomic orbitals η_κ: in an

exact form if a complete set of orbitals are used: but in practice, a truncated set of, say m, functions are used as an approximation of the LCAO form.

$$\phi_i = \sum_{\kappa=1}^{m} C_{i\kappa}\ \eta_\kappa \qquad (1.61)$$

This may be presented in matrix form, where the basis functions η_κ form an m-dimensional row vector and are transformed into the molecular orbitals ϕ_i by matrix multiplication with the (mxn)-dimensional matrix of coefficients, $\underline{C}$.

$$\underline{\phi} = \underline{\eta}\ \underline{C} \qquad (1.62)$$

The Hartree-Fock eigen-problem equation (1.60) may be written as:

$$\hat{F}\phi_i = \varepsilon_i \phi_i$$

or (1.63)

$$\underline{\hat{F}}\ \underline{\phi} = \underline{\phi}\ \underline{\varepsilon}$$

where ε is a diagonal matrix. Taking the inner product with ϕ_i gives:

$$\langle \phi_i \mid \hat{F} \mid \phi_i \rangle = \langle \phi_i \mid \phi_i \rangle \varepsilon_i$$

or (1.64)

$$\underline{F}^{\phi} = \underline{S}^{\phi}\underline{\varepsilon}$$

Clearly if the molecular orbitals ϕ are orthogonal then $\underline{S}^{\phi} = \underline{1}$, and this would imply that the matrix representative of an operator over the eigenvector space is a diagonal matrix. However since the molecular orbitals ϕ are constructed by the LCAO method using a basis set which generally does not consist of orthogonal functions, then the coefficient matrix which diagonalises $\underline{F}$ cannot be found by an orthogonal trans-

formation. It is therefore necessary to transform the non-orthogonal set {η} into an orthogonal set {χ}. In the orthogonalisation procedure, the matrix $\underline{V}$ is introduced with the condition for generating an orthogonal set.

$$\underline{V}\,\underline{V}^{+} = \underline{S}^{-1} \tag{1.65}$$

Where $\underline{C}$ is non-orthogonal:

$$\underline{F}^{\eta}\,\underline{C} = \underline{S}^{\eta}\,\underline{C}\,\underline{\varepsilon}$$

then $\underline{F}^{\eta}\,\underline{1}\,\underline{C} = \underline{S}^{\eta}\,\underline{1}\,\underline{C}\,\underline{\varepsilon}$

since $\underline{V}\,\underline{V}^{-1} = \underline{1}$ $\quad \underline{F}^{\eta}\,\underline{V}\,\underline{V}^{-1}\,\underline{C} = \underline{S}^{\eta}\,\underline{V}\,\underline{V}^{-1}\,\underline{C}\,\underline{\varepsilon}$

premultiplying by $\underline{V}^{+}$ $\quad (\underline{V}^{+}\,\underline{F}^{\eta}\,\underline{V})\,(\underline{V}^{-1}\underline{C}) = (\underline{V}^{+}\,\underline{S}^{\eta}\,\underline{V})\,(\underline{V}^{-1}\underline{C})\underline{\varepsilon}$

where $\underline{V}$ is orthogonal $\quad \underline{V}^{+}\,\underline{F}^{\eta}\,\underline{V} = \underline{F}^{X}$

and $\quad \underline{V}^{+}\,\underline{S}^{\eta}\,\underline{V} = \underline{S}^{X} = \underline{1}$

therefore $\quad \underline{F}^{X}\,\underline{U} = \underline{U}\,\underline{\varepsilon}$ $\quad$ where $\underline{V}^{-1}\underline{C} = \underline{U}$ $\quad$ (1.66)

Expanding $\underline{\phi}$ in terms of the orthonormal basis set {x}, in (1.64) gives:

$$\underline{F}^{\phi} = \underline{U}^{+}\,\underline{V}^{+}\,\underline{F}^{\eta}\,\underline{V}\,\underline{U} = \underline{U}^{+}\,\underline{V}^{+}\,\underline{S}^{\eta}\,\underline{V}\,\underline{U}\,\underline{\varepsilon} \tag{1.67}$$

Lowdin showed that the orthogonalising matrix V may be chosen to be $S^{-\frac{1}{2}}$. This is known as the Symmetric or Lowdin[20], orthogonalisation. Therefore:

$$\underline{F}^{X} = \underline{S}^{-\frac{1}{2}}\,\underline{F}^{\eta}\,\underline{S}^{-\frac{1}{2}} \tag{1.68}$$

and

$$\underline{F}^{\phi} = \underline{U}^{+}\,\underline{F}^{X}\,\underline{U} = \underline{U}^{+}\,\underline{S}^{X}\,\underline{U}\,\underline{\varepsilon}$$

Since {x} is orthonormal, $\underline{S}^{X} = 1$, therefore:

$$\underline{F}^{\phi} = \underline{U}^{+}\,\underline{U}\,\underline{\varepsilon}$$

$\underline{U}$ is orthogonal thus $\underline{U}^{+}\,\underline{U} = 1$, and

$$\underline{F}^{\phi} = \underline{\varepsilon} \tag{1.69}$$

Clearly, the real symmetric matrix $\underline{F}^x$ is diagonalised by the unitary matrix $\underline{U}$ in a similarity transformation. A widely used method for the diagonalisation of real symmetric matrices is that of Jacobi which is based upon a succession of plane rotations. If in (1.69) above, the matrix $\underline{F}^x$ is finally diagonalised by the κ^{th} rotation. then the matrix $\underline{U}$ above. is obtained as the product of the κ preceding unitary matrices.

In the HF matrix equation over the original basis $\{\eta\}$:

$$\underline{C}^+ \underline{F}^{\eta} \underline{C} = \underline{C}^+ \underline{S}^{\eta} \underline{C} \underline{\varepsilon}$$

where

$$\underline{F}^{\eta} = \underline{h}^{\eta} + \underline{G}^{\eta} \tag{1.70}$$

$$\underline{C} = \underline{V}\,\underline{U} \qquad \underline{C}^+ = \underline{U}^+ \underline{V}^+$$

and $$S^{\eta}_{pq} = \langle \eta_p \mid \eta_q \rangle$$

The corresponding matrix elements are given by

$$h^{\eta}_{pq} = \langle \eta_p \mid \hat{h} \mid \eta_q \rangle \tag{1.71}$$

$$G^{\eta}_{pq} = \langle \eta_p \mid \hat{G} \mid \eta_q \rangle = \sum_{j=1}^{n} \left(2\langle \eta_p \mid \hat{J}_j \mid \eta_q \rangle - \langle \eta_p \mid \hat{K}_j \mid \eta_q \rangle\right)$$

$$= \sum_{j=1}^{n} \sum_{r,s}^{m} C_{rj}\, C_{sj}^{*} \left(2\langle \eta_p(\mu)\, \eta_s(\nu) \mid \hat{g} \mid \eta_q(\mu)\, \eta_r(\nu) \rangle \right.$$

$$\left. - \langle \eta_p(\mu)\, \eta_s(\nu) \mid \hat{g} \mid \eta_r(\mu)\, \eta_q(\nu) \rangle \right)$$

$$= \sum_{r,s}^{m} R_{rs} \left(2\langle ps \mid \hat{g} \mid qr \rangle - \langle ps \mid \hat{g} \mid rq \rangle\right) \tag{1.72}$$

where $R_{rs} = \sum_{j=1}^{n} C_{rj}\, C_{sj}^{*}$ defines the matrix elements of the first-order density matrix in the matrix representation, assuming n doubly occupied orbitals. Thus:

$$F^{n}_{pq} = h^{n}_{pq} + G^{n}_{pq} \qquad (1.73)$$

Comparing the expression for E in (1.48) with (1.71), (1.72) and (1.73), then writing E in terms of the basis functions, gives:

$$E = \sum_{i=1}^{n} C_i^{+}\, {}^{n}{}^{+}\, (2h^{\phi} + G^{\phi})^{n}C_i = \sum_{i=1}^{n} C_i^{+}\, (2h^{n} + G^{n})C_i$$

$$= \sum_{i=1}^{n} C_i^{+}\, (h^{n} + F^{n})C_i$$

$$E = \mathrm{tr}\ \{\underline{R}\ (\underline{h}^{n} + \underline{F}^{n})\} \qquad (1.74)$$

Clearly from (1.74) the expression for the total energy may be written in several forms:

i.e. $E = 2\ \mathrm{tr}\ \underline{R}\ \underline{h}^{n} + \mathrm{tr}\ \underline{R}\ \underline{G}^{n}$

$= 2\ \mathrm{tr}\ \underline{R}\ \underline{F}^{n} - \mathrm{tr}\ \underline{R}\ \underline{G}^{n}$

$= \mathrm{tr}\ \underline{R}\ (\underline{h}^{n} + \underline{F}^{n})$ as in (1.74)

$= 2\ \mathrm{tr}\ \underline{R}\ (\underline{h}^{n} + \tfrac{1}{2}\underline{G}^{n}) \qquad (1.75)$

Where from the diagonalisation of the H-F matrix (1.69) and (1.70) it is evident that each element of the diagonal matrix is an associated orbital energy; in (1.75) diagonalisation is over the occupied orbitals only; however it is important to note that the total energy is not just twice the sum of the SCF orbital energies (two electrons in each orbital): for each orbital energy includes the interaction between its electron and the electrons in all other orbitals and, in summing, the interactions are counted twice. Referring again to (1.75), the second expression introduces the sum of the orbital energies, reduced by the electron-electron repulsions to cancel out doubly-counted interactions. The final form shows that the total energy can be written as a sum of

modified orbital energies.

1.3.2 A Summary of the SCF Procedure

Since $\underline{F}$ depends upon $\underline{R}$ and hence upon the solution of the problem, iteration is necessary: with an assumed $\underline{R}$, $\underline{F}$ is set up and solved; from the lowest energy orbitals, $\underline{R}$ is re-calculated, $\underline{F}$ revised, and the process repeated. Eventually, assuming that the process converges, the $\underline{R}$ which emerges will differ inappreciably from that used in setting up $\underline{F}$ (i.e. $\underline{R}$ of the previous cycle) and the solution is then Self Consistent. In practice, the total energy is calculated, using one of the expressions in (1.74) and (1.75) at each iteration as a more convenient means of determining convergence and this is discussed in a later section.

The first step in the procedure is the approximation of the LCAO method to define the molecular orbitals, in terms of a finite set of basis functions. These are then used to calculate the molecular integrals h^{η}_{pq} (1.71) and G^{η}_{pq} (1.72), as considered in a subsequent section. The basis functions used are unlikely to be orthogonal and therefore an orthogonalisation matrix $\underline{V}$ is introduced, which is constructed from the overlap matrix $\underline{S}$ as $\underline{S}^{-\frac{1}{2}}$ (1.65).

At this point, the iterative cycle begins. The initial density matrix $\underline{R}$ is constructed from the molecular orbital coefficients $\underline{C}$ (1.72), which are usually obtained by diagonalising the one-electron Hamiltonian matrix (1.71). The $\underline{G}$ matrix is then constructed from $\underline{R}$ and the two electron integrals, (1.72) (the computational aspects of this procedure are considered in due course), therefore allowing an energy value to be calculated.

The Fock matrix is constructed from (1.70) and transformed to orthogonal basis using procedure (1.66). This is then diagonalised using a technique† such as that of Jacobi yielding $\underline{U}$ as in (1.69), and hence $\underline{C}$ from (1.70). A revised density matrix $\underline{R}'$ may now be constructed and the procedure repeated until the total energy E and hence $\underline{R}$ be reproduced within a given threshold.

1.4 Open Shell SCF Methods

In general it is not possible to express the HF wave function for an open shell atom or molecule as a single determinant. However, the HF wave functions for the ground states of most radicals (open-shell species) can be written as single determinants. In particular, an electron configuration with only a single electron outside closed shells (spin multiplicity 2) is of common occurrence and will be described in this manner. However there are two approaches to this problem within the LCAO MO framework. The Restricted Hartree-Fock (RHF) Method, treats the two wavefunctions and spin states as equivalent in the absence of a magnetic field, and only by convention examines that with the larger spin eigenvalues. The Unrestricted Hartree-Fock approach removes the assumption that the spatial parts of each pair of spin-orbitals be identical and for this reason has been termed both; "the Spin Unrestricted Hartree-Fock (SUHF)" method and the "Different Orbitals for Different Spins (DODS)" approach.

---

† Footnote: Attention is drawn to reference 21 for a discussion of alternative methods for matrix diagonalisation.

Those molecular excited states of chemical interest which are usually represented by the RHF wave functions have only a few electrons outside closed shells. For this reason, the number of determinants, taken as a linear combination, which is required to give the correct spin and spatial symmetry to the RHF function is usually quite small. A brief discussion of these methods will be given below in terms of their differences and analogies to the closed shell case.

1.4.1 Restricted Hartree-Fock (RHF) Theory

Discussions in this section will be of a suitably general nature so that the equations mentioned may be applicable to both, open-shell states of maximum multiplicity where only a single determinant is required, and states of less than maximum multiplicity using a linear combination of determinants. The initial constraints of the system are that n_1 orbitals are doubly occupied whilst the remaining n_2 orbitals are singly occupied.

The MO of the closed and open shells may be collected in matrices $\underline{T}_1$ and $\underline{T}_2$ with n_1 and n_2 columns respectively, and density matrices for each shell are defined,

$$\underline{R}_1 = \underline{T}_1 \underline{T}_1^+, \qquad \underline{R}_2 = \underline{T}_2 \underline{T}_2^+ \tag{1.76}$$

where the subscripts 1 and 2, imply closed and open respectively.

The energy expression which replaces (1.48) is as follows:

$$E = 2\sum_{i} \hat{h}_{ii} + \sum_{i,j}(2J_{ij}-K_{ij}) + f\left[2\sum_{r} h_r + \sum_{r,s}(2aJ_{rs}-bK_{rs})\right]$$

$$+ 2f \sum_{i,r} (2J_{ir}-K_{ir}) \qquad (1.77)$$

where i and j refer to the closed shell orbitals and r and s the open shell.

The constants a and b depend upon the particular state considered, and f may be thought of as a "fractional occupation number" $0 \leq f \leq 1$ per spin orbital. These values may be obtained by setting up the appropriate combinations of determinants and writing down the expressions for the energy. Many of these have been listed for different states by Roothaan[22] who developed the procedure. In the case where the electron spins are parallel (maximum multiplicity) then the values $f = \frac{1}{2}$, $a = 1$ and $b = 2$ are appropriate. Proceeding in a manner equivalent to the derivation of (1.74) and hence (1.75), this may be expressed as follows:

$$E = 2\,\mathrm{tr}\ \underline{R}_1 (\underline{h} + \tfrac{1}{2}\underline{G}_1) + 2f\ \mathrm{tr}\ \underline{R}_2 (\underline{h} + \tfrac{1}{2}\underline{G}_2) \qquad (1.78)$$

where the two shells have slightly different electron interaction matrices

$$\underline{G}_1 = \underline{G}(2\underline{R}_1) + \underline{G}(2f\,\underline{R}_2) \qquad \text{Closed shell}$$

$$\underline{G}_2 = \underline{G}(2\underline{R}_1) + \underline{G}'(2f\,\underline{R}_2) \qquad \text{Open shell} \qquad (1.79)$$

expressed in terms of coulomb and exchange matrices, through

$$\underline{G}(R) = \underline{J}(R) - \tfrac{1}{2}\underline{K}(R)$$

$$\underline{G}'(R) = a\underline{J}(R) - \tfrac{1}{2}b\underline{K}(R) \qquad (1.80)$$

In $\underline{G}_2$, the $\underline{G}$-term represents the coulomb-exchange effect

of the closed shell electrons, while the $\underline{G}'$-term refers to the other open-shell electrons.

Application of the variation principle in an analagous manner to that previously described for the closed shell case shows that the two sets of orbitals (closed and open shells) are eigenfunctions of two molecular Fock operators:

$$\hat{\underline{F}}_1 \underline{T}_1 = \underline{T}_1 \underline{\varepsilon}_1 \qquad \text{Closed shell}$$

$$\hat{\underline{F}}_2 \underline{T}_2 = \underline{T}_2 \underline{\varepsilon}_2 \qquad \text{Open shell} \tag{1.81}$$

(where orthogonalisation of the basis functions may be assumed since an orthogonalisation method has been described for the closed shell case (1.66)).

Consequently, there are two HF matrices.

$$\underline{F}_1 = (\underline{h} + \underline{G}_1)$$

$$\underline{F}_2 = (\underline{h} + \underline{G}_2) \tag{1.82}$$

The ooject is to obtain one equation, by re-defining the Fock operator,

i.e. $$\hat{\underline{F}}\,\underline{T} = \underline{T}\,\underline{\varepsilon} \tag{1.83}$$

The matrix $\underline{F}$ must combine the properties of $\underline{F}_1$ and $\underline{F}_2$, having the same eigenvectors, $\underline{T}_2$, as $\underline{F}_2$, and giving zero when multiplying $\underline{T}_1$ and any other matrix with eigenfunctions of $\underline{F}_1$, and zero when multiplying $\underline{T}_2$. Any additive combination of two such matrices has the property of $\underline{F}$.

Assuming $\underline{T}$ to be orthogonal and normalised

$$\underline{T}^+ \underline{T} = \underline{1} \tag{1.84}$$

Since $\underline{T}_1$ and $\underline{T}_2$ are partitions of $\underline{T}$ then:

$$\underline{T}_1^{+}\,\underline{T}_1 = \underline{1}$$

and (1.85)

$$\underline{T}_2^{+}\,\underline{T}_2 = \underline{1}$$

Since $\underline{T}_1$ and $\underline{T}_2$ have no column of $\underline{T}$ in common.

$$\underline{T}_1^{+}\,\underline{T}_2 = \underline{T}_2^{+}\,\underline{T}_1 = 0$$

These properties of orthogonality and normalisation of the $\underline{T}$ matrices define the matrix products with $\underline{R}$.

$$\begin{aligned}
\underline{R}_1\,\underline{T}_1 &= \underline{T}_1\,\underline{T}_1^{+}\,\underline{T}_1 = \underline{T}_1 \\
\underline{R}_2\,\underline{T}_2 &= \underline{T}_2\,\underline{T}_2^{+}\,\underline{T}_2 = \underline{T}_2 \\
\underline{R}_1\,\underline{T}_2 &= \underline{T}_1\,\underline{T}_1^{+}\,\underline{T}_2 = \underline{0} \\
\underline{R}_2\,\underline{T}_1 &= \underline{T}_2\,\underline{T}_2^{+}\,\underline{T}_1 = \underline{0}
\end{aligned} \qquad (1.86)$$

Thus the matrices $(\underline{1} - \underline{R}_1)$, and $(\underline{1} - \underline{R}_2)$ have the properties:

$$\begin{aligned}
(\underline{1} - \underline{R}_1)\,\underline{T}_1 &= \underline{0} \\
(\underline{1} - \underline{R}_1)\,\underline{T}_2 &= \underline{T}_2 \\
(\underline{1} - \underline{R}_2)\,\underline{T}_1 &= \underline{T}_1 \\
(\underline{1} - \underline{R}_2)\,\underline{T}_2 &= \underline{0}
\end{aligned} \qquad (1.87)$$

These relations may now be used to form $\underline{F}$. Consider,

$$(\underline{1} - \underline{R}_2)\,\underline{F}_1\,(\underline{1} - \underline{R}_2) \qquad (1.88)$$

operating on $\underline{T}_2$. Using the above relations

$$\begin{aligned}
(\underline{1} - \underline{R}_2)\,\underline{F}_1\,(\underline{1} - \underline{R}_2)\,\underline{T}_1 &= (\underline{1} - \underline{R}_2)\,\underline{F}_1\,(\underline{T}_1 - \underline{0}) \\
&= (\underline{1} - \underline{R}_2)\,\underline{T}_1\,\underline{\varepsilon}_1 \\
&= \underline{T}_1\,\underline{\varepsilon}_1
\end{aligned} \qquad (1.89)$$

Operating on $\underline{T}_2$ gives:

$$(\underline{1} - \underline{R}_2)\,\underline{F}_1\,(\underline{1} - \underline{R}_2)\,\underline{T}_2 = \underline{0} \qquad (1.90)$$

(1.88) has the same eigenvectors as $\underline{F}_1$ and gives zero when operating on the eigenfunctions of $\underline{F}_2$.

A similar analysis of

$$(\underline{1} - \underline{R}_1)\, \underline{F}_2\, (\underline{1} - \underline{R}_1) \qquad (1.91)$$

on $\underline{T}_1$ and $\underline{T}_2$ gives $\underline{0}$ and $\underline{T}_2\, \underline{\varepsilon}_2$ respectively. Therefore any matrix which is a linear combination of (1.88) and (1.91) has eigenvectors $\underline{T}_1$ and $\underline{T}_2$ as required by $\underline{F}$.

$$\text{i.e.} \quad a(\underline{1} - \underline{R}_2)\, \underline{F}_1\, (\underline{1} - \underline{R}_2) + b(\underline{1} - \underline{R}_1)\, \underline{F}_2\, (\underline{1} - \underline{R}_1) \qquad (1.92)$$

where a and b are arbitrary constants.

This may be extended to include the virtual orbitals also.

$$\underline{F} = a(\underline{1} - \underline{R}_2)\, \underline{F}_1\, (\underline{1} - \underline{R}_2) + b(\underline{1} - \underline{R}_1)\, \underline{F}_2\, (\underline{1} - \underline{R}_1) + c(\underline{1} - \underline{R}_3)\, (2\underline{F}_1 - \underline{F}_2)\, (\underline{1} - \underline{R}_3) \qquad (1.93)$$

where $\underline{R}_3 = \underline{T}_3\, \underline{T}_3^{+}$ and $\underline{R}_3 = (\underline{1} - \underline{R}_1 - \underline{R}_2)$

It is convenient to allow a, b and c to be equal to unity.

Again, the equation must be solved iteratively until self consistency is achieved: the matrix $\underline{T}_1$ may be found from the first n_1 eigenvectors and $\underline{T}_2$ from the next n_2, so determining $\underline{R}_1$, $\underline{R}_2$ and a revised $\underline{F}$ for the next iteration. In fact, the technique is as in the closed shell case, and the additional steps are all simple matrix multiplications. The eigenvalues have no simple meaning (unlike those calculated for the closed shell) and may not be thought of as orbital energies since $\underline{F}$ is non-unique. Only the total energy E and the densities $\underline{R}_1$ and $\underline{R}_2$ have an invariant significance[9].

1.4.2 Unrestricted Hartree-Fock(UHF) Theory

As previously noted, the UHF method is an extension of the RHF method in that the restriction, that the spatial functions of each closed shell pair of spin-orbitals are identical, is removed[23]. The wave function is therefore written as a single determinant of n_α orbitals occupied by electrons of α spin and n_β orbitals, with β spins, where for the open shell case $n_\alpha \neq n_\beta$. Clearly, this differs from the RHF classification according to closed and open shells. To determine the orbitals which minimise the energy for a function of this form, it is convenient to write the total energy in terms of two R-matrices, one for orbitals in the α-spin manifold $\underline{R}^\alpha$ and one for those in the β-spin manifold $\underline{R}^\beta$.

Again, the two different types of MO may be collected in matrices $\underline{T}^\alpha$ and $\underline{T}^\beta$ with n_α and n_β columns respectively.

$$\underline{R}^\alpha = \underline{T}^\alpha \, \underline{T}^{\alpha+}$$

$$\underline{R}^\beta = \underline{T}^\beta \, \underline{T}^{\beta+} \tag{1.94}$$

The energy expression in this case is:

$$E = \mathrm{tr}\, \underline{R}^\alpha \, \underline{h} + \tfrac{1}{2} \mathrm{tr}\, \underline{G}^\alpha \, \underline{R}^\alpha$$

$$+ \mathrm{tr}\, \underline{R}^\beta \, \underline{h} + \tfrac{1}{2} \mathrm{tr}\, \underline{G}^\beta \, \underline{R}^\beta \tag{1.95}$$

where

$$\underline{G}^\alpha = J(\underline{R}^\alpha) - K(\underline{R}^\alpha) + J(\underline{R}^\beta)$$

$$\underline{G}^\beta = J(\underline{R}^\beta) - K(\underline{R}^\beta) + J(\underline{R}^\alpha) \tag{1.96}$$

and h, J and K are of their usual form (1.72). The conditions for a stationary value may again be formulated in terms of a matrix eigenvalue equation for the sets of orbital coefficients,

and there is one equation for the orbitals of each type.

$$\hat{\underline{F}}^{\alpha}\,\underline{T}^{\alpha} = \underline{T}^{\alpha}\,\underline{\varepsilon}^{\alpha}$$

and (1.97)

$$\hat{\underline{F}}^{\beta}\,\underline{T}^{\beta} = \underline{T}^{\beta}\,\underline{\varepsilon}^{\beta}$$

and where the two Fock matrices are

$$\underline{F}^{\alpha} = \underline{h} + \underline{G}^{\alpha}$$

and (1.98)

$$\underline{F}^{\beta} = \underline{h} + \underline{G}^{\beta}$$

A self consistent solution may again be achieved by iteration, in exactly the same manner as for the closed shell case, but the resultant wave function will no longer in general contain doubly occupied orbitals, i.e. α-type and β-type spin orbitals with a common orbital factor.

Because the orbital factors are split in the UHF method, the resulting UHF function is not a spin eigenfunction[24], and is therefore, strictly speaking unsuitable for representing a real spectroscopic state.

The most straightforward way of making the UHF wave function an exact eigenfunction of S^2 is to apply a spin projection operator[25]. The resulting wave function may be referred to as the Projected Unrestricted Hartree Fock (PUHF) wave function, but this wave function is not strictly variational, and the energy is still minimised for the UHF wave function.

1.5 Configuration Interaction

1.5.1 Correlation Energy

The Hartree-Fock energy is usually within less

than 1% of the experimental value, for organic systems and although this may seem a very good agreement, it must be noted that absolute energies are not of much significance to practical problems. Generally, of interest are energy differences, such as the energy difference between two spectroscopic states. However, the energy differences are often no larger than 1% of the total energy of either state, and therefore small errors in the total energies may lead to large relative errors in their differences. In the HF approximation, the motion of each electron is solved in the presence of the average potential created by the remaining (n-1) electrons and as such, the approximation therefore neglects the instantaneous repulsions between pairs of electrons. The contribution to the total energy due to instantaneous repulsions is termed the correlation energy, E_{corr}.

More specifically, the correlation energy is seen as the energy difference between the HF limit energy (the limit approached by restricted self-consistent field calculations as the basis set approaches completeness) and the exact solution of the non-relativistic Schrödinger equation[26].

Although it is evident that in such cases as the calculation of heats of atomisation, heats of reaction and dissociation energies; especially when applied to excited states; these are inadequately treated within the HF formalism; there are many instances in which chemical phenomena are well described.

Molecular geometries, and some one-electron properties predicted from RHF wave functions, are frequently in good agreement with experiment, and generally, changes in E_{corr} have been shown to be small for both barriers to rotation[27]

and in the specific case of heats of isodesmic reactions[28].

One of the main methods for calculating ionisation potentials is the ΔSCF method. In this technique, ionisation potentials are given by

$$IP = E^{HF}_{(ion)} - E^{HF}_{(neutral)} \qquad (1.99)$$

where it is assumed that correlation corrections uniformly lower the total energy of the ground and ionised states of a given molecule and this will be discussed in greater detail within the content of the following chapters.

Of those features showing the inadequacies of the HF method, the most important is its inability to correctly describe molecule formation and dissociation, due to incorrect behaviour at large internuclear separations. This is illustrated in Figure (1.1).

Figure (1.1) A comparison of the HF and experimental potential energy curves for a diatomic molecule

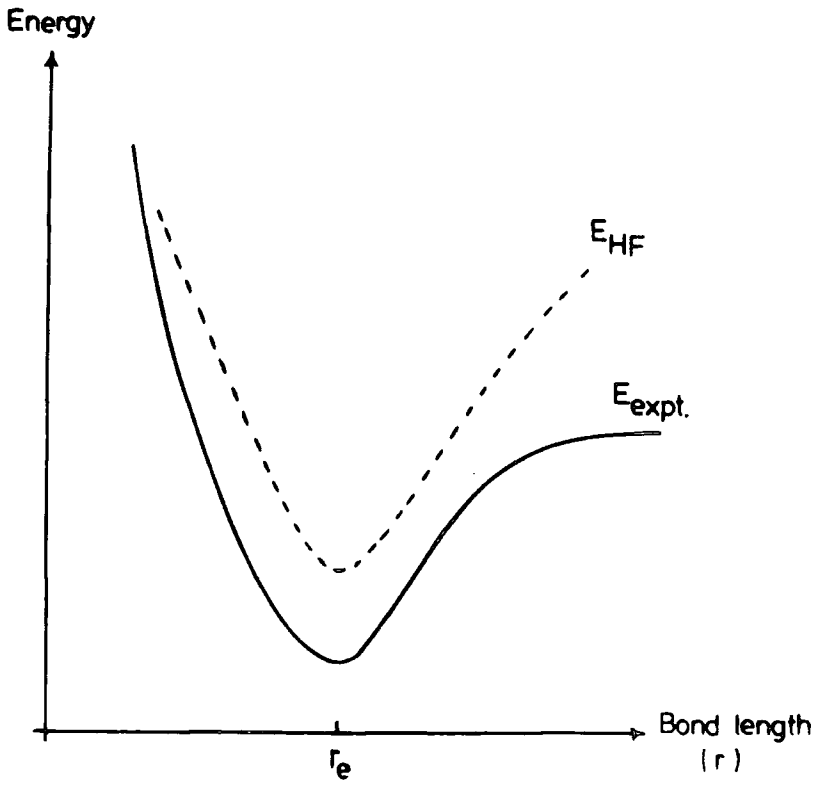

However, from the discussions of Cade and coworkers[29], it is evident that some important aspects of potential energy surfaces, namely equilibrium geometries and force constants can be successfully predicted within the Hartree-Fock formalism. Clearly, from Figure (1.1), comparison of the computed and experimental potential energy curves of a diatomic molecule shows that although the HF curve lies above the experimental, the shapes of the two curves are similar around their minima and they are almost parallel. Consequently, the computed equilibrium bond distances are normally close to the observed values (usually underestimated by a few hundredths of an Angstrom) and also the vibrational frequencies, and therefore force constants are well reproduced by HF functions (usually overestimated with a reduction in size of basis set). Equivalent observations are made in multidimensional potential energy surfaces of polyatomic molecules where equilibrium geometries and force constants can be successfully computed from HF wave functions.

1.5.2 Solving the Correlation Energy Problem

The most frequently used approach to the problem of correlation energy is the incorporation of the method of configuration interaction (CI). However, since no use of CI has been made in the calculations in this thesis, only a brief discussion will be included, but a brief introduction is given in Schaefer[4], and attention is drawn to two recent texts for a more detailed discussion[8,10].

For any atom or molecule, there are an infinite number of orbitals in addition to the HF orbitals, which may be used to construct other configurations. A CI wavefunction is a

linear combination of such configurations with coefficients variationally determined, and is therefore of the form

$$\psi_e = \sum_i C_i \Phi_i \qquad (1.100)$$

where the Φ's are an orthonormal set of n electron configurations, and the coefficients C_i are determined to minimise the energy $\int \psi_e^* \hat{H}_e \psi_e \, d\tau$.

Application of the Variation Principle leads to the eigen value problem, in the manner previously discussed (Section 1.2.2).

$$(\underline{H} - \underline{E}1)\,\underline{C} = \underline{0} \qquad (1.101)$$

$\underline{H}$ is composed of matrix elements between configurations

$$H_{ij} = \int \Phi_i^* \hat{H}_e \Phi_j \, d\tau \qquad (1.102)$$

If M configurations are included in the CI calculations, then solution of (1.101) gives M distinct eigenvalues (energies), and from MacDonald's Theorem[30] the k^{th} lowest eigenvalue of (1.101) is a rigorous upper bound to the k^{th} lowest exact energy. With each energy E is associated an eigenvector composed of coefficients C_i, defining the corresponding CI wave function.

Hamiltonian matrix elements H_{ij} between configurations i and j of different symmetries are zero, and therefore a consideration of only those configurations having the total symmetry of the investigated electronic state, greatly simplifies the secular equation.

Of general interest, is the lowest eigenvalue and corresponding eigenvector solution, and therefore methods for obtaining these particular values only, have been developed,[31,32] making possible the consideration of much larger CI problems than are usually considered practical.

At this stage, it is necessary to introduce the terminology to be used in the discussion of CI. An orbital occupancy is a collection of orbitals, written without regard to those quantum numbers not affecting the orbital energy (e.g. M_l and M_s values) and is usually referred to as the electron configuration.

A configuration, however, is defined as a symmetry-adapted linear combination of Slater determinants. 'Symmetry-adapted' implies that the chosen linear combination of determinants possesses all the symmetry of the molecular state being described by the approximate wave function. A Slater determinant D_i is defined as in Section 1.2.1 and thus the configuration Φ is written:

$$\Phi = \sum_i C_i D_i \qquad (1.103)$$

It is often found that several different configurations arise from a single orbital occupancy, and a consideration of only the electrons outside closed shells determines what configurations are possible. Having determined the manifold for a given orbital occupancy,[33] it is then necessary to find which configurations of this manifold give rise to the desired spin multiplicity. A less tedious approach to the problem than the direct application of angular momentum operators is the use of projected wave functions. In particular Nesbet's method[25] is simple to apply, and time saving in CI studies in that it reduces the number of terms involved in matrix elements.

It is often the case that a CI wavefunction is dominated by a single configuration, the HF wavefunction and that approximately 95% of the correlation energy can be accounted for by configurations which differ by only one or two orbitals from this.

A singly excited configuration (or single excitation) differs from the reference configuration in the nature of the occupancy of only one orbital whilst a double excitation is a configuration arising from an orbital occupancy differing by two orbitals. Thus, where D_o is the reference or HF configuration.

$$D_o = |\phi_1(1)\ \phi_2(2) \ldots \phi_i(i) \ldots \phi_p(p) \ldots \phi_n(n)| \quad (1.104)$$

then a single excitation obtained by promoting an electron from the p^{th} spin orbital to the q^{th} spin orbital is represented as:

$$D_p^q = |\phi_1(1)\ \phi_2(2) \ldots \phi_q(p) \ldots \phi_n(n)| \quad (1.105)$$

and a double excitation as:

$$D_{pi}^{qj} = |\phi_1(1)\ \phi_2(2) \ldots \phi_j(i) \ldots \phi_q(p) \ldots \phi_n(n)| \quad (1.106)$$

where excitation is from spin orbitals ϕ_i and ϕ_p to spin orbitals ϕ_j and ϕ_q respectively.

The matrix elements H_{ij}, now expressed in terms of these determinantal functions D_i may be evaluated by the use of Slater's Rules for the calculation of Matrix Elements,[34] summarised in Table (1.1).

The electronic wavefunction may now be written as

$$\psi_e = C_o D_o + \sum_{p,q} C_p^q D_p^q + \sum_{p,q,i,j} C_{pi}^{qj} D_{pi}^{qj} + \ldots \quad (1.107)$$

which is termed the CI expansion.

Within an orthonormal set of orbitals, if two determinants differ by three or more spin orbitals, the H matrix element between these two determinants is identically zero. It is essentially for this reason that when the HF configuration dominates the wavefunction, only singly and doubly

TABLE 1.1 A Collection of Useful Slater Rules

1. Overlap Integral

$$\langle D_o|D_o\rangle = \qquad \langle D_o|D_p^{\,q}\rangle = \langle D_o|D_{pi}^{\,qj}\rangle = 0$$

2. One-electron Operators

$$\langle D_o|\sum_i \hat{P}(i)|D_o\rangle = \sum_{p}^{\text{occupied}} \langle \phi_p(1)|P(1)|\phi_p(1)\rangle$$

$$\langle D_o|\sum_i \hat{P}(i)|D_p^{\,q}\rangle = \langle \phi_p(1)|\hat{P}(1)|\phi_q(1)\rangle$$

$$\langle D_o|\sum_i \hat{P}(i)|D_{pi}^{\,qj}\rangle = 0$$

3. Two-electron Operators

$$\langle D_o|\sum_{i<j} \hat{P}(i,j)|D_o\rangle = \sum_{p<q}^{\text{occupied}} \langle \phi_p(1)\phi_q(2)|\hat{P}(1,2)|\phi_p(1)\phi_q(2)\rangle - \langle \phi_p(1)\phi_q(2)|\hat{P}(1,2)|\phi_p(2)\phi_q(1)\rangle$$

$$\langle D_o|\sum_{i<j} \hat{P}(i,j)|D_p^{\,r}\rangle = \sum_{p}^{\text{occupied}} \langle \phi_p(1)\phi_q(2)|\hat{P}(1,2)|\phi_p(1)\phi_r(2)\rangle - \langle \phi_p(1)\phi_q(2)|P(1,2)|\phi_p(2)\phi_r(1)\rangle$$

$$\langle D_o|\sum_{i<j} \hat{P}(i,j)|D_{pq}^{\,rs}\rangle = \langle \phi_p(1)\,\phi_q|\hat{P}(1,2)|\phi_r(1)\phi_s(2)\rangle - \langle \phi_p(1)\,\phi_q(2)|P(1,2)|\phi_r(2)\phi_s(1)\rangle$$

$$\langle D_o|\sum_{i<j} \hat{P}(i,j)|D_{pqi}^{\,rsj}\rangle = 0$$

where $\sum_i \hat{P}(i)$ and $\sum_{i<j} \hat{P}(i,j)$ are general one- and two- electron operators respectively.

excited configurations will give significant contributions to the wave function.

In HF Theory, the expansion is limited to the first determinant, with a coefficient of unity and then the spin orbitals are optimised. In CI, the spin orbitals are fixed, but the coefficients C_k are optimised. Ideally the calculation should be a combination of these two ideas and indeed this is the aim of the Multi Configuration SCF procedure, where both spin orbitals and coefficients are simultaneously varied to give the lowest MCSCF wave function. Although this method is increasing in popularity, solution of the MCSCF equations is computationally difficult and very time consuming.

The generalised valence bond wave function, briefly referred to in Section 1.2.2, is a particular form of an MCSCF wave function in which each chemical bond is described in terms of a pair of localised, nonorthogonal, optimised orbitals. At large internuclear distances, this description is advantageous since each orbital of a pair would tend to localise on one atom (or molecular fragment, in general), providing a simple description of the dissociation process in terms of a single-configuration wave function. Such orbitals would be expected to have a beneficial effect upon the convergence of a CI expansion, but they cannot be used conveniently without orthogonalisation. Near equilibrium bond length, orthogonalisation renders their expression inferior in performance. However, Raffenetti and Kahn have found that the orthogonalised form is preferable as a basis for a CI expansion whenever the original G.V.B. orbitals have an overlap integral smaller in magnitude than $\sqrt{2}-1$.[10]

Due to the nature of the information required, the use of these methods have not been necessary, and therefore a detailed discussion of the procedures will be neglected, but attention is again drawn to the excellent texts available on these topics and methods of solution.[9,10]

1.5.3 The Relativistic Correction

In the previous section, the correlation energy has been described as the difference between the exact non-relativistic H.F. energy and the exact non-relativistic energy of a given system. The relativistic correction is the energetic consequence of the relativistic effects suffered by the electrons on passing the nucleus. A consideration of the Virial Theorem, ($V = -2T$ where V is the potential energy and T the kinetic energy) shows that an electron in a given region of high potential will have a correspondingly high kinetic energy. The relativistic effect is a function of atomic number, being small for the first row atoms but considerably larger for the heavier elements. For the heavier atoms it is not inconceivable that this may become significant in calculations on photoionisation. Fortunately, relativistic corrections to shifts in core-electron binding energies are small, and it is assumed that the effects for atoms are unchanged upon molecule formation:

$$\text{i.e.} \qquad E_R^{mol} = \sum_{k}^{\text{Total No. of atoms}} (E_R^{atom})_k \qquad (1.108)$$

Tabulations of relativistic expectation values for atoms have been made,[35] allowing detailed comparison with non-relativistic results. Also, neutral atom ΔSCF binding energies from relativistic HF calculations ($2<Z<106$) have been published,[36] allowing a comparison between these and

Koopmans' values to be made.

1.6 Population Analysis

The population analysis is frequently used in qualitative discussions of electronic structure. Following Mulliken,[37] overlap integrals between the basis functions are used to analyse an SCF wave function so that a certain number of electrons is assigned to each basis function.

More generally, if the molecular orbitals (MO) are expressed as a linear combination of atomic orbitals (AO):

$$\phi_i = \sum_j C_{ij} \eta_j \tag{1.109}$$

then, the MO probability density function is given by

$$\begin{aligned} \phi_i^2 = (\sum_j C_{ij} \eta_j)^2 = (\sum_j C_{ij} \eta_j)(\sum_k C_{ik} \eta_k) \\ = \sum_j \sum_k C_{ij} C_{ik} \eta_j \eta_k \end{aligned} \tag{1.110}$$

The sum of the squares of the coefficients of η_j in all ϕ_i gives the total "occupation number" of AO η_j. This is the sum of the squares of the i^{th} row of $\underline{C}$ multiplied by the number of electrons in each spatial MO (N_i). If in (1.110), the specific case of j=k is excluded, then multiplying the coefficients of $\eta_j \eta_k$ by Ni and summing gives the population of the overlap region.

Integrating over all space, the orbital population Ni is:

$$N_i = N_i \int \phi_i^2 \, d\tau = N_i \sum_j \sum_k C_{ij} C_{ik} \int \eta_j \eta_k \, d\tau$$

$$= N_i \sum_j \sum_k C_{ij} C_{ik} S_{jk} \qquad (1.111)$$

where S_{jk} is the overlap integral $\int \eta_j \eta_k \, d\tau \equiv \langle \eta_j | \eta_k \rangle$.

Summing over all occupied MO gives:

$$N = \sum_i N_i = \sum_i N_i \sum_j \sum_k C_{ij} C_{ik} S_{jk}$$

$$= \sum_j \sum_k S_{jk} \left(\sum_i C_{ij} C_{ik} \right) \qquad (1.112)$$

where N is the total number of electrons. In the general case, the orbital occupancy N_i would be incorporated into the density matrix (i.e. (1.72) would be modified). In a closed-shell system, $N_i = 2$ for all of the occupied MO. Therefore, from (1.72):

$$R_{jk} = \sum_i^{\text{MO occupied}} C_{ji} C_{ik}^{+} = \sum_i^{\text{MO occupied}} C_{ji} C_{ki}^{*} = \sum_i C_{ji} C_{ki}$$

(1.113)

Since the M.O. are real. Thus (1.112) becomes:

$$N = 2 \sum_j \sum_k R_{jk} S_{jk} \qquad (1.114)$$

A population matrix $\underline{P}$ may be defined

$$P_{ij} = 2 R_{ij} S_{ij} \qquad (1.115)$$

Along the principal diagonal, the P_{ii}, equal to $2R_{ii}$ (since $S_{ii} = 1$), represent the electronic populations, or the

"atomic charge" in units of electrons, whilst the off-diagonal elements P_{ij} are overlap populations, related to the simple idea of "bond order". Since both $\underline{R}$ and $\underline{S}$ are symmetric, then $P_{ij} = P_{ji}$.

Clearly, from (1.114)

$$\sum_i \sum_j P_{ij} = N \tag{1.116}$$

The summation of all P_{ij} elements associated with a given pair of atoms A and B reduces the "orbital by orbital" population matrix $\underline{P}$ to an "atom by atom" matrix $\underline{Q}$.

$$QAB = \sum_{i}^{\text{AO in A}} \sum_{j}^{\text{AO in B}} P_{ij} \tag{1.117}$$

The total number of electrons associated with atom A, N_A, is given by:

$$\begin{aligned} N_A &= Q_{AA} + (\tfrac{1}{2}) \sum_{B \neq A}^{\text{atoms}} Q_{AB} + (\tfrac{1}{2}) \sum_{B \neq A}^{\text{atoms}} Q_{BA} \\ &= Q_{AA} + \sum_{B \neq A}^{\text{atoms}} Q_{AB} \\ &= \sum_{B}^{\text{all atoms}} Q_{AB} \end{aligned} \tag{1.118}$$

Since Mulliken has suggested that the electron density be equally partitioned between A and B. Where Z_A is the nuclear charge associated with atom A then the net charge on atom A is given by $Z_A - N_A$.

1.7 Orbitals and Basis Functions

1.7.1 Molecular Integral Evaluation

The expression of the MO in terms of a linear combination of basis functions has been focussed upon frequently in the previous sections. Molecular calculations are generally carried out in terms of basis functions centred on each atom in the molecule, and the choice of these functions is important in that the accuracy of the wavefunction is determined by the quality of the basis set from which it is constructed.

The term linear combination of atomic orbitals (LCAO) has also arisen in previous discussions, and this is historical in that basis functions were chosen by physical analogy to orbitals, however since the number of computationally difficult two electron integrals increases with the number of basis functions as N^4, these so called Slater-type orbitals (STO) have been replaced by the more mathematically and computationally convenient Gaussian type functions (G.T.F.) in many cases.

A clear advantage of the Gaussian function is seen in its expression, in that the product of such functions will always produce another Gaussian function, as will be seen, and this is not inherent in the form of the Slater-type function. Consequently, for the GTF, three and four centre integrals which are very time-consuming in LCAO MO calculations are reduced to relatively simple two centre integrals.

Thus,

$$\langle G_a G_b \left|\frac{1}{r_{12}}\right| G_c\, G_d \rangle = \langle G_e \left|\frac{1}{r_{12}}\right| G_f \rangle \qquad (1.119)$$

The clear disadvantage of using G.T.F. is that they do not resemble atomic orbitals in form. In particular, the s-type GTF lacks a cusp at the nucleus, and also at large distances decreases too rapidly as illustrated in Figure (1.2).

Figure 1.2. A comparison of Slater- and Gaussian-type functions

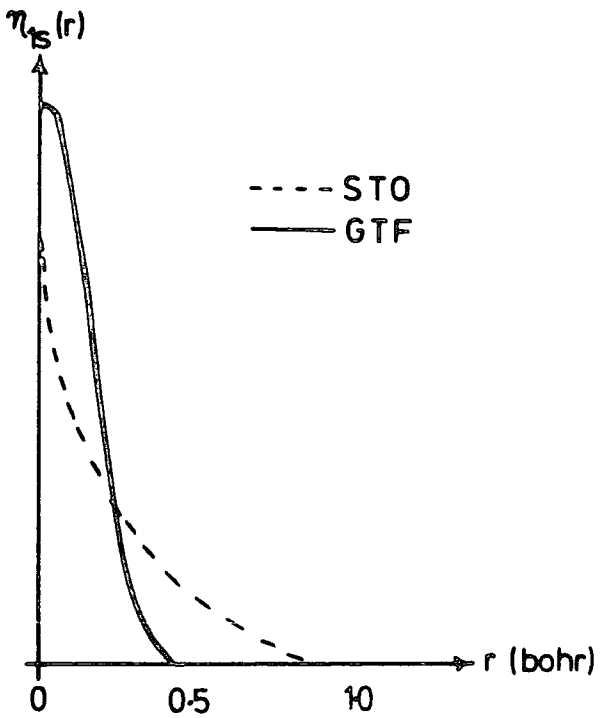

However, this is not a serious problem, as it merely means that more GTF must be used to approximate this behaviour and since all GTF type integrals may be evaluated as standard forms the desired result is obtained more rapidly.

1.7.2 Slater Type Functions

The use of exponential functions was first suggested by Slater,[38] and prior to the early 1960's almost

all MO calculations were performed with STO of the form:

$$\eta_{nlm}(r,\theta,\phi) = A_n \; r^{n-1} \; e^{-\zeta r} . \; Y_{lm}(\theta,\phi) \qquad (1.120)$$

where A_n is a normalisation factor;

n,l,m are the principle, azimuthal and magnetic quantum numbers;

ζ is the orbital exponent;

and $Y_{lm}(\theta,\phi)$ are the spherical harmonics, introducing the required angular dependence.

1.7.3 Gaussian Type Functions

The use of Gaussian functions in electronic structure calculations was first suggested by Boys[39] and in past years many large scale MO calculations have used G.T.F.[40] The radial dependence of a G.T.F. may be written as:

$$\eta = B_n \; r^n \; e^{-\alpha r^2} \qquad (1.121)$$

where B_n is again a normalisation factor;

and n is the analogue of the principal quantum number; taking values 1, 1+2, 1+4, etc.

Angular dependence in this case is introduced by a function of the form:

$$C \; x^p \; y^q \; z^s \; e^{-\alpha r^2} \qquad (1.122)$$

where p, q and s are integers and the resulting function is therefore termed a cartesian gaussian.

Preuss[41] and Whitten[42], independently, have developed another procedure termed the gaussian lobe method which uses only S-type gaussians of the form $Be^{-\alpha r^2}$ and floating the centres of these functions away from the atomic centres to simulate s, p, d .... orbitals.

1.7.4 The Minimal Basis Set

A minimal basis set includes only one function for each AO occupied in each atom of the molecule and is usually considered to be of Slater type. (e.g. for carbon: 1s 2s 2px 2py). The choice of orbital exponent ζ was originally made using the set of empirical rules deduced by Slater,[38] where:

$$\zeta = \left(\frac{Z-S}{n^*}\right) \qquad (1.123)$$

Here, Z is the actual charge on the nucleus;

S is a screening constant;

and n^* is an effective quantum number.

A more direct approach by Clementi and coworkers[43,44] was to variationally optimise ζ values for each atom, producing tables of best atom exponents, used repeatedly in this work. In principle, the exponents should be re-optimised for each molecule under consideration, but this is prohibitively expensive and therefore if greater accuracy is required then the basis set is expanded.

As previously noted, the computation of multicentre two-electron integrals involving STO is difficult although the minimal basis set may be conceptually simple. To overcome this problem, the concept is retained, but each STO is replaced by a linear combination of n-GTF and the basis set is termed STO-nG, being fundamentally gaussian in nature.[45,46,47] It has been shown[46,47] that even when n is equal to six, the total molecular SCF energies are ≈1eV above the exact STO values and that since it is energy differences which are of importance, four gaussians to each STO are adequate.

The coefficients and exponents of the gaussians are optimised by a least squares procedure to fit a Slater orbital of unit exponent. The Slater exponent is then chosen, and the gaussian exponent scaled accordingly;

(Scaled gaussian exponent = least squared optimised exponent X (Slater exponent)^2)

to be used in the STO-nG expansion.

Virtually all of the current semi-empirical SCF methods in use are in principle based upon a minimum set of STO and many of the concepts in organic chemistry (e.g. resonance structures, hybridisation) can only be discussed in these terms.

1.7.5 Split Valence Shell Basis Sets

Greater flexibility in the description of valence orbitals is introduced by splitting of the valence-shell in each heavy atom and this allows for orbital distortion upon bond formation. A commonly used example of this type, used extensively in this work, is the STO-4-31G basis set,[48] in which the inner (1s) shell of the first-row atoms is represented by a linear combination of 4 G.T.F., whilst the valence shells (2s,2p) are divided into "inner" and "outer" components represented by 3 and 1 GTF respectively. Hydrogens are represented by a split 1s shell, again comprising of "inner" (3GTF) and "outer" (1GTF) parts.

As emphasised by Nesbet,[49] the inclusion of functions having a higher l value in the description of each atom, termed polarisation functions, can lead to a substantial lowering in SCF energy and an improvement in the computed expectation values of various properties of the molecule (e.g. dissociation energies and dipole moments). Thus a further improvement is

obtained by addition of a single set of gaussian d functions to the basis set for each first row atom, a commonly used basis set being STO-6.31G*; addition of a single set of gaussian p functions to that for each hydrogen atom gives the following terminology:

STO - 6.31G.**[50]

For reasons of economy, the exponents of the polarisation functions are not optimised in the course of the calculations, but are obtained from calculations on small molecules,[51] since fortunately calculated total energies are not particularly sensitive to small variations in exponents. A reasonable value for the gaussian exponent for hydrogen would be $\alpha(1s)=1.0$ and for the first row atoms, $\alpha(3d)=0.8$. In general, a trend of increasing optimum 3d exponents is assumed for both Slater and gaussian functions in going across the period.

1.7.6 Double Zeta and Extended Basis Sets

The double zeta basis set, in which twice as many functions as would be used in the minimal basis are included, yields a considerable improvement in total energy. For the carbon atom therefore the basis set consists of two 1s Slater functions, two 2s functions and two sets of 2p functions (px, py and pz), each pair having two different exponents ζ and ζ' optimised by successive ground state SCF calculations.[52,53]

After the double zeta level has been reached for a first row atom, the next most important contribution to the total energy is again provided by the addition of polarisation functions in the form of five 3d functions corresponding to the $5m_l$ values associated with $l=2$. Equally important for

molecules containing hydrogen is the inclusion of 2px, 2py and 2pz functions in each H atom expression. The STO exponents are obtained in the manner previously referenced and a reasonable value for the hydrogen and first-row atoms is $\zeta(2p) = \zeta(3d) = 2.0$.

SCF energies very close to the HF value may be gained by using STO basis sets larger than the double zeta level, and these are termed extended basis sets. An example of such a basis is the triple zeta, the form of which is self explanatory in being analogous to the above-mentioned double zeta basis set.

1.7.7 Gaussian Basis Sets

The above discussions have largely centred upon the use of the Slater function and Gaussian approximations to it, as a basis for molecular calculations. However, the rapid computation of the multicentre integrals due to the form of the gaussian function, despite increases in their numbers proportional to N^4, as previously noted, allows a more direct approach in that the electronic wave function may be expanded as large sets of nuclear centred gaussian functions. Indeed, optimised gaussian basis sets of several sizes have been reported in the literature,[54] with exponents α (as in (1.121) and (1.122)) optimised for each atom by variation until a minimum in the SCF energy is computed.

Although the required integrals resulting from such basis sets may be computed efficiently, the iterative solution of the matrix HF equations can be time consuming. Numerous techniques have been devised to accelerate the convergence of the solutions as will be seen in the next section, however,

rather than reducing the number of iterations, if the basis functions could be grouped together in some manner then a reduction in the time required per iteration would ensue and this is the fundamental concept of basis set contraction.

If there are n functions in the primitive set and m functions in the contracted set, then contraction reduces the number of integrals to be manipulated by $(m/n)^4$. In practice, little accuracy is lost if $m=n/2$[55] so that the contracted set contains 1/16 the number of integrals and will require only 1/16 of the time per iteration.

In grouping together the primitive gaussian functions, fixed coefficients are assumed[56] and therefore in solving the SCF equations, only the coefficients related to each SCF orbital of the contracted function must be determined.

The contraction of gaussian basis sets requires great care.[55] A complete contraction to atomic SCF orbitals may seem an obvious move, and for the gaussian (9s5p) primitive set of Huzinaga,[54a] having 24 functions per atom, this would be designated (9s5p/2s1p) or [2s1p]†. However, the use of such a basis set would be a mistake as it is drastically overcontracted and would lead to erroneous descriptions of molecular properties (e.g. unrealistically large bond distances and small dissociation energies). This is due to a lack of flexibility in describing the rearrangement of the electron distribution upon molecule formation, and therefore a minimum STO basis set is preferable to such an energetically superior gaussian contraction.

---

† Uncontracted sets are denoted by parentheses, while contracted sets are denoted by brackets.

Surveying previous work[52,53] indicates that the aim in performing a basis set contraction is to obtain a contracted gaussian basis comparable to the double zeta Slater-function sets. Indeed, one of the most effective gaussian basis sets is the double zeta [4s3p][55] contraction of the (9s5p) primitive set[54a] referred to previously. In this context, the term double zeta implies that two contracted GTF contribute to each AO and the contraction scheme in the above follows that, which experience has shown to be most efficient for molecular calculations, in that the outermost (smallest exponent) primitive functions remain uncontracted, whilst a single contracted function is formed from the innermost (largest exponent) primitives. This permits the outer functions, having maximum amplitude in the interatomic regions to respond to changes which occur upon molecule formation whilst the inner functions describe regions which are largely atomic in character. The double zeta [4s3p] contraction has been used in a number of calculations in this thesis, providing economically viable computations of comparatively good quality as will be seen in subsequent chapters.

1.8 Computational Aspects of *ab initio* Calculations

The theories relating to quantum mechanics and in particular, MO theory, were largely elaborated during the second quarter of this century however, only with the advent of modern electronic computers in the 1960's together with appropriate well documented computer programs has the *ab initio* technique become an established tool in modern science. Man-years of effort have now produced a number of these programs, and a selection of those available through international organisations such as the Quantum Chemistry Program

Exchange (Q.C.P.E.)[57], reads as follows: ALCHEMY[58], GAUSSIAN 70[59], IBMOL V[60], MOLECULE[61], and POLYATOM 2[62].

The calculations in this thesis have been carried out using the ATMOL 3[63] suite of programs and this section will be devoted to a limited discussion of points of interest in the packages; a more detailed description may be found in the appropriate ATMOL 3 documentation.

ATMOL consists of several packages, which were originally devised by Hillier and Saunders in the late 1960's as extensions of the POLYATOM and IBMOL systems. In common with most *ab initio* programs, it has the following essential stages:

(i) The computation of single and multi-centre integrals over a set of basis functions, together with the transformation of these integrals over contracted functions should this be required.

(ii) An iterative assembly and diagonalisation of the Fock matrix until the required self-consistency is reached.

(iii) Analysis of the molecular wave function in the form of a Mulliken population analysis, electron density contour plots and the calculation of expectation values of some 1-electron operators (e.g. dipole moments, etc.)

1.8.1 Integral Considerations

The topic of research regarding integral evaluation has largely centred around the computation, storage and

retrieval of molecular integrals, since these areas are the most time-consuming in any MO calculation. This is particularly evident in the case of the multi-centre integrals, although ATMOL 3 has extensive integral file handling facilities provided by a SERVICE program which allows the copying, editing and merging of integral files and the INTEGRALS package itself has both restore and restart facilities to overcome problems attributing to integral storage space and the computational time-factor.

Details of the numerical procedures used for the evaluation of molecular integrals over G.T.F., together with a discussion of the general strategy employed are given by Saunders[64]. For STO, single-centre two-electron integrals are computed analytically, whilst all other two-electron integrals are computed by the gaussian transform technique of Shavitt and Karplus[65].

The matrix of one-electron integrals can be conveniently stored in a two-dimensional array in the fast store of the computer or where storage space is important, only distinct elements need be saved and therefore, due to the Hermitian symmetry of the one-electron Hamiltonian operator, only $\frac{1}{2}m(m+1)$ unique integrals are stored, where m is the number of basis functions.

The treatment of the four-centre repulsion integrals differs from that where space saving is not considered since this would involve a four dimensional array containing m^4 elements and would neglect a number of important equalities among the integrals which would permit a considerable saving of storage space, thereby allowing the method to be used for only the smallest molecules.

Due to the permutations of the indices p, q, r and s being independent of molecular symmetry, only one of the following integrals need be computed and stored:

$$\langle ps|\hat{g}|qr\rangle = \langle qs|\hat{g}|pr\rangle = \langle pr|\hat{g}|qs\rangle = \langle qr|\hat{g}|ps\rangle$$
$$= \langle sq|\hat{g}|rq\rangle = \langle rp|\hat{g}|sq\rangle = \langle sq|\hat{g}|rp\rangle = \langle rq|\hat{g}|sp\rangle \qquad (1.124)$$

Clearly, depending upon the equalities among p, q, r and s, there are 1, 2, 4 or 8 integrals with the same value as $\langle ps|\hat{g}|qr\rangle$ and an ordering convention, among the indices, is needed in storing this integral. The convention used by ATMOL is:

$$p \geq q; \quad s \geq r; \quad [pq] \geq [sr] \qquad (1.125)$$

where $[pq] = \frac{1}{2}p(p-1) + q$ and this converts the otherwise 4-dimensional array into a pseudo-2-dimensional matrix, with the number of distinct elements given by $\frac{1}{8}(m^4 + 2m^3 + 3m^2 + 2m)$ m being the number of basis functions.

The integrals are stored on an external file by first computing and storing them in blocks in the fast store and then writing these blocks as units to a disk or tape using the following scheme:

(i) assign a block of storage in the fast store - a "buffer" - for temporary storage of the integrals;

(ii) set up loops ranging over p, q, r and s satisfying the ordering convention $p \geq q$; $s \geq r$; $[pq] \geq [sr]$;

(iii) using the current labels p, q r and s and the molecular geometry, orbital specifications, etc. compute the current integral $\langle ps|\hat{g}|qr\rangle$;

(iv) add the computed $\langle ps|\hat{g}|qr\rangle$ to the buffer; if this fills the buffer go to (v). if not go to (vi);

(v) write the contents of the buffer to disk;

(vi) increment p, q, r, s, consistent with the ordering convention of (ii);

(vii) if the loops on p, q, r, s are exhausted i.e. q=m go to (viii), if not go to (iii);

(viii) close the integral storage file and finish.

The computed integrals, in storage, need to be accessed and identified for use in the orbital basis calculation. The two general methods for unique identification of each integral in such a file are:

(a) store the values of the labels p, q, r, s and of the integral $\langle ps|\hat{g}|qr\rangle$, together in the file;

or (b) store the integrals $\langle ps|\hat{g}|qr\rangle$ in a particular order in the file so that values of p, q, r and s are determined by the position of the value of $\langle ps|\hat{g}|qr\rangle$ in the file.

Both methods have their relative advantages and disadvantages however, although requiring more space for storage method (a) has the distinct advantage in that any integrals which are zero may be omitted from the file, thus giving greater flexibility in the case where such an approximation as the neglect of small electron repulsion integrals is invoked.

In reality, each block of storage in the ATMOL 3 system is limited to a value of 340 integrals, and the maximum number of contracted functions which may be handled by the VRSINTEG program is 127 with a maximum number of primitives within a contraction being 6. An improved program (BIGINTEG) has recently been documented which increases the contracted functions parameter to 250. Within both programs, there exists

the facility to use the symmetry properties of the molecule to improve the efficiency of calculation of the two-electron integrals.

1.8.2 Computational Aspects of the Closed Shell SCF Procedure

As previously noted, (Section 1.3.2) the SCF calculation proceeds in an iterative manner, with each cycle consisting basically of three steps:

(i) Construction of the Fock matrix (1.70);

(ii) Solution of the pseudoeigen value equation (1.70);

(iii) Recognition as to whether or not self-consistency has been reached; if not the re-input of the new trial vectors, ($\underline{C}$ in 1.70) by the construction of $\underline{R}$ (1.72), for the next cycle.

Each of these steps requires some auxiliary calculations such as the formation of the density matrix $\underline{R}$ in step (iii). At each iteration, the total energy E (1.74) is calculated and the trial vectors orthonormalised. In this section, the aim is to briefly draw attention to the approach of the ATMOL 3, VRSSCF program and some of its facilities.

From (1.73) and (1.72) it is clear that a general element of the Fock matrix is described by

$$Fpq = hpq + Gpq = hpq + \sum_{rs} Rrs \left(2\langle ps|\hat{g}|qr\rangle - \langle ps|\hat{g}|rq\rangle\right) \qquad (1.126)$$

In building the Fock matrix therefore, it is necessary to first construct the $\underline{G}$ matrix from the density matrix $\underline{R}$ and the file of 2 electron repulsion integrals remembering that this file contains only one representative form of the

integral equalities (1.124). Since the reading of an external file is a slow process, in the computational scheme used this procedure must occur only a minimal number of times. It is therefore unsatisfactory to approach the problem by immediately calculating all of the repulsion integrals, as this would involve reading the file $\frac{1}{2}m(m+1)$ times in total. However, looking at each integral $\langle ps|\hat{g}|qr\rangle$ and its labels p, q, r, s, within the context of the previous storage convention gives the possible elements which it contributes to the matrix $\underline{G}$ thereby only requiring to read the file once. It is possible to write a simple algorithm for the formation of the $\underline{G}$ matrix[66].

The standard method for solution of the Roothaan equation (1.63) for the closed shell system, in the form of a transformation to an eigenvalue problem by Lowdin orthogonalisation[20a] and obtaining the eigenvalues and eigenvectors of the real, symmetric matrix by a diagonalisation technique such as that of Jacobi, has been referred to in a previous Section (1.3.1). However, of interest is the nature of the trial vectors used to calculate the density matrix $\underline{R}$ in the initial stages of the calculation and at the end of each cycle, since comparison of these vectors after each iteration to establish their agreement within a fixed threshold, is the criterion for convergence being achieved.

Clearly a good choice of initial vectors, in the sense that they are similar in form to the solution set, will be advantageous on two counts, since fewer iterations will be needed to achieve the required result, and the possibility of trapping the solution in a local minimum is diminished. The flexible file-handling capabilities of ATMOL 3 allow such

choices to be made either for a molecular fragment, or a related molecule, from the vectors produced in previous calculations. Alternatively, trial vectors may be formed by diagonalisation of the one-electron Hamiltonian operator matrix. The solution eigenvectors are ordered according to increasing eigenvalue.

Where a trial set of vectors is a poor representation of the exact solution, it is not inconceivable that convergence problems may arise. In ATMOL 3 therefore an unconditional guarantee of convergence may be obtained according to the procedure proposed by Saunders and Hillier[67]. In a 2n electron system, over m basis functions, n doubly-occupied molecular orbitals may be constructed (DOMOS) and therefore (m-n) virtual MO (VMOS), such that the complete set of MO is orthonormal. Where η, ϕ_1 and ϕ_3 represent the row vectors of basis functions, DOMOS and VMOS respectively, then:

$$(\phi_1 \,\vdots\, \phi_2) = (\eta)\ (C_1 \,\vdots\, C_2) = \underline{n}\ \underline{C} \qquad (1.127)$$

where a column of $\underline{C}$ gives the atomic orbital coefficient of a given MO.

Since the total wave function and Energy are invariant to mixing between DOMOS only, consideration need only be given to the mixing between DOMOS and VMOS. Where $\underline{I}_1$ denotes the identity matrix of order n, and Δ is the "mixing" matrix of order (m-n)Xn with arbitrary elements of small value this may be represented as:

$$\underline{\phi}_1' = (\phi_1 \,\vdots\, \phi_2) \begin{pmatrix} I_1 \\ \cdots \\ \Delta \end{pmatrix} \qquad (1.128)$$

From a consideration of the overlap matrix, it is evident that with these variations, the DOMOS remain orthonormal to the first order. Thus:

$$\underline{S} = \phi_1'^{+}\ \phi_1' = (I_1 \vdots \Delta^+) \begin{pmatrix} \phi_1 \\ \vdots \\ \phi_2 \end{pmatrix} (\phi_1 \vdots \phi_2) \begin{pmatrix} I_1 \\ \vdots \\ \Delta \end{pmatrix}$$

$$= (I_1 \vdots \Delta^+) \begin{pmatrix} I_1 \\ \vdots \\ \Delta \end{pmatrix}$$

$$= \underline{I}_1 + \underline{\Delta}^+ \underline{\Delta} \qquad (1.129)$$

From perturbation theory, the electronic energy change accompanying the variations in the DOMOS may be written as:[68]

$$E \longrightarrow E_o + 4 \sum_{k}^{\text{virtual}} \sum_{i}^{\text{occupied}} \Delta_{ki} F_{ki}^{\phi} + \text{higher terms} \qquad (1.130)$$

where E_o is the energy of the unperturbed wavefunction and F_{ki}^{ϕ} denotes the matrix element connecting the k^{th} VMO with the i^{th} DOMO over the Fock operator in the trial MO basis set. Clearly, the conditions for self-consistency (i.e. $\left(\frac{\delta E}{\delta \Delta_{ki}}\right)_{\Delta}=0$) are satisfied when all $F_{ki}^{\phi} = 0$ and if all Δ_{ki} are chosen such that they be of opposite sign to the corresponding F_{ki} (making the first order energy contribution negative) and sufficiently small in magnitude so as to make the higher terms smaller in magnitude than those of the first order, an iterated wave function of lower energy than the unperturbed function is generated and convergence guaranteed. This does not, however, guarantee convergence to the lowest energy, stationary point on the potential energy surface.

Equivalent results may be obtained by diagonalising the Fock matrix constructed in the basis of the trial MO:

$$\underline{F}^{\phi} = (C_1 \vdots C_2)^{+}\, \underline{F}^{\eta}\, (C_1 \vdots C_2)$$

$$= \left[\begin{array}{c:c} C_1^{+} F^{\eta} C_1 & C_1^{+} F^{\eta} C_2 \\ \hdashline C_2^{+} F^{\eta} C_1 & C_2^{+} F^{\eta} C_2 \end{array}\right] \qquad (1.131)$$

where $\underline{C}_1^{+}\, \underline{F}^{\eta}\, \underline{C}_1$ and $\underline{C}_2^{+}\, \underline{F}^{\eta}\, \underline{C}_2$ correspond to the Fock matrices in the bases of the DOMOS and VMOS respectively and the off diagonal partitions represent the Fock matrices connecting DOMOS with VMOS.

The closed shell SCF program constructs a modified Fock matrix in which the elements of the off-diagonal DOMO-VMO blocks are multiplied by a "damp-factor" (λ) whilst a "level-shifter" (α)$\underline{I}_2$ is added to the diagonal elements of the Fock matrix in the basis of the VMOS where $\underline{I}_2$ is the identity matrix of (m-n) order.

$$\underline{F}^{\phi MOD} = \left[\begin{array}{c:c} C_1^{+} F^{\eta} C_1 & \lambda C_1^{+} F^{\eta} C_2 \\ \hdashline \lambda C_2^{+} F^{\eta} C_1 & C_2^{+} F^{\eta} C_2 + \alpha I_2 \end{array}\right] \qquad (1.132)$$

The modified Fock matrix is diagonalised, and the eigenvectors ordered according to the 'aufbau' principle based upon the resulting eigenvalues.

The diagonalisation of $F^{\phi MOD}$ may be analysed by first order perturbation theory, and assuming that the canonicalisation of the trial MO is such as to give the diagonal blocks in diagonal form, then:

$$\Delta_{ki} = \frac{\lambda F^{\phi}_{ki}}{(F^{\phi}_{ii} - F^{\phi}_{kk} - \alpha)} \qquad (1.133)$$

If it is assumed that the damp-factor (λ) takes its normal value of unity and the level-shifter (α) is positive and sufficiently large in magnitude then:

(i) the first order analysis will be valid;

(ii) the trial MO can be forced to obey the 'aufbau' principle with respect to the level-shifted Fock operator, so that swapping of MO between the virtual and occupied shells will not occur;

(iii) the Δ_{ki} can be chosen to be of opposite sign to the F_{ki}^{ϕ} and arbitrarily small in magnitude so that the first order energy variation is negative and larger in magnitude than the higher order terms.

Hence, a sufficiently level-shifted procedure will always give convergence to a stationary point on the energy surface.

As previously noted, since the MO ordering procedure is dependent upon the eigenvalues of the level-shifted Fock operator, convergence to excited states not necessarily obeying the 'aufbau' principle, and often characterised by an unreasonably low first ionisation potential when applying Koopmans' Theorem, is possible when the non-level shifted Fock operator is applied. A feature of ATMOL 3 which has proven particularly useful in such cases is the AUTO directive which allows molecular orbital switching to occur at user defined intervals in the calculation.

Conversely, it is not advisable to use excessively large values for the level shifter since, although guaranteeing convergence, the rate of its achievement becomes unduly slow. Ideally large values (~4 to 5 hartrees) are used in the first few iterations thus stabilising the calculation, and then typical values are ~0.3 to 1 hartree.

Convergence is recognised at the end of a given iteration if each component of the vectors corresponding to the occupied orbitals, differs from that used in building the Fock matrix by a value less than the set threshold. Careful consideration must be given to this threshold value, since if this is set too large then the results will be unnecessarily inaccurate; in the alternative case a perfectly adequate calculation may be rejected as divergent.

In general, due to the more rapid convergence of the total energy value, this is established, using (1.74), before the program considers the limits of variation in the values of the vectors. Confirmation that convergence has been achieved may also be found in the form of the Fock matrix, in that off-diagonal elements will have the form $F_{ki}^{\phi} = 0$ at convergence.

1.8.3 Computational Aspects of the Open-Shell SCF Procedure

For the open-shell case, the procedure is by and large equivalent to that for the closed shell. Again the calculation is an iterative one incorporating the three stages referred to in the previous section, but differs in that two Fock matrices are constructed, representing the closed and open shells respectively in the Restricted Hartree-Fock Theory (Section 1.4.1), and allowing for the different spin factors in the Unrestricted Hartree-Fock Theory (Section 1.4.2). Since all of the open-shell calculations reported in this thesis have been carried out within the RHF formalism it is the computational aspects of the ATMOL 3 programs relating to this theory which will be discussed.

Two Fock matrices arise as a consequence of the two density matrices $\underline{R}_1$ and $\underline{R}_2$ (1.76). from both closed and open shells respectively, combining with the repulsion integrals to form two $\underline{G}$ matrices (1.79). Computationally, these are easily formed by minor changes to the closed shell routine previously referenced. Following the arguments in Section 1.4.1, the two Fock matrices may be combined to give a single matrix of the form (1.93) which is then diagonalised. As a logical extension to the closed-shell case, a "level-shifting" technique has also been developed for the open-shell system[69], thereby permitting guaranteed convergence as in the previous section. The general method used is similar to that already discussed but is necessarily more complicated due to the inclusion of terms relating to the singly occupied molecular orbitals (SOMOS).

In the energy minimisation procedure, the blocking in the matrix, equivalent to (1.131), is now nine-fold, and with the inclusion of the 'damp-factors' and 'level-shifters', again introduced by the program, appears as follows:

$$F^{\phi MOD} = \left[\begin{array}{c|c|c} C_1^{+} F^{\eta} C_1 & \lambda_{12} C_1^{+} F^{\eta} C_2 & \lambda_{13} C_1^{+} F^{\eta} C_3 \\ \hline \lambda_{12} C_2^{+} F^{\eta} C_1 & C_2^{+} F^{\eta} C_2 + \alpha I & \lambda_{23} C_2^{+} F^{\eta} C_3 \\ \hline \lambda_{13} C_3^{+} F^{\eta} C_1 & \lambda_{23} C_3^{+} F^{\eta} C_2 & C_3^{+} F^{\eta} C_3 + (\alpha+\beta) I \end{array}\right] \qquad (1.134)$$

Where indices 1, 2 and 3 are related to the DOMOS, SOMOS and VMOS respectively and the λ values are the 'damp factors' whilst α and β represent the 'level shifters', then the elements of (1.134) are clearly defined as in (1.131). Proceeding as before, with the introduction of first order perturbation

theory, the following results are obtained.

$$(\Delta_1)_{ki} = \frac{\lambda 13\ F_{ki}^{\phi}}{F_{ii}^{\phi} - F_{kk}^{\phi} - \alpha - \beta}$$

$$(\Delta_2)_{kj} = \frac{\lambda 23\ F_{kj}^{\phi}}{F_{jj}^{\phi} - F_{kk}^{\phi} - \beta} \qquad (1.135)$$

$$(\Delta_3)_{ji} = \frac{\lambda 12\ F_{ji}^{\phi}}{F_{ii}^{\phi} - F_{jj}^{\phi} - \alpha}$$

where the indices i, j and k correspond to DOMOS, SOMOS and VMOS respectively.

Following the previous arguments, if the 'damp factors' are allocated their normal value of unity, then providing that the values of α and β are sufficiently large in magnitude and positive, convergence to a stationary point on the energy surface is guaranteed. The convergence of the calculation is again determined by examination of the total energy (1.78) at the end of each iterative cycle before consideration is given to the variation in the eigenvectors with respect to a threshold limit. These eigenvectors may be ordered according to the 'aufbau' principle, or by the use of the LOCK directive which causes iterated molecular orbitals to be selected on the principle of maximum overlap with the trial MO.

In the case of excited states with parallel spins, this directive is particularly useful combined with the lesser generalised energy equation, where a=1, b=2 and f=$\frac{1}{2}$ in (1.77), (1.78) and (1.79), in what is termed the RHF module. The totally general case which is applicable to both the above, and excited singlets is called the GRHF module and does not need such a facility.

Whilst the former is useful in such cases as core hole state species as encountered in the calculation of core binding energies, the latter is necessary in establishing the energies of Auger transitions, due to the two electron nature of the process, as will become evident in the following chapter.

CHAPTER TWO

ELECTRON SPECTROSCOPY FOR CHEMICAL APPLICATIONS (E.S.C.A.)

2.1 Introduction

In this chapter, the fundamental processes involved in E.S.C.A. (XPS) will be outlined, followed by a description of the instrumentation used, and the main features of the spectra obtained. The technique is primarily concerned with the study of core electrons (unlike UPS which is strictly a valence electron technique), however the manner in which this reflects the environment of the valence electrons is also included. In particular such valence processes as shake-up and shake-off are considered and the relationship of E.S.C.A. to Auger and X-ray fluorescence spectroscopy is noted. Also discussed are the various schemes for calculation of core electron binding energies (BE) and relaxation energies (RE), with emphasis given to *ab initio* quantum mechanical methods.

In addition to the works of Siegbahn *et al*,[70,71] several texts and reviews are available regarding both the technique[72-77] and theoretical aspects[78-82] of E.S.C.A.

2.2 X-Ray Photoemission Processes

Following the initial work by Einstein[83] and independent investigations of the photoelectric effect by Robinson[84-86] and De Broglie[87] in the early 20th century, it was not until the early 1950's that Siegbahn and co-workers constructed an iron-free high resolution electron spectrometer and the term E.S.C.A. (Electron Spectroscopy for Chemical Applications) was applied.

The early development of electron spectroscopy (i.e. pre-Siegbahn) has been documented by Jenkin, Leckey and Liesengang.[88]

2.2.1 Photoemission

The sample to be investigated is irradiated using a monoenergetic beam of soft X-rays, typically $Ti_{k\alpha}$, $Al_{k\alpha_{1,2}}$ or $Mg_{k\alpha_{1,2}}$ with photon energies of 4510 eV, 1486.6 eV and 1253.7 eV respectively. Photoemission of electrons with BE lower than these thresholds is clearly possible, and the process is complete in 10^{-17} seconds. The total kinetic energy (KE) of such an electron is given by:

$$KE = h\nu - BE - E_r \qquad (2.1)$$

where $h\nu$ is the energy of the incident photon;

h is Planck's constant;

ν is the frequency of the X-rays;

BE is the binding energy of the photoejected electron, defined as the energy required to remove an electron to infinity with zero KE;

and E_r is the recoil energy of the atom or molecule.

Since in this work, comparison is made with experimental data for samples irradiated using soft X-rays, it is generally accepted[70] that the recoil energy is negligible and that the gas phase equation (2.1) is reduced to:

$$KE = h\nu - BE \qquad (2.2)$$

However, recent studies by Cederbaum and Domcke[89] have shown that with high energy photon sources the vibrational band envelopes in the E.S.C.A. spectra of molecules are modified

due to recoil-induced excitations. It is not inconceivable that as increased technology yields spectra of higher resolution then this will be more readily observed.

2.2.2 Relaxation Phenomena

In any atom or molecule, the major contribution to the total energy is due to the core electrons and as previously noted, although these do not explicitly take part in bonding, they do monitor valence-electron distributions. Therefore, upon core ionisation, due to an effective increase in nuclear potential, a substantial electronic reorganisation occurs, termed "relaxation".

Theoretical and experimental studies have shown that the relaxation process is a sensitive function of the electronic structure of the molecule[90-93] and that within a series of related molecules, the differences in relaxation energy (RE) are small but significant in that they are responsible for shifts in BE of the core electrons. Of particular importance to this section are recent studies showing that within the limitations of the RHF ΔSCF formalism, relaxation energies may be partitioned amongst the various occupied orbitals,[94-98] and this will be elaborated in a later section.

2.2.3 Shake-Up and Shake-Off Phenomena

There is a finite probability that simultaneous electronic excitations may accompany core-ionisation as a manifestation of electronic relaxation. Where excitation is from a valence occupied orbital to a virtual orbital, the process is termed shake-up, as illustrated in Figure (2.1) and in the case of simultaneous emission of the valence electron,

shake-off. These processes are often clearly discernible as satellite peaks to the low kinetic-energy side of the main photoionisation peak.

Figure 2.1 A schematic representation of the basic processes in E.S.C.A.

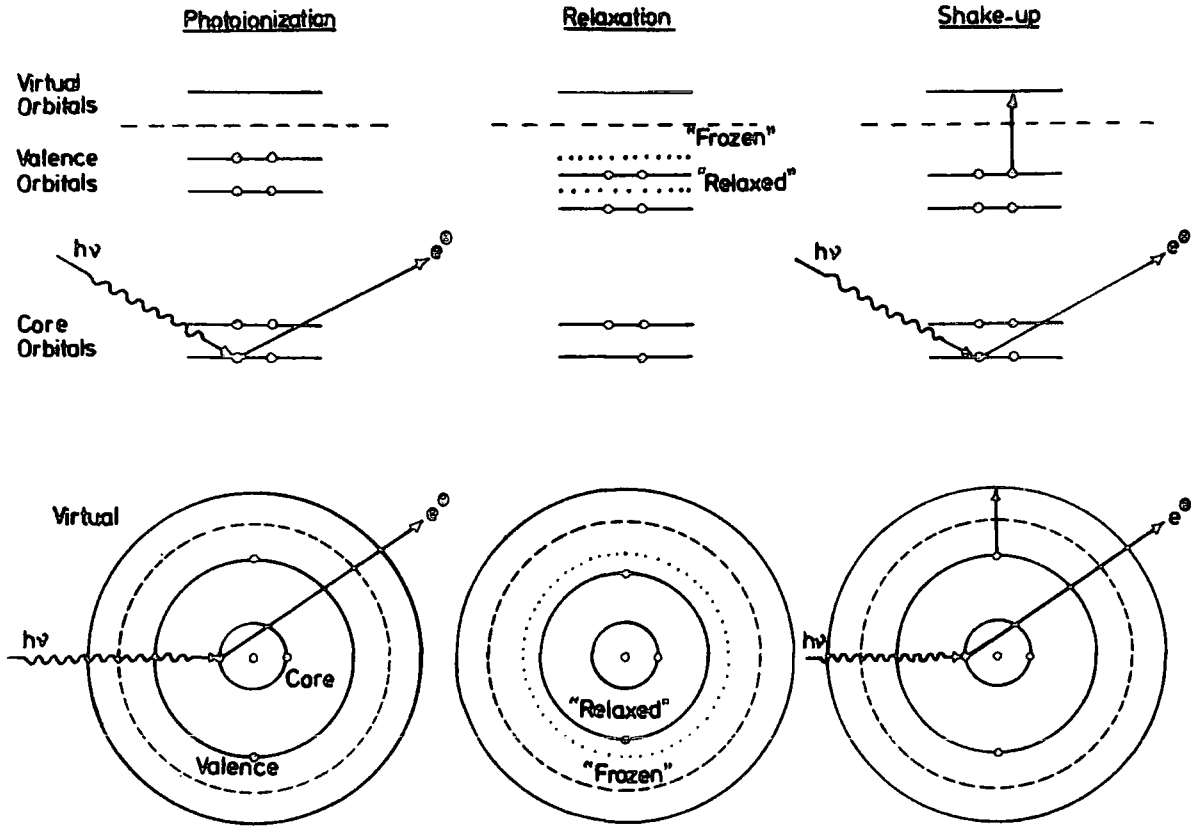

The transition intensity of a shake-up process may be treated within the sudden approximation,[99] as being directly related to the sum of the overlap terms involving the occupied orbitals of the ground state system and virtual orbitals of the hole state species under consideration. In the approximation, it is assumed that due to the rapid time-scale of the ionisation process, upon removal of an electron at t=0, the change in Hamiltonian as a function of time will be almost

discontinuous. However, the wave function must be a continuous function of time at t=0, and therefore

$$\psi_o\ (x_1 \ldots x_i \ldots x_N) = \sum_n\ a_n(x_i)\phi_n(x_1 \ldots x_{i-1},\ x_{i+1}, \ldots x_n) \qquad (2.3)$$

for all values x_i.

Where the initial wavefunction ψ_i for the neutral system is given by:

$$\psi_i \ = \ \sum_{\mu=1}^{n}\ C_{\mu i}\ \ \phi_\mu \qquad (2.4a)$$

and for the ion, the final state wavefunction ψ_f by:

$$\psi_f \ = \ \sum_{\nu=1}^{n}\ K_{\nu f}\ \ \phi'_\nu \qquad (2.4b)$$

then the probability of such a transition is given by:[100]

$$P_{f \leftarrow i} \ = \ N \mid \sum_{\mu=1}^{n} K_{\mu f}\ \ C_{\mu i}\ \ \phi'_\mu \mid \phi_\mu > \mid^2 \qquad (2.5)$$

n is the total number of basis functions and N the number of electrons involved in the process.

Since this probability involves the overlap of the two orbitals the selection rules governing the shake-up excitation are of monopole type, i.e.

$$\Delta J = \Delta L = \Delta S = \Delta M_J = \Delta M_L = \Delta M_S = 0 \qquad (2.6)$$

Clearly, from this result, since such an excitation may be thought of as arising from the doublet core ionised state, then there are only two possibilities (within a simple orbital model) which may constitute allowed transitions. Either the unpaired electrons in both valence and virtual orbitals are of opposite spins ("singlet origin") or both

have parallel spins whilst the remaining core electron is of opposite spin ("triplet origin") as shown in Figure (2.2).

Figure 2.2 A schematic representation of singlet/triplet shake-up

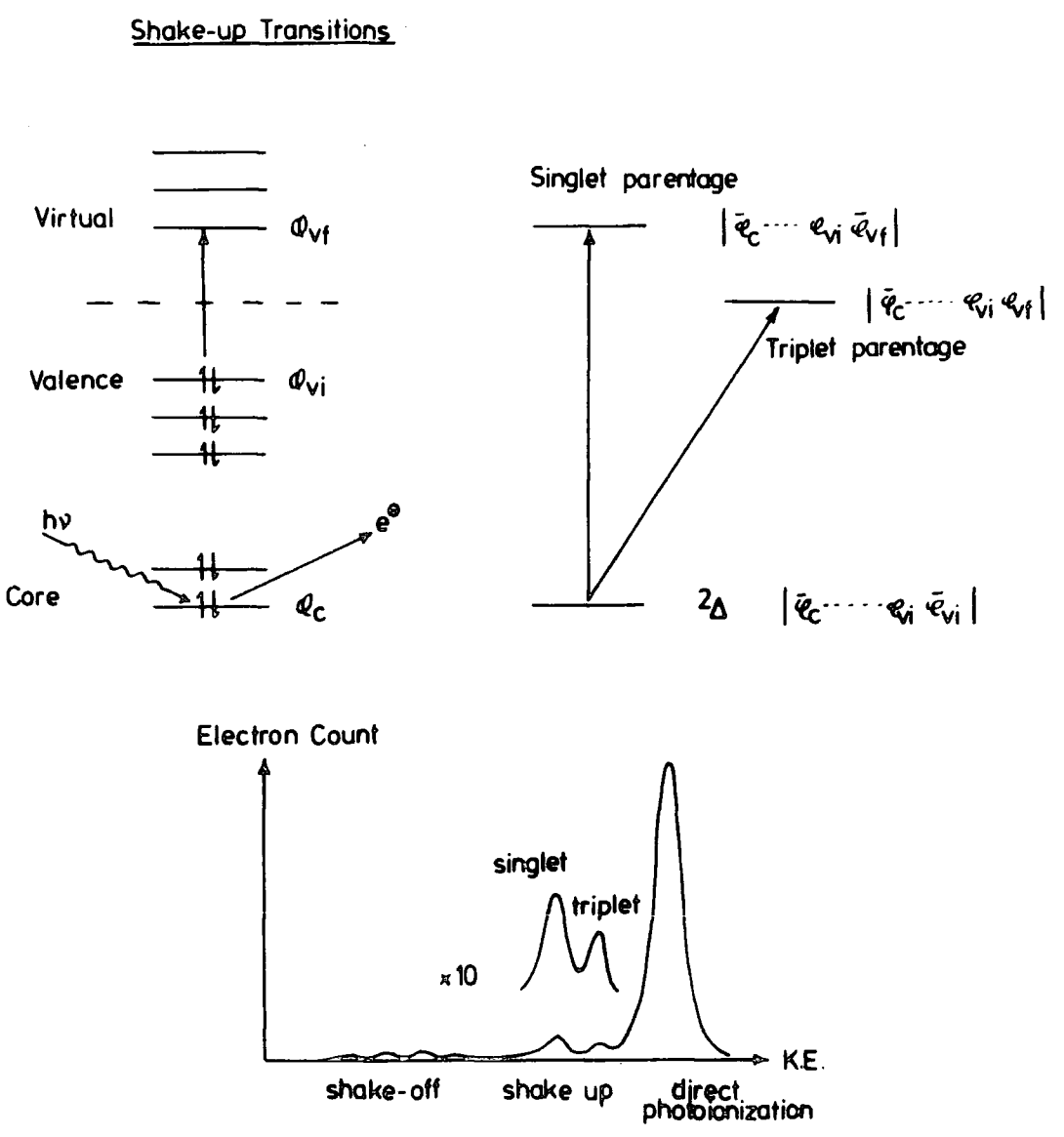

Whilst that of "triplet origin" is the lower energy state, the state of "singlet origin" would naively be expected to be the more intense, and in principle it should be possible to observe the energy separations and intensities of these components. This simplified approach to the theoretical treatment of shake-up states provides a starting point for the discussions in later chapters; a more detailed discussion is given by Martin and Shirley.[101]

Manne and Åberg[102] have studied the relationship between relaxation, shake-up and shake-off and have shown how the weighted average over the direct photoionisation shake-up and shake-off peaks correspond to the B.E. appropriate to the unrelaxed system (given by Koopmans' Theorem). Since R.E. fall within a narrow range for a given core level (e.g. for C_{1s}, a typical BE for a neutral system is ~ 290 eV whilst RE might typically fall in the range 12 $\pm$ 2 eV), it is clear that shake-up and shake-off processes are present in every system; only the transition intensities vary from system to system. Transitions of highest probability should be evident close to the weighted mean since the intensity of the high energy shake-off processes ought to be small.

In principle, therefore, the R.E. should be available from experiment, as illustrated in Figure (2.3), providing that all of the relevant shake-up and shake-off processes may be estimated in terms of energy shifts and intensities.

Figure 2.3 An illustration of the relationship between RE, the direct photoionisation peak, and shake-up and shake-off processes

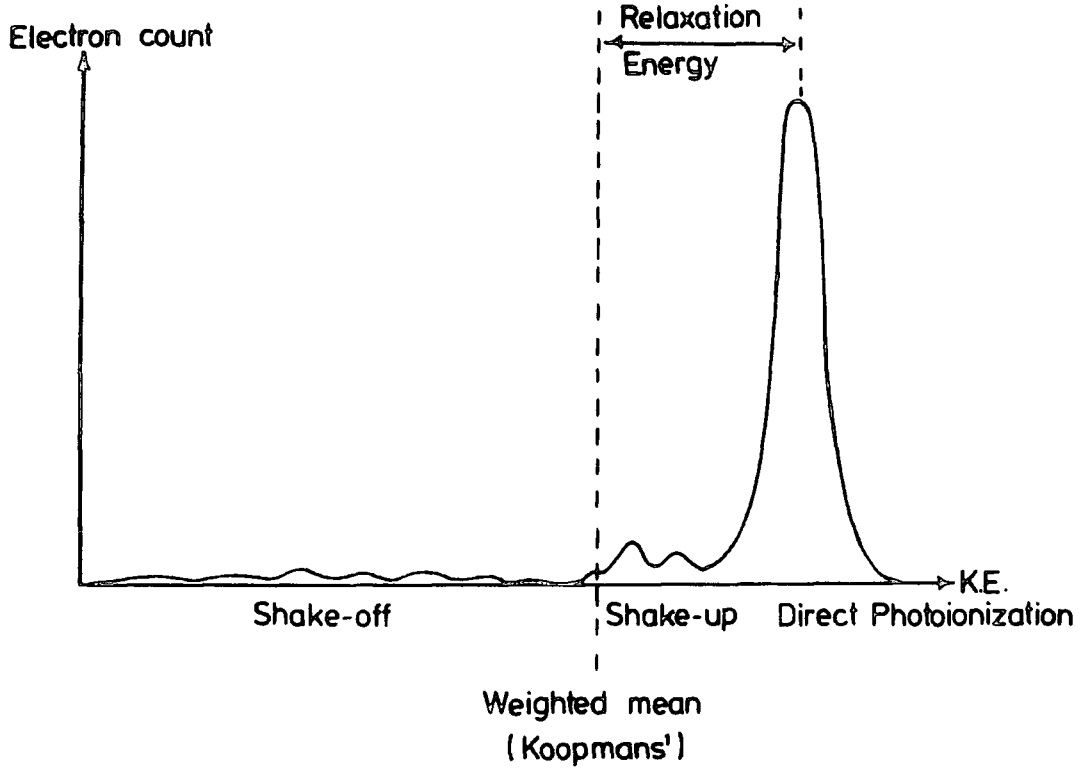

In practice however this is complicated by the presence of the general inelastic tail,[103,104] arising from photoionisation of a given core level, followed by energy loss due to a variety of scattering processes, which give rise to a broad energy distribution, generally obscuring any underlying shake-off features in the case of condensed phase studies.

2.2.4 De-Excitation Processes

Decay of a highly excited core-ionised state occurs by one of two mechanisms:[71] X-ray fluorescence, or the emission of a secondary electron in the radiationless Auger process. In both cases, the core vacancy is filled by the transition of an electron from another subshell of lower binding energy as illustrated in Figure (2.4).

Figure 2.4 A schematic illustration of de-excitation by Auger and X-ray Fluorescence

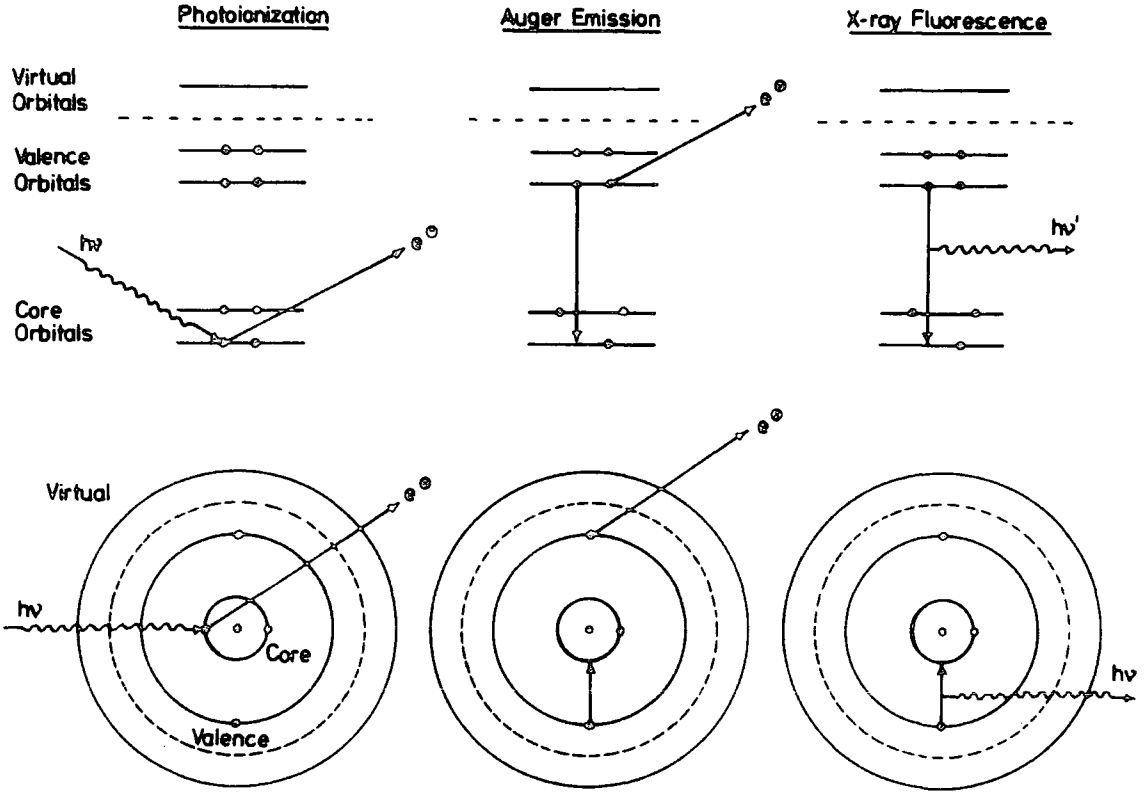

Both X-ray fluorescence and the Auger effect form the basis for important spectroscopic methods complementary to E.S.C.A. in many of its applications: these are X-ray emission spectroscopy (XES) and Auger electron spectroscopy (AES) respectively. In XES the spectrum of emitted X-rays is measured and this has proven an excellent means of qualitative analysis: concentrations of 0.1% for most elements and 0.01% for elements such as Fe, Co and Ni have been detected.[105] In AES the kinetic energy distribution of the Auger electron is measured and in practice it has been shown that whilst both the Auger mechanism and X-ray emission contribute to the decay of core-hole states, their relative probabilities are highly dependent upon the atomic number of the element concerned (Figure (2.5))[71].

Figure 2.5 Probability of Auger Electron Emission and X-ray Fluorescence as a function of Atomic Number

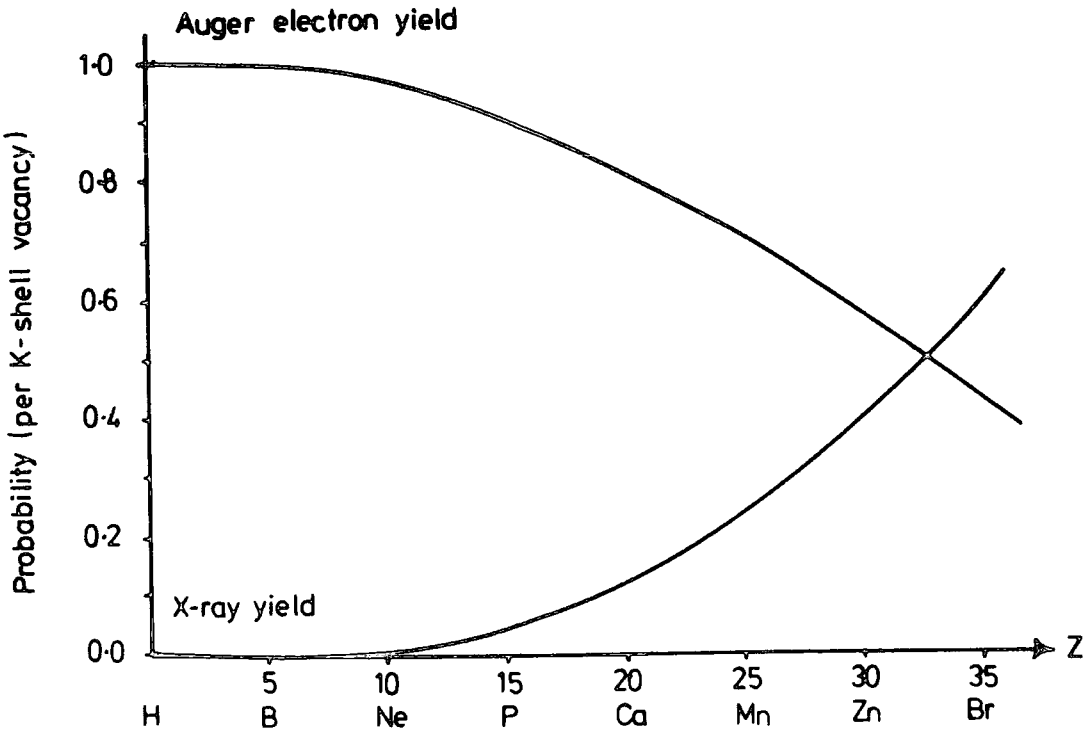

Clearly, Auger emission predominates for the lighter elements, especially those encountered in organic systems, where X-ray emission is negligible.

Auger spectra, like X-ray emission spectra are normally excited by electron bombardment, but Auger electrons can alternatively be studied in conjunction with E.S.C.A., since the electron spectra excited by X-rays contain Auger structure in addition to core photo electron signals.[106] Although AES has been widely used as a tool for elemental analysis of the surfaces of solids, only recently has it become apparent that the Auger lineshapes are sensitive to chemical environment.[107-109]

Concern in this thesis is with the case where the original core hole is in a carbon K shell and the decay involves two valence electrons, a process denoted as C(KVV). Theoretical analysis of the Auger process has been dealt with elsewhere[110] and will only briefly be discussed in this section. The Auger electron energy, neglecting vibrational effects, is written as the difference between the initial state total energy, given by the expression

$$E_i = E_o + I_c \qquad (2.7)$$

where E_o is the total energy of the neutral molecule and I_c is the ionisation potential (IP) of the core level, and the final state energy for holes in the j and k molecular orbitals (MO) with spin s:

$$E_f\ (j,k,s) = E_o + I_j + I_k - V_{jk}^{s} + S_{jk} \qquad (2.8)$$

where V_{jk}^{s} is the spin dependent hole-hole interaction term[111] and S_{jk} is the static relaxation term.[112] The Auger transition probabilities may be calculated according to the method

described by Jennison,[110] whereby separate RHF-SCF calculations are performed upon the initial state and the ground state of the neutral molecule, and the initial state valence orbitals are used to formulate Auger matrix elements, $M_{j'k'}$ which may be transferred into the true matrix elements M_{jk} using projection coefficients:

$$M_{jk} = \sum_{p'q'}^{\text{occupied orbitals}} C_{nkp'q'} M_{p'q'} \qquad (2.9)$$

The sum is restricted to occupied, initial-state, valence orbitals and the coefficient C is the overlap matrix between the pseudo final state (written in terms of relaxed initial state valence orbitals) and the "true" final state.

2.3 Instrumentation

Since the appearance of the first commercial E.S.C.A. instrument in 1969, several designs have been marketed commercially. Although the work in this thesis was carried out on an AEI ES200 AA/B spectrometer, an ES300 has recently been acquired, and attention will be drawn to the design features of this instrument. A schematic of the essential components of a typical E.S.C.A. spectrometer is given in Figure (2.6).

The description of the apparatus may be considered under four headings:

Figure 2.6 A schematic of E.S.C.A. instrumentation

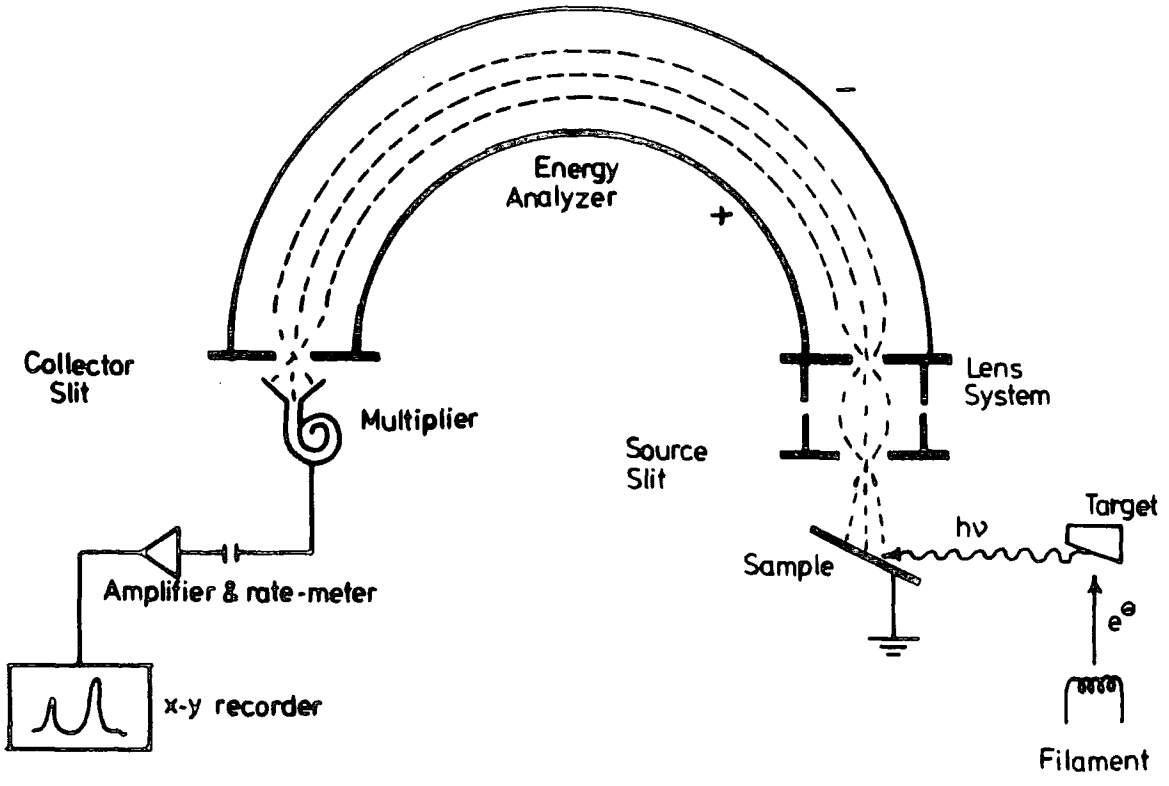

(i) X-ray Generator

(ii) Sample Chamber

(iii) Analyser

(iv) Electron Detection and Data Acquisition

2.3.1 X-ray Generator

The generator for the ES200 AA/B spectrometer consists of a Marconi Elliot GX5 high voltage generator whilst that for the ES300 is a solid state generator of Kratos design. The X-ray photon sources are of the hidden filament or Henke[113] design, (reducing the risk of contamination of the target by

evaporated tungsten), and in the former spectrometer consist of a non-monochromatised $Mg_{k\alpha_{1,2}}$ (typical operating conditions: $<10^{-7}$ torr- 12kV; 15mA) and a monochromatised $Al_{k\alpha_{1,2}}$ source, ($<10^{-7}$ torr; 15kV; 35mA). While retaining a monochromatised $Al_{k\alpha_{1,2}}$ source, a special feature of the ES300 is a dual anode ($Mg_{k\alpha_{1,2}}$ and $Ti_{k\alpha}$) source in which two filaments are fitted and the two different anode materials may be switch selected by the appropriate choice of filaments without the need to break vacuum. The X-ray flux is of the order of 0.1 millirad $sec.^{-1}$ which for the majority of samples causes little or no radiation damage.[114]

In both systemsthe non-monochromatised sources are isolated from the sample chamber by a thin (~0.003") Al window which ensures that electrons scattered from the target or filament do not enter the sample region. In order to reduce the risk of scattered electrons exciting X-radiation from the Al window, the filament is operated at near ground potential (+10 V) and the anode at high positive voltage.

In the case of the Al source, monochromatisation improves the resolution by reducing the linewidth and elminating unwanted background, and X-ray satellites. The wavelength λ of $Al_{k\alpha}$ radiation is 8.34Å, and by diffraction from the $(10\bar{1}0)$ planes of quartz at an incident angle θ of 78.5°, the required conditions for the Bragg relation are satisfied.[71] Thus,

$$n\lambda = 2d \sin \theta \qquad (2.10)$$

where n is an integer giving the order of diffraction (n=1 in this case) and d is the lattice spacing (2d = 8.5Å for quartz).

After separating the $Al_{k\alpha}$ radiation from the background, the linewidth may be reduced by one of three techniques:

(i) "slit-filtering"[91] (using a slit mechanism);

(ii) "dispersion compensation" (passing photoelectrons through a lens to allow for the peak-shape of the k_{α} radiation);

(iii) "fine-focussing"[115] (employing an electron-gun and a rotating anode).

In principle, an ultimate linewidth of 0.2eV can be attained by these techniques[116] and that adopted by the instruments referred to in this chapter is method (i).

2.3.2 Sample Chamber

The sample chambers of both E.S.C.A. instruments are equipped with several access ports for sample introduction and treatment facilities. The preferred method of introduction is via an insertion lock system and high vacuum gate or ball valves, which allows samples to be studied on the tip of a probe whilst maintaining a base-pressure of $\sim 10^{-8}$ torr in the system. Also, by probe rotation, the optimum signal intensity may be obtained, or angular dependent studies performed.

Solid samples are mounted on the probe-tip by means of double-sided 'Scotch' insulating tape or film solvent cast onto a gold substrate. Liquid or volatile samples may be studied in the condensed phase by cooling of the probe tip using liquid nitrogen or alternatively may be directly sublimed onto a cryogenic tip within the spectrometer source. A method for gas phase studies is included in a subsequent chapter.

2.3.3 Analyser

The function of an electron energy analyser is to measure the energy distribution of electrons emitted from a sample. For E.S.C.A. studies the analyser should have a resolution of 1 in 10^4, and that used on both the ES200 and ES300 is a hemispherical, double-focussing analyser based on the principle described by Purcell.[117] The inherent resolution of the analyser is given by:

$$\frac{\Delta E}{E} = \frac{R}{W} \qquad (2.11)$$

where E is the energy of the electrons;

R is the mean radius of the hemispheres;

and W is the combined widths of the entrance and exit slits.

Clearly, the resolution may be improved in three distinct ways:

(i) reducing the slit widths, which reduces the signal intensity;

(ii) increasing the radius of the hemispheres, which increases engineering costs and pumping requirements;

(iii) retarding the electrons before they enter the analyser.

With reasonable compromise made on the slit widths to obtain sufficient signal intensity, and on the size of the hemispheres to prevent manufacturing problems, the Kratos E.S. series retard the electrons by means of a lens assembly before entry to the analyser. Helmer and Weichert[189] first pointed out that, for the general class of dispersive analysers used in E.S.C.A., it is possible to retard before analysis, and, for a given absolute resolution ΔE, to gain in overall efficiency in a system with single-channel detection. Since the transmitted electron current (I) of an E.S.C.A. spectrometer is

given by:

$$I = BA\Omega \qquad (2.12)$$

where B is the brightness of the electron illumination of the entrance slit, determined by the strength of X-radiation at the sample;

and $A\Omega$ is the luminosity of the spectrometer (A is the area of the entrance slit and Ω the solid angle aperture as viewed from the entrance slit);

it is clear that, depending upon the nature of $A\Omega$, the brightness and hence the transmitted electron current will be reduced in a retarding field. However, since the luminosity is proportional to the square of the fractional resolution ($\Delta E/E_S$) then retarding the electrons will increase I by a factor equal to the square of the previous reduction. If electrons, leaving the sample, with kinetic energy E_S are retarded to an energy E_0 for transmission through the analyser, then the resolving power of the complete system, $\Delta E/E_S$, will be improved by a factor equal to the retarding ratio E_S/E_0. Electrons of the required K.E. may be focussed at the detector slit by either of two methods:

(i) the analyser voltages can be held constant to give a fixed analyser transmission energy (FAT) (usually 65eV for the ES200)[118] while the lens potentials are varied to maintain constant focal position and constant magnification although the energy of electrons selected from the sample is changing;

or (ii) the analyser operates at constant resolution ($\Delta E/E$) so that peak widths vary across a spectrum.

A fixed retardation ratio (FRR) (usually 1/23rd of the KE at the source for the ES200)[118] is used and a spectrum is obtained by scanning the retarding potential and the potential between the hemispheres given by:

$$V_{out} = E_o \left[3 - 2 \left(R_o / R_{out} \right) \right]$$

$$V_{in} = E_o \left[3 - 2 \left(R_o / R_{in} \right) \right]$$

where the mean radius $R_o = \frac{(R_{in} + R_{out})}{2}$

and R_{in} and R_{out} are the radii of the inner and outer hemispheres respectively.

For a given flux and analyser slit size, the variation of sensitivity with electron kinetic energy from the sample depends upon the mode of analyser scanning selected: FRR or FAT. The overall sensitivity variation of a spectrometer with energy (the transmission function) is obtained by combination of the sensitivities of its components; the analyser and the retarding optics. Since the sensitivity of the analyser is directly proportional to E_o and in FRR mode the lens voltage ratio E_s/E_o is fixed then the lens sensitivity is fixed and the overall transmission function is as that of the analyser indicating that in FRR mode sensitivity increases with electron KE.

In the FAT mode, E_o is fixed and the overall transmission function is now that of the retarding optics. The entrance half angles into the analyser α_o, β_o are fixed at some selected values by an angle defining slit. Electrons of varying energy E_s are selected and focussed into the analyser: variation in

the voltage ratio E_s/E_o will cause variation in the acceptance angle at the lens input which may be described by the Abbe-Helmholtz sine law.

For unit magnification and small angles

$$\alpha_s E_s^{\frac{1}{2}} = \alpha_o E_o^{\frac{1}{2}} \text{ (in the dispersion plane)}$$
$$\text{and } \beta_s E_s^{\frac{1}{2}} = \beta_o E_o^{\frac{1}{2}} \text{ (in the perpendicular plane)} \qquad (2.13)$$

Combining the equation gives:

$$\alpha_s \beta_s = \alpha_o \beta_o \, (E_o/E_s) \qquad (2.14)$$

Clearly, as lower KE are scanned, the acceptance solid angle at the sample, $\alpha_s \beta_s$, increases thus increasing the sensitivity I. However, the recent study by Cross and Castle[118] pertaining specifically to the investigation of the transmission function in FAT mode for the ES200 spectrometer concluded that this is almost independent of KE contrary to Kratos recommendations.[119]

The overall resolution, $\Delta E_{M/E}$, of the system also depends upon contributions from sources other than the analyser:

(i) The width of the X-ray line inducing the emission, ΔE_X;

(ii) The natural width of the electron energy distribution in the level being studied, ΔE_{CL};

(iii) The line-broadening due to spectrometer irregularities which can vary with electron emission energy E, and slit widths, ΔE_S.

Thus:

$$(\Delta E_M)^2 = (\Delta E_X)^2 + (\Delta E_{CL})^2 + (\Delta E_S)^2 \qquad (2.15)$$

If solid samples are studied, this is further modified by addition of a factor $(\Delta E_{ss})^2$ which allows for line broadening due to solid state effects. ΔE_s can be varied on both the ES200 and ES300 by means of adjustable entrance and collector slits on the analyser.

2.3.4 Electron Detection and Data Acquisition

The electrons focussed by the analyser are detected by an electron multiplier and the pulses obtained are amplified and fed into the counting electronics. The signals fed into the counting system generate the E.S.C.A. spectra in two ways:

(i) The continuous scan, where the electrostatic field is increased from the present starting KE continuously, while the signals from the multiplier are monitored by a rate meter. When the signal to background ratio is sufficiently high, a graph of the electron counts per second versus the KE of the electrons is plotted onto an X-Y recorder.

(ii) The step scan, in which the field is increased by pre-set increments (typically 0.1eV) and at each increment, (a) the counts may be measured for a fixed length of time, or (b) a fixed number of counts may be timed. The data obtained from the step scans is stored in a multichannel analyser (MCA), so that many scans can be accumulated to average random fluctuations in the background.

2.4 Energy Referencing

It is important to understand the relationship that exists between the experimentally observed BE for E.S.C.A. applied to solids, as opposed to free molecules and values calculated using the *ab initio* LCAO MO SCF technique. Whilst for gaseous samples, the reference level normally taken in E.S.C.A. is the vacuum level, for a conducting solid the most convenient reference is the Fermi level[70] (defined, strictly, at absolute zero, for a metal as the highest occupied level) since as there is electrical contact between the sample and spectrometer their Fermi levels are equivalent.

The work-function for a solid ϕ_s is defined to be the energy gap between the free electron (vacuum) level and the Fermi level in the solid. Although the Fermi levels of both the solid and the spectrometer are equivalent their vacuum levels may be different, and then the electron will experience either an accelerating or retarding potential equal to $\phi_s - \phi_{spec}$, where ϕ_{spec} is the work function of the spectrometer.[120,121] In E.S.C.A. it is the KE of the electron when it enters the analyser that is measured, and taking zero BE to be the Fermi level of the sample, the following equation results:

$$BE = h\nu - KE - \phi_{spec}. \qquad (2.16)$$

This is illustrated in Figure (2.7).

The BE referred to the Fermi level does not depend on the work function of the sample but only on that of the spectrometer ϕ_{spec}, and this represents a constant correction to all BE.

With non-conducting samples or samples not in electrical contact with the spectrometer, in order to correct for sample

Figure 2.7 An illustration of the BE reference level in solids

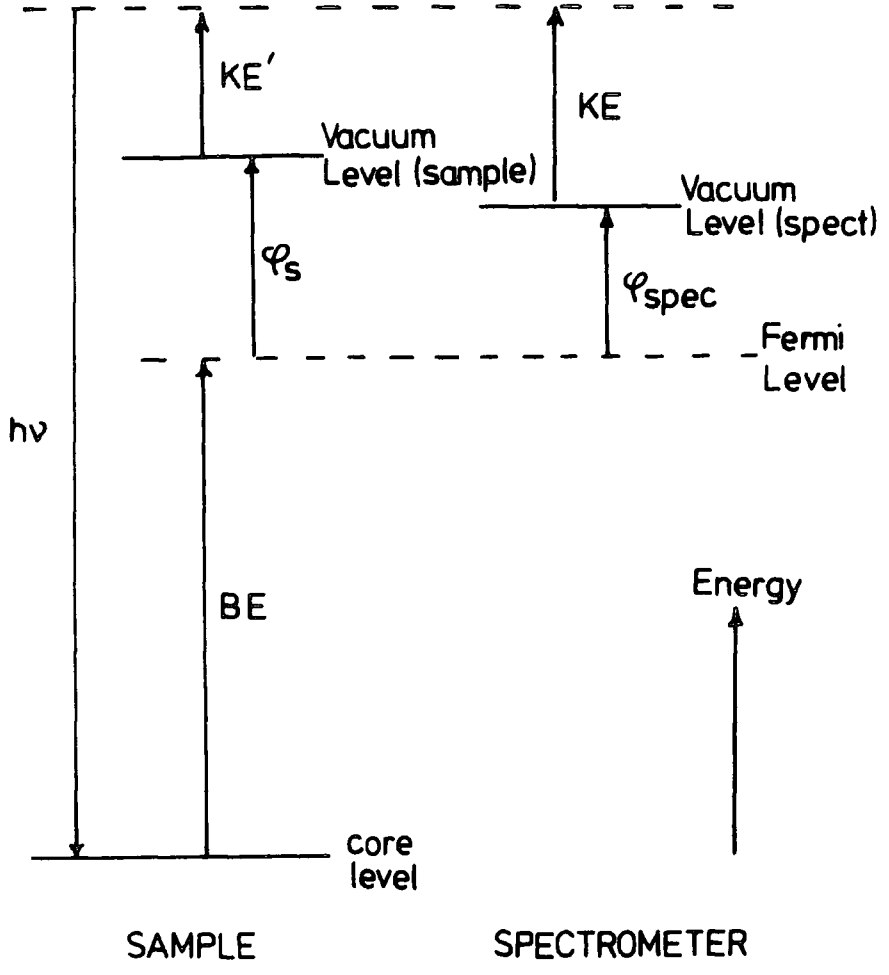

charging due to photoionisation from the surface regions some calibration procedure must be adopted.[122] For gaseous samples referencing (vacuum level) is most readily accomplished by simultaneous leakage into the gas cell of an appropriate standard for which absolute BE are accurately known (e.g. Ar).[122]

For samples deposited in thin film on a conducting substrate in the spectrometer source, since the mean free path of the incident X-ray beam is very large[70] it is possible, depending on conditions, for films of the order of 10^3 Å to have sufficient charge carriers to remain in electrical contact with the spectrometer. This is most readily shown by

applying a bias voltage to the sample probe and if this is the case then the apparent shift in energy scale will exactly follow the applied bias. By shifting the position of the true zero of the KE scale, it is possible to study the secondary electron distribution and this provides a direct energy reference.[123] If the sample has been deposited on a substrate such as gold it is possible to measure the core levels of the sample whilst monitoring the $Au4f_{7/2}$ core level (84.0eV) and this provides a convenient means of energy referencing.[124]

Where in such cases as thick insulating samples are studied and only a fortuitous possibility of electrical contact with the spectrometer exists, the most reliable method of energy referencing is to follow a controlled build up of hydrocarbon at the surface (BE C_{1s} 285eV).[122] This may be accomplished by using a cooled cap assembly on the X-ray source. Such material almost always goes down in uniform coverage and at sub monolayer coverage acquires the same surface potential as the sample. Work from this laboratory has shown how the build up of extraneous hydrocarbon material in the ES200 spectrometer may be selectively controlled.[125]

2.5 Features of Core Electron Spectra

2.5.1 Binding Energies and Chemical Shifts

The BE of core electrons, which can be thought of as being essentially localised, are sensitive to the electronic environment of the atom in question.[124] Thus for a given core level of an element, while the absolute BE for that level is characteristic of the element, differences

in electronic environment of a given atom in a molecule give rise to a small range of binding energies, "chemical shifts", often representative of a given structural feature. This is perhaps best illustrated in data pertaining to C_{1s} levels in carbon-oxygen containing systems.[126] An extensive theoretical study, over a range of functionalities in such systems, carried out by Clark and co-workers,[127] has suggested the additive nature of these shifts in BE as being a function of the number of bands to the oxygen substituents. Thus a shift of ∿1.5eV corresponds to carbon singly bonded to an oxygen, whilst a shift of ∿3eV can correspond to either a carbon singly bonded to two oxygens or doubly bonded to one oxygen. On this basis, carboxylic acids and esters, and carbonates would be expected to exhibit shifts of ∿4.5eV and 6eV respectively, in good agreement with experimentally determined values.[70,71,126,128,129]

This scheme has proven to be particularly useful in considering data related to polymer oxidation by 'oxygen plasmas'[130] since an extensive variety of oxygen-containing structural features are produced at the polymer surface. An example of this is its application to the C_{1s} E.S.C.A. spectrum of an oxidised polystyrene sample.[127] If an analogue, curve-fitting procedure is employed with gaussian curves positioned at ∿286.6, 287.9, 289.0 and 290.4eV, in addition to that at ∿285.0eV (referenced to the extraneous hydrocrabon, as mentioned in the previous section) and treating only the peak height as a variable, then a unique deconvolution can be achieved with a full width at half maximum (FWHM) of 1.7eV. In general, for a given core-level (with due allowance for any shake-up or shake-off processes), the peak intensities are proportional to the number of atoms in a particular environment.

2.5.2 Line Shape Analysis

The need for line shape analysis arises from the unfavourable ratio of chemical shift to line-widths which is one of the major weaknesses of E.S.C.A. compared to say n.m.r.[124] The dominant contribution to the line-widths with most commercial instrumentation is the inherent widths of the polychromatic X-ray photon source. However, great improvements can be made if monochromatisation procedures are employed. The effects contributing to the total line-width ΔE_M have been discussed in (2.15). Whilst the contributions to ΔE_M from ΔE_S (due to spectrometer aberrations) are considered to be Gaussian line-shapes, those from both ΔE_X and ΔE_{CL} are Lorentzian in nature and are related to the lifetime of the core hole state via the Uncertainty Principle:[131]

$$\Delta E . \quad \Delta t \simeq \frac{h}{2\pi} \qquad (2.17)$$

where Δt is the lifetime of the state.

A linewidth of ~1eV corresponds to a lifetime of approximately 6.6×10^{-16}s from (2.17).

The convolution of these line-shapes produces a hybrid with a Gaussian distribution dominating overall and Lorentzian character in the tails of the distribution. The use of pure Gaussian shapes therefore introduces only small errors into the lineshape analysis.[71] The deconvolution of a given envelope may be approached in the manner briefly mentioned in Section (2.5.1) using information obtained theoretically or experimentally from prototype systems, regarding both BE shifts and line-widths, or in a digital manner using a computer. Alternatively, derivative spectroscopy may be applied to the problem;[132-134] the 2nd and 4th order derivatives providing

information on the number of components making up a line-shape and an approximation to their KE.

The use of deconvolution has been discussed by Ebel and Gurker,[135] and criticisms of the technique by Wertheim.[136]

2.5.3 Multiplet Splitting

Multiplet splitting of core levels is the result of spin interaction between an unpaired electron, resulting from the photoionisation process and other unpaired electrons present in the system. The theoretical interpretation of multiplet effects is only straightforwardly understood for S-hole states and is based upon Van Vleck's vector coupling model.[137]

If S is the total spin of the 1^n configuration in the ground state, then the two possible final states have a total spin of $S \pm \frac{1}{2}$ and an energy difference, ΔE, proportional to the multiplicity of the ground state:

$$\Delta E = (2S + 1)K \qquad (2.18)$$

where K is the exchange integral between the core (C) and valence (V) electrons under consideration, defined by

$$K = \langle \phi_C(1)\ \phi_V(2)\ \left|\frac{1}{r_{12}}\right|\ \phi_C(2)\ \phi_V(1) \rangle \qquad (2.19)$$

The intensities of the peaks are proportional to the degeneracies of the final spin states, viz:

$$\begin{aligned}(2(S+\tfrac{1}{2}) + 1) : (2(S-\tfrac{1}{2}) + 1) &= 2S + 2 : 2S \\ &= S + 1 : S\end{aligned} \qquad (2.20)$$

Multiplet splitting in E.S.C.A. has been discussed in detail by Fadley.[138] The magnitude of the splitting for a given ion can give valuable information concerning the localisation or delocalisation of the unpaired, valence electrons

in compounds: the greater the spin-density on an atom, the greater the splitting.[139]

2.5.4 Spin-Orbit Splitting

If photoionisation occurs from an orbital with orbital quantum number (l) greater than zero then a doublet structure is observed in the resultant spectrum.[89] This arises from a coupling of the spin (S) and orbital angular momenta (L) of the electrons to yield a total momentum (J). When spin-orbit coupling is weak, the Russell-Saunders (RS)[140] scheme is followed (L+S=J). When the spin-orbit coupling energy is large, the orbital and spin momenta couple individually and the resultants then couple. This is termed the j-j coupling scheme.

The RS scheme is appropriate for lighter elements up to thelanthanides and the jj scheme for the heavier elements.[141] The intensities of the signals in the doublet structure are proportional to the ratio of the degeneracies of the states defined by the 2J+1 rule. The relative signal intensities are shown in Table (2.1).

Table 2.1 Intensity Ratios for Different Levels

	Orbital Quantum Number	Total Quantum Number	Intensity Ratio
	l	$J = (l \pm S)$	(2J+1) : (2J+1)
s	0	$\frac{1}{2}$	No splitting
p	1	$\frac{1}{2}$ 3/2	1 : 2
d	2	3/2 5/2	2 : 3
f	3	5/2 7/2	3 : 4

2.5.5 Electrostatic Splitting

This type of splitting has been interpreted as arising from the differential interaction of the external electrostatic field with the spin states of the core levels involved.[142,143] Correlations have been observed between this type of splitting and the quadrupole splittings obtained from Mossbauer spectroscopy[144] which arise from the interaction of the nuclear quadrupole moment with the inhomogeneous electric field. These splittings have been observed for a number of systems.[145,146]

2.5.6 Satellite Peaks

Peaks of this nature, arising to the low kinetic energy side of the direct photoionisation peak, as a result of shake-up and shake-off processes have been discussed in Section (2.2.3), and a detailed theoretical framework for calculating such satellite peaks has been given by Martin and Shirley.[147]

Other satellite peaks may be observed:

(i) "Configuration Interaction" peaks arise whenever there are final states with the same symmetry, and with energies close to but greater than, the single hole-state energy.[148] They may be considered as arising from doubly excited states of the hole-state, as opposed to shake-up and shake-off, which are singly excited states. Such peaks have been observed in alkali metal halides.[148,131]

(ii) In solids, discrete peaks can arise from surface and bulk loss and interband transitions.[70]

(iii) In gases, satellite peaks may be caused by energy loss of the photoelectron after emission, if it undergoes a secondary collison with an atom or molecule, leading to their excitation.[71]

(iv) In the case of metals, plasmon excitations may occur during the formation of a core hole. Tailing on the high binding energy side of many E.S.C.A. peaks is due to intrinsic processes (the parent excitation is accompanied by additional excitations which reduce the observed kinetic energy giving rise to electron energy-loss satellite peaks). Other photoelectrons suffer extrinsic losses (electrons from primary excitation lose energy in escaping to the solid's surface). Plasmon energy-loss peaks contain contributions from both intrinsic and extrinsic processes.[188]

(v) The X-ray source itself may be a cause of satellite features with higher KE than the direct photoionisation peak. These peaks are formed by the small percentage of $K\alpha_{3,4}$ and $K\alpha_{5,6}$ radiation[71] but may be eliminated by monochromatisation of the X-ray source.

2.6 Methods for the Calculation of Binding Energies and Relaxation Energies

2.6.1 Koopmans' Theorem

Upon diagonalisation of the Fock matrix (Section 1.3.1) the eigen values obtained (εp) are termed the orbital energies of the associated molecular orbitals, which are displayed as basis function contributions in eigenvector form.

Koopmans' Theorem[149] states that these orbital energies for a closed-shell system may be associated with the BE (or ionisation potentials) of the atom or molecule for which the SCF wavefunction has been obtained:

$$BE = -\varepsilon p \qquad (2.21)$$

From (1.48)

$$\varepsilon p = hpp^{\phi} + \sum_{q}^{n} (2J_{pq}^{\phi} - K_{pq}^{\phi}) \qquad (2.22)$$

If the total energy for a neutral molecule is evaluated using (1.48) and also that from a single determinant neglecting one of the above SCF orbitals, then Koopmans showed that the energy difference between molecule and positive ion is the value εp given by (2.22).

The main defects of using Koopmans' Theorem as a quantitative model for B.E. are that it does not allow for the reorganisation or "relaxation" of the remaining electronic structure upon ionisation and does not account for defects inherent in the MO model itself, such as correlation and relativistic corrections.[150]

2.6.2 The ΔSCF Method and Relaxation Energy

In the ΔSCF method, the BE of an electron is calculated as the difference between the total energies of the ground state and ionised state of an atom or molecule:

$$BE = E_{HF}^{*} - E_{HF} \qquad (2.23)$$

where the asterisk indicates a vacancy in a core-level. Since the computed hole-states are not necessarily orthogonal to all lower energy states of the same symmetry,[151] there is therefore no guarantee that variational upper bounds to the true total energies for the ionised species are obtained.

To overcome this problem, the ATMOL suite of programs discussed in (Section 1.8) has incorporated a LOCK directive which forces convergence upon the required state. The core hole states are found to be so far away from other bound states of the ionised system that there is no attempted "mixing" and therefore these are not subject to variational collapse.[82,152]

In molecules containing non-equivalent centres, the problem of delocalised core holes does not arise, however Bagus and Schaefer[153] performing calculations on the delocalised and localised 1s hole-states of O_2 found that the calculations with gerade or ungerade symmetry, imposed on the hole-state, gave a BE of 554.4eV whereas that for a localised core-hole on an oxygen atom was 542.0eV, in reasonable agreement with the experimental value of 543.1eV. There is now a large body of literature in favour of a localised description of core hole states.[154,155] As pointed out by Siegbahn,[156] the difference in energies of localised and delocalised hole-state species for a given system disappears when a procedure taking correlation into account is adopted, regardless of the extent of localisation in the initial HF wavefunctions.

The major defect in Koopmans' Theorem is the neglect of electronic relaxation. The relaxation energy may be defined as the difference between the BE of an electron described by Koopmans' Theorem, and the ΔSCF method:

$$RE = (-\varepsilon) - \Delta SCF\ BE \qquad (2.24)$$

The physical interpretation of the relaxation process was discussed in Section 2.2.2. Since Koopmans' Theorem uses the ground state wavefunction only, no account is taken of the change in spatial distribution of the electrons caused

by photoionisation. For the Δ SCF calculations however, this effect is explicitly considered. The relationship between Koopmans' Theorem, Δ SCF BE and experimental BE is shown in Figure (2.8).

Figure 2.8 The Relationship between Koopmans' Theorem ΔSCF and Experimental B.E.

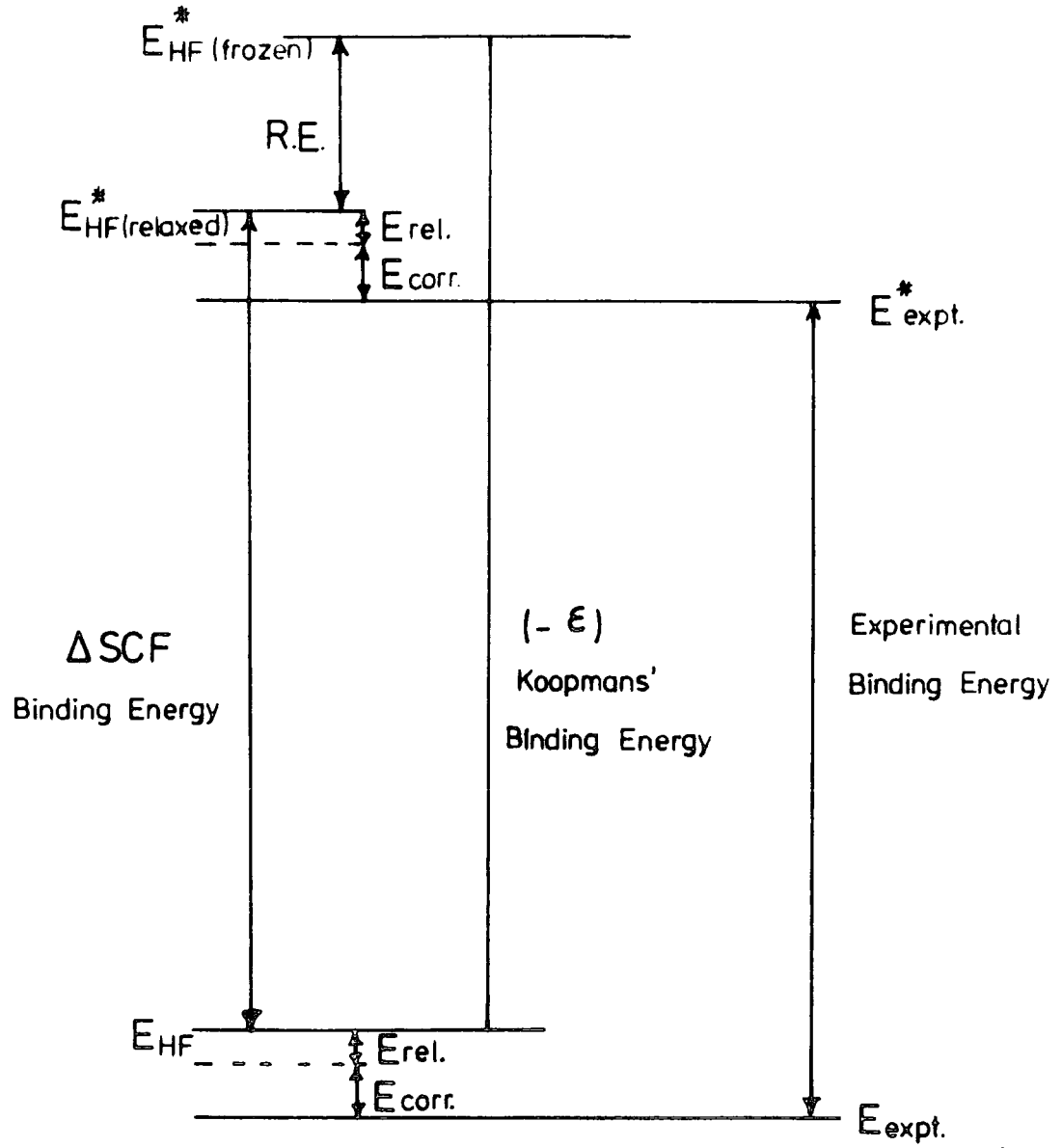

A further insight into this reorganisation process, has been given by Clark and co-workers.[94-98] The approach is illustrated in Figure (2.9), where ψ_o refers to the ground state, and ψ_o^+ and ψ_f^+ to the "Koopmans'" and hole-state wavefunctions. The relaxation process is illustrated by the use of dotted lines to show the unrelaxed orbital energies; hole-state spin-orbitals are indicated with a prime.

Figure 2.9 A Schematic Illustration of the Method for obtaining Single Orbital Relaxation Energies

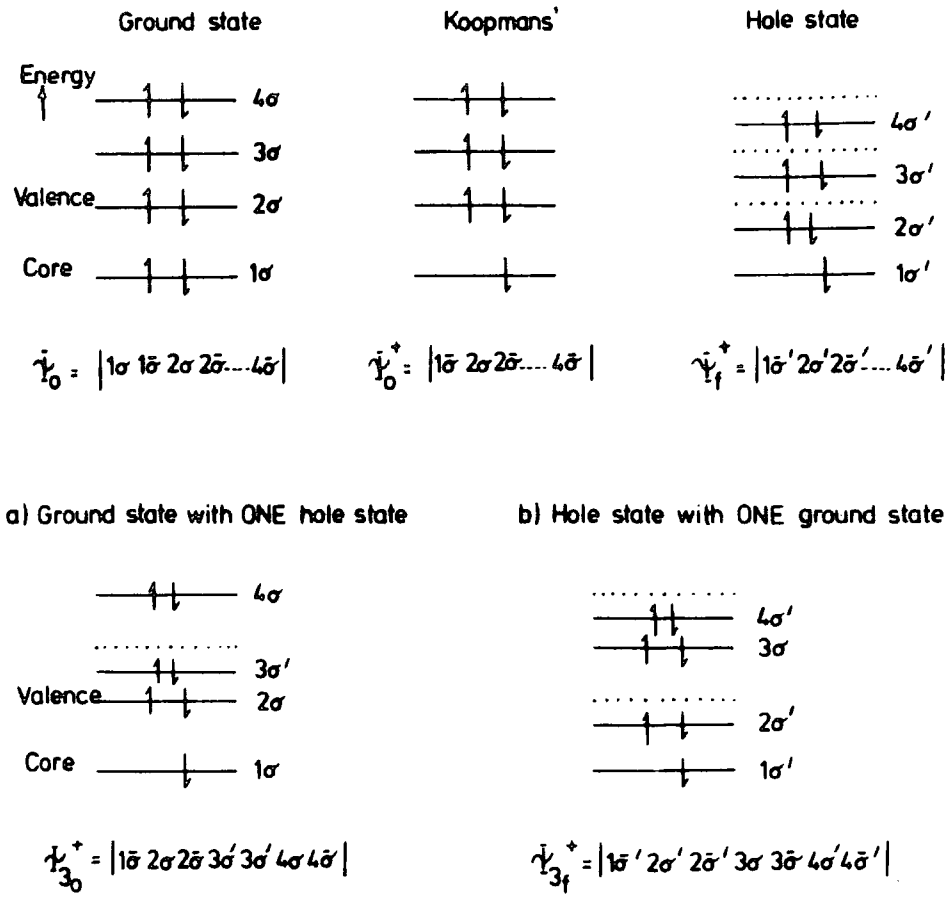

The contribution to the total relaxation energy due to each orbital may be calculated using the ground and core hole-state eigen vectors in two distinct but complementary calculations:

(i) the total energy of a hypothetical state for the core ionised species in which all of the orbitals are "frozen", save that orbital under study, (ψ_{30}^+ Figure (2.9) which is "relaxed" is calculated. A comparison of the binding energy obtained from this hypothetical state with that obtained from the completely "frozen" system (corresponding to the Koopmans' BE), gives a value for the single orbital relaxation.

(ii) the converse situation, where a hypothetical state for the core-ionised species is now constructed corresponding to all "relaxed" orbitals, save that orbital under study, (e.g. ψ_{3f}^{+} in Figure (2.9)) which is "frozen". The binding energy appropriate to this state is compared with that for the completely "relaxed" system (corresponding to the ΔSCF BE) to give a value for the single orbital relaxation energy.

The value obtained from calculation (i) provides an upper, and that from (ii) a lower, bound to the single orbital relaxation energy. Taking the simple average of the two calculations (i) and (ii) gives a value for the single orbital relaxation energy. The sum of all single orbital relaxation energies in a system corresponds to the total relaxation energy for that system, calculated directly.

So far, it has been assumed that both the molecule and its core hole state are in their vibrational ground-states, and zero point energies have not been considered. Although vibrational fine structure accompanying valence-ionisation in UPS is well documented and comparatively well understood,[157,158] it is only with the advent of high-resolution E.S.C.A. instrumentation, incorporating fine-focus X-ray monochromatisation,[115,159] that the presence of vibrational fine-structure accompanying core-ionisation, manifest as a broadening and asymmetry of the observed photoionisation peak, has been observed. When a core-electron leaves a molecule, there will be a change (generally a decrease) in the bond lengths; a new equilibrium bond-distance, with a different force constant, in the core-ionised species will replace the previous ground-state values.

Two types of ionisation potential may now be calculated:

(i) a vertical transition, which is a transition involving the most likely vertical change from a vibrational level $\nu'' = o$ in the ground state. This implies that no changes in nuclear geometry occur during photoemission. This assumption by consideration of the time-scale of photoemission $(\sim 10^{-17}s)$[160] as compared with a typical vibrational frequency $(\sim 10^{-13}s)$ [161] is clearly valid;

(ii) an adiabatic transition, representing a change from a vibrational level $\nu'' = o$ in the ground-state to a vibrational level $\nu' = o$ in the core-ionised species.

The new, core ionised potential contains various vibrational states which will be populated by Franck-Condon transitions. The Franck-Condon principle[162-164] gives the transition probability between vibrational states $\psi_{\nu''}$ and $\psi_{\nu'}$ as:

$$P_{\nu''\nu'} \propto |\int \psi_{\nu''} \psi_{\nu'} d\tau|^2 \qquad (2.25)$$

These quantities are commonly referred to as Franck-Condon factors.

In the harmonic approximation, the Franck-Condon factors depend on the three parameters $\alpha_{\nu''}$, $\alpha_{\nu'}$ and $\Delta r = r_{\nu''} - r_{\nu'}$, where Δr is the difference in equilibrium bond-length, $\alpha_{\nu i} = (\mu K_{\nu i})^{\frac{1}{2}}/\hbar$, μ is the reduced mass for the system, and $K_{\nu i}$ is the molecular force constant for the state i. Thus, from knowledge of the potential surfaces (equilibrium bond-lengths, force constants) for the ground and core hole states, and from the recurrence relationships defined by Ansbacher,[165] it is possible to compute the Franck-Condon factors. These

may be used to quantitatively explain fine structure in E.S.C.A. spectra, as illustrated in Figure (2.10) for methane using the CI calculations of Meyer,[166] and the experimental data of Siegbahn *et al.*[167]

Figure 2.10 A Schematic Representation of Vibrational Excitation in Methane and Analysis of the C_{1s} line Structure

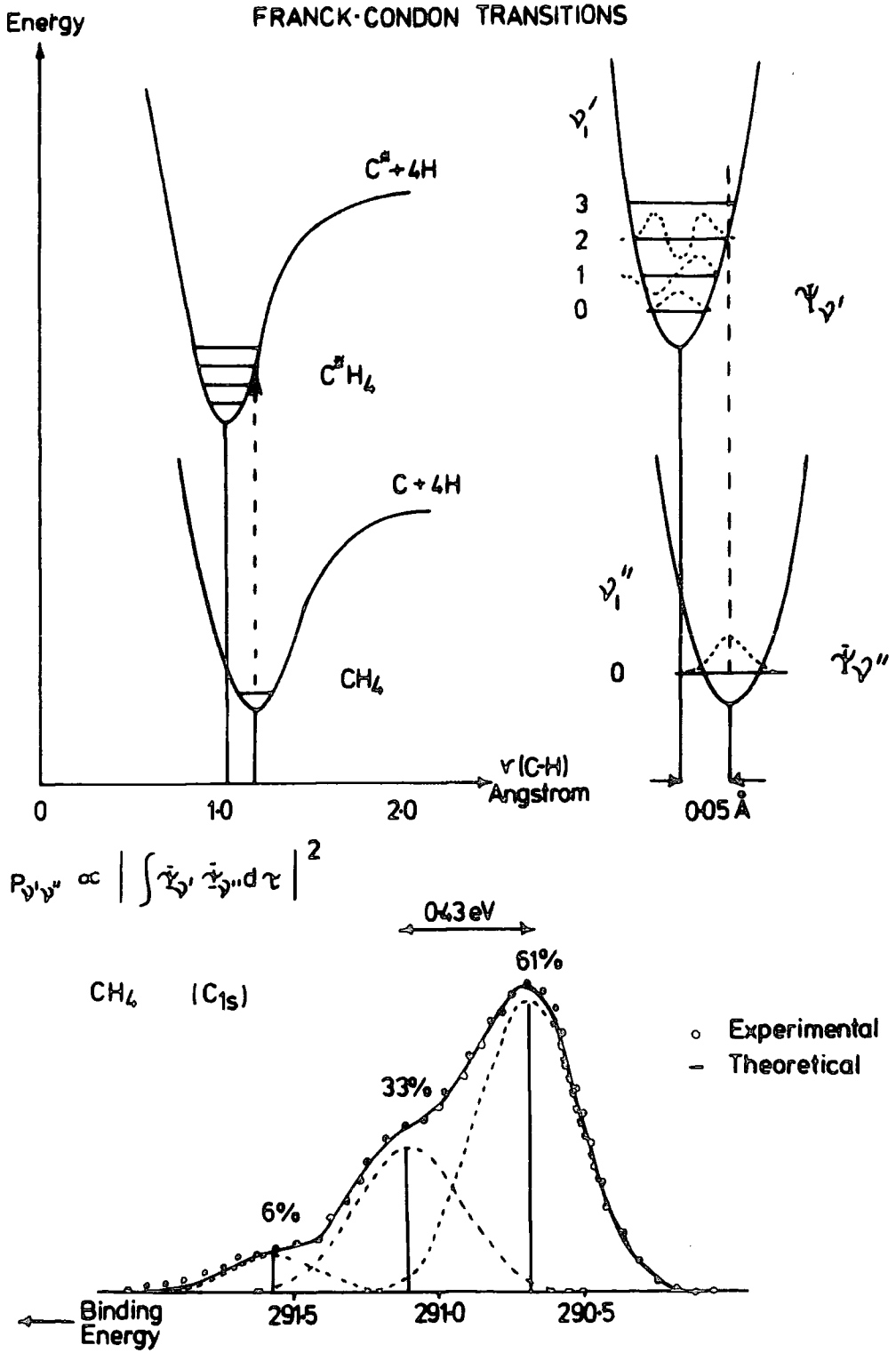

The failure of Koopmans' Theorem to agree with experimental BE's need not solely be due to relaxation effects. The BE may more precisely be defined as:

$$\Delta BE = \Delta E_{HF} + \Delta E_{corr} + \Delta E_{R} \qquad (2.26)$$

where ΔE_{HF} is the difference in the HF energies between the ground and core hole states, previously defined as the ΔSCF BE (2.23);

ΔE_{corr} is the difference in correlation energies;
and ΔE_{R} is the difference in relativistic energies.

Strictly, the difference between the vertical and adiabatic ionisation potentials (ΔE_{vib}) should be included in (2.26); however this has been shown to be sufficiently small as to be ignored.[168] Also, as was noted earlier in Section (1.5.3), although for heavier atoms the relativistic energy contribution to the BE increases in importance, for core-ionisation of first-row atoms, ΔE_{R} can in general be neglected.[169]

The correlation energy E_{corr} has also been discussed previously (Section 1.5.1). Although ΔE_{corr} is relatively small, and may be ignored in many cases, particularly where BE shifts are considered in this work, this may not generally be true, since for molecules, due to the contraction of the outer orbitals upon core ionisation, there is generally a resulting increase in the correlation energy as compared to that of the ground state. However, this will be offset, to some extent, by the reduction in the number of electron pair interactions in the molecular ion as discussed by Clementi[170] and Bagus[171] and therefore when absolute BE are considered ΔE_{corr} may well be small but care must be exercised in determining its significance.

2.6.3 The Equivalent Cores Approximation

Inherent in the equivalent cores approximation is the assumption that the valence-electrons will be affected by the ionisation of a core-electron in essentially the same manner as if a proton were added to the nucleus. This method of predicting chemical shifts was first reported by Jolly and Hendrickson.[172]

For the shift in C_{1s} BE between CH_4 and CH_3-X (where X is a general functionality), the scheme is as follows:

$$CH_4 \longrightarrow CH_4^{*+} + e^-; \quad \Delta E = (BE)_{CH_4} \qquad (2.27)$$

where * indicates a core hole vacancy i.e. C_{1s}

$$C^*H_4^+ + N^{5+} \longrightarrow NH_4^+ + \overset{*}{C}^{5+}; \quad \Delta E = \delta_o \qquad (2.28)$$

The reaction (2.28) involves the exchange of the $\overset{*}{C}^{5+}$ core and the equivalent core species N^{5+}; δ_o is the 'core exchange' energy.

Summing (2.27) and (2.28) gives

$$CH_4 + N^{5+} \longrightarrow NH_4^+ + \overset{*}{C}^{5+} + e^-; \quad \Delta E = (BE)_{CH_4} + \delta_o \qquad (2.29)$$

Similarly for CH_3-X:

$$CH_3\text{-}X + N^{5+} \longrightarrow NH_3\text{-}X^+ + \overset{*}{C}^{5+} + e^-; \quad \Delta E = (BE)_{CH_3X} + \delta_1 \qquad (2.30)$$

Subtracting (2.29) from (2.30) gives

$$CH_3\text{-}X + NH_4^+ \longrightarrow NH_3\text{-}X + CH_4^+; \quad \Delta E = (BE)_{CH_3X} - (BE)_{CH_4} + (\delta_1 - \delta_o) \qquad (2.31)$$

δ_o and δ_1 are assumed small since $\overset{*}{C}H_4$ and NH_4^+, $\overset{*}{C}H_3$-X and NH_3-X^+, and $\overset{*}{C}^{5+}$ and N^{5+} are chemically equivalent. The strong form of the equivalent cores approximation sets δ_o and δ_1 independently to zero, but it is sufficient to adopt the weak form ($\delta_1 - \delta_o = 0$) to determine a chemical shift.

When experimental, thermodynamic data is unavailable, ground state SCF calculations for both the molecules and ions provide the required heats of reaction for the isodesmic processes involved, thus allowing the shifts to be calculated. An interesting development of this approach, first suggested by McWeeny and Velenick,[173] is the use of a modest basis set such as the STO-4-31G using the ΔSCF method, but employing valence exponents of the equivalent core species for the core hole state wavefunction. A detailed investigation of basis set optimisation for CO by Clark and Müller[174] led to the conclusion that for small basis sets (such as STO-4-31G), the calculated absolute BE, with the optimum best-atom valence exponents on the core-hole atom, is in close agreement with that calculated using valence exponents appropriate to the equivalent core species. The latter basis sets are loosely referred to as "optimised" basis sets, and are found to give excellent values of the absolute BE at the STO-4-31G[175] level. Differences in BE, however, are adequately described with the previously described ΔSCF calculations at the STO-4-31G level, certainly for molecules composed of first-row elements.

2.6.4 Methods Involving Perturbation Theory

When there are many ionic states of the same symmetry in the same energy region, (a problem encountered in valence ionisation) a single configuration is a poor quantitative description of such near degeneracy.[176,177] Also the SCF MO model contains different correlation defects for the different states, and procedures such as the PNO-CI and CEPA methods of Meyer[178] are required to explicitly account for the electron correlation energy.

The study of valence-ionisation by UPS. has inspired several perturbation approaches. These include the Transition Operator Method of Gosinski and Pickup,[179] the Equations of Motion method developed by Rowe[180] and extended by Simons *et al*,[181] the Multiple Scattering X_α Method first suggested by Slater,[182] to describe valence ionisation; Rayleigh-Schrödinger Perturbation Theory developed by Chong *et al*[183] and Time-Independent Perturbation Theory developed and applied by Hubac and Kvasnicka.[184]

Several authors have used Green's function techniques to calculate corrections to Koopmans' Theorem. In particular, a general survey[185] of the Green's function has been specifically discussed by Lindenberg and Ohrn.[186] Cederbaum *et al*[187] have developed an approach based on the second-quantisation formulation of many-body perturbation theory, in which the B.E. are found from the negative real parts of the poles of the one particle Green's function. With an HF reference state for the perturbation scheme, the zero order poles correspond to BE = $-\varepsilon_p$ for the occupied MO which is just Koopmans' Theorem. First order terms vanish in this formulation, and higher-order terms are analysed by diagram techniques. The second-order expansion of the self-energy operator contains sums over three orbital indices and it becomes increasingly difficult to consider higher-order expansions though methods have been developed to do this.

CHAPTER THREE

SOME THEORETICAL ASPECTS OF CORE-IONISATION PHENOMENA IN A SERIES OF PROTOTYPE SYSTEMS FOR NITROGEN AND OXYGEN FUNCTIONALITIES IN POLYMERS

LCAO MO SCF computations (in the ΔSCF formalism) have been performed on the ground and core hole states of a range of nitrogen containing model systems, encompassing most of the common functionalities of interest in the study of polymers. The data complement that previously presented on oxygen functionalities and show that for specific cases, dependent upon the nature of the functionality (e.g. nitrate esters and nitriles) substituent effects can be substantially different than would be normally anticipated on the basis of a simple additivity model.

Comparison is drawn, in appropriate cases, with experimental data on both simple model systems and on polymers.

3.1 Introduction

From the range of information levels available upon completion of a single E.S.C.A. experiment, as outlined in the previous chapter, and the distinctive nature of core levels, it is clear that providing an appropriate calibration exists, the relative intensities and shifts in binding energy for components of a given core level, may be used to identify structural features.

As an example, the wide scan spectrum of a polyamide (figure 3.1) shows the ease of elemental identification

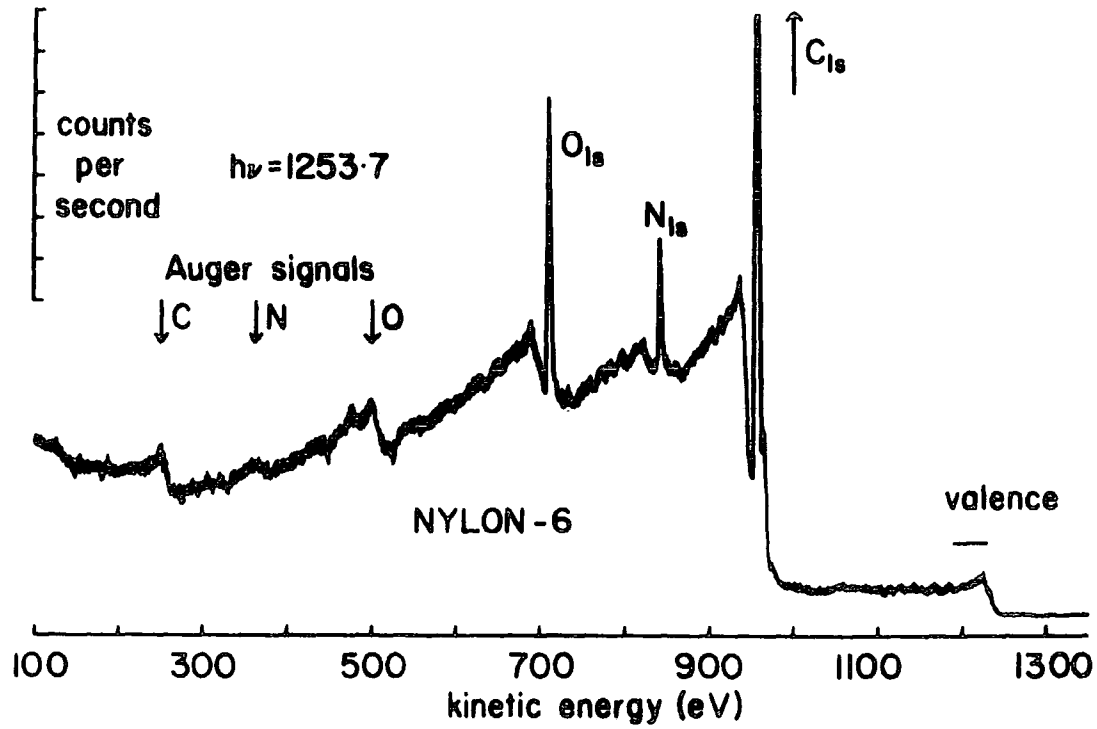

Figure 3.1 Wide scan spectrum of the Nylon-6 Polyamide

from the core ionisation data, and the high resolution O_{1s}, N_{1s} and C_{1s} core level spectra (figure 3.2) characterise the configuration as being that of Nylon 6 from a consideration of the intensity ratio (1:1:4) of the structural features evident in the C_{1s} envelope. The surface nature of the technique has therefore rendered the above useful in delineating the complexity of chemical reactions occurring at the gas/solid interface as might be experienced by natural weathering of a polymer or its oxidation by inductively coupled ratio-frequency plasmas

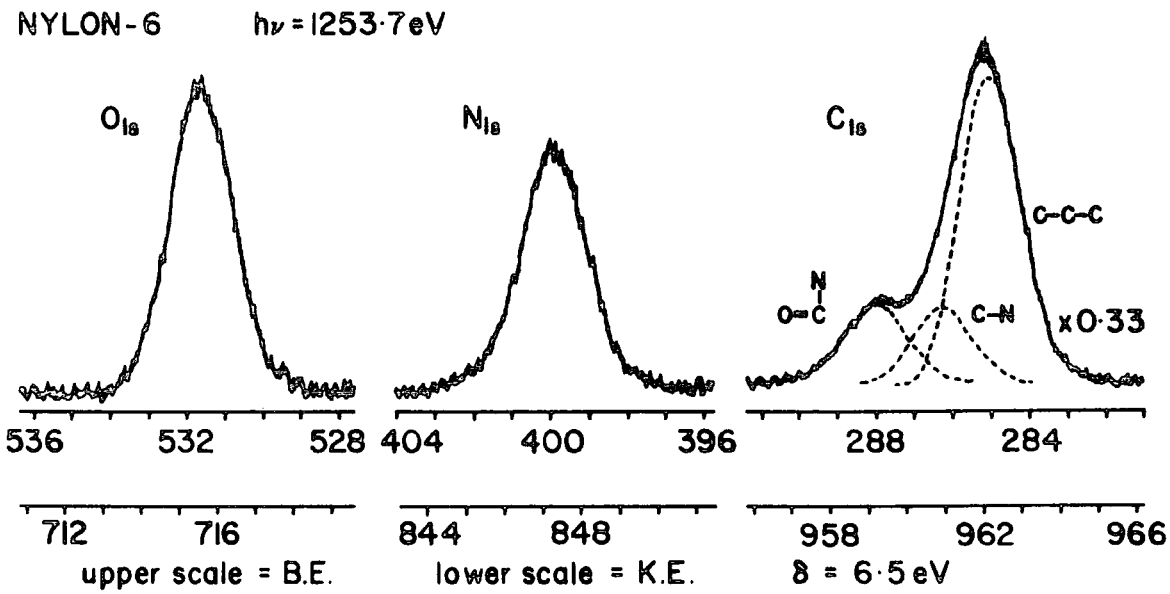

Figure 3.2 High Resolution O_{1s}, N_{1s} and C_{1s} spectra for Nylon-6

excited in oxygen. To reiterate the brief discussion in section 2.5.1 in more detail, the C_{1s} and O_{1s} core level spectra for polystyrene[127] treated in an 'oxygen plasma' are included (Figure 3.3).

In such a treatment, it is known that an extensive variety of oxygen containing structural features is produced at the surface of the polymer,[130] ranging from simple alcohols and esters to peroxyacids and carbonates. It is clear from the C_{1s} spectrum and the knowledge that a sample

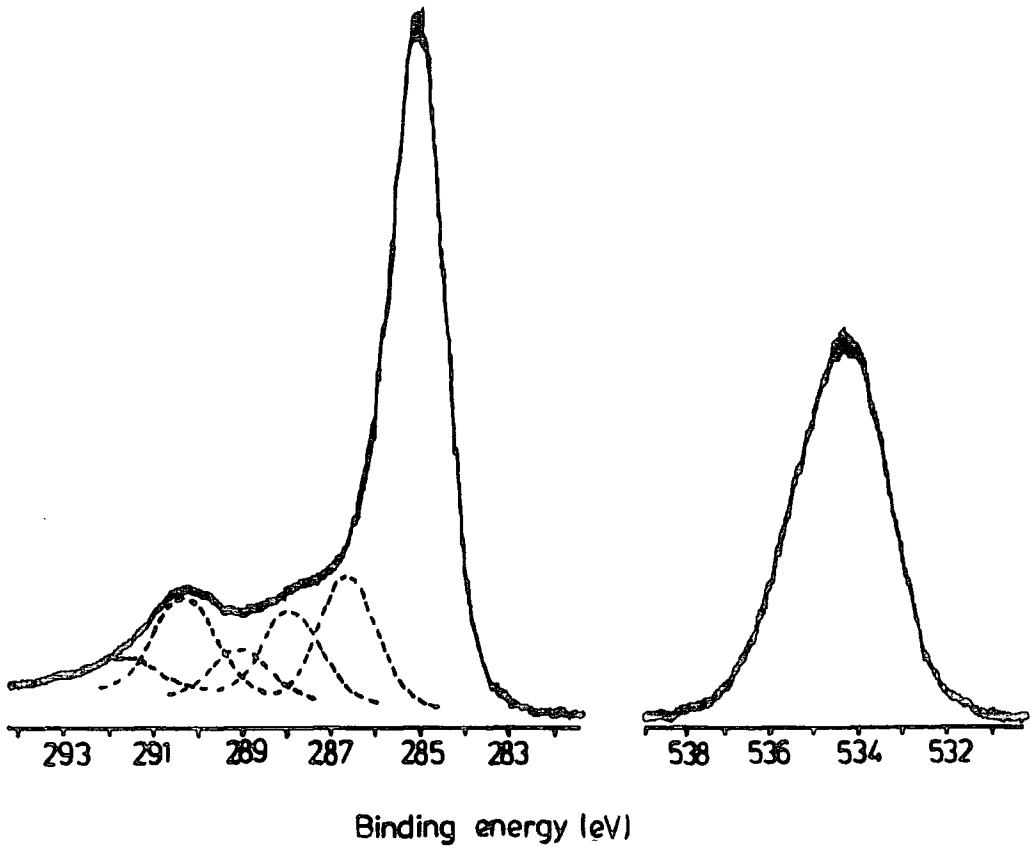

Figure 3.3 C_{1s} and O_{1s} core level spectra for polystyrene after exposure to an inductively coupled radio-frequency glow discharge excited in oxygen. (0.2 torr, 0.1 watt, 16 seconds).

exhibiting a 'clean' surface would produce only a single peak with shake-up satellite (arising from $\pi \rightarrow \pi^*$ excitations accompanying core ionisation), that substantial modification of the surface has occurred. It is apparent, that deconvolution of such a complex spectrum by a curve fitting analysis would be difficult, and this prompted a non-empirical theoretical study of the binding energies and relaxation energies for an extensive series of oxygen

containing organic systems encompassing most of the common functionalities.[127] Trends in binding energy arising from this study are shown in Figure 3.4

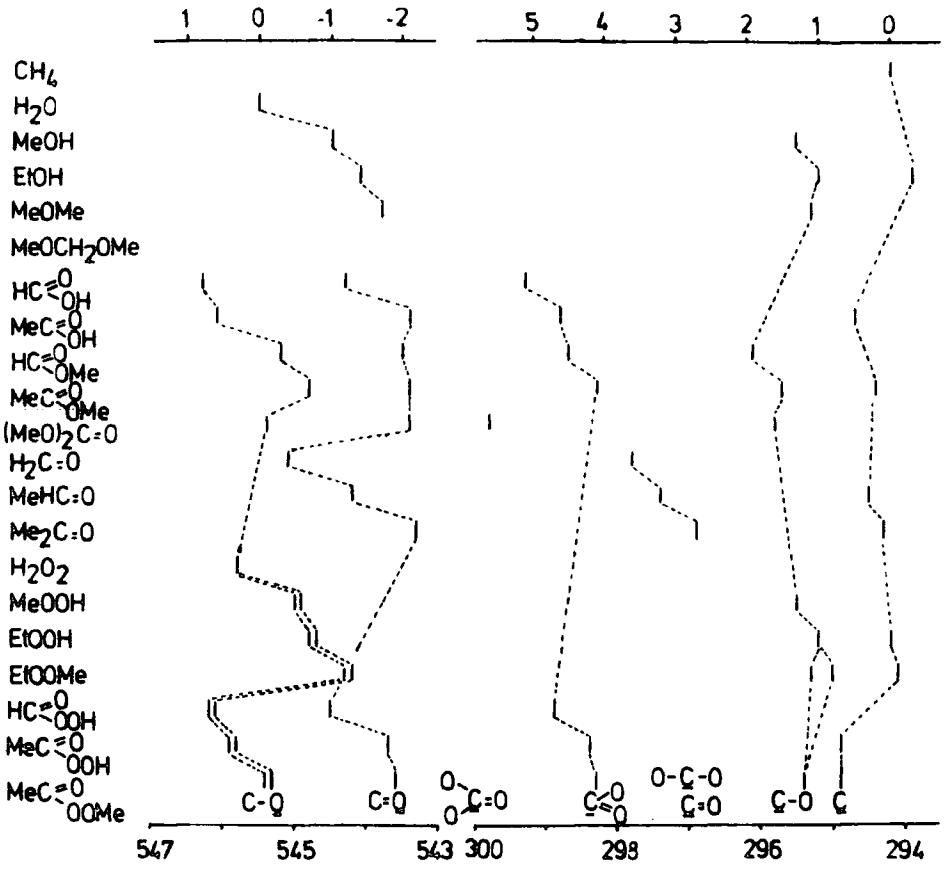

Figure 3.4 Trends in absolute and relative ΔSCF binding energies (in eV) as a function of electronic environment

From the data displayed in Figure 3.4 it was found that by employing an analogue curve fitting procedure, with gaussian curves positioned at ∿ 286.6, 287.9, 289.0 and 290.4 eV as shown in Figure 3.3, and treating the height as a variable, a unique deconvolution was achieved with a full width at half maximum (FWHM) of 1.7 eV . For

the O_{1s} spectrum it is clear that shifts in binding energy span a much smaller range, but in a similar manner, it was suggested that peaks at ~532.8, 533.7, 534.3 and 535.2 eV corresponding to doubly bonded oxygen; singly bonded oxygen in alcohols, ethers and peroxides; singly bonded oxygen in acids, esters and hydroperoxides; and singly bonded oxygen in carbonates, peroxyacids and peroxyesters respectively provide a unique deconvolution.

An interesting result from the theoretical study, which aids the above deconvolution procedure for the C_{1s} spectrum, is the approximately additive nature of the substituent effects. The determining factor for this was found to be the number of bonds to the oxygen substituents; a shift to higher binding energy of ~1.5 eV per carbon-oxygen bond as previously noted (Section 2.5.1). Secondary, or β substituent effects of oxygen, however, are found to be relatively small. The relaxation energies for the C_{1s} levels, in the wide range of oxygen functionalities studied, were found to exhibit a strong linear dependence on binding energies; a higher binding energy being associated with a lower relaxation energy; and correlations were found to be characteristic of a given structural type. From the substantial range covered by the relaxation energies (~1.4 eV) it was evident that shifts in binding energy could not be described in terms of Koopmans' Theorem.

A considerable body of data[126-130, 190-192] is now available on the influence of a wide range of substituents on the core level binding energies for both C_{1s} and O_{1s} levels, ensured by the importance of such oxygen containing

functional groups in simple systems (e.g. alcohols, ethers, aldehydes, ketones and carboxylic acids) and abstracting the relevant data for prototype systems of interest, allows an interpretation of the surface chemistry of simple polymer systems, as in the manner previously described. Although a good understanding has been reached on the relative importance of differential changes in relaxation energies in determining the absolute magnitudes of shifts in binding energy for C_{1s} and O_{1s} core levels, to date, there has been no comparable systematic study of the equally important nitrogen functionalities.

Polymer surfaces are often contaminated, not only in natural weathering or ageing processes, but also in their preparation and application. Thus, the surfaces of mouldings often involve specific segregation of release agents, whilst polymers produced by emulsion polymerisation often show evidence of segregation of entrained emulsifying agents at the surface.[193] More specifically, those possessing hydrophilic centres ($-NH_2$, $-CONH_2$, $>C=O$ etc.) may well become specifically contaminated at the surface by hydrogen bonded water.[126] It is therefore important that the composition of the surface be well understood, to avoid misinterpretation of observed phenomena.

E.S.C.A. is becoming increasingly important as a tool for 'trouble-shooting' problems in these areas and a readily available example is adhesive failure at a surface. Indeed part of this study was motivated by current work concerning the homogeneity of a series of polyether- and polyester-based, polyurethane adhesives, before and after a specified curing

procedure. Polyester film, vacuum coated with aluminium and with a layer of coloured lacquer covering the aluminium surface, is used for decorative purposes. The lacquer, is frequently based on a polyurethane resin and it is therefore important that the resin cures adequately, otherwise resistance to wear is poor. This process has been monitored using MIR (multiple internal reflection) spectroscopy where disappearance of the band relating to the isocynate group (2280 cm^{-1}) is noted as a function of time.[194] In the first instance, the sample depth of 10000Å could be improved by at least a factor of ~200, for what is essentially a surface phenomenon, if E.S.C.A. were used, and with a knowledge of the shifts in B.E. for the polyurethane and isocyanate systems, it is conceivable that the disappearance of not one, but three peaks (in the C_{1s}, N_{1s} and O_{1s} envelopes) could be monitored.

From the fact that in an E.S.C.A. spectrum, as in that for Nylon-6 shown earlier, the components contributing to the envelope for each core level, display relative intensities often clearly characteristic of molecular stoichiometry it is suggested that the technique would be useful in establishing the composition of co-polymers. Indeed much of the early work by Clark and co-workers[195] in E.S.C.A. applied to polymers involved the study of simple fluorocarbon monomers, which provided essential data to enable the compositions of co-polymers of ethylene and tetrafluoroethylene, which are largely alternating in character, to be determined. This was shown to be possible by two means: comparison of the

integrated ratios for the F_{1s} and C_{1s} levels; and from the individual components of the C_{1s} levels. Despite individual importance in the textile industry and in coatings for aircraft respectively, the polyamides and -imides together form a co-polymer which derives increased thermal stability but a decrease in flexibility from the imide/amide ratio.[196] Again, with a knowledge of the shifts in binding energies and relaxation effects for these systems E.S.C.A. studies would prove useful.

A particularly important class of co-polymers, termed ABS, (Acrylonitrile, Butadiene, Styrene), consist of two types. Type A is a blend of two co-polymers, styrene-acrylonitrile and butadiene-acrylonitrile, whilst type B involves copolymerising the styrene-acrylonitrile blend with polybutadiene dissolved in the monomer blend. Priebe *et al*[197] studied the oxidation of these two types in natural weathering, and from I.R. transmission spectra concluded formation at the surface of (-OH) hydroxyl, aldehyde (-CHO), ketone (>C=O), peroxide (-C-O-O-) and carboxyl (-COOH) groups with a decrease in 1,4-trans double bonds, and 1,2 vinyl bonds. After six months exposure, the double bonds of the polybutadiene component had completely disappeared, but it was suggested that the styrene and acrylonitrile units remained unaffected. The susceptibility of polystyrene to oxidation is clearly displayed earlier in Figure 3.3, and it is feasible that the minimum sampling depth of 20μm in the I.R. study is responsible for the above result. Clearly for E.S.C.A. to be applied, a detailed study of the acrylonitrile group is warranted to allow data relating to the

oxidised polystyrene to be abstracted from the C_{1s} core level spectrum. Confirmation of the above is presented in a study of the oxidised polyalkyl acrylates.[126] The O_{1s} spectrum consists of two components of unequal intensity, with the increased component being due to C=O structural features. High resolution I.R. studies reveal only a single peak in the range 1734 ± 6 cm^{-1}, consistent with

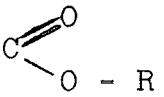

structural features. This is readily understood, since the I.R. data pertains essentially to the bulk.

A current area of research is the kinetics and mechanism of nitration and denitration in cellulose.[198] The main point of interest concerns the question of how the degree of substitution relates to the composition of the acid mix (range HNO_3 17-27% H_2SO_4 66-50% and 17-23% H_2O). The maximum degree of substitution is 3, but in reality, the highest value observed is $\sim$2.8 from Kjeldahl analysis. This can be rationalised in terms of two extreme models. The first may be attributed to the micro- and macroscopic structure of the cellulose. Thus inhomogeneities in the bulk structure could conceivably give rise to accessible and inaccessible regions which would correspond to completely nitrated and unreacted material respectively. An alternative model suggests that since nitration is a reversible esterification process then the $\sim$2.8 degree of substitution represents an equilibrium value. In such a heterogeneous process rationalisation of the possible explanations requires a technique which can distinguish between surface and bulk phenomena. To consider the E.S.C.A. data,

information is necessary on such functionalities as the nitrite and nitrate esters, as well as the nitro-alkane and amide, since the latter may be produced by photo-reduction.

To date, there appear to have been no previous theoretical investigations of core ionisation phenomena involving the wide range of nitrogen functionalities outlined above. To partially rectify this situation, detailed ΔSCF computations have been carried out on these, and a number of other nitrogen functionalities to establish trends in absolute and relative core-binding energies and relaxation energies. New data are also included on oxygen functionalities which extend the work previously reported. In appropriate cases, the theoretical work has been complemented by experimental studies.

3.2 Theoretical and Experimental Considerations

3.2.1 Computational Details

Non-empirical LCAO MO SCF calculations have been carried out, within the Hartree-Fock formalism, on the ground and localised core hole states of a range of molecules involving nitrogen functionalities, using the best-atom exponents referred to in Section 1.7.4.[43] An STO-4.31G basis set (Section 1.7.5) was used, as previous investigations have shown[199] that shifts in core binding energies and differences in relaxation energies accompanying core ionisation, are well described at this level, within the Hartree-Fock

formalism. The core binding energies and relaxation[147] energies were calculated according to the methods described in Section 2.6.2.

Subject to availability, experimental or optimised geometries were taken from the literature,[200-213] supplemented, where necessary, by standard bond lengths and bond angles. For those systems where insufficient co-ordinate-geometry data were available, geometry optimisations were performed using the routine incorporated into the MNDO programs of Dewar and Thiel.[214,215]

3.2.2 Experimental Details

Spectra described in this work have been recorded on an AEI200AA/B spectrometer using $Mg_{k\alpha_{1,2}}$ radiation. Where necessary, liquids were injected into a reservoir shaft and the vapour condensed as thin film onto a cold probe (gold substrate) at $\sim$-110°C. Powdered samples were mounted onto the sample probe by means of double sided "Scotch" insulating tape. For such insulating samples, energy reference was by means of the hydrocarbon peak at 285eV, which arises from deposition of the extraneous hydrocarbon in the spectrometer, upon the sample surface (as described in Section 2.4). This can be built up over a lengthy time period once cooling to the end cap of the X-ray source has been removed.[125] For the films deposited *in situ* on gold, monitoring the $Au_{4f_{7/2}}$ level of the substrate, in the early stages of deposition, allows a direct

reference with respect to the Fermi level (c.f. Section 2.4). The $Au_{4f_{7/2}}$ level at 84eV binding energy, used for energy reference in this study had a full width at half maximum (FWHM) of 1.15eV under the conditions of these experiments. Spectra were recorded in the fixed retardation ratio mode (FRR) (c.f. Section 2.3.3) and area ratios and line shape analysis were carried out using a Du Pont 310 curve resolver.

The following samples have been studied as thin films deposited *in situ* on a cooled gold substrate; isopropyl nitrate, propyl nitrate, N-butyl nitrate, butyl nitrite and nitromethane. In each case, the samples were commercially available and of a purity greater than 97%, and were used without further purification. The following polymer samples have been studied in powder form: polymethacrylonitrile, and polyacrylonitrile. As a model for the urethane linkage, a sample of a polyether based (Holden Surface Coatings, Birmingham Ltd.) urethane adhesive was studied as a thin film coated onto a gold substrate.

3.3 Results and Discussion

The complete set of theoretical core binding energy data generated from this study are displayed in Figure (3.5). Using the ΔSCF method with an STO-4.31G basis set, it is well known that the absolute magnitudes of the relaxation energies tend to be slightly underestimated; as a result, the calculated absolute binding energies are somewhat larger than those determined experimentally. However previous studies have shown that calculations at the STO-4.31G level

provide an excellent description of differences in relaxation energies and binding energies and the data in Figure (3.5) are therefore, for convenience, referenced both to the gas phase (vacuum level) and to the solid phase (Fermi level) (c.f. Section 2.4). For comparison purposes some data are also included from previous studies (e.g. C_{1s}, N_{1s} and O_{1s} binding energies for CH_4, NH_3 and H_2O respectively). The span in shifts for the model systems is ∿7eV, ∿8eV and ∿6eV for the C_{1s}, N_{1s} and O_{1s} levels respectively.

With such a large body of data, it is convenient to make a detailed consideration of each core level in turn.

3.3.1 C_{1s} Levels

(a) Oxygen as a Primary Substituent

As previously noted it has been shown that relaxation energies often follow the trends in overall core binding energies for C_{1s} levels (viz. a higher binding energy being associated with a lower relaxation energy) and that substituent effects are additive in nature. Thus in the previous study of prototype systems for oxidative functionalisation of polymers, (Figure 3.4) the additive nature of the shifts in binding energy for oxygen as a substituent, was noted, and for the range of functionalities studied, a primary substituent effect of 1.5 ± 0.4 eV for each carbon-oxygen bond was obtained which, as shown in Figure 3.3, adequately describes the appearance of simple carbon-oxygen and peroxy-features in the spectrum. A recent study by Harding and

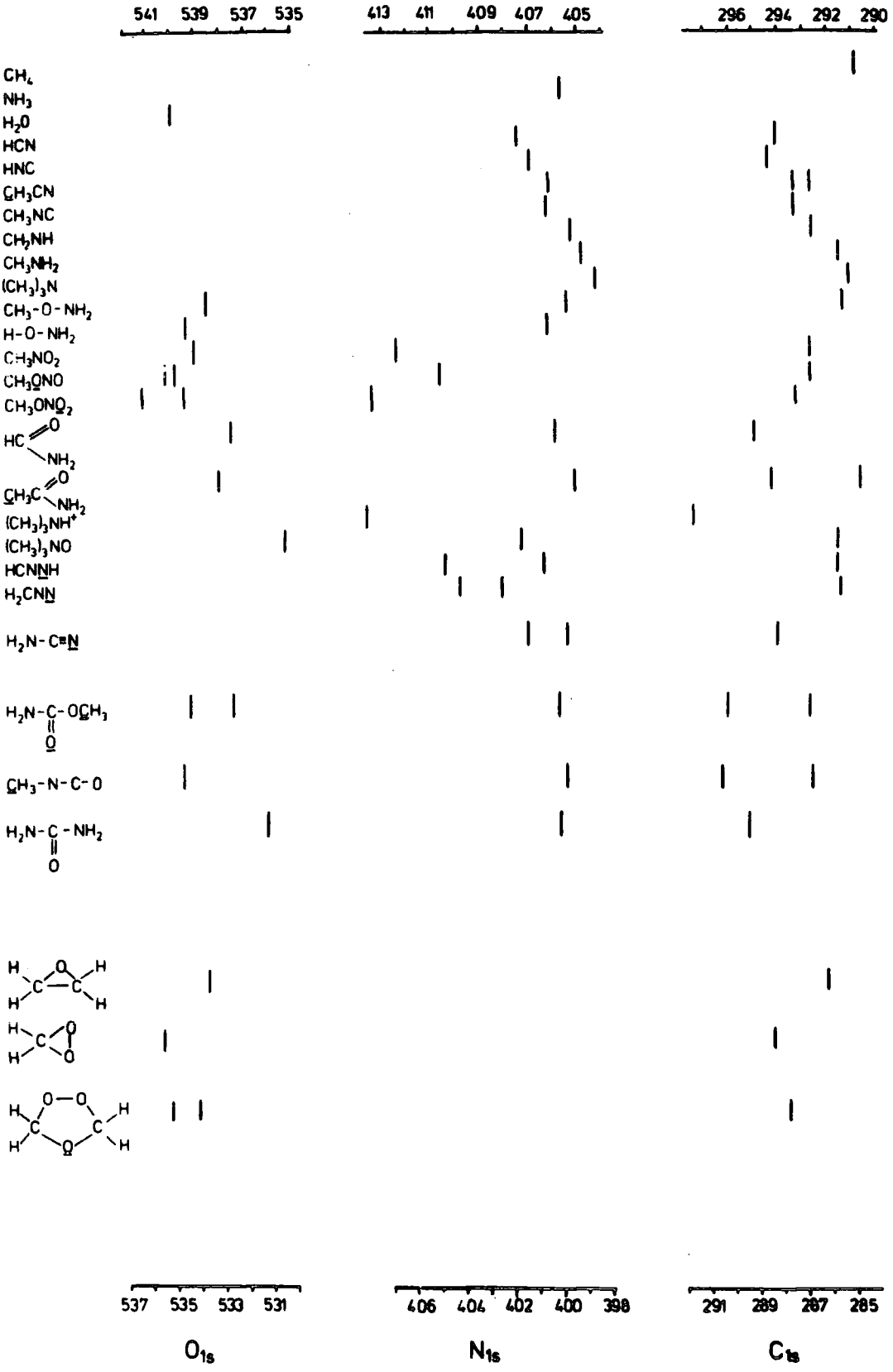

Figure 3.5 Trends in absolute ΔSCF binding energies (in eV) as a function of electronic environment

Goddard III[200] concerning the mechanisms of ozonolysis confirm the isolation of the 1,2,4 trioxolane species upon reaction with olefins, but note the stability of the dioxirane species in preference to the peroxymethylene intermediate (36 Kcal mol^{-1}), and the formation therefore of dioxymethylene as the reactive intermediate. It was therefore of interest to calculate the binding energies for oxirane, dioxirane and the 1,2,4-trioxolane (ethylene ozonide) as an extension of the previous work to heterocyclic carbon-oxygen ring systems, and the data are presented in Table 3.1).

Table 3.1

ΔSCF Binding Energies and Koopmans' Binding Energies (STO-4.31G)

	C_{1s} Levels (eV)				O_{1s} Levels (eV)			
Molecule	ΔSCF		Koopmans'		ΔSCF		Koopmans'	
	B.E.	ΔB.E.	B.E.	ΔB.E.	B.E.	ΔB.E.	B.E.	ΔB.E.
CH_4	294.2	(0)	305.1	(0)				
H_2O					545.5	(0)	560.8	(0)
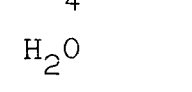	295.4	+1.2	306.9	+1.8	544.2	-1.3	561.6	+0.8
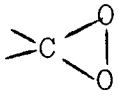	297.6	+3.4	308.8	+3.7	546.0	+0.5	563.3	+2.5
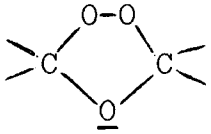	297.0	+2.8	308.5	+3.4	544.6 545.7	-0.9 +0.2	561.8 563.4	+1.0 +2.6

Where ambiguity may arise underlining denotes atoms of lower B.E.

Trends are clearly discernible; for the C_{1s} levels the tolerable agreement between the shifts in Koopmans' binding energies and those calculated within the ΔSCF formalism indicates that within the electronic environments of these carbon-oxygen systems, the shifts in ΔSCF binding energies are largely due to changes in relaxation energy only. The O_{1s} levels also show the distinctive high binding energy components associated with a peroxy-linkage, which has previously been noted, and are consistent with recent studies of the dibenzoyl peroxide system.[216]

The range of functionalities studied to date suggest that for $\rightarrow$C - O - X functionalities (where X is a general carbon-oxygen functional group), the secondary influence of the substuent X is very small (e.g. for X = H, CH_3, OH, CH_2OCH_3, COH, $COCH_3$, OCH_3, OCH_2CH_3 and $OCOCH_3$ the primary substituent effect is 1.5 ± 0.4 eV) and clearly the data for oxirane, dioxirane and the 1,2,4-trioxolane also fall into this pattern.

The present study provides examples which fall outside the scope of such a simple additivity model and it would appear that the large electronic effect of nitrogen can provide a substantial secondary shift. Thus for X = NH_2 the shift is considerably reduced to ∿0.5 eV compared to that for X = $CONH_2$ where the computed shift with respect to methane as a standard is 1.8eV. (Studies of polyurethane based adhesive systems confirm the shift data as will become apparent in a later section). By contrast with strongly electron withdrawing nitrogen functionalities the shift is

considerably increased over that predicted on a simple additivity model. Thus for nitrate esters, X = NO_2, the shift with respect to methane increases to ∿2.4eV. The strong secondary influence of a nitrate ester group at first sight might seem surprising since nitrite esters adhere well to the general scheme, with a shift in binding energy, equivalent to that of the urethane grouping, substituent, of 1.8eV.

As has been noted, whilst the absolute magnitudes of relaxation energies are underestimated and the absolute binding energies are consequently slightly overestimated at the STO-4.31G level, such calculations provide an excellent description of differences in relaxation and binding energies accompanying core-ionisation. The ΔSCF calculations briefly referred to, show therefore that changes in relaxation energy are not responsible for the increased shift in binding energy, since the difference in relaxation energy between X = NH_2 and X = NO_2 is computed to be only 0.3eV, whilst the shifts in binding energy relative to methane as a standard are 0.5eV and 2.4eV respectively.

To investigate this further, the core level spectra for a series of model compounds have been recorded. The experimental data for the C_{1s}, N_{1s} and O_{1s} levels for these systems are compared with the theoretical data for model systems in Table 3.2.

The comparison is in two sections since gas phase data (vacuum level) are available for some of the model systems whilst solid phase (Fermi level) data are available for others.

TABLE 3.2 A comparison of ΔSCF binding energies of C_{1s}, N_{1s} and O_{1s} levels in the model systems with experimental data

Molecule	Solid Phase Experimental B.E. (eV)					Theoretical B.E. (eV) (Corrected)				
	C_{1s}		N_{1s}	O_{1s}		C_{1s}		N_{1s}	O_{1s}	
CH_3CN						286.8	287.5	400.4		
$(C(C)(C)C(N))_n$	285.0	286.4	399.5							
$(C(C)C(N))_n$	285.0	286.3	399.3							
CH_3NO_2		286.8	406.8	534.3			286.8	406.8	534.1	
CH_3ONO							286.8	404.9	534.9	535.3
$CH_3CH_2CH_2CH_2ONO$	285.0	286.7	405.0	534.2	535.2					
CH_3ONO_2							287.4	407.7	536.2	534.5
$CH_3CH_2ONO_2$	285.0	287.0	408.1	535.0	534.2					
$CH_3CH_2CH_2ONO_2$	285.0	287.1	408.0	535.5	534.1					
$CH_3CH_2(ONO_2)CH_3$	285.0	287.0	408.1	535.3	534.1					
$CH_3CH_2CH_2CH_2ONO_2$	285.0	286.5	408.0	535.5	534.3					
$CH_3C(=O)NH_2$						284.8	288.4	399.5	533.1	
$-C(=O)N$		288.1	399.8	532.8						
$CH_3-O-C(=O)-NH_2$						286.8	290.2	400.3	534.4	532.
$-O-C(=O)-N(H)-$		289.8	400.4	534.1	532.5					

Molecule	Gas Phase Experimental B.E. (eV) (ref. 192)						Theoretical B.E. (eV) (Corrected)			
	C_{1s}			N_{1s}		O_{1s}	C_{1s}		N_{1s}	O_{1s}
CH_4	290.8						290.8			
NH_3				405.6					405.6	
H_2O						539.7				539.7
HCN	293.5			406.8			294.0		407.4	
CH_3CN	292.7			405.6			292.6	293.3	406.1	
$(CH_3)_3CCN$	291.1	291.8	292.4	405.1						
CH_3NH_2	291.5			405.2			291.4		404.8	
$(CH_3)_3N$	291.3			404.8			291.0		404.2	
$(CH_3)_3NO$	291.8					537.7	291.5		407.3	535.1
CH_3NO_2	293.0			411.2		539.1	292.6		412.4	538.8
$(CH_3)_3CNO_2$	291.43	292.6		411.5		538.7				
NH_2CHO	294.5			406.4		537.7	294.9		405.9	537.3
$(NH_2)_2CO$	294.8			406.1		537.2	295.1		405.8	535.9

Where ambiguity arises underlining denotes atoms of lower B.E.

Characteristic of the nitrate esters, are the C_{1s} core level spectra of n-propyl and iso-propyl nitrates displayed in Figure 3.6. As an aid to deconvolution, these are accompanied by their twice differentiated analogues which are indicative of stationary points on the C_{1s} lineshapes in the form of clearly defined maxima or minima (c.f. Section 2.5.2).

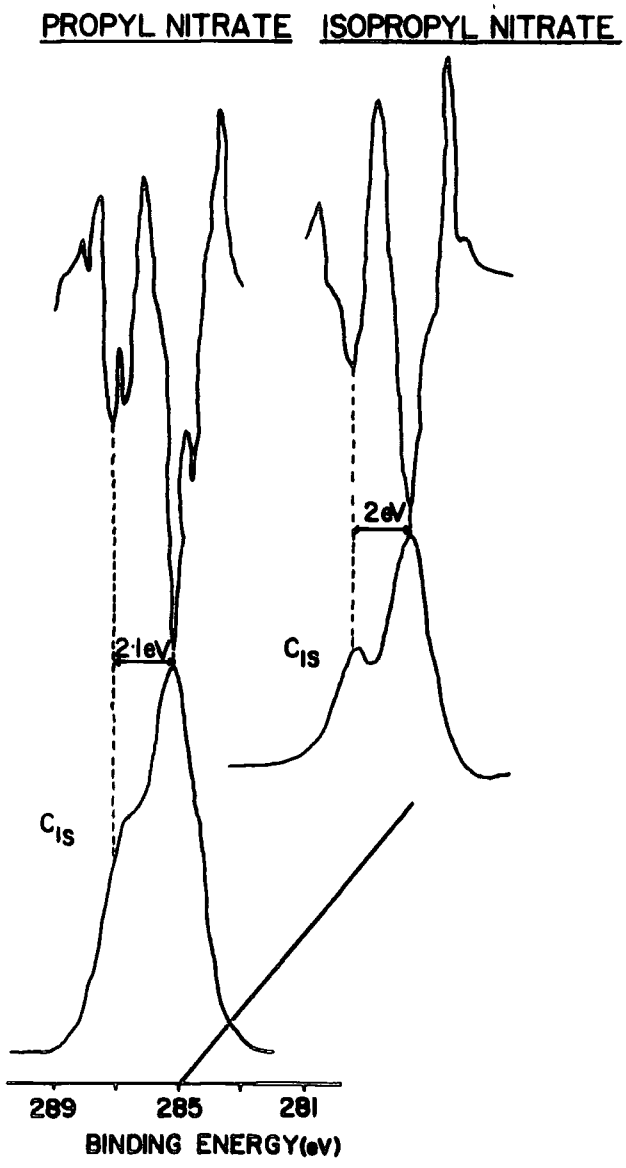

Figure 3.6 C_{1s} core-level spectra for n-propyl and isopropyl nitrates and their Derivative Spectra (2nd)

In each case, the measured shift in binding energy is ∿2 eV and clearly the data confirm that a nitrate ester functionality has a substantially larger shift than might have been anticipated on the basis of a simple additivity model. Both C_{1s} envelopes are deconvoluted in terms of two components in 2:1 ratio with the higher binding energy component being the lower in intensity in both cases. It is clear from the nature of these spectra that for the nitrate ester functionality only primary shifts are observed in the C_{1s} core levels.

The increased shift at carbon associated with the conversion of an alcohol into its nitrate ester ($\rightarrow C-OH \longrightarrow \rightarrow C-O-NO_2$) gives rise to distinctive changes in overall C_{1s} line profiles and endows E.S.C.A. with considerable potential for monitoring changes in surface chemistry associated with nitrate ester formation. The C_{1s} and O_{1s}, and C_{1s} N_{1s}, and O_{1s} core level spectra for cellulose and nitrocellulose samples respectively are presented in Figure 3.7.

Comparing the two C_{1s} envelopes, it is evident from their shape that the C_{1s} level for the carbons directly attached to oxygen in the nitrate ester groups, is distinctively shifted to higher binding energy. Employing the shift-data from the present study assigns the central component at ∿287.4 eV, and although this component arises predominantly from the carbons C2, C3 and C6 (using the standard ordering convention) bearing the nitrate ester functionality, broadening of the line encompasses contributions from C4 and C5, and also, depending upon the degree

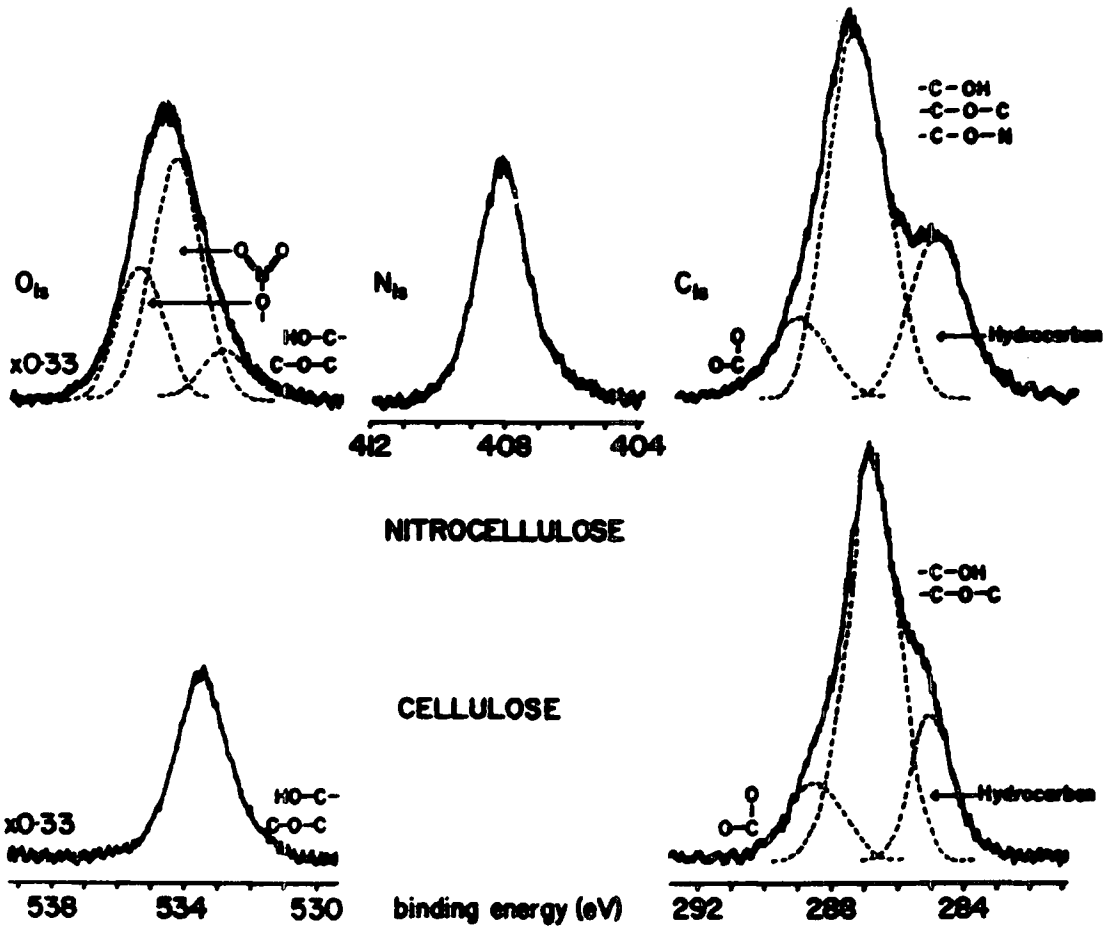

Figure 3.7 Core level spectra for Cellulose (C_{1s}, O_{1s}) and Nitrocellulose (C_{1s}, N_{1s}, O_{1s})

of substitution unreacted C2, C3 and C6 features. The third component arises in both cases from C1, which is uniquely attached to 2 oxygens in the cyclic hemiacetal formulation of the β-D-glucopyranose ring. In principle, with the theoretical data now accumulated, a precise deconvolution of the spectrum is possible, but in this case unnecessary. As already described, the point in question is that of degree of substitution and with the existence of a distinctive, single-component N_{1s} envelope (as discussed in a later section), a recent study[198] has shown that this may be calculated from the integrated C_{1s}/N_{1s} area ratios, when the extraneous hydrocarbon component is neglected, and the appropriate sensitivity factors for the various core levels are known.

(b) Nitrogen as a Primary Substituent

The data presented in Figure (3.5) may be used to systematically extend the range of nitrogen containing substituents for which primary substituent effects on C_{1s} core levels have been evaluated theoretically. It is convenient in discussing this data to present it in a processed tabular form (Table 3.3).

The results of an earlier study[217] have shown that at whatever level of theoretical sophistication the electronic structure of acetonitrile is studied, it is apparent that the same gross feature emerges, in that the electron population is much lower on the methyl carbon, than on the carbon attached to nitrogen. Also, the shift in core binding energy for the C_{1s} levels of acetonitrile is reported to be small, despite the large difference in electron

Table 3.3

Shifts in ΔSCF binding energy and relaxation energy for methyl in CH_3-X

CH_3-X	C_{1s} B.E. (Shift) (eV)	R.E.	N_{1s} B.E. (Shift) (eV)	R.E.
CH_3-N≡C	2.5	0.2	0.6	0.9
CH_3-C≡N	1.8	0.3	0.5	0.7
CH_3-NO_2	1.8	0.3	6.8	0.7
CH_3-ONO	1.8	0.4	5.0	0.6
CH_3-ONO_2	2.4	0.2	7.8	1.1
CH_3-NCO	1.7	0.4	0.0	1.2
CH_3-ONH_2	0.5	0.5	-0.2	0.8
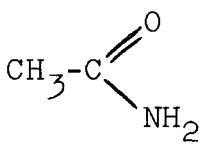	-0.2	0.5	-0.5	0.6
CH_3-NH_2	0.6	0.3	-0.8	0.6
$(CH_3)_3$-N	0.2	0.6	-1.4	1.7
$(CH_3)_3$-NO	0.7	0.7	1.7	2.0
$(CH_3)_3$-NH^+	6.6	0.4	8.0	1.5
CH_3-O-C(=O)-NH_2	1.8	0.4	0.3	0.8

C_{1s} shift referenced to CH_4 294.2 eV R.E. 11.0 eV
N_{1s} shift referenced to NH_3 409.9 eV R.E. 13.6 eV

population.

Allowing for the fact that a Mulliken population analysis is a relatively inaccurate way of describing the electron distribution about an atom as a result of the arbitrary division of overlap density (c.f. Section 1.6), in the previous work a difference of ∿1 electron between the two carbon atom populations has been noted, and this is comparable with the present study in which a difference of 0.7 electrons is

computed. The different electronic environments are however reflected in the significant difference in the computed relaxation energies. Thus for the cyanide carbon (of acetonitrile) the computed relaxation energy of 10.5 eV compares with that of 11.3 eV for the methyl carbon and indeed the computed shift in binding energy of ∿0.7 eV arises almost solely from this difference in relaxation energy. It should be noted however that the calculations predict a substantial secondary effect of the cyanide substituent upon the attached C_{1s} levels. Thus the methyl carbon in acetonitrile is predicted to be shifted to higher binding energy by ∿1.8 eV compared with methane. The gas phase data in Table (3.2) confirm these results; the shift in binding energy between the C_{1s} level of methane and the average of the two C_{1s} levels of acetonitrile being 1.9 eV; in excellent agreement with the theoretical computations.

Previous studies of acetonitrile in both the gas phase and solid state confirm that the shift in binding energy between the carbons is small and to investigate this and the large secondary shift in some detail in related systems, the core level spectra of both polyacrylonitrile and polymethacrylonitrile have been measured. The C_{1s} and N_{1s} levels are shown in Figure 3.8, and the necessity for the core level spectra of both materials to be studied, in the determination of the shifts in binding energy relative to methane, and their structural dependence, is argued as follows.

The C_{1s} core level spectrum for polyacrylonitrile may be analysed in terms of a doublet with intensity ratio 2:1, full width at half maximum of 1.4 eV, and shift in binding

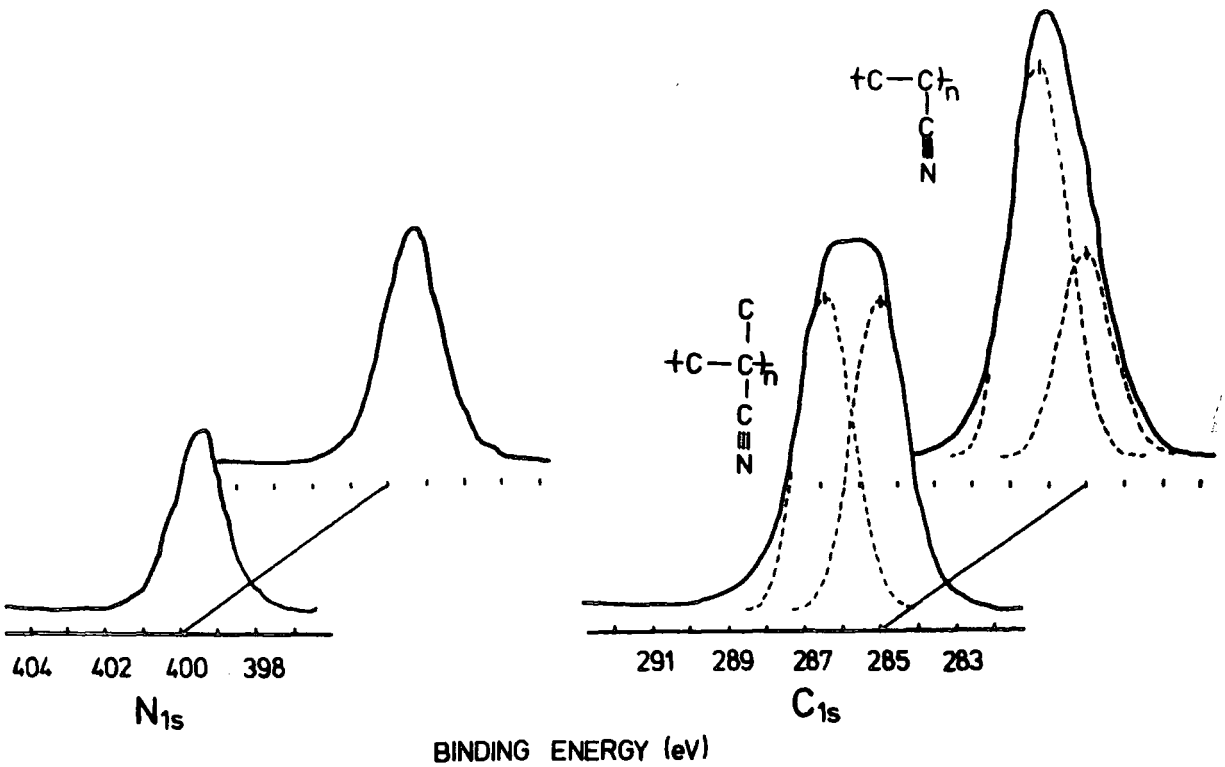

Figure 3.8 C_{1s} and N_{1s} solid phase core level spectra for polymethacrylonitrile and polyacrylonitrile

energy between the peaks of 1.3 eV, showing that either two carbons in each monomer unit in the given structure promote a shift to higher binding energy, as the theoretical calculations suggest, or that the electronic environment of the cyano-carbon in each unit is such that upon core ionisation, an uncharacteristic lowering of the binding energy to a level below that of the backbone methylene groups is observed. To clarify this situation, the C_{1s} levels for polymethacrylonitrile are directly analysed in terms of two peaks of equal intensity, corresponding to C-CN and

$\underline{C}$ - $\overset{CH_3}{\underset{|}{C}}$ respectively, with full width at half maximum of 1.4 eV and again a shift in binding energy between the two peaks of 1.4 eV. In both cases, the shifts in binding energy are comparable, and using either of the two samples, left in the spectrometer over a lengthy time period, with the cooling to the end cap of the X-ray source removed, increases the intensity of the peak at lower binding energy in the C_{1s} envelope due to deposition of the extraneous hydrocarbon in the spectrometer, onto the sample. This is a further indication that this peak arises due to core ionisation of the backbone methylene groups.

The immediate inference from this study therefore, is that if E.S.C.A. were applied to the problem of weathering in the ABS terpolymers, as previously suggested, depending upon their composition, an unusually large contribution in the region corresponding to carbon/oxygen single bonds must be rationalised in terms of two equivalent C_{1s} ionisations from the acrylonitrile unit and not one.

As previously noted, the small shift in binding energy, occurring in the acetonitrile system is attributed to relaxation phenomena accompanying core ionisation. In such a small system, only limited relaxation may occur, however in polymer systems, relaxation will be at a maximum and this is manifest in the equivalence of the binding energy upon core ionisation of both the cyano- and the adjacent carbon in both the polymethacrylonitrile and polyacrylonitrile systems. Intermediate in this effect, are the gas phase data for tertiary butyl nitrile, since the carbon envelope

is analysed in terms of three peaks. A shift of 1.3 eV between the peaks highest and lowest in binding energy compares well with the above results, however the extent of relaxation is such that the shift between the C_{1s} lineshapes for the cyano- and adjacent carbon is comparable with that calculated and observed for acetonitrile and the secondary shift at the latter is consequently considerably diminished to 0.7 eV.

The data in Table 3.3 suggest that the substituent effect of the isocyanide group is somewhat larger than for the cyanide group, and this is as expected since in terms of bonding characteristics nitrogen is a primary substituent for the former and a secondary substituent for the latter functionality. The substituent effect of a nitro group is essentially the same as for a nitrite ester and for an isocyanate group. An interesting comparison may be drawn in the series CH_3-X for which X = NH_2, $N(CH_3)_2$, $NO(CH_3)_2$, and $\overset{+}{N}H(CH_3)_2$. The effect of introducing successive methyl groups in going from X = NH_2 to $N(CH_3)_2$ is a small shift to lower binding energy by approximately 0.2 eV per methyl group which is as a direct result of parallel increases in relaxation energy. The secondary effect of oxygen is small but significant. Thus the shift on going from X = $N(CH_3)_2$ to the corresponding N-oxide is 0.5 eV and since this is accompanied by a slight increase in relaxation energy (0.1 eV) then clearly this is not due to relaxation effects.

For the isolated systems, the effect of protonation is substantial. Thus in going from X = $N(CH_3)_2$ to the protonated system the computed shift is 6.4 eV. In the

solid state, the lattice potentials will be such as to substantially reduce the shift. For example,[218] in a series of simple polypeptides, the measured shift between protonated and backbone nitrogen is only 1.5 eV compared with a predicted shift of approximately 7.5 eV, thus emphasising the importance of counterions in the lattice.

In summary, the primary substituent effect of a nitrogen functionality is markedly dependent upon the nature of the substituent and varies over a wider range than for the typical oxygen functionality. At one extreme, the effect of $N(CH_3)_2$ as a substituent is very small (0.2 eV) whilst isocyanate and nitro substituent effects are substantial (1.8 eV). The nitrile group is of special interest since the primary substituent effect of nitrogen is somewhat similar for both the singly and triply bonded carbon atoms.

3.3.2 N_{1s} Levels

It is evident from the data in Figure 3.5 and in Table 3.3 that N_{1s} core binding energies fall into distinctive regions for each functionality.

At lowest binding energy are amides and amines, whilst at highest binding energy are the oxygen containing nitrogen functionalities such as nitrate esters, nitro alkanes and nitrite esters. The binding energies for the latter 3 classes are distinctively different and whereas the primary substituent effect on C_{1s} levels of the isomeric

$-NO_2$ and -ONO functionalities are the same, the N_{1s} levels are most certainly different. This enables a ready distinction to be drawn between nitro alkanes and nitrite esters on the basis of the N_{1s} binding energies and therefore unambiguously assigns the lower binding energy component at ∿405 eV, often found in industrial scale, nitrated, cellulose samples, as being due to nitrite ester groups.[198] Having previously remarked upon the distinctive nature of the N_{1s} levels for nitrate esters, it is interesting to compare the shift in binding energy in going from a nitrite to a nitrate ester, and in going from a nitro-alkane to a nitrate ester. The shifts in binding energy are 2.8 eV and 1.0 eV respectively; the former corresponding roughly with the distinctive shift in converting a tertiary amine to its N-oxide which is 3.1 eV.

This therefore confirms that monitoring the N_{1s} core level ionisation for a series of nitrocellulose samples, as previously described, is a ready means of studying the degrees of substitution corresponding to the range of acid mixes, and E.S.C.A. studies have shown that in both the surface and the bulk, these are dependent upon the equilibrium between the nitration and denitration processes.

At intermediate binding energies between the two extremes are nitriles, isonitriles, isocyanates and urethanes. An extensive study of polyurethane based adhesives has recently been completed, and in all cases, a N_{1s} peak is found at ∿400.5 eV in binding energy. This compares with a typical amide nitrogen binding energy of ∿399.8 eV corresponding to a shift of ∿0.7 eV, in excellent agreement with the theoretically calculated shift, (0.8 eV for CH_3CONH_2 and CH_3-$OCONH_2$ using these as prototype systems).

To investigate the contribution of changes in relaxation energy to the shifts in core binding energies, consideration of the extremes of shift encompassed by the CH_3ONO_2 and $(CH_3)_3N$ systems may be considered. The difference in relaxation energies of 0.6 eV is seen to contribute ~10% to the total shift range in this case.

The theoretical data allow a comparison of the influence on core binding energies of various substituents X in the series NH_2-X and the data is collected in Table 3.4.

Table 3.4

Shifts in SCF binding energy and relaxation energy for NH_2 in the series NH_2-X

NH_2-X	N_{1s} B.E. (Shift) (eV)	R.E.
NH_2-CH_3	-0.8	0.6
$NH_2-C\equiv N$	1.6	0.4
$NH_2-\overset{\overset{O}{\|}}{C}-H$	0.3	0.7
$NH_2-\overset{\overset{O}{\|}}{C}-CH_3$	-0.5	0.6
$NH_2-\overset{\overset{O}{\|}}{C}-NH_2$	0.2	0.7
$NH_2-\overset{\overset{O}{\|}}{C}-OCH_3$	0.3	0.7
NH_2-O-H	0.6	0.4
NH_2-O-CH_3	-0.2	0.8

N_{1s} shift referenced to NH_3 409.9 eV R.E. 13.6 eV

Whilst for the C_{1s} levels the typical effect of replacing hydrogen by methyl is small, and largely dependent upon relaxation, for the N_{1s} levels, the effect is substantial, and appears generally to be unrelated to relaxation phenomena. Thus, in going from X = H to X = CH_3, X = CHO to X = $COCH_3$, and from X = OH to X = OCH_3 the computed shifts are to lower binding energy by approximately 0.8 eV in each case, whilst the accompanying relaxation energy shifts are 0.6 eV, -0.1 eV and 0.4 eV respectively. It is interesting to note, that although in general the effect of a given substituent is different for C_{1s} and N_{1s} core levels (e.g. the primary effect of singly bonded oxygen ∿1.5 eV for C_{1s} levels; ∿0.6 eV for N_{1s} levels; primarily because β-substituent effects are enhanced for the latter), in the particular case of the nitrile functionality, the shift for the attached atom (e.g. C in CH_3CN and N in NH_2CN) is virtually the same ∿1.7 eV.

3.3.3 O_{1s} Levels

In previous work,[127] and indeed in an earlier section of this chapter, it has been shown that in systems containing only carbon, hydrogen and oxygen, the shifts in O_{1s} levels fall into distinctive patterns dependent upon functionality (Figure 3.4). The data relating to the oxirane, dioxirane and 1,2,4-trioxolane systems included in this study therefore fall into this same consistent pattern with the substituent effects previously described. The nitrogen containing oxygen functionalities extend the range

of substituent effects and illustrate the considerable complexity of the interplay between the various electronic factors which determine overall shifts.

In this earlier study, it is noted that the oxygen in a carbonyl group is typically at low binding energy and the data in Figure 3.5 provides two examples which show that when nitrogen functionalities are involved, the substantial electronic effects can modify the characteristic binding energy pattern quite significantly. Thus the introduction of a strongly electron donating amino substituent in going from an amide to a urea results in a substantial shift to lower binding energy of 1.9 eV. By contrast the O_{1s} level for the isocyanate functionality is shifted by ∿1.6 eV to higher binding energy. Whilst the shifts in binding energy characteristic of the C_{1s} and N_{1s} core levels, are notably similar for the urethane and isocyanate functionalities, two components describe the O_{1s} envelope for the former, (∿532.6 eV and ∿534.4 eV in good agreement with experiment) and only one for the latter (∿534.7 eV). Since the higher binding energy component in the urethane is comparable in binding energy to the O_{1s} level for the isocyanate functionality then conceivably, a mixture of the two species would show only two components in the O_{1s} envelope, with the appreciable shift of ∿1.8 eV as previously observed. Clearly, a useful method for monitoring the urethane curing process mentioned earlier, would be to compare the intensities of these components for the mixture, on the premise that when these are equal, only the urethane system is present and the curing process is complete. The formal valence bond pairing scheme usually

written to describe N-oxides suggests substantial negative charge on the oxygen and the computed value in this case is 0.4e. In keeping with this idea, the binding energy is very low (c.f. Figure 3.5). The nitro,nitrite ester and nitrate ester functionalities form an interesting and distinctive comparison. The theoretical calculations at the STO-4.31G level suggest that the binding energies for the two oxygens in a nitrite ester should be in the order C - O - N - < - O - N - O and that the average binding energies should be higher than for the oxygens in a nitro alkane. This being the case, comparison with the experimental data shows that for the oxygen line profiles at lower binding energy, there is excellent agreement with the theoretical values. Although partially confirming the above assignment, the computed binding energy shift-difference, between the two oxygens in the nitrite ester, of 0.4 eV is somewhat smaller than that determined experimentally from the resolved spectrum (1.0 eV).

A further series of calculations using the Dunning (4s3p/2s) contraction[55] of the Huzinaga (9s5p) gaussian basis set,[54a] (c.f. Section 1.7.7) on the nitrite and nitrate esters, also confirm the above assignments and shift differences (Table 3.5).

The experimental data provides an average shift difference of 0.5 eV for the nitrite ester with respect to the nitro-alkane, compared with a theoretically computed difference of 1.0 eV. The introduction of a third oxygen, in going from a nitrite or nitro alkane to a nitrate ester is computed to give rise to shifts in binding energy of 1.3 eV

Table 3.5

Binding and relaxation energies (eV) as a function of basis set, for the nitrite and nitrate esters

	STO-4.31G			Dunning (4s3p/2s)		
	O_{1s}(RE)	N_{1s}(RE)	C_{1s}(RE)	O_{1s}(RE)	N_{1s}(RE)	C_{1s}(RE)
$CH_3\underline{O}NO$	545.4(17.6)	414.9(14.2)	296.0(11.4)	540.2(21.7)	412.1(17.7)	293.9(14.0)
$CH_3O\underline{N}O$	545.8(17.5)			540.5(21.6)		
$CH_3ON\underline{O}_2$	545.0(17.3)	417.7(14.7)	296.6(11.2)	540.0(22.0)	415.4(18.2)	294.6(13.8)
$CH_3\underline{O}NO_2$	546.7(17.7)			541.8(22.3)		

(C$\underline{O}$N) and -0.4 eV(ON$\underline{O}$) or 0.4 eV (O-N$\underline{O}$) for the former and latter respectively. One consequence of this is that the assignment for the oxygens is reversed in going from the nitrite ester to the nitrate ester. The experimental data in Table 3.2 support this assignment and the O_{1s} core level spectra for the cellulose and nitrocellulose samples (Figure 3.7) clearly show that the components due to the nitrate ester functionality are shifted to higher binding energy relative to that of the unreacted alcohol and ether groups. The shift-difference between the two line profiles at higher binding energy (intensity ratio 1:2) is $\sim$1.3 eV and compares well with the other experimental values (1.2 eV) determined. For the methyl derivative however, this shift is slightly overestimated (1.7 eV), but a good agreement is found between the theoretically calculated, absolute binding energy values for the terminal oxygens in both the nitrate and nitrite esters, and also for those of the nitro-alkane (Table 3.2). This therefore indicates that the higher absolute values of the computed binding energies, for the inner oxygens of both the nitrite and nitrate esters, (as compared to experiment, Table 3.2) may be an artefact of the extent of relaxation possible as a result of such a core ionisation in the relatively small methyl model systems.

From the limited data available, it is clear that for C_{1s}, N_{1s} and O_{1s} levels, substitution of a directly attached hydrogen by a methyl group leads to a shift to lower binding energy; the shift increasing in going from C_{1s} to O_{1s} levels (Table 3.6).

Table 3.6

ΔSCF binding and relaxation energy shifts (eV) for H, CH_3-X substitution

X	C_{1s}	RE	N_{1s}	RE	O_{1s}	RE
NH_2			-0.8	0.6		
$(NH_2 \rightarrow (CH_3)_2N)$			-1.4	1.6		
CN	-0.7	0.5	-1.3	0.5		
NC	-1.0	0.6	-0.7	0.4		
ONH_2			-0.8	0.4	-0.9	0.7
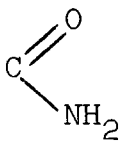	-0.7	0.4	-0.8	-0.1	0.5	-0.6

Analysis of the shifts in binding energy and changes in relaxation energies shows that the largest contribution to the shifts arises from the increased relaxation energy of the methyl substituted derivatives. While this is generally true for the atom at which replacement occurs and in many cases, at the adjacent atoms, this is not so in the case of acetamide, as previously noted. For substitution at the carbon, this is clearly the case, however whilst a decrease in the binding energy for the N_{1s} level is noted, a very slight decrease in relaxation energy is also seen and an increase is observed in the oxygen binding energy which is accompanied by an equivalent decrease in relaxation energy.

These results pertain to the eclipsed acetamide conformer in which a methyl hydrogen, the two carbons, nitrogen and

oxygen atoms are assumed co-planar, and there is a spatial distance of $\sim$2.5 Å between the co-planar hydrogen and oxygen atoms. This arrangement is calculated to be 2.3 K cal mol^{-1} more favourable in energy than the staggered conformer at the STO-4.31G level, and the resulting shifts in binding and relaxation energies are equivalent to those previously noted.

Consideration of the relative energies for the core ionised systems confirms that the eclipsed conformer is indeed the more stable form, but there is little indication that this is so, due to hydrogen bonding, or that such an interaction is responsible for the increased binding energy upon core-ionisation of the O_{1s} level relative to that of formamide.

A more detailed discussion of the arguments used in this determination will be presented in the next chapter.

CHAPTER FOUR

A THEORETICAL AND EXPERIMENTAL INVESTIGATION OF CORE IONISATION PHENOMENA IN β-DICARBONYL COMPOUNDS AND RELATED ENOL TAUTOMERS

Non-empirical LCAO-MO SCF calculations have been performed on the ground and core hole states of the C_S and C_{2v} structures for malonaldehyde, and for a range of geometries describing the acetylacetone molecule. The theoretical studies have been complemented by gas phase E.S.C.A. studies of both the O_{1s} and C_{1s} core levels for the latter. A comparison of the theoretical data for both systems with the present experimental data, and that previously available for the O_{1s} levels only, shows excellent agreement with unsymmetrical C_S enol structures. A discussion of the low energy shake-up satellites accompanying both C_{1s} and O_{1s} core ionisations is also presented and consideration is given to the relative energies of the various tautomeric models as a function of the hole state locations.

4.1 Introduction

For limited series of closely related molecules, Koopmans' Theorem (discussed in Section 2.6.1) gives an adequate interpretation of chemical shifts between core levels. However, this depends upon the fact that, for related molecules with similar valence electron distributions, relaxation energies, (ignored in Koopmans' Theorem) tend to be closely similar. If this is not the case, then

Koopmans' Theorem cannot be expected to apply. Clark and co-workers[219] have illustrated the validity of this approach in a structural determination of a mixture of the isomeric 1,1,3,4,5,6,7- and 1,1,2,4,5,6,7- heptafluoroindenes. Clearly, the complexity of such systems renders a more rigorous approach impossible, however the shifts in binding energies from charge potential type calculations showed excellent agreement with the C_{1s} E.S.C.A. spectrum if a 1:4 mixture in favour of the latter was assumed. More important, by using the experimentally determined binding energy shifts for the C_{1s} and F_{1s} levels of tetradecafluorotricyclo [6,2,2,0] dodeca-2,6,9-triene, the study demonstrated the feasibility of inversion of the process to provide experimental charge distributions. Comparison with the theoretical data by least squares analysis gave correlation coefficients better than 0.99. It is evident therefore, that although not taking part in bonding directly, core electrons nonetheless provide a convenient and instructive monitor of valence electron distributions.

The range of information levels available from the study of core electron spectra has been discussed extensively in Chapter Two, as has the time scale of the phenomena involved. However, the capability deriving from this of studying dynamic equilibria, often entailing only weak interactions, has only been exploited in a few cases.[220,27] For example, in the situation described above concerning the mixture of the two isomeric heptafluoroindenes, the 4:1 ratio was established by conventional spectroscopic techniques (^{1}H and ^{19}F n.m.r. measurements, and i.r. studies),

however these were unable to identify the major component. Since the lifetimes of core hole states are typically in the range 10^{-14} - 10^{-17}s E.S.C.A. is therefore, in principle, capable of distinguishing between non-classical and rapidly equilibrating classical cations. Olah and co-workers[220] have therefore investigated the norbornyl cation and related model systems with varying degrees of charge localisation, and these studies will be discussed in greater detail in a subsequent chapter. With the advent of instrumentation capable of generating spectra of high resolution on an extremely rapid time scale, it may be anticipated that this particular virtue of E.S.C.A. as a spectroscopic tool will be of increasing importance.

Since only a limited range of related organic and polymeric systemsof interest to chemists, may be studied within the confines of Koopmans' Theorem, and hence by the use of charge potential type calculations, it is necessary to model most functionalities by related small molecules enabling non-empirical calculations to be performed, which permit a consideration of relaxation effects as a function of electronic environment. Following earlier studies by Clark and co-workers concerning relaxation in a small number of C, O, N type molecules[221] and the halogen diatomics,[223] a more detailed investigation of C, O, systems[127] has been outlined in the previous chapter, which also provides an extensive study of nitrogen containing functionalities.

The potential energy surfaces for both the N_2 and CO molecules have also been investigated,[223] in the ground state

and as a function of core hole location. Studies for the neutral molecule have shown that these are adequately described within the Hartree-Fock formalism to varying degrees of accuracy, as a function of basis set. Changes in bondlength accompanying core ionisation, as determined by hole state calculations are also well described (viz. an increase in bondlength for O_{1s} in CO, and decreases in bondlengths for C_{1s} and N_{1s} in CO, and N_2 respectively) and as a sidelight, it was noted that better agreement with experiment was found for these and absolute binding energies if the equivalent cores approach (discussed in Section 2.6.3) was adopted. From the discussions of Section 2.6.2, it is evident that such studies are important in determining the associated vibrational fine structure accompanying core ionisation, however, a more important point, of particular relevance to this work, is that interactions which are weak (e.g. hydrogen bonds) in the ground state manifold are often enhanced on going to the core hole state manifold.[224,225]

As noted in the previous chapter, polymers which possess hydrophilic centres ($-NH_2$, $-CONH_2$, $\geq C=O$, etc.) may well become specifically contaminated at the surface by hydrogen bonded water. This was found to be evident by E.S.C.A. studies of commercially produced low density polyethylene films both before, and after desiccation.[126] The substantial signals corresponding to the O_{1s} levels exhibited an unresolved structure, one of the components of which, disappeared on storing the sample over P_2O_5. Comparison with previous studies indicated that the higher binding

energy component, which subsequently disappeared, corresponded to H_2O, while the lower binding energy peak corresponded to carbonyl oxygen. This was verified in the C_{1s} spectra where a small shoulder to the high binding energy side of the main peak ($\sim$3eV shift) was evident (c.f. previous chapter).

The study of hydrogen bonded dimers and trimers[226] also provides prototype model systems for the investigation of changes in extra-molecular contributions to relaxation energies, on going from an isolated molecule to the condensed phase. Although the hydrogen-bond strengths for the neutral H_2O systems are found to be quite small (<0.02eV), the associated shifts in core binding energies are substantial. Thus in going from the monomer to the dimer, the O_{1s} level of the component providing the hydrogen for hydrogen-bond formation decreased in binding energy, whilst the other increased, such that the computed shift was in excess of 2eV. Furthermore, the relaxation energies were in each case, noted to be larger for the associated species.

With attention thus far having been focussed upon relatively simple systems such as hydrogen bonded dimers and trimers involving first row hydrides, it is of interest to extend this work to more complicated systems, particularly those which can form stable internal hydrogen bonds. In this chapter therefore, comparisons are drawn between theoretical analyses of the core ionised states of malonaldehyde (MA), acteylacetone (acac), and their enol forms. However,

emphasis has been placed upon the study of the methyl-derivative since the structure of this system has remained a point of contention for many years.

A non-empirical investigation of the hole states of this molecule is particularly apposite at this time since experimental data has recently become available,[227,228] and semi-empirical charge-potential-type calculations have recently been reported[229] on some aspects relevant to the interpretation of the experimental data. Previous experimental gas phase, E.S.C.A. studies of the O_{1s} levels of acac reveal two main components together with a low intensity component to the low kinetic energy side. The original interpretation of the data[227] in terms of an unsymmetrical enol form with the lower intensity component being due to the presence of a small percentage of keto form has subsequently been revised in the light of data on other systems. Analysis of the O_{1s} levels of the tropolone system[228] and its methyl derivative into two peaks in ∿3:2 ratio, is indicative of the former's existence as a C_S symmetric enol form, and also that a preferential shake-up process occurs from ionisation of the lower binding energy, carbonyl oxygen, which detracts from the intensity of its assigned peak. Brown and co-workers have now suggested therefore that the low intensity component at high binding energy corresponds to $\pi \rightarrow \pi^*$ shake-up satellites accompanying core ionisation of the O_{1s} levels of the enol form.

In a recent theoretical study of the core ionised states of acac by a semi-empirical procedure of the charge potential variety,[229] the discrepancy between the computed O_{1s} core levels for the enol form of acac and the experimental data was again attributed to the presence of both keto and enol forms in the gas phase. Although the charge potential model of Maksic and co-workers also treated the likely core hole state spectra for the C_{1s} levels, no experimental data has been available to date for direct comparison. Clearly, a core hole state study of the C_{1s} levels is particularly apposite at this time, since, as outlined in the previous chapter, this should be as reliable a fingerprint of tautomeric form as the O_{1s} levels. For comparison, theoretical studies at a non-empirical level are required, since the use of semi-empirical methods for the quantitative discussion of core level data indicates thatchanges in relaxation energies are not explicitly considered. An instance[219] where such a study may be applied to gain shifts in binding energy is illustrated at the beginning of this chapter and in the previous chapter, the substantial effect of relaxation upon the shifts in carbon/oxygen systems is noted.

In view of this, included in this chapter are detailed experimental (gas phase) E.S.C.A. spectra for the C_{1s} and O_{1s} levels of acac, and comparisons are drawn between the results of *ab initio* ΔSCF computations for the core hole states, of the various models, for the above system and those of MA.

The following points of interest have been considered:

(i) the computed (ΔSCF) core binding and relaxation energies for the C_{1s} and O_{1s} levels of acac and MA, and their various possible tautomeric structures, and comparison of these results with the experimental data;

(ii) the change in potential energy surfaces for the internally hydrogen bonded, tautomeric enol models as a function of the hole state; and

(iii) the investigation of possible low energy shake-up satellites accompanying C_{1s} and O_{1s} core ionisation in the enol model systems.

4.2 Computational and Experimental Considerations

4.2.1 Computational Details

The calculations were once again performed using the ATMOL 3 suite of programs (Section 1.8), and since only shifts in core binding energies and differences in relaxation energies were required, these were adequately described using the basis set and exponents employed in the previous chapter. The ground and localised core hole state computations for proposed C_S and C_{2v} MA structures[230] are compared with various tautomeric models for acac. The geometries used for the latter are a representation of those suggested by both experimental and theoretical studies, incorporating asymmetric C_S and symmetric C_{2v} enol forms, and the diketone. These include the proposed structures for the keto and enol tautomers from

an electron diffraction study by Lowrey *et al*,[231] along with the non-linearly, hydrogen bonded, symmetric form proposed from an extensive INDO geometry optimisation carried out by Gordon and Koob.[232] Geometries for the two asymmetric enol tautomers were taken from a theoretical investigation by Catalan *et al*,[233] using *ab initio* methods to determine the potential energy curve for malonaldehyde as a function of O-O distance; and substituting the hydrogen atoms of the aldehyde groupings by methyl groups, assuming standard bond lengths and angles. The geometry for the second tautomer was modified by rotation of the enolic hydrogen 30° out of the plane of the molecule about the C-O bond.

4.2.2 Experimental Details

Gas phase spectra were recorded on an AEI ES 200 AA/B spectrometer using a gas cell designed specifically for the purpose. The cell, basically a titanium cube with a central chamber, connecting input- and output-ports of flexible tubing extended by two lengths of non-magnetic stainless steel tubing, and with a variable slit and window assembly, was designed such that it interlocked with the cold cap at the end of the X-ray source. Its installation involved the removal of the insertion locks, which were refitted around the extended input- and output-tubing.

Clearly, in operation an independent flow system is possible, but in this case it was preferred that the output aperture be closed and differential pumping occured via the slit, and sample chamber of the spectrometer. The vapour was introduced through a leak valve, which regulated the sample chamber pressure to $\sim 5 \times 10^{-6}$ torr. Spectra were recorded using a $Mg_{K\alpha_{1,2}}$ X-ray source operated at 12 KV and 15 mA (c.f. Section 2.2.1) in the fixed retardation ratio mode (FRR) of scanning (c.f. Section 2.3.3). Referencing, as also described in Chapter Two, was achieved by leaking argon into the system, and under the conditions of the experiment, the $Ar_{2p_{3/2}}$ core ionisation of 248.6eV binding energy, used for this calibration, had a full width at half maximum of 1.3 eV.

4.3 Results and Discussion

The electronic structure of simple diketones and corresponding enol forms has been the subject of much theoretical work over the past few years.[229-233] However little attention seems to have been paid to the direct theoretical investigation of the energetic stabilising effect, of the internal hydrogen bonding in the enol form. Experimental estimates for the strength of this intramolecular hydrogen bond in the enol form of acac are suggested to be in the region of $\sim$10Kcal mol^{-1},[234] and on this basis alone, the presence of significant proportions of keto-form in gas phase E.S.C.A. studies is not likely.

At present, there is considerable interest in the nature of the potential function describing this bond. A single well potential function is indicative of a C_{2v} geometry whilst a double potential well would describe a C_S structure. The INDO semi-empirical study by Gordon and Koob[232] has suggested that acac has C_{2v} symmetry in the gas phase and indeed this was supported by electron diffraction determinations by Lowrey *et al*,[231] who further suggested that the OHO arrangement was linear in nature. Whilst electron diffraction is relatively insensitive to the position of light nuclei such as hydrogen, support for the symmetrically hydrogen bonded enol forms is evident in the semi-empirical studies of the MA system by Catalan *et al*.[233]

In contrast, Roos and co-workers[230] extended the CNDO/2 calculations of Schuster,[235] allowing full geometrical optimisation of the MA system and obtained qualitatively similar results, which showed stabilisation of the C_S tautomer by $\sim$2 Kcal mol^{-1}. A further series of calculations at an *ab initio* level were in agreement with later non-empirical studies performed by Catalan and co-workers,[233] which have suggested that for the enol form of MA there is a double potential well, the computed barrier height with respect to the C_{2v} form being $\sim$11 Kcal mol^{-1}. The latter study also concluded that single potential minima (viz. a symmetrically hydrogen bonded system) tend to be artefacts of semi-empirical treatments, and the non-empirical investigations published to date agree that in the particular case of malonaldehyde, the intramolecular hydrogen bond is unsymmetrical (C_S symmetry).

Comparable computations have not been reported for acac itself, however it is interesting to note that from a consideration of the ^{2}H spin-lattice relaxation times, determined for the enol form of acac and its perdeuterated analogue, in detailed n.m.r. studies,[234] the deuterium quadrupole coupling constants, are calculated to be in the region 150-210 kHz. Since those of single minimum type are noted to be of ∿5 kHz as compared to a range of ∿100-200 kHz for quadrupole coupling constants corresponding to hydrogen bonds of the double minimum type, then the acac structure in the solution phase is unambiguously assigned as being of C_S symmetry.

With this background therefore consideration will be made, firstly of the computed ground state energies for the keto and enol systems for which *ab initio* computations have been carried out. Discussion will then be made of the C_{1s} and O_{1s} hole state spectra and a comparison made with the experimental data. Since, as outlined above, non-empirical methods have established the structure of MA as being of C_S symmetry, it is of interest to compare the results for hole state calculations on the above system with those for acac.

4.3.1 Ground State Energies

The total energies and configurations for the acac models studied in this work are shown in Figure 4.1.

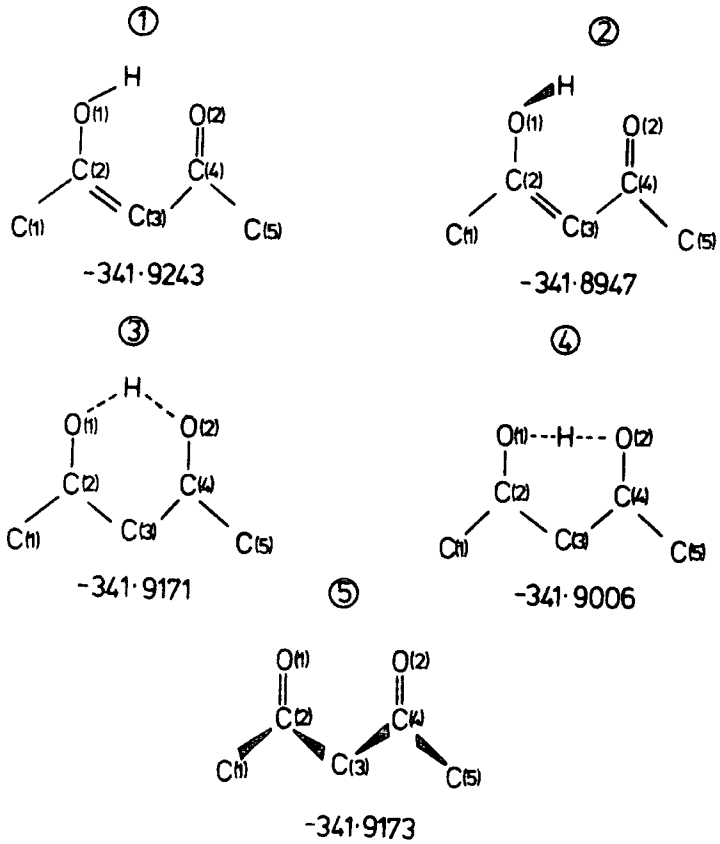

Figure 4.1 Total energies and configurations for the acac models studied

The unsymmetrical (C_S) internally hydrogen-bonded system is calculated to be 4.4 Kcal mol^{-1} more stable than the keto form. Two models which have previously been proposed in the literature for symmetrically (C_{2v}) hydrogen-bonded systems have also been studied and from this it would appear that the non-linear hydrogen-bonded system (enol 3) is greatly preferred in equilibration between the unsymmetrical structures (enol 1), to the linear system (enol 4) proposed on the basis of electron diffraction studies.

This is consistent with the *ab initio* theoretical investigations of the simpler MA system.

The internal hydrogen bond is unusually strong and in keeping with this, rotation about the C(2)-O(1) bond to displace the hydrogen from the planar 6-membered ring configuration by 30^{o} leads to an energy increase of 18.6 Kcal mol^{-1}. The relevance of this distortion to the discussion of the core hole state spectra will become apparent in a later section. A 10^{o} distortion from planarity however involves $\sim$2.5 Kcal mol^{-1} increase in energy. Complete rotation about the C(2)-O(1) bond removes the hydrogen bond contribution to the total energy and since the hydrogen and methyl substituent at C(2) are then in close proximity, the energy difference for this configuration with respect to the planar internally hydrogen-bonded system is increased to $\sim$35Kcal mol^{-1}.

4.3.2 Core Hole State Spectra

Previous experimental investigations[227,228] of corehole states, have concentrated on the O_{1s} core levels in the belief that the distinctive nature of these core levels and the inherently rapid time scale of the phenomena would lead to an unambiguous assignment of structure. There appears to have been no previous investigation of the C_{1s} core level spectra, and in order to present a consistent picture, the gas phase spectra for acac have been measured, and these are displayed in Figure 4.2.

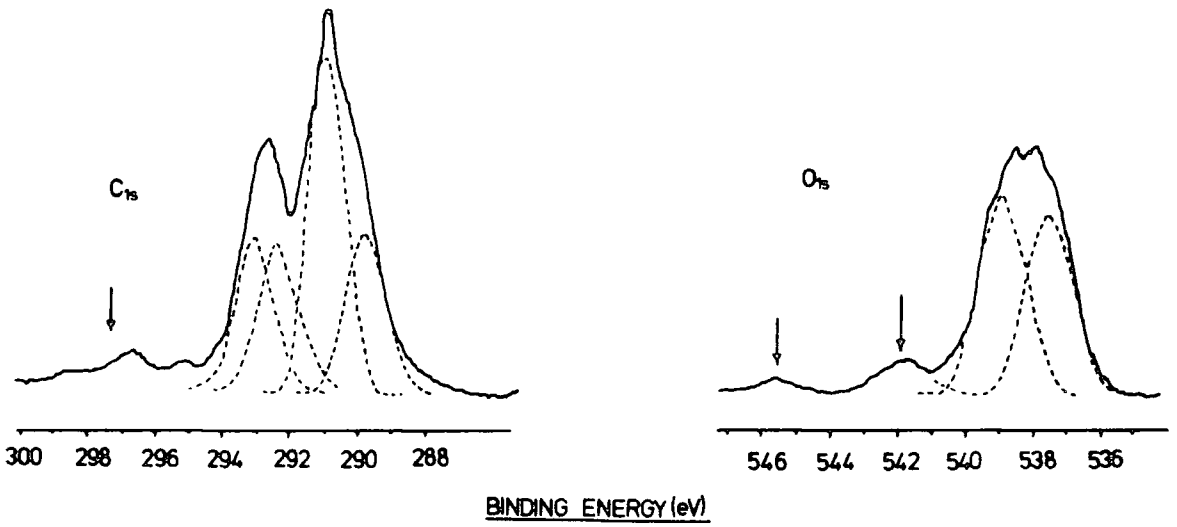

Figure 4.2 C_{1s} and O_{1s} gas-phase core-level spectra for acetylacetone

The O_{1s} levels are qualitatively similar in shape to those previously reported by Brown and co-workers for both acac[228] and MA,[227] however since the FWHM is substantially lower than for previous investigations, slightly more detail becomes apparent. Line shape analysis of the main unresolved peak provides two components of relative intensity 1.1:1 with an energy separation of 1.3eV; the FWHM for the components being identical (1.4eV). The O_{1s} levels also show evidence for satellite structure to the low kinetic energy

side of the main photoionisation peak, as reported previously.

Analysis of the O_{1s} levels of the tropolone system and its methyl derivative into two peaks in ~3:2 ratio, as previously outlined, has demonstrated its existence as a C_S, unsymmetrical enol form and also that a preferential shake-up process occurs from ionisation of the lower binding energy, carbonyl oxygen, which detracts from the intensity of its assigned peak. Clearly, where the lower intensity peak for acac is that at lower binding energy, then this is in agreement with the above analysis. For MA however, whilst the main photoionisation peak is resolved into two components of unequal intensity, (0.96:1.0) that at lower binding energy is also reported to be of higher intensity, and these values are inconsistent with the extent of satellite structure also evident. Since the O_{1s} spectra for the MA and acac systems are qualitatively similar then it is conceivable that the former may be re-analysed in a manner similar to that of the latter and a preliminary investigation of the reported spectra indicates that this is possible. The line shape subjected to a computer deconvolution by Brown has therefore been re-generated from a consideration of the reported FWHM, relative intensities and shifts in binding energy for its components (Figure 4.3).

The solitary nature of the satellite component suggests that the FWHM proposed by Brown (1.6eV) is a reasonable value and this estimate will be used for all three components in

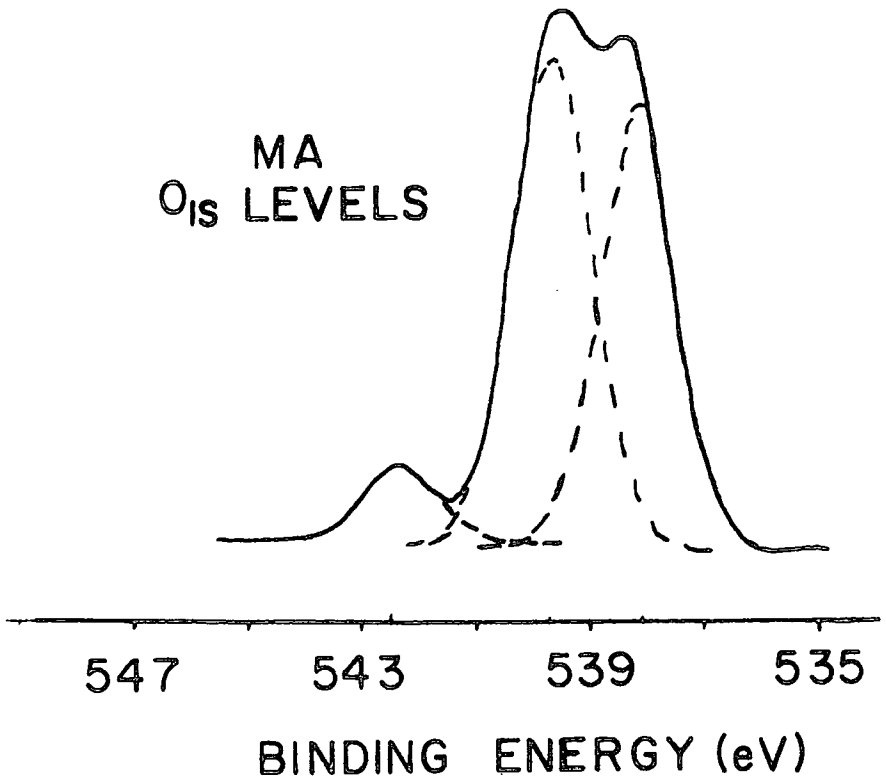

Figure 4.3 The O_{1s} core level spectrum for MA

the re-deconvolution, the reason for this will become apparent in a later section. The main photoionisation peak is resolved into two components (shift 1.6eV) with intensity ratio 1.0:0.87, that corresponding to the carbonyl oxygen, at lower binding energy being the lower in intensity. An intensity of 0.13 for the satellite structure relative to the more intense component is now consistent with the detraction of intensity from the lower binding energy peak, and this will be further discussed in a later section.

The C_{1s} levels for the acac system consist of two major components and line shape analysis shows that there are four individual components of relative intensity 1:1:2.3:1; the FWHM for each component being 1.3eV. There is also evidence for satellite structure to the high binding energy side and once again, this will be discussed in a subsequent section. It should be noted however that even in the absence of any detailed theoretical treatment, the data are only compatible with an enol structure (c.f. the discussions concerning relative intensities of components within an envelope and their relationship to functionalities in a given structure - Chapter Three).

4.3.3 Core Hole State Energies

Discussion in the literature has largely centred on the distinctive nature of the O_{1s} levels,[227,228] however previous assignments have rested either in comparison with Koopmans' Theorem for the MA system,[230,233] or on results of semi-empirical calculations[229] which do not explicitly consider changes in relaxation energies. The experimental data presented in this Chapter for the O_{1s} levels of acac are slightly different than those previously documented in the literature both in terms of the relative intensities of the two major components, their FWHM and their separation.

The total energies computed for the C_{1s} and O_{1s} core hole states of enol forms 1-3 and of the keto form are given in Table 4.1, whilst Table 4.2 lists the absolute binding and relaxation energies.

TABLE 4.1 Total energies (eV) for the ground states and C_{1s} and O_{1s} core hole states for the acac models studied.

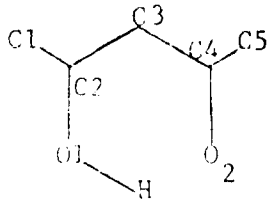

ENOL

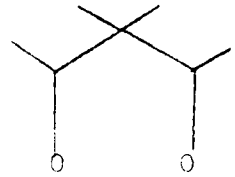

KETO

		1	2	3	4	
	GS	-341.9243	-341.8947	-341.9171	-341.9006	-341.9173
	C1	-331.1057	-331.0741	-331.0959	-331.0798	-331.1016
	C2	-331.0452	-331.0183	-331.0222	-331.0005	-331.0078
Hole States	C3	-331.1620	-331.1303	-331.1443	-331.1254	-331.0951
	C4	-331.0189	-330.9975	-331.0222	-331.0005	-331.0076
	C5	-331.1089	-331.0842	-331.0959	-331.0798	-331.1016
	O1	-321.9391	-321.8895	-321.9612	-321.9296	-321.9466
	O2	-321.9730	-321.9577			

TABLE 4.2 ΔSCF core binding energies, relaxation energies and completed shifts (eV) for the Acac configurations

	ENOL				KETO	EXPT.	SHIFTS ENOL				KETO	EXPT.
CORE HOLE	1	2	3	4			1	2	3	4		
O1*	538.2 (17.6)	538.8 (17.5)	537.4 (18.1)	537.8 (17.8)	537.8 (17.8)	538.7	-0.7	-0.1	-1.5	-1.1	-1.1	-0.2
O2*	537.3 (18.2)	536.9 (18.3)	537.4 (18.1)	537.8 (18.2)	537.8 (17.8)	537.4	-1.6	-2.0	-1.5	-1.1	-1.1	-1.5
C1*	291.0 (11.6)	291.0 (11.6)	291.1 (11.6)	291.0 (11.6)	290.9 (11.6)	290.7	0.2	0.2	0.3	0.2	0.1	-0.1
C2*	292.6 (12.2)	292.6 (12.3)	293.1 (12.0)	293.2 (12.1)	293.5 (11.5)	292.3	1.8	1.8	2.3	2.4	2.7	1.5
C3*	289.5 (12.0)	289.5 (12.1)	289.7 (12.1)	289.8 (12.1)	291.1 (11.9)	289.5	-1.3	-1.3	-1.1	-1.0	0.3	-1.2
C4*	293.3 (11.7)	293.1 (11.7)	293.1 (12.0)	293.2 (12.1)	293.5 (11.5)	293.0	2.5	2.3	2.3	2.4	2.7	2.3
C5*	290.9 (11.6)	290.8 (11.6)	291.1 (11.6)	291.0 (11.6)	290.9 (11.6)	290.7	0.1	0.0	0.3	0.2	0.1	-0.1

O_{1s} referenced to MeOH Expt. 538.9

C_{1s} referenced to Methane Expt. 290.8

As noted earlier, ΔSCF computations at the STO - 4.31G level accurately reproduce shifts in binding energy, although absolute relaxation energies are somewhat underestimated, and in order to correct for this, binding energies have been referenced to CH_4 (for C_{1s} levels) and to CH_3OH (O_{1s} levels) both at the vacuum level.[71,236]

Considering firstly the O_{1s} levels, it is clear that the experimental data are only compatible with a C_S enol form. For enol 1, the calculations unambiguously assign the higher binding energy (slightly more intense) component to the enol oxygen O(1), O(2) being at significantly lower binding energy (energy separation 0.9 eV). This is in agreement with the assignment based on the semi-empirical calculations reported by Maksic and co-workers.[229] The symmetrical enol form (enol 4) is predicted to have an O_{1s} binding energy which is closely similar to that of the keto form, and this indicates that if the O_{1s} levels did not have a doublet structure, then it might well have been difficult, on the basis of the O_{1s} levels alone, to decide between alternative keto and enol forms of C_{2v} symmetry.

The results of equivalent calculations on the C_S and C_{2v} conformers of MA which relate to enols 1 and 3 of the acac system are also compared with the revised experimental data of Brown and co-workers.[227] (Table 4.3)

Clearly, the experimental data (once again only the O_{1s} levels have been reported) confirm the assignment of previous theoretical studies in that they are only compatible with an

Table 4.3

ΔSCF core binding energies, relaxation energies and computed shifts (eV) for the C_S and C_{2v} conformers of Malonaldehyde

				Shifts		
Core Hole	C_S	C_{2v}	Expt.	C_S	C_{2v}	Expt.
O(1)*	539.6(17.2)	538.3(18.0)	539.7	0.7	-0.6	0.8
O(2)*	537.8(18.2)	538.3(18.0)	538.1	-1.1	-0.6	-0.8
C(2)*	293.1(12.0)	293.6(11.7)	-	2.3	2.8	-
C(3)*	290.3(11.9)	290.2(11.8)	-	-0.5	-0.6	-
C(4)*	293.8(11.2)	293.6(11.7)	-	3.0	2.8	-

O_{1s} referenced to MeOH Expt. 538.9

C_{1s} referenced to Methane Expt. 290.8

unsymmetrical, C_S, enol form. As in the case of acac, the computations assign the higher binding energy component to the enol oxygen O(1), O(2) being at lower binding energy with an energy separation of 1.8 eV. The assignment is again consistent with that of Maksic and co-workers,[229] and the shift in binding energy between the two line profiles is in good agreement with experiment (1.6 eV). In terms of absolute binding energies, for MA there is fairly good agreement with experiment, especially for O(1), however the slight deviation in energy shift between the two O_{1s} levels appears to accrue from an underestimation of the absolute binding energy for O(2) in the C_S form. By contrast, in the acac system, (enol 1) for O(2) of the corresponding C_S form, the absolute binding energy is in excellent agreement with the experimental data; however, the shift is slightly smaller (0.9 eV) than that observed experimentally (1.3 eV).

To investigate how this might be influenced by the planarity of the ring system, ΔSCF computations were carried out on the system with 30^{o} displacement of the O(1)-H bond as illustrated in Figure (4.4).

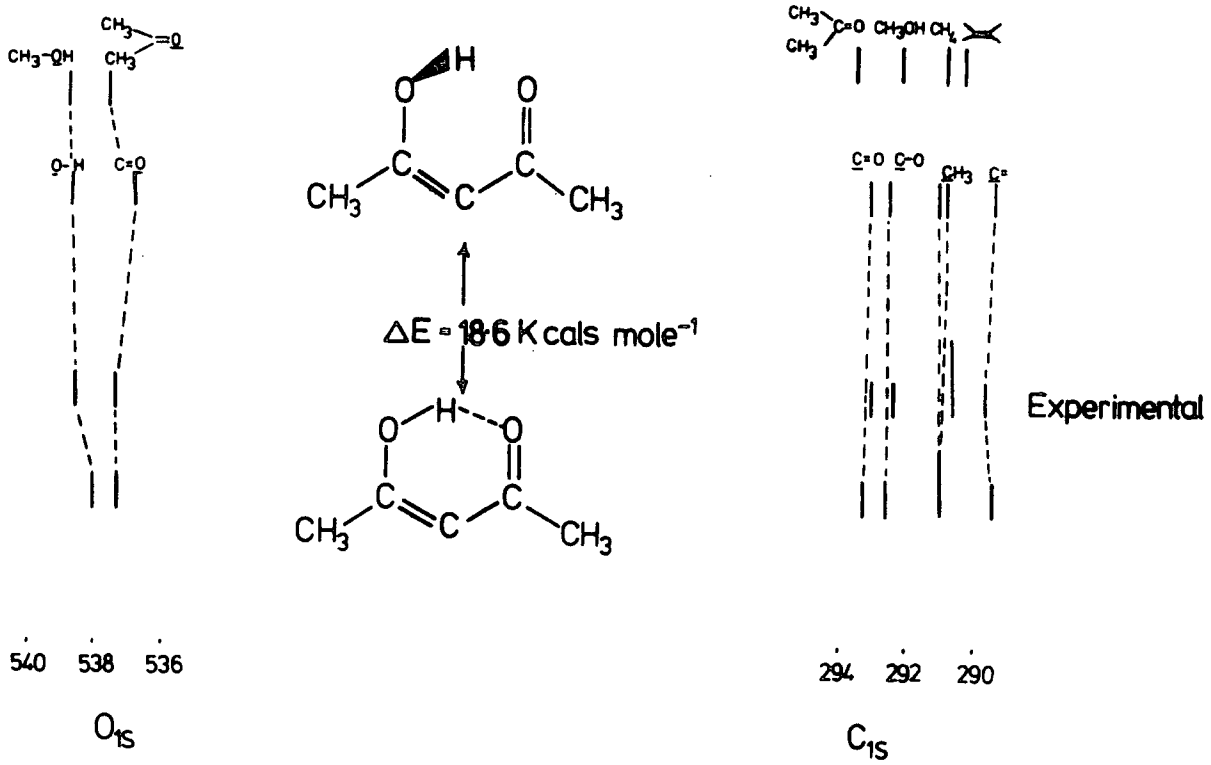

Figure 4.4 An illustration of the shifts in BE as a function of planarity

For comparison, data for the binding energies of systems relating to each functionality are also included, from Figure 3.4.

In the non-planar system, the O_{1s} shift increases substantially to 1.9 eV and this arises from a shift of O(1) to higher binding energy, of 0.6 eV and a shift to lower binding energy of O(2) of 0.4 eV compared with the planar unsymmetrical structure (enol 1). The fact that the shifts bracket the experimentally determined data both in an absolute and relative sense is interesting and suggests that a relatively small deviation from planarity could qualitatively account for the observed data. This is not inconceivable since from a previous computation it was noted that a 10° deviation from planarity gives rise to a small energy increase and it could well be the case, that the energy minimum lies in the region between 0 and 10° from planarity. Since correlation energy effects (c.f. Section 1.5.1) are likely to be important in determining such small energy differences for different conformers, speculation may only be made as to the likely energy minimum, however the E.S.C.A. data would suggest that the system may not be planar, although deviations from planarity must be small.

The C_{1s} core level data are distinctively different for the keto and enol forms and this is best illustrated in Figure 4.5, the striking feature being the very low binding energy for the vinylic C(3) carbon which as population analyses show, carries significant negative charge (Figure 4.6).

The symmetrical enol system shows some differences with respect to the unsymmetrical enol forms, particularly for C(2) (C(4)) and this is confirmed in the MA data. The C_{1s} levels are relatively insensitive to the displacement of the

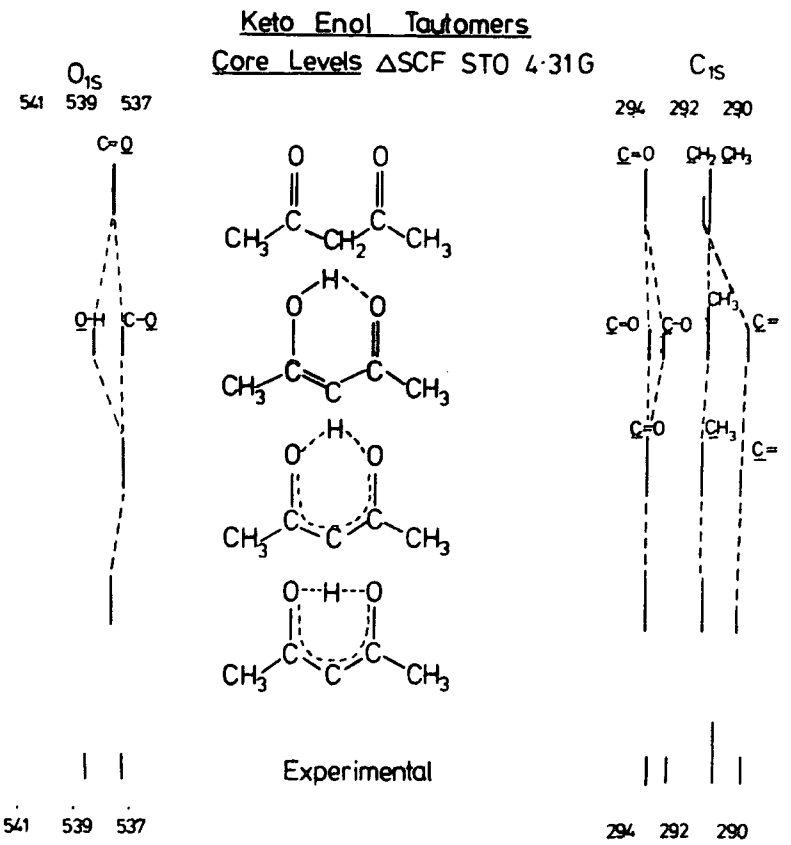

Figure 4.5 A comparison of the C_{1s} and O_{1s} BE shifts for the keto and planar, enol forms of acac

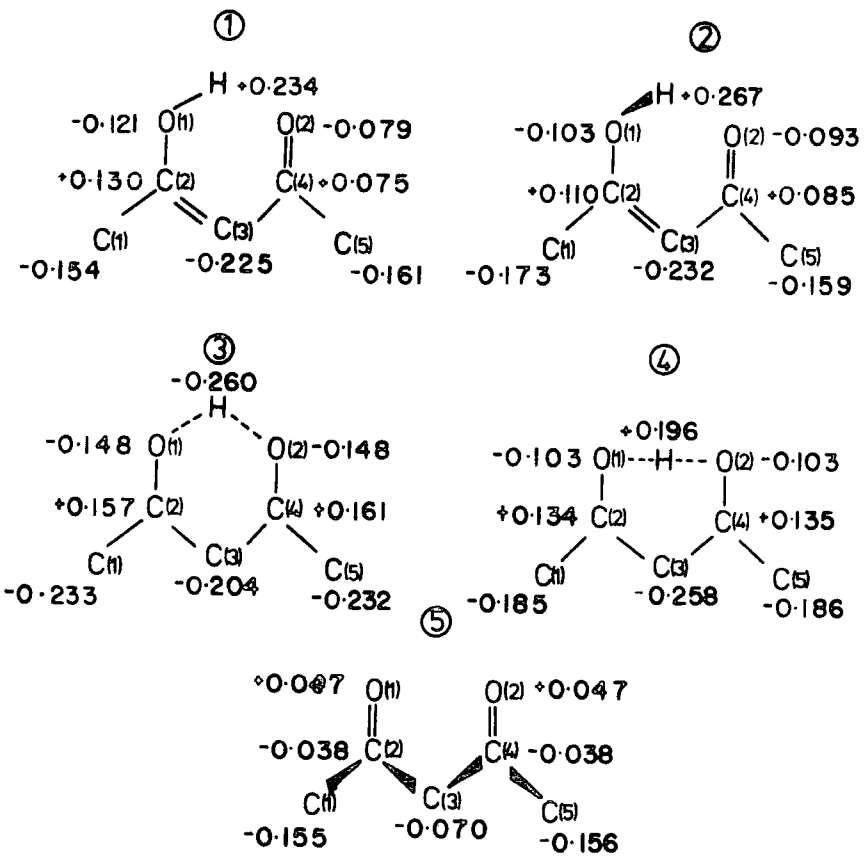

Figure 4.6 Charge distributions for the models studied

O(1)-H bond from the plane of the ring. Thus the computed absolute and relative binding energies for enols 1 and 2 are virtually the same.

The comparison with the experimental data (at this time only available for acac) is striking, the agreement being within $\pm$ 0.3 eV. A general comparison of the core level data for enols 1 and 3 with those of the MA system, shows a lowering in binding energy in each instance, consistent with the increased relaxation upon substitution of a hydrogen atom by a methyl group, as outlined in the previous chapter. This is particularly evident in the adjacent enol and carbonyl, carbons which are shifted to higher binding energy by 0.5 eV in both the C_S and C_{2v} forms of MA. Since the shifts in binding energy compare readily with those observed for the acac system and these are in turn, in good agreement with experimental data, it is not inconceivable that the data for MA will be a good representation of the experimental data also.

The results for the C_{1s} levels therefore complement those for the O_{1s} levels and both lead unambiguously to the assignment of unsymmetrical, internally hydrogen-bonded, enol forms for acac and MA, the O_{1s} data for the former further suggesting a small deviation from planarity. It is interesting to compare the results of the ΔSCF computations with assignments based on a charge potential model as described by Maksic and co-workers.[226] The total span in C_{1s} binding energies from the ΔSCF calculations are 3.8 eV for acac (enol 1), in excellent agreement with the experimental data

(3.5 eV), and 3.5 eV for the C_S form of MA. By contrast, the semi-empirical calculations underestimate the total spreads in C_{1s} binding energies (2.3 eV and 2.0 eV respectively) by some 50%.

The semi-empirical calculations based on MINDO/3 unfortunately also lead to an incorrect ordering of the core levels for enol 1 of the acac system. Thus the methyl carbons are predicted to have virtually the same binding energy as C(3) and this is incompatible with both the *ab initio* ΔSCF treatment and with the experimental data. The latter reveals a distinctive asymmetry to the low binding energy side of the main component of the C_{1s} levels arising from C(3) and the methyl carbons respectively, (experimental shift -1.2 eV, ΔSCF -1.1 eV and semi-empirical 0.0 eV). Part at least of this discrepancy can be traced to differences in relaxation energies. For enol 1 and the C_S form of MA for example, the various C_{1s} levels span a difference of 0.6 eV and 0.8 eV in relaxation energies respectively and this also points to the deficiencies of Koopmans' Theorem in attempting any quantitative comparison with the experimental data, as previously suggested.

4.3.4 Relative Energies of Tautomers as a Function of Hole State

In view of the examples at the beginning of this chapter (N_2 and CO), it is clear that the substantial reorganisation of valence-electron distribution accompanying core ionisations substantially modify potential energy surfaces.

To reiterate an earlier discussion, in the particular case of simple hydrogen bonded systems, hydrogen bond energies can be substantially different in the ground and core hole state manifolds consequent upon the change in electron demand brought about by creation of a core hole. It is therefore of interest to investigate the relative energies for unsymmetrical and symmetrical hydrogen bonded enol forms for MA and acac, together with the keto form of the latter as a function of the location of the core hole. The relevant data are collected in Table 4.4 (MA) and Table 4.5 (acac).

Table 4.4

Relative energies (K cal mol^{-1}) for the C_S and C_{2v} enol forms of malonaldehyde as a function of core hole location

	Species	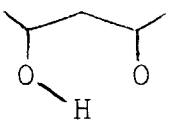	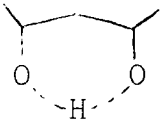
	GS	(0)	3.5
Hole States	O(1)	(0)	-27.3
	O(2)	(0)	14.2
	C(2)	(0)	16.0
	C(3)	(0)	2.9
	C(4)	(0)	-0.1

For the ground state, the C_S tautomer is the more stable for MA at this level, whilst for acac theenergies are in the order enol 1< keto< enol 3< enol 2 (enol 2 with the O1-H bond twisted 30^{o} with respect to the plane).

Table 4.5

Relative energies (K cal mol^{-1}) of the unsymmetrical and symmetrical hydrogen-bonded enol forms and the keto form of acetyl-acetone as a function of core hole location

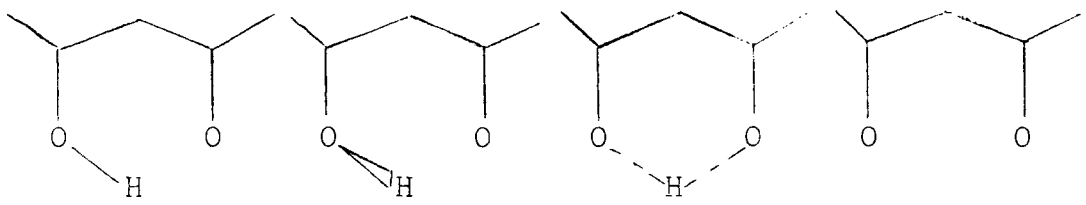

	SPECIES		RELATIVE ENERGIES (Kcal mol^{-1})		
	GS	(0)	18.6	4.5	4.4
	O1	(0)	31.1	-13.9	-4.7
	O2	(0)	9.6	7.4	16.6
	C1	(0)	19.8	6.1	2.6
Hole	C2	(0)	16.9	14.4	23.5
States	C3	(0)	19.9	11.1	42.0
	C4	(0)	13.4	-2.1	7.0
	C5	(0)	15.5	8.2	4.6

Considering firstly the relative energies of the enol 1 and keto forms, creation of a C_{1s} core hole at C(1), C(4) and C(5) lead to very little change in the relative energies whilst creation of a core hole at O(1) stabilises and at O(2), C(2) and C(3) destabilises the keto form with respect to the enol 1. This emphasises the fact that it is not only the hydrogen bond component which contributes to the energy difference between the enol 1 and keto forms. Thus from simple model systems[225] it is known that creation of a core hole on the atom to which the hydrogen involved in hydrogen bonding is attached leads to an increase in hydrogen bond

energy whilst creation of a core hole on the atom providing the lone pair for the hydrogen bond leads to a substantial decrease in bond energy. Naively therefore it might be anticipated that creation of a core hole on O(1) would lead to an increased hydrogen bond energy and hence greater energy stabilisation of the enol 1 compared with the keto tautomer, the reverse being expected in the case of creation of a core hole at O(2). If other factors were equal, this is just the effect which would be produced.

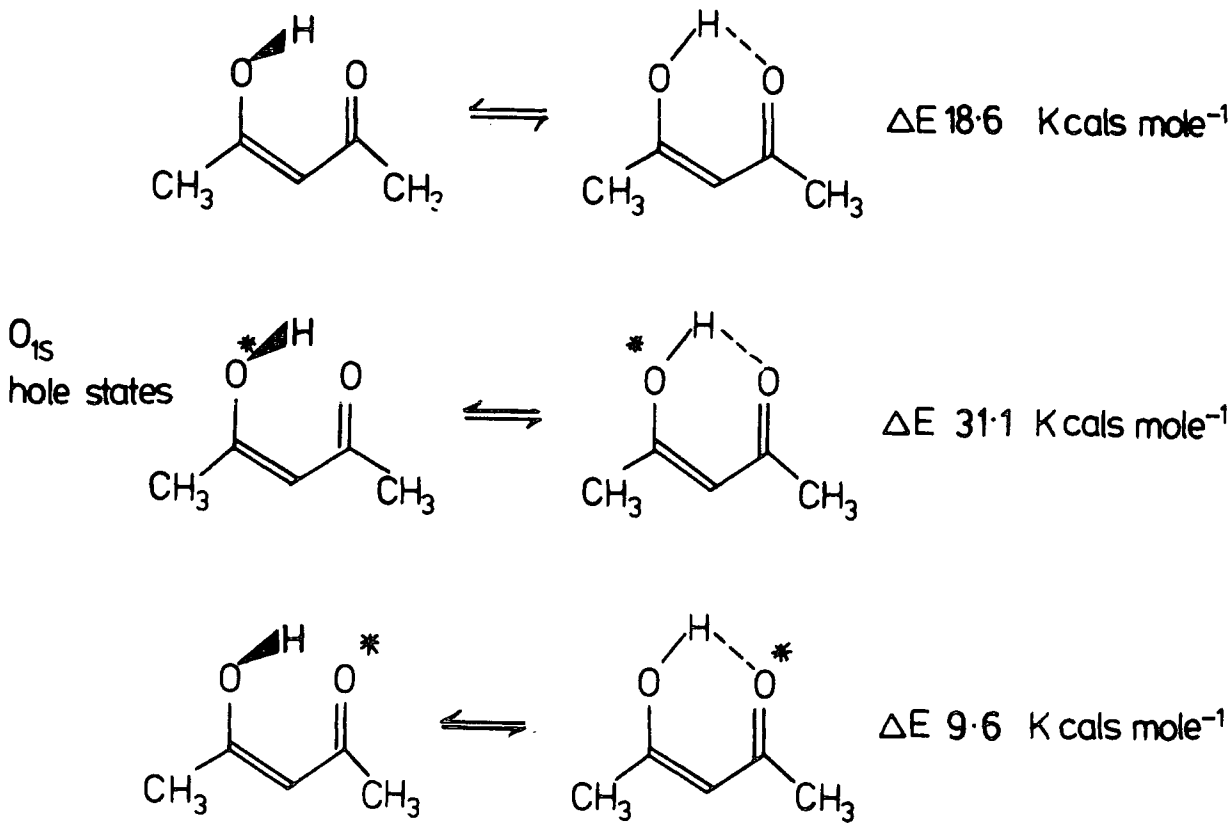

Figure 4.7 Comparison of the relative energies of enol 1 and enol 2 as function of O_{1s} hole states

Thus comparison of the relative energies of enol 1 and enol 2 (Figure 4.7) shows that creation of a core hole on O(1) stabilises the planar hydrogen bonded system by $\sim$12 K cal mol^{-1} compared with the ground state, whilst for the O(2) core ionised system a destabilisation of $\sim$9 K cal mol^{-1} is computed. For comparison, data for the changes in hydrogen-bond energies for core ionisation in the water dimer[226] are also included in Figure 4.8.

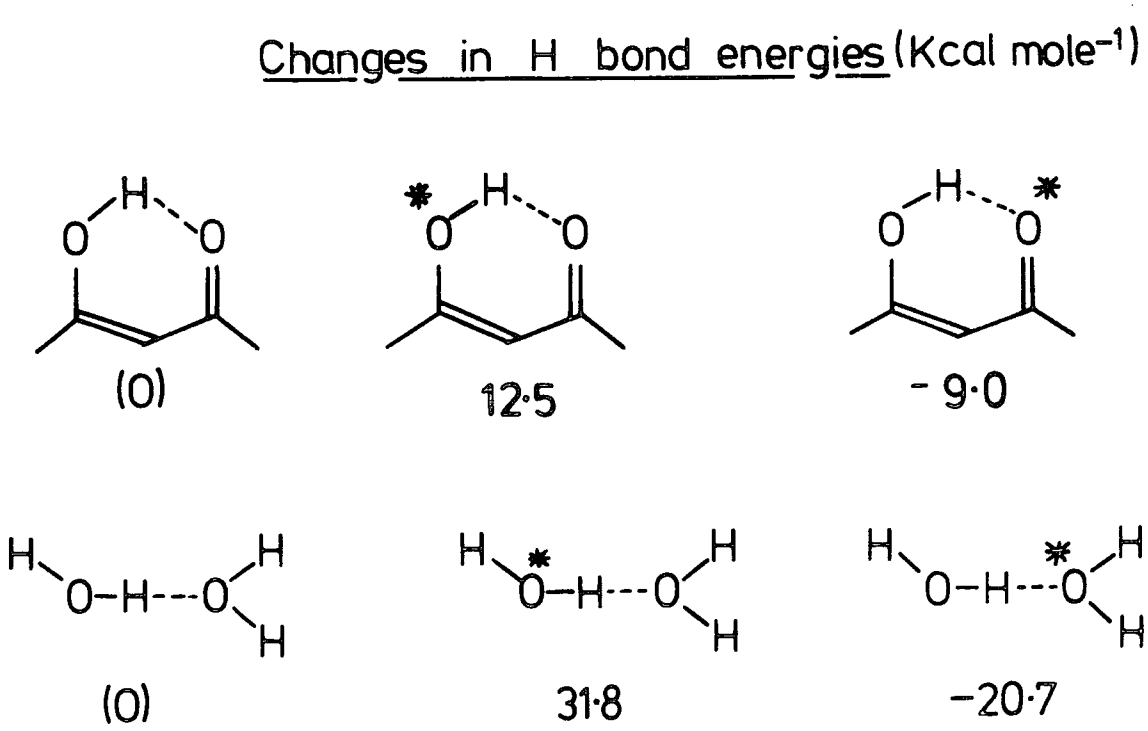

Figure 4.8 Changes in H-bond energies as a function of hole state (K cal mol^{-1})

The different bonding situation in the keto form compared with the enol, and its response to core ionisation cannot therefore be straightforwardly inferred from a consideration of the portion of the system involved in hydrogen bonding. Creation of a core hole on O(1) and to some extent C(4) leads to stabilisation of the symmetrical hydrogen bonded systems with respect to the unsymmetrical enol 1 and the corresponding C_S tautomer of MA, whilst for the O(2) hole states and those of C(1) and C(5) in acac, there is little change with respect to the ground-state energy differences (Figure 4.9).

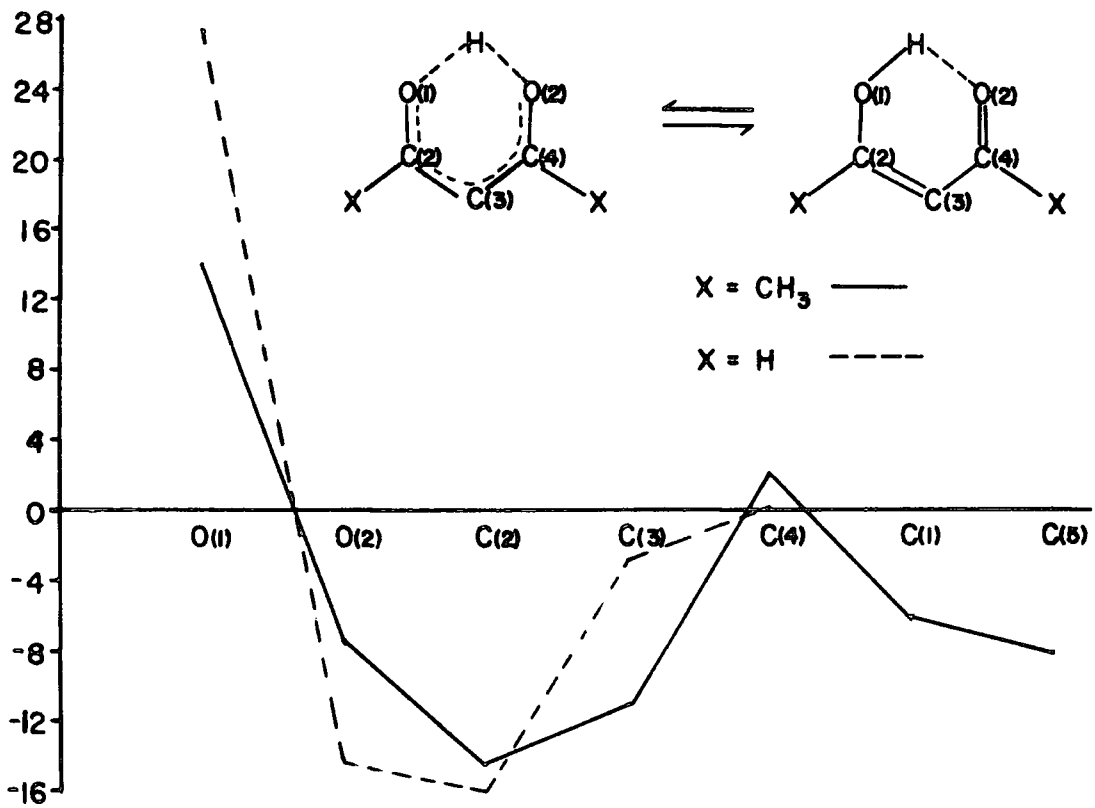

Figure 4.9 Comparison of the relative energies (K cal mol^{-1}) of enol 1 and enol 3, and the C_S and C_{2v} forms of acac and MA as a function of core hole location.

Creation of core holes at C(2) and C(3) however, leads to significant destabilisation of the symmetrical hydrogen bonded system for acac but this is only seen in the case of C(2) in MA, with little change for C(3).

The line shape analysis of the experimental envelope for the O_{1s} levels recorded in this work may be adequately described in terms of two dominant components of the same FWHM. Differences in line-width can conceivably arise from two main effects (assuming that spectra are recorded at sufficiently low pressure such that formation of dimers, etc. is unimportant) namely, differences in lifetime for the core hole states, (Section 2.5.2), and secondly from vibrational effects (Section 2.6.2).

The question of differences in lifetime for a given core hole state as a function of electronic environment has only received qualitative discussion in some simple systems[237] since in general there have been no detailed theoretical investigations of Auger transition rates which dominate lifetime effects for molecules containing first row atoms.

It is interesting to note, that the total electron population on O(1) is very similar to that on O(2) (Figure 4.6) and the computed relaxation energies are also almost the same. This would tend to suggest that major differences in lifetime would be unlikely. The 0.3 eV difference in FWHM proposed by Brown and co-workers[228] if attributed solely to differences in lifetime effects would require a difference in lifetime for the two hole states well in excess of an order of magnitude, as is apparent from a consideration

of the Uncertainty Principle (Section 2.5.2). The other factor which could also tend towards differential broadening (which however would be asymmetric) would be vibrational effects. The relative changes in energy for the various acac tautomers, indicated in Table 4.5, suggest that it is only in the case of the O(1) core hole state that any significant vibrational effects might be of importance, since it is only for this core ionised state that the symmetrically hydrogen-bonded structure is energetically preferred. It might therefore be anticipated that there will be vibrational excitation of the OH stretching modes. It is difficult to estimate the likely stretching frequencies for the symmetrical hydrogen bonded species, but a reasonable estimate would suggest vibrational components separated successively by $\sim$0.4 eV.

In an extensive study of the overall band profiles for a series of isoelectronic, saturated, and unsaturated, polyatomic systems,[238] it was noted that in going from methane to ethane there would be a substantial reduction in the composite line width for the C_{1s} levels since the changes in both equilibrium geometries and force constants are much smaller. Computations of the Franck Condon factors (Section 2.6.2) suggested that >90% of the signal intensity in the 00 transition for ethane compared with $\sim$62% in the case of methane. It is clear therefore that a probability for vibrational excitation in the region of $\sim$40% from transitions above the fundamental are required to drastically alter the FWHM. For methanol, estimates of the Franck Condon factors

for the C-O and OH stretching vibrations accompanying O_{1s} core ionisation, suggested ∿54 and 98% of the intensity constituted 0-0 transitions. Although the calculations predicted substantial vibrational excitation of the CO stretching mode, a vast reduction in force constant was also noted which with the close spacing of the individual components (∿0.1 eV) ensured that the FWHM for the O_{1s} levels remained small. From these results, it seems unlikely that the FWHM for the O_{1s} levels of acac would be drastically altered by vibrational excitation.

4.3.5 Shake-Up Spectra

The experimental data previously reported for the O_{1s} levels of both systems[227,228] and the data reported here for both the O_{1s} and C_{1s} levels of acetylacetone, reveal low intensity satellites to the high binding energy side of the main photoionisation peaks. Although in the particular case of the O_{1s} levels the initial assignments of satellite structure as arising from a low concentration of keto form have subsequently been revised in favour of an interpretation based on shake-up structure accompanying core-ionisation of the O_{1s} levels of the enol form, no attempt has previously been made to investigate this theoretically. Before considering the shake-up structure in detail it is worth noting that the ΔSCF computations reported here rule out any interpretation of the satellite structure in terms of the keto form, since the O_{1s} binding energy is computed to be somewhat lower than for the enol oxygen in the unsymmetrical enol form.

For the enol forms (1-4) of acac and the C_S and C_{2v} forms of MA, the HOMOS and LUMOS may be described approximately in terms of the corresponding orbitals for a 6π pentadienyl system. From the detailed discussions of Chapter Six relating to previous experimental and theoretical studies, it is apparent that low energy satellites of appreciable intensity arise from HOMO-LUMO shake-up transitions,[239-242] and evidence has previously been presented (Section 2.2.3) that the energies and intensities of such satellites may be semi-quantitatively described within the sudden approximation. Energies and intensities for the HUMO-LUMO transitions for the various model systems have therefore been computed, from the relevant ground and core hole state eigenvectors and eigenvalues for both the O_{1s} and C_{1s} levels, and the data are presented in Table 4.6 (acetylacetone) and Table 4.7 (malonaldehyde).

Considering firstly the O_{1s} levels of acetylacetone, where as the straightforward $\pi \rightarrow \pi^*$ transition for the keto form is calculated to have zero intensity, for the enol forms satellites of approximately the same transition energy ($\sim$5 eV) are computed for both O(1) and O(2). In the MA systems, the transition energies for O(1) and O(2) differ slightly in the C_S form (5.5 eV and 4.3 eV respectively) whilst those for the C_{2v} form are equal, corresponding to that for O(2) previously mentioned (4.4 eV). For the unsymmetrical enol forms of both systems, the satellites are computed to be of unequal intensity, that deriving from the lower binding energy, keto-oxygen being the more intense.

TABLE 4.6

Computed Energies (eV) and Intensities (%) for Shake-Up HOMO-LUMO Transitions for the Various Model Systems

Hole State	Enol				Keto	Exp.
	1	2	3	4		
O-1*	3.2%(5.7eV)	3.9%(5.8eV)	5.1%(5.1eV)	5.2%(5.0eV)	0.0%	see text
O-2*	8.6%(5.0eV)	6.2%(5.0eV)	5.1%(5.1eV)	5.2%(5.0eV)	0.0%	12.0%(4.6eV)
C-1*	0.0%	0.0%	1.3%(8.8eV)	1.4%(6.5eV)	0.0%	0.0%
C-2*	5.1%(4.5eV)	6.3%(4.4eV)	5.0%(3.8eV)	4.2%(3.8eV)	1.4%(9.9eV)	(4.3eV)
C-3*	2.9%(6.2eV)	0.1%(6.1eV)	0.0%	0.0%	0.0%	6.0%(5.7eV)
C-4*	2.7%(5.0eV)	0.6%(4.2eV)	5.0%(3.8eV)	4.2%(3.8eV)	1.4%(9.9eV)	(5.4eV)
C-5*	0.0%	0.0%	1.3%(8.8eV)	1.4%(6.5eV)	0.0%	0.0%

Table 4.7

Computed energies (eV) and intensities (%) for shake-up HOMO-LUMO transitions for the malonaldehyde systems

Hole State	C_s	C_{2v}	Expt.
O(1)*	2.9%(5.5 eV)	6.6%(4.4 eV)	see text
O(2)*	11.7%(4.3 eV)	6.6%(4.4 eV)	1%
C(2)*	4.5%(4.1 eV)	5.5%(3.3 eV)	-
C(3)*	1.5%(5.6 eV)	0.0	-
C(4)*	2.6%(3.7 eV)	5.5%(3.3 eV)	-

Fortuitously, the relative intensities for the two direct photoionisation peaks based on these crude estimates of intensity for both systems, would be 1.07:1 for acac and 1.1:1 for MA, in surprisingly good agreement with experiment (1.1:1), and the revised estimates of Brown's data (1.1:1).

The energy separations of the satellite peaks from the lower binding energy components of 4.7 eV (acac) and 4.4 eV (MA) also compare surprisingly well with those calculated theoretically (5.0 eV and 4.3 eV respectively) and the absolute measured intensities of ∿12% and ∿13% are also in tolerable agreement with the theoretical estimates of 9% and 12% respectively. Unfortunately the spectra in this work and clearly that due to Brown[227] also, are not of sufficiently high signal/noise ratio to detect the satellites for O(1) in both systems, however the data for acac are not inconsistent with a transition energy of 5.7 eV and an intensity of 1/30 of that of the main photoionisation peak. It would therefore appear that the acac data is consistent with that for MA and that the calculations confirm the assignment of the high binding energy

satellites as originating from HOMO-LUMO, $\pi \rightarrow \pi^*$ shake-up satellites from the unsymmetrical enol forms.

The C_{1s} spectra (acac) also show evidence for a relatively broad unresolved shake-up region and the computations suggest transitions from the carbons involved in the system in order of intensity C(2)>C(4)≈C(3), the transition energies being in the order C(3)>C(2)≈C(4), and this is confirmed in the MA computations. Since C(3) (in acac) is not at very low binding energy, the predicted shake-up satellites should all fall within a relatively narrow energy region centred ∿5 eV to the high binding energy side of the main component of the C_{1s} levels (C(1), C(5)). The total calculated intensity of ∿3% for this satellite (as a percentage of the total C_{1s} envelope) would then seem to be consistent with the experimental data.

In the hierarchy of information levels available from an E.S.C.A. experiment, after the absolute binding energies and, relative intensities and internal shifts of the observed peaks, the shake-up satellites may be regarded as secondary levels of information. As is evident in the above assignments, these satellites are as distinctive in nature as are the primary sources. In a subsequent chapter examples are given which emphasise the importance of such structure.

CHAPTER FIVE

A THEORETICAL CONSIDERATION OF CORE-IONISATION IN CARBOCATIONS

ΔSCF computations have been performed on a range of geometries for both the cyclopentyl and 2-butyl cations. Although the actual E.S.C.A. spectrum has not been published for the cyclopentyl cation, the simulated C_{1s} core level spectra calculated at the STO-4.31G level indicate that the experimental shift data available are consistent with a classical structure. The manner in which such shifts in binding energy are well described at this non-empirical level and particularly characteristic of a classical or non-classical configuration has prompted a structural determination for the 2-butyl cation. The enhancement of weak interactions on going to the core hole state manifold potentially provides a straightforward means of distinguishing between the given isomers, since the computed E.S.C.A. spectra are found to be so distinctive.

5.1 Introduction

Ab initio molecular orbital theory has played an impressive role in the discussion of the structure and stability of reactive chemical intermediates.[243-246] Since such species do not in general exhibit a sufficiently long lifetime as to be amenable to direct spectroscopic observation and characterisation, it has been by the use of theoretical rather than experimental means that an insight into the properties of these systems has been gained. Theoretical

studies of this type refer to the gas phase and the calculations therefore reflect the fundamental electronic properties of the isolated ion. Caution must therefore be exercised in making comparisons with experimental data in solution, where the results may depend strongly on interactions with solvent molecules.[247]

It is evident from the comprehensive volumes edited by Olah and Schleyer[248] that the carbonium ions occupy a special place in the studies of reactive chemical intermediates. In order to account properly for their properties, Olah[249] proposed two classes of carbocation (the most general name for all cationic carbon compounds, c.f. carbanions for the negative ions):

(i) carbenium ions, which are trivalent ("classical") ions with an electron-deficient central carbon atom;

(ii) carbonium ions, which are penta- (or tetra-) co-ordinated ("non-classical") ions.

The topic of non-classical carbocations has aroused much controversy; with reviews by Kramer,[250] Brown[251] and Olah[252] giving good accounts of the different viewpoints; and a more recent text by Brown[253] attempting to give a critical examination of this whole area.

In particular cases, theoretical calculations at various levels of sophistication agree in that the energy difference between the classical and non-classical formulations for such species are small. A simple example of this genre is studies relating to the classical and non-

classical (hydrogen-bridged) ethyl cation. Kohler and Lischka[255] at a non-empirical SCF level have shown the classical species to be ∿2 K cal mol^{-1} the more stable, in agreement with earlier calculations by Clark and Lilley.[256] However, with the inclusion of estimates of the correlation energy for both species, the non-classical structure is favoured by ∿3 Kcal mol^{-1}. It would therefore seem reasonable to focus attention on properties of the systems which would provide a direct means of distinguishing between their classical or non-classical nature. For those amenable to experimental investigation the only technique which would *a priori* appear capable of effecting such a distinction is E.S.C.A., for which the time-scale precludes any ambiguities arising from rapidly equilibrating structures. Indeed, it was realised at an early stage that the core binding energy shifts would be particularly suitable for definitive studies of the carbocations. Thus Olah and co-workers have applied the technique to the study of the tert-butyl,[254] cyclopentyl- and 2-norbornyl- cations.[220]

The manner in which valence electronic reorganisation accompanying core ionisation, can substantially modify the potential energy surface with respect to the ground-state, has been outlined in the previous chapter with reference to the dicarbonyl systems. Consequently the enhancement of weak interactions such as hydrogen bonding, illustrates the significance of core ionisation as sufficiently strong a perturbation, to provide a monitor of overall valence-electron distributions. Returning to the discussion concerning the nature of the ethyl cation, at the STO-4.31G level a classical

ground-state is favoured by ∿7 K cal mol^{-1}.[256] However, the effect of core ionisation is dramatic; a core-hole on thecarbon bearing the positive charge in the classical species, favours a non-classical cation by ∿42 K cal mol^{-1}; whilst creation of a core hole on the alternative carbon favours the classical cation by ∿60 K cal mol^{-1}. As will become apparent, in a later section, analyses of this type have proven useful in the categorisation of the structures of such systems as the 1-propyl and 2-norbornyl cations.[257] The manifestation of the results for these systems has been that their core hole state spectra were found to be highly characteristic for the isomeric species, and differed quite significantly for systems which on an absolute energy scale were closely similar.

In view of the reported E.S.C.A. data and the distinctive nature of previous theoretical studies, in this chapter it will be shown how shifts in binding energy computed at a non-empirical level, are well described in the case of the cyclopentyl cation, and the manner in which such calculations show that E.S.C.A. data may be decisive in the debate concerning the structure of the 2-butyl cation.

5.2 A Non-Empirical Investigation of the Ground and Core Hole States of the Cyclopentyl Cation

Over the past decade, much of the work concerned with the classical or non-classical nature of carbocations has centred upon the 2-norbornyl system. Following earlier n.m.r. studies,[258] the necessity to neglect possible intra-

and intermolecular interactions (e.g. Wagner-Meerwein rearrangements, hydride shifts, proton exchange, etc.) prompted Olah *et al* to utilise the inherently rapid time scale of the ionisation processes in E.S.C.A. In these studies, comparisons of the degrees of charge localisation were made with those from the spectra pertaining to the cyclopentyl and tertiary butyl cations. Whilst for the tertiary butyl cation, the reported core-level spectrum consists of a doublet structure (intensity ratio 1:3) with C_{1s} binding energy shift of 3.9 $\pm$ 0.2 eV, the E.S.C.A. spectrum for cyclopentyl cation has not been published but is stated to consist of two peaks (intensity ratio 1:4) with a separation of 4.3 $\pm$ 0.5 eV. For these two systems, such separations are seen as being characteristic of cationic species with charge localisation. However, for the 2-norbornyl system, technical difficulties in obtaining appropriate core level spectra, due to extraneous hydrocarbon contamination from the spectrometer, have confused the issue and the available data have been interpreted as supporting both possibilities.

Dewar *et al*,[259] using the semi-empirical MINDO/3 method have studied the above systems within the equivalent cores approximation of Jolly, outlined in Chapter Two. Contrary to the interpretation of the E.S.C.A. data, by Olah and coworkers, these results indicated that all three species were of a classical nature. More important, whilst only fair agreement was established between the simulated C_{1s} core level spectrum for tertiary butyl cation and experiment (peak separation 3.4 eV) that for cyclopentyl cation has failed completely, (peak separation 1.8 $\pm$ 0.1 eV) with regard to the

E.S.C.A. data (c.f. 4.3 $\pm$ 0.5 eV) and was insensitive to the spectral resolution used. Non-empirical computations[260] have since confirmed the non-classical nature of the 2-norbornyl system and for the tertiary butyl cation have shown that at the STO-4.31G level, excellent agreement with the experimental core binding energy shifts may be obtained.

Abstracting the shift data from the study ofthe 2-norbornyl cation allows the core hole state spectra for the classical and non-classical species to be synthesised, if components of an appropriate line-shape (gaussian) and line-width are used. Taking the component FWHM to be 1.8 eV, these are compared with the spectrum reported by Olah and co-workers (Figure 5.1).

From Figure 5.1, interpretation of the experimental data in terms of the classical ion is clearly unlikely. However, to date no comparable non-empirical investigations have been made concerning the cyclopentyl cation. Such an investigation is clearly warranted on at least two counts:

(i) in view of the difficulties and controversy in obtaining and interpreting the E.S.C.A. spectrum for the 2-norbornyl cation, it is unfortunate that the actual C_{1s} core level spectrum for cyclopentyl cation has not been published;

(ii) whilst reasonable agreement with experiment is inferred from semi-empirical calculations relating to the tertiary butyl system, a parallel study of the cyclopentyl cation using the MINDO/3 method fails to agree with the interpretation of the E.S.C.A. spectrum in terms of the shift between C_{1s} core levels.

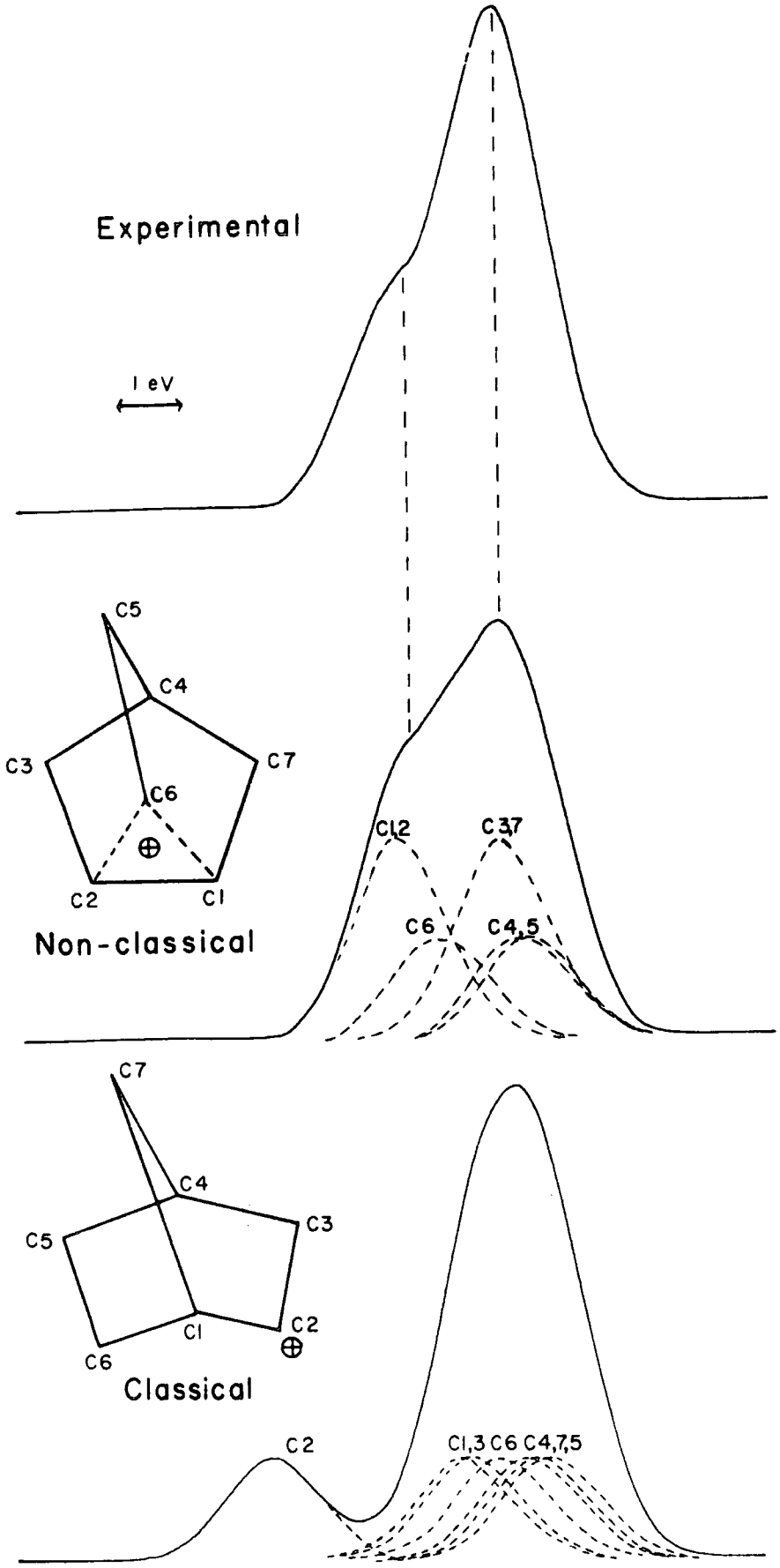

Figure 5.1 C_{1s} spectra for the classical and non-classical, 2-norbornyl cation

Also in a recent study by Schleyer *et al*[261] it was noted that at both semi-empirical and *ab initio* levels a non-classical, pyramidal structure was found to be a local energy minimum on the potential energy surface for cyclopentyl cation. With this background, the present study will largely be concerned with a comparison of the ground and core-hole states of the classical and non-classical species, and the previously published experimental and semi-empirical, theoretical data.

5.2.1 Computational Details

A series of calculations[272] concerning the methyl and ethyl cations, at both the Slater Double Zeta and STO-4.31G levels have on comparison, shown that the tendency for the latter basis set to over-estimate absolute binding energy (as a result of an underestimation of the magnitude of the relaxation energy) is also apparent when applied to studies of the carbocations. However, the results show that *shifts* in binding energy and in relaxation energy are well-reproduced at the STO-4.31G level.

Non-empirical LCAO MO SCF calculations have therefore been performed for the representative, classical and non-classical models for the cyclopentyl cation using this basis set. The classical structure was that predicted using the multivariational, geometry optimisation routine contained in the MNDO program[214] and that for the non-classical ion was referenced from the recent study by Schleyer and co-workers.[261] The 'best-atom' exponents taken from the study

by Clementi and Raimondi were again used in the evaluation of the one- and two-electron integrals, employing the ATMOL 3 suite of programs. Binding energies were calculated directly as energy differences (c.f. Section 2.6.2) with differences between Koopmans' Theorem and the ΔSCF binding energy values providing estimates of the relaxation energies accompanying core ionisation.

5.2.2 Results and Discussion

(a) Ground States

The configurations studied and their total energies, calculated at the STO-4.31G level are displayed in Figure 5.2.

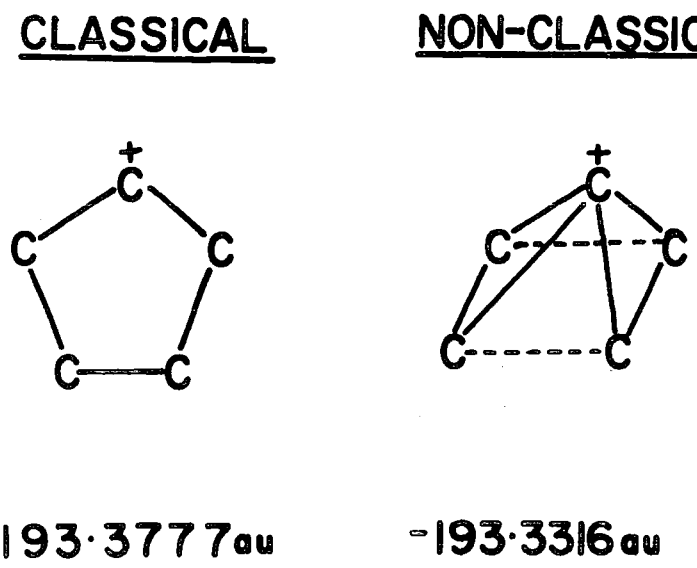

Figure 5.2 Total Energies (Hartrees) for the Classical and Non-Classical Cyclopentyl Cation Configurations

The classical cyclopentyl cation structure, optimised using the MNDO subroutine is predicted to consist of a planar carbon ring, and is calculated to be 45.4 K cal mol^{-1} more stable than thenon-classical configuration at the semi-empirical level. This value is in perfect agreement with that obtained by Schleyer and co-workers[261] at an *ab initio* theoretical level using the STO-3G basis set. The present study suggests that the figure is overestimated by some 50%, since at this level the classical ion is calculated to be the more stable by only 28.9 K cal mol^{-1}. It is not inconceivable that more accurate calculations including the effects of polarisation functions and correlation energy corrections may further reduce this value, but it is highly unlikely that this lowering in energy would be so significant as to render the non-classical configuration the more stable on an absolute scale.

(b) Core Hole States

The results outlined for the 2-norbornyl-and tertiary butyl- cations suggest that there exists a good agreement between theory and experiment with regard to shifts in binding energies and relaxation energies, calculated at the STO-4.31G level. The computed absolute and relative binding energies, and relaxation energies for the classical and non-classical species are presented in Table (5.1). For comparison, also included are semi-empirical data calculated using the equivalent cores method. Since the mode of sample preparation used for the E.S.C.A. investigation involves a frozen solvent matrix, the absolute values have been corrected to a binding

energy scale on which the hydrocarbon (solid phase) line profile is assigned a value of 285 eV.

Considering firstly the non-empirical data, it is clear that the computed spectra are distinctively different for theclassical and non-classical forms. Whereas for the classical species, a C_{1s} core level spectrum exhibiting three peaks with intensity ratio 1:2:2 is predicted, in the case of the non-classical cyclopentyl cation only two peaks are evident, with that of higher intensity also arising at higher binding energy: the intensity ratio for the latter two peaks being 4:1.

Significant differences in core level binding energy shifts are also characteristic of a given structural type. The span in binding energy shifts for the classical cation is calculated to be 5.3 eV and is greatly inexcess of that for the non-classical species (0.4 eV) computed at the STO-4.31G level. Regarding the relaxation energy shifts, for the classical species the span is compressed to 0.6 eV, however a trend which associates increasing relaxation energy with a lowering in binding energy is evident. A value numerically equivalent to that found for the binding energies is observed in the case of the alternative cation structure indicating that changes in binding energy in this configuration may be as a result of the differences in relaxation effects.

In the study by Olah and co-workers,[220] absolute binding energy values relating to the unpublished spectrum for the cyclopentyl cation are not reported. However, it is stated that the C_{1s} envelope is analysed in terms of two line profiles

Table 5.1

The absolute and Relative Binding Energies (eV) and Relaxation Energies (eV) for the Cyclopentyl Cation configurations studied

	ΔSCF Method				Equivalent Cores	
	Classical		Non-Classical		Classical	
Hole State	STO-4.31G		STO-4.31G		MNDO	MINDO/3[a]
	B.E.	R.E.	B.E.	R.E.	B.E.	B.E.
C(1)	294.8	11.3	290.8	12.4	293.7	292.3
C(2)	290.9	11.7	291.2	12.0	291.1	290.8
C(3)	289.5	11.9	291.2	12.0	290.2	290.3
C(4)	289.5	11.9	291.2	12.0	290.2	290.3
C(5)	290.9	11.7	291.2	12.0	291.1	290.8
	ΔB.E.	ΔR.E.	ΔB.E.	ΔR.E.	ΔB.E.	ΔB.E.
C(1)	9.8	0.3	5.8	1.4	8.7	7.3
C(2)	5.9	0.7	6.2	1.0	6.1	5.8
C(3)	4.5	0.9	6.2	1.0	5.2	5.3
C(4)	4.5	0.9	6.2	1.0	5.2	5.3
C(5)	5.9	0.7	6.2	1.0	6.1	5.8

ΔB.E. and ΔR.E. are relative to methane (B.E. 285.0 R.E. 11.0 eV) (a) Ref.259.

with a relative intensity ratio of 1:4, and internal shift of 4.3 $\pm$ 0.5 eV. Although the FWHM for the two peaks are not mentioned explicitly, it is noted that the more intense line profile, at lower binding energy, is by comparison significantly broadened.

Even without a detailed consideration of the differences in internal binding energy shifts predicted for the classical and non-classical species, it is clear from the ordering and relative intensity ratios of the peaks, that the actual C_{1s} core level spectrum cannot arise from the non-classical configuration. Since in the computed core level spectrum for the classical cation structure, the two lineshapes which are equivalent in intensity are separated by as much as 1.4 eV, it is conceivable that if this portion of the spectrum was resolved in terms of only one peak then this would then account for the increased linewidth. From the data in Table (5.1) estimations may be made as to the internal binding energy shift between the centroid of the above lineshape and that arising from core ionisation of the carbon atom bearing the localised charge distribution (Table 5.2).

Table 5.2

Internal B.E. shifts (e.V) for the classical cyclopentyl cation

	ΔSCF METHOD		EQUIVALENT CORES	
	STO-4.31G	EXPT.	MNDO	MINDO/3
Cyclopentyl Cation	4.6	4.3$\pm$0.5	3.0	1.8$\pm$0.1

It is clear from the data in Table (5.2) that within this scheme, there exists a very good agreement between the shift difference calculated at the non-empirical level and the peak separation determined experimentally. If components of appropriate, gaussian line-shape (as discussed in Chapter Two) and linewidth, are taken then it is possible to synthesise the core hole state spectrum which should, in principle, be a good representation of the unpublished spectrum. Simulated spectra are therefore included representing the C_{1s} core level ionisations in the classical and non-classical species (Figure 5.3).

That the broadening in the more intense lineshape of the actual spectrum occurs as a result of core ionisation of inequivalent centres, as in the manner described, is evident from two points:

(i) it is unlikely to be due to vibrational excitation accompanying core ionisation, since such excitations are difficult to detect even for small molecules studied in the gas phase and would most certainly remain undetected for carbocations studied in the condensed phase;[235]

(ii) if this were due to a difference in lifetimes for the core holestates, then that of the carbon bearing the localised charge distribution, would need to be significantly longer.

As previously noted, Dewar *et al* have studied the cyclopentyl, classical, cation system using the MINDO/3 semi-empirical method and the results are presented in Tables (5.1)

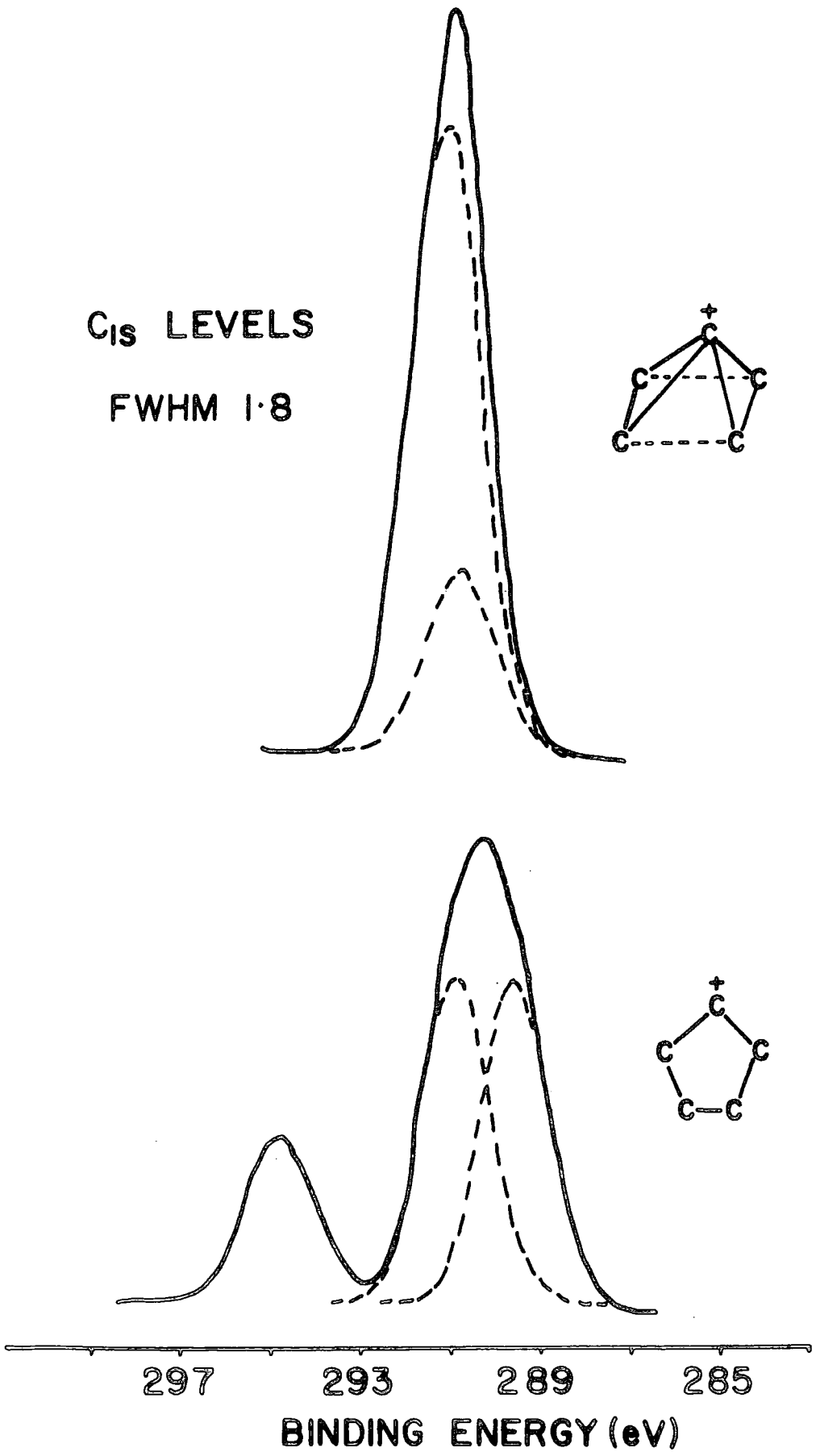

Figure 5.3 Computed C_{1s} Core Level Spectra for the Classical and Non-Classical Cyclopentyl Cation

and (5.2). Since the classical geometry for the present study was determined using a semi-empirical method (M NDO) the above results are compared with an equivalent cores investigation at this level. From the data pertaining to the STO-4.31G study, it is evident that the spans in binding energy for the MNDO (3.5 eV) and MINDO/3 (2.0eV) investigations are grossly underestimated although the former semi-empirical method shows some improvement. More important, whilst calculations at this level agree that the C_{1s} spectrum for the classical species is composed of three components (intensity ratio 1:2:2) arising from three inequivalent core ionisations, from Table (5.2) it is clear that on the basis of the previous assumption, the shift difference between the centroid of the lower binding energy peaks and that at high binding energy is inadequately expressed in both cases. Once again, improvement is noted in the results of the MNDO calculations.

Clearly, since in the non-empirical study a good agreement with the E.S.C.A. data is observed using a classical configuration, optimised at a semi-empirical level, it is significant that the MNDO and MINDO/3 calculations fail in this respect. This implies that the inability for the MINDO/3 study to predict the correct shifts in binding energy was not an artefact of an incorrect geometry optimisation, but was more likely due to the inadequacy of the method for calculating heats of reaction for the isodesmic core-exchange processes involved in the equivalent cores concept.

5.3 A Non-Empirical Investigation of the Ground and Core Hole States of the Secondary Butyl Cation

The expedience of E.S.C.A. as a technique for the determination of structure and bonding is clearly evident in the previous chapters, and in the particular case of the carbocations, is demonstrated in the studies of the tertiary butyl, cyclopentyl, and 2-norbornyl cations outlined earlier. In spite of this, experimental investigations of the 2-butyl cation have remained a continuation of the early N.M.R. studies by Saunders and co-workers,[262] and despite its inherent simplicity, there is still no overall agreement as to its structure.

Early attempts by Olah *et al*,[263] to prepare the 2-butyl cation from 2-fluorobutane, n-butane or butanol-2, in 'magic acid' media (SbF_5 - HSO_3F) led directly to tertiary butyl cation. However, Saunders *et al*, in the study referred to above, found that if 2-butyl chloride was slowly added to SbF_5/SO_2ClF solution at -110°C and with the aid of vacuum line techniques, then the 2-butyl cation was generated. This was evident in the ^1H N.M.R. spectrum and its temperature dependence. Thus, the spectrum recorded at -112°C consisted of three peaks; the central being due to tertiary butyl cation formed in the preparation and the two remaining peaks were assigned as arising from the 2 and 3, and 1 and 4 protons of 2-butyl cation, averaged by very rapid 3,2-hydride shifts. As the sample was warmed, the tertiary butyl cation peak remained unchanged, however those assigned as being due to the 2-butyl cation coalesced and above 40°C rapid conversion to the former occurred.

A second process which scrambles all of the protons in the cation was detected from these observations of line broadening and coalescence at temperatures from -112°C to -40°C.[264] Line shape analysis of the N.M.R. spectrum showed the activation energy for this process to be low (7.5 ± 0.1 K cal mol^{-1}) and a mechanism which had previously been suggested for the interchanging of hydrogens in the isopropyl cation, was thought to be unlikely, since reversible rearrangement to the primary ion would be expected to require about 9 additional K cal mol^{-1}.

An alternative mechanism, also suggested for the isopropyl cation, is favoured. This involves cyclisation to a protonated methylcyclopropane intermediate, which was originally thought to be either 'edge' or 'corner' protonated, followed by proton scrambling rearrangement and reopening, to sec-butyl cation. However, subsequent studies[264] on the isopropyl cation have shown the edge-protonated cyclopropane to be a transition state, at least a few K cal mol^{-1} less stable than the corner-protonated intermediate. This is supported by the non-empirical calculations of Pople *et al*[265] on the $C_3H_7^+$ ion. Only two potential minima on the energy surface were found, corresponding to the expected isopropyl cation, extended chain structure, and to a distorted form of the corner-protonated cyclopropane, related to n-propyl cation. This is a structure which will be clarified later, when described as a 'partially bridged' or 'bent', n-propyl cation. The edge-protonated cyclopropane was calculated to be ~10 K cal mol^{-1} higher in energy than the corner protonated structure and the face-protonated cyclopropane was predicted to be very unstable.

If these observations are apparent for the 2-butyl cation also, then the most probable mechanism involves closure to a form resembling the corner-protonated methylcyclopropane intermediate, followed by degenerate corner-to-corner proton rearrangement and reopening, in a manner similar to that described by Saunders *et al.*

More recently, Olah and co-workers[266] have made an investigation of the high resolution ^{13}C N.M.R. spectra of solutions of the C_3 to C_8 alkyl cations in SbF_5/SO_2ClF, a low nucleophilicity solvent. The effect of methyl substituents was determined by comparing the ^{13}C N.M.R. shifts of related carbocations, and was found to be constant. An attempt to estimate the ^{13}C shifts of the degenerate and non-degenerate equilibrating cations, whilst giving good agreement for the tertiary-tertiary case on comparison with experimental values, showed significant deviations in the particular case of the 2-butyl cation. Two methods were used to evaluate estimates for the ^{13}C shifts of the 2-butyl cation from methyl substituents. The first involved substituting a methyl group β from the carbenium centre in the isopropyl cation and using the estimated substituent effects, along with the shifts in the static isopropyl cation, to estimate the ^{13}C shifts for 2-butyl cation. A similar process involving the removal of a methyl group from a position adjacent to the carbenium centre in the tertiary-amyl cation produced equivalent results. A comparison of the experimental and calculated values showed deviations of 9.2 and 19.8 p.p.m. per carbon for the methyls and the equilibrating carbocation centres respectively.

The ^{13}C spectrum reported by Olah and co-workers consists of two quartets and it was noted that this is certainly inconsistent with that expected from a static hydrogen bridged intermediate, since this, when fully coupled, would show a doublet of doublets and quartet for the hydrogen-bridged carbons and methyl carbons respectively. It was suggested that rapid exchange of the three hydrogens attached to the central carbons may explain the ^{13}C spectra, however this was discounted on the basis that there is no method available to accurately estimate the ^{13}C shifts of an equilibrating, hydrogen bridged, 2-butyl cation, and if comparison lies with those in the bridged ethylene halonium ions then greater shielding would be expected than is observed experimentally. A further possibility was that if the hydrogen bridged species exhibited a similarity in thermodynamic stability when compared with the extended chain species, then both intermediates would contribute to average ^{13}C N.M.R. shifts. However this must be rejected on the basis of recent calculations by Köhler and Lischka,[267] which with estimates of correlation energy find a difference in energy between the two species of $\sim$10 K cal mol^{-1}.

The ^{13}C N.M.R. spectrum for the 2-butyl cation does not exclude the possibility of rapidly equilibrating classical (extended chain) structures but indicates that some additional effect may be causing the discrepancy between the averaged and observed ^{13}C shifts. Indeed, the discussions of Saunders *et al* outlined earlier are supported in this study.

In a series of solid state, magic angle, cross polarisation studies, Myhre and Yannoni[268] have noted that N.M.R. spectra for the 2-chlorobutane-antimony pentafluoride system recorded within the temperature range -85°C down to -130°C show lines characteristic of the 2-butyl cation and these resonances are in good agreement with chemical shifts observed in the solution state. No significant spectral change was observed upon warming to -60°C, when on the basis of solution studies coalescence would be expected to occur. This indicates that the rate of carbon scrambling in the 2-butyl cation must be significantly slower than in solution. A recent estimate[269] for the barrier, in solution, for the degenerate hydride shift was that it was less than 2.4 K cal mol^{-1}. This value can only be an upper bound since the parameter used in the fast exchange limit approximation, $k = (\pi/2) \times (\Delta^2/W)$, was the change in line width (W) at a given temperature. The validity of this approach is based upon the idea that line broadening in the fast exchange limit is proportional to frequency squared, and in the case of the 2-butyl cation, no broadening was observed. Assuming a suppression of the rate for this process, as was noted for the carbon scrambling, it is indeed interesting that evidence for a 'static' 2-butyl cation in a spectrum recorded at -190°C is still not observed. These observations indicate therefore, that either the barrier in solution for the hydride shift is considerably less than 2.4 K cal mol^{-1} or the rapid equilibriation of classical ions does not occur.

A number of possible structures for the 2-butyl cation have been investigated theoretically over the past decade. An early *ab initio* study by Pople and co-workers[265b] at the STO-3G level, which considered the effects of C-X and C-H hyper-conjugation as a function of substituent X in the isopropyl cation, indicated that when X = CH_3, (2-butyl cation) a conformational preference was observed. For the classical (extended chain) configuration staggered conformations were concluded to be significantly more stable than the eclipsed form studied (by ∿8 K cal mol^{-1}) and a general tendency considerably favouring C-C hyperconjugation as opposed to C-H hyperconjugation was apparent. This latter point is emphasised in further studies by Pople *et al*[265c] concerning the relative energies of the $C_3H_7^+$ species, as mentioned earlier. As illustrated in Table 5.3, whilst at the STO-4.31G level, the energies for the n-propyl (extended chain), partially bridged 1-propyl (bent) and corner-protonated cyclopropane are noticeably similar, relative to 2-propyl cation, using an STO-6.31G* basis set, with the inclusion of polarisation functions on carbon, the partially bridged and fully bridged structures are stabilised by ∿3 and 4 K cal mol^{-1} respectively due to increased hyperconjugative effects.

Recent studies by Köhler and Lischka[267] have been carried out at both the STO-3G and MINDO/3 levels to optimise both, classical and non-classical structures for the 2-butyl cation, thereby allowing further computations to be made with the use of extended basis sets, and including estimates of electron correlation effects. Unfortunately, only the classical

Table 5.3

Relative energies of $C_3H_7^+$ ground state structures (in K cal mol^{-1})[a]

	STO-4.31G	STO-6.31G*
2-propyl	0	0
n-propyl	17.4	17.0
'bent' 1-propyl	16.9	14.1
corner-protonated cyclopropane	17.3	13.0

a. Ref. 265c.

(extended chain) structure and symmetrically, hydrogen-bridged configuration have been considered. At the SCF level, the former is noted to be the more stable by as much as 10 K cal mol^{-1}, however with the inclusion of polarisation functions on both carbon and hydrogen this value is reduced to a level comparable with earlier results reported by Pople *et al*[265c] using the STO-4.31G basis set ($\sim$1 K cal mol^{-1}). An estimation of the correlation effects for the systems reverses the above trend, since as noted previously, the stability of the hydrogen bridged species is then favoured by $\sim$10 K cal mol^{-1}. If such a stabilisation is evident, then the compatibility of this result with the ^{13}C N.M.R. observations of Olah *et al*[266] has been discussed earlier.

It is clear from the previous investigations outlined above that the present situation is unsatisfactory in at least two respects. Firstly, the theoretical computations

have not adequately explored regions of the potential energy surface forthe 2-butyl system, corresponding to partially bridged and non-classical fully bridged species such as corner protonated, methyl substituted, cyclopropanes. This is indeed surprising in view of the extensive range of geometries investigated for the 1-propyl cation, and the nature of the intermediates suggested in the mechanism for the proton scrambling process. Secondly, experimental investigations have reached a stage where it is clear that the N.M.R. time scale is such that the technique is incapable of distinguishing between rapid equilibration of classical ions, or indeed various non-classical ions and a static non-classical structure for the 2-butyl cation.

The focus of attention for the rest of this chapter is therefore on both of these aspects. Results described earlier have indicated that shifts in binding energy are well described at the STO-4.31G level and therefore detailed *ab initio* computations, employing this basis set, have been carried out on structures for the 2-butyl cation which would potentially be compatible with the N.M.R. data. By considdering the localised core hole states for each system in turn, it will be shown how the inherently very fast time scale of the E.S.C.A. technique, drawn upon in the previous chapter, is in principle also capable of distinguishing unambiguously between alternative possibilities for the structure of the 2-butyl cation.

5.3.1 Computational Details

Calculations of the type described in the case of the cyclopentyl cation have been carried out for a number of structures compatible with available N.M.R. data on the 2-butyl cation. These included the classical (extended chain) structure and methyl-corner-protonated cyclopropane since the latter has been suggested as an intermediate in the scrambling processes observed in both the solution-phase[262,264,266] and solid-state N.M.R. spectra.[268] Such a structure was first suggested with regard to hydrogen and carbon interchange in the isopropyl cation and in an elegant investigation of the potential energy surface by Pople and co-workers,[265c] a distorted form of the above configuration pertaining to a partially bridged species was noted to be the more stable at the STO-4.31G level (c.f. Table 5.3). A partially bridged analogue for the 2-butyl cation was therefore also included.

The geometries used in this study were based upon the results of the earlier work by Pople *et al*;[265] taking the optimised geometries for the isomeric forms of the 1-propyl cation and employing standard bond lengths and angles for the substituent methyl groups from a study of the 2-propyl cation, provided prototype structures for the isomeric 2-butyl cations.

5.3.2 Results and Discussion

(a) Ground States

The focus of previous theoretical investigations on the 2-butyl cation has been a conformational study on the classical (extended chain) structure[265b] showing the preference of C-C as opposed to C-H hyperconjugation, and a comparison of the above configuration[267] with that optimised for the symmetric (hydrogen bridged) non-classical isomer. This limited range of structures clearly contrasts with the extensive range of geometries which have been investigated for the 1-propyl cation, and a straight analogy would suggest that both partially methyl bridged and fully bridged (methyl substituted corner protonated cyclopropane) structures should be considered also. Previous discussions have already indicated that this is particularly apparent in the light of low temperature solution phase and solid state N.M.R. data.

Further computations on the 1-propyl cation[257] have confirmed that the relative energies of an extended chain, partially bridged and fully bridged (corner protonated cyclopropane) are all very similar at the STO-4.31G level. A consideration of the population analyses for these structures, as shown in Figure 5.4, coupled with the knowledge that at a more sophisticated level of calculation[265c] (Table 5.3), the partially bridged and fully bridged, corner protonated cyclopropanes are the more stable, suggests however, that the effect of methyl substitution at the carbon bearing the positive charge, in going to the 2-butyl cation might lead to substantial stabilisation of the partially bridged structure.

Figure 5.4 Population analyses for the 1-propyl cation isomeric forms

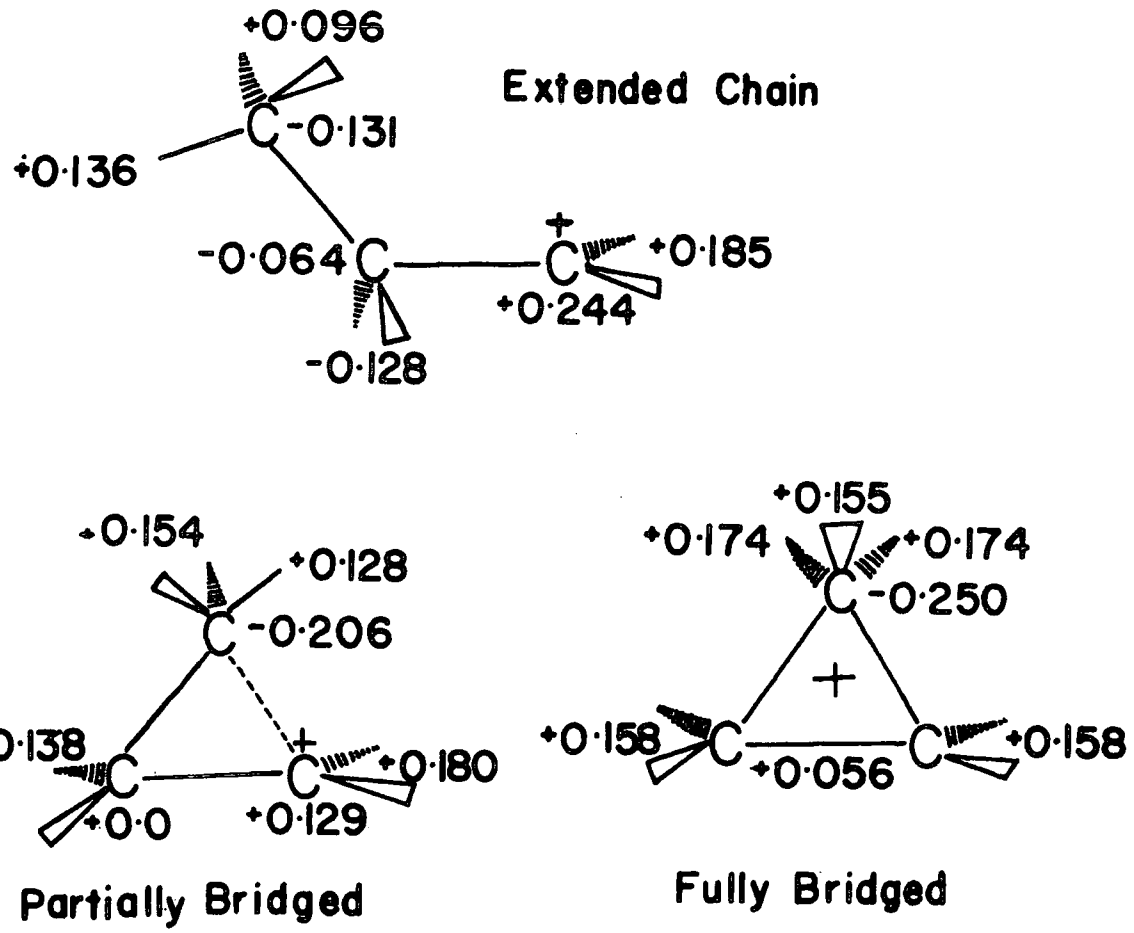

The localisation of the positive charge clearly diminishes in going from extended chain to fully bridged structures and surveying the populations at the bridging carbons and associated hydrogen atoms, indicates that the increased stabilisation of the latter two configurations, as compared to the extended chain, at the STO-6.31G* level, is due to increased C-C hyperconjugation. Pople[265c] has noted, that the apparent, small, stabilisation of the fully bridged structure as compared to the partially bridged cation may be an artefact of the addition of d functions to carbon, since this is known to preferentially lower the energy of

three membered rings. Indeed, the calculations of Clark *et al*[257] agree with theoriginal assignment by Pople and co-workers in finding the partially bridged structure slightly the more stable. Substitution of a methyl group as suggested, would therefore stabilise a more localised charge, and diminish the tendency for hyperconjugation.

Evidence for such a premise may be taken from recent work by Schleyer *et al*[270] who have compared the heats of formation for non-classical, corner-protonated, cyclopropane structures and their classical (extended chain) counterparts. Whilst for the 1-propyl system, the fully bridged form is clearly found to be the more stable ($\sim$6K cal mol^{-1}), for the 1,2-dimethyl-1-propyl cation, the classical isomer is slightly favoured ($\sim$1K cal mol^{-1}). The large difference in energy for the 1-propyl isomers as compared to the results of Clark *et al* and Pople and co-workers is clearly due to the assumption of a ground state geometry which has limited C-C hyperconjugative properties (H from $\overset{+}{C}H_2$, and CH_3 group eclipsed). Pople and co-workers have computed the energy difference for these 1-propyl classical, conformers and a lowering ofthe above value by $\sim$3 K cal mol^{-1} is a reasonable estimate but does not change the original argument.

Computations have therefore been carried out on the ground states of the extended chain, partially bridged, and fully bridged structures for the 2-butyl cation, which are analogous to those shown in Figure 5.4, and the results are displayed in Figure 5.5.

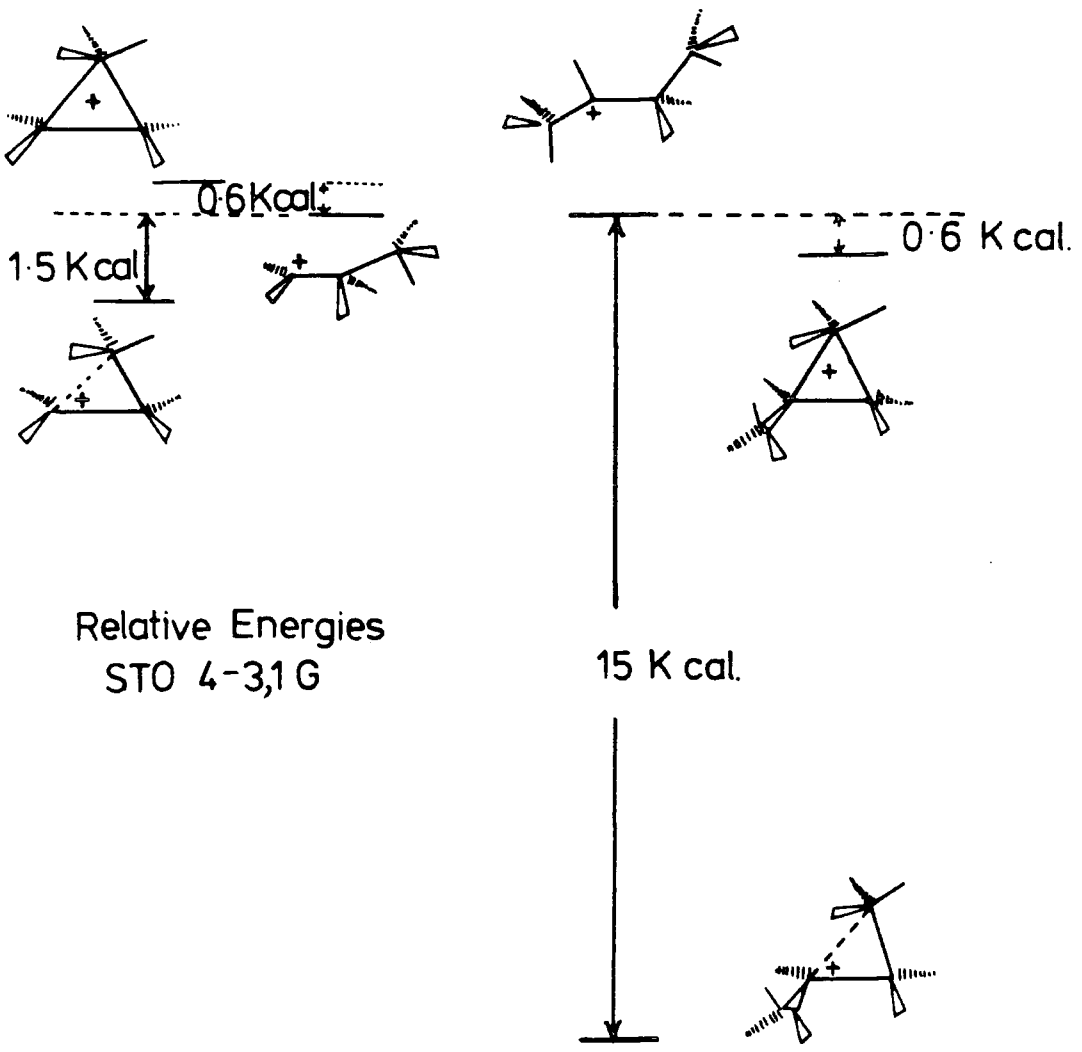

Figure 5.5 Relative energies of the extended chain, partially bridged and non-classical 1-propyl and 2-butyl carbocations at the STO-4.31G level

Whereas for the 1-propyl cation at the STO-4.31G level the order of stability is predicted to be partially bridged > extended chain > fully bridged, that for the 2-butyl cation is predicted to be partially bridged > fully bridged > extended chain. Whilst the effect of methyl substitution substantially lowers the energy for the partially bridged isomer as was

suspected, the reversal of trend concerning the energies for the extended chain and fully bridged isomers at this level, is not as a direct result of this. The ground state geometry assumed for the extended chain, classical 1-propyl cation is that which allows maximum C-C hyperconjugation (i.e. H from $\overset{+}{C}H_2$ and CH_3 staggered c.f. Figure 5.5) and calculated to be the more stable conformer by Pople and co-workers. The conformer assumed for the 2-butyl cation (extended chain), is that in agreement with the computations by Köhler and Lischka,[267] enabling a direct comparison to be made, and does not allow C-C hyperconjugation (see Figure 5.5). Pople and co-workers have again calculated the difference in energy for these two conformers (at the STO-3G level) and note that the extended chain conformer allowing a degree of C-C hyperconjugation is the more stable by $\sim$2 K cal mol^{-1}. Taking this value into consideration, shows the extended chain isomer for 2-butyl cation to be slightly more stable than the fully bridged form (at the STO-4.31G level) in agreement with observations for the 1-propyl cation. Indeed, a value of $\sim$1.4 K cal mol^{-1} shows a relatively greater stabilisation of the classical form than is observed in the 1-propyl case (0.6 K cal mol^{-1}) and is therefore also in agreement with the recent trends shown by Schleyer *et al* as noted above.

In emphasising the lack of hyperconjugation possible for the above classical 2-butyl cation, conformer, it is interesting to consider the relative stability of a 'bent', 'partially bridged' structure in which the hydrogen at C(2) and methyl bridging group are eclipsed (Figure 5.6).

Figure 5.6 Relative energies of classical and partially bridged, non-hyperconjugative forms for 2-butyl cation (K cal mol^{-1})

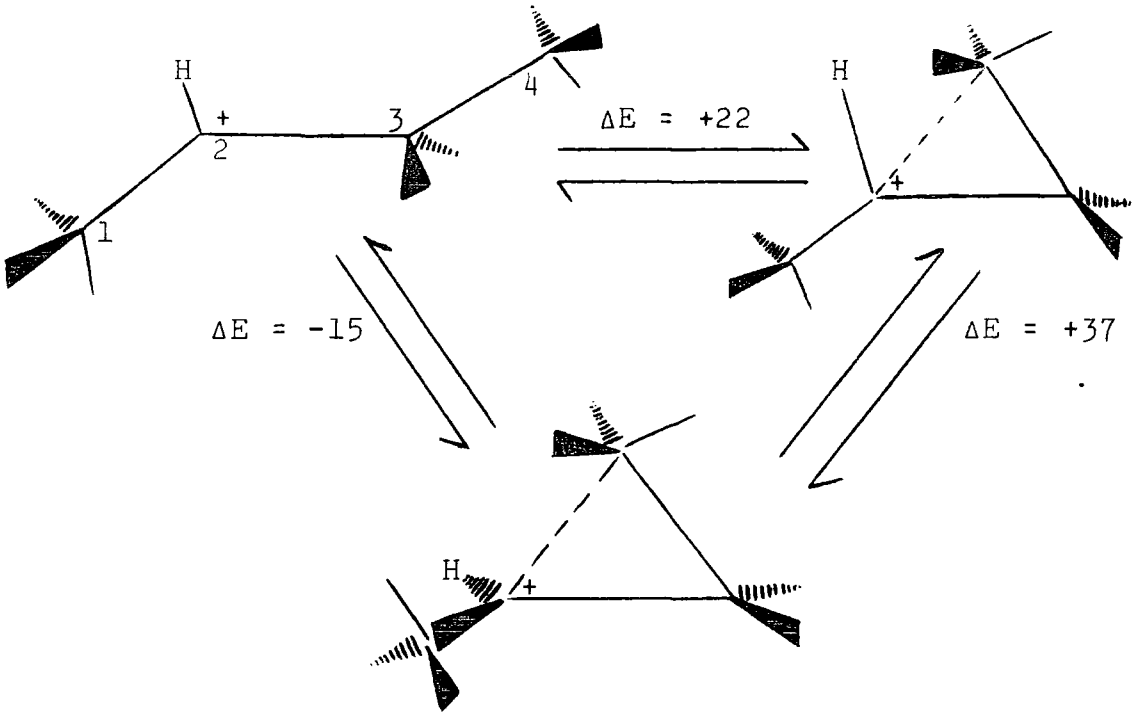

Such a structure is clearly 22 K cal mol^{-1} less stable than the extended chain configuration and 37 K cal mol^{-1} less stable than the staggered structure which is favoured at the STO-4.31G level.

Köhler and Lischka have also considered the symmetrically hydrogen bridged isomer for the 2-butyl cation[267] using extended basis sets. As previously noted, even with the addition of polarisation functions on both carbon and hydrogen, at the SCF level this structure is still found to be slightly less stablethan the classical conformer also studied. An increase in the relative stability for the former is only evident when estimates of correlation effects are considered.

As was shown in Table 5.3, in the case of the 1-propyl cation, addition of polarisation functions to the STO-6.31G basis set leads to an increased stabilisation of the partially bridged and fully bridged isomers relative to the classical cation. The effects of polarisation functions and correlation energy corrections[267] for the 2-butyl cation should therefore stabilise the bridged non-classical species relative to the extended chain, the stabilisation being somewhat larger for the fully bridged as opposed to the partially bridged species. It is expected that such effects would therefore outweigh the conformational preferences outlined above, although it seems unlikely that the order of stability for the fully bridged and partially bridged forms indicated by the SCF calculations would be overturned. The ordering of stabilities as a result of polarisation and correlation energy considerations should therefore be exactly as shown in Figure 5.5, (viz. partially bridged > fully bridged > classical), the only proviso being that such effects might well decrease the relative energetic preference for the partially bridged as opposed to the fully bridged non-classical structure as already noted.

On the basis of the above discussions, comparison with the theoretical computations of Köhler and Lischka[267] reveals that both the partially (methyl) bridged and the methyl substituted corner protonated cyclopropane configurations are lower in energy than the symmetrically hydrogen bridged structure (and by inference the corresponding partially bridged structure). The calculations of the ground state energies at the STO-4.31G level suggest therefore that the 2-butyl cation may well adopt a partially bridged structure.

(b) Core Hole States

Discussions of the previous chapter have shown how weak interactions in the ground state hypersurface may be greatly enhanced on going to the core hole state manifold. The manner in which such phenomena are evident in the case of core ionisation of the ethyl cation has been outlined earlier with regard to both classical and non-classical hydrogen-bridged, isomers. In the particular cases of the 1-propyl cation and the 2-norbornyl cation, the creation of a core hole at a given site within the molecular frameworks leads to substantial electronic reorganisation[257] and in consequence core hole state spectra, even for species which differ very little in ground state energies, can be strikingly different. Thus, in Figure 5.7, showing the relative energies of the classical and non-classical 2-norbornyl cation as a function of holestate location, such trends are clearly evident. Whilst a core hole on C(2) enhances participation with C(1) and C(6), resulting in the non-classical species being favoured by $\sim$48 K cal mol^{-1}, creation of a core hole on either of the latter two donor atoms, leads to the classical cation being stabilised by $\sim$25 and 19 K cal mol^{-1} respectively.

It is evident that in the case of the 2-norbornyl cation, the extremely rapid time scale of the phenomena involved (essentially dictated by the lifetimes of the C_{1s} hole states) provides core hole state spectra which are entirely diagnostic of a classical or non-classical structure and comparisons with available E.S.C.A. data as was shown in Figure 5.1, has revealed that in a solid magic acid matrix the structure of the 2-norbornyl cation is non-classical.

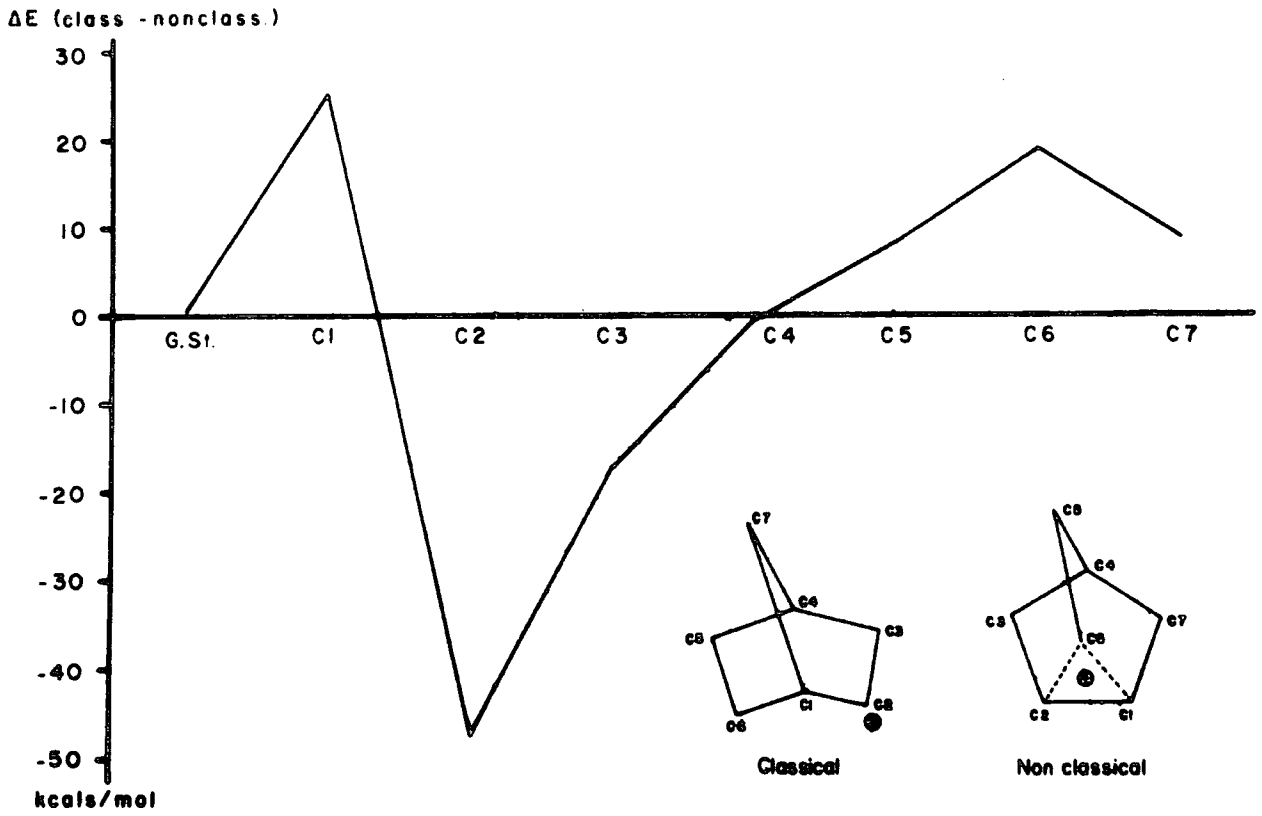

Figure 5.7 Relative energy-differences between the classical and non-classical forms of the 2-norbornyl cation

The investigation of the localised C_{1s} hole states of the various possible structures for the 2-butyl cation provides a further striking example of the general phenomena of enhancement of weak interactions in going to the core hole state manifold. The total energies for the ground and core hole states relating to the structures studied are presented in Table 5.4.

Table 5.4

Total energies (hartrees) for the ground and core hole states of the 2-butyl cation models studied

	Extended Chain	Partially bridged	Fully bridged
GS	-155.6427	-155.6669	-155.6436
C(1)*	-144.5957	-144.6385	-144.6336
C(2)*	-144.4500	-144.5225	-144.5559
C(3)*	-144.5950	-144.6262	-144.5645
C(4)*	-144.6711	-144.6377	-144.5974

Creation of a core hole at a given site within a carbocation structure represents the ultimate in electron demand and the distortion of the potential energy surfaces arising from the valence electron response becomes clear from the data presented in Figure 5.8.

Whilst the solid line shows the stability of the partially bridged 2-butyl cation structure relative to the classical ion, as a function of core hole location, the dashed line is representative of information concerning the fully bridged configuration relative to the extended chain isomer. As might be expected, core ionisation of the substituent methyl carbon adheres to the predicted ordering of the relative stabilities in the ground state with both partially bridged and fully bridged structures showing an almost equivalent stabilisation. However, in the case of the creation of a core hole at C(2), participation by the methyl

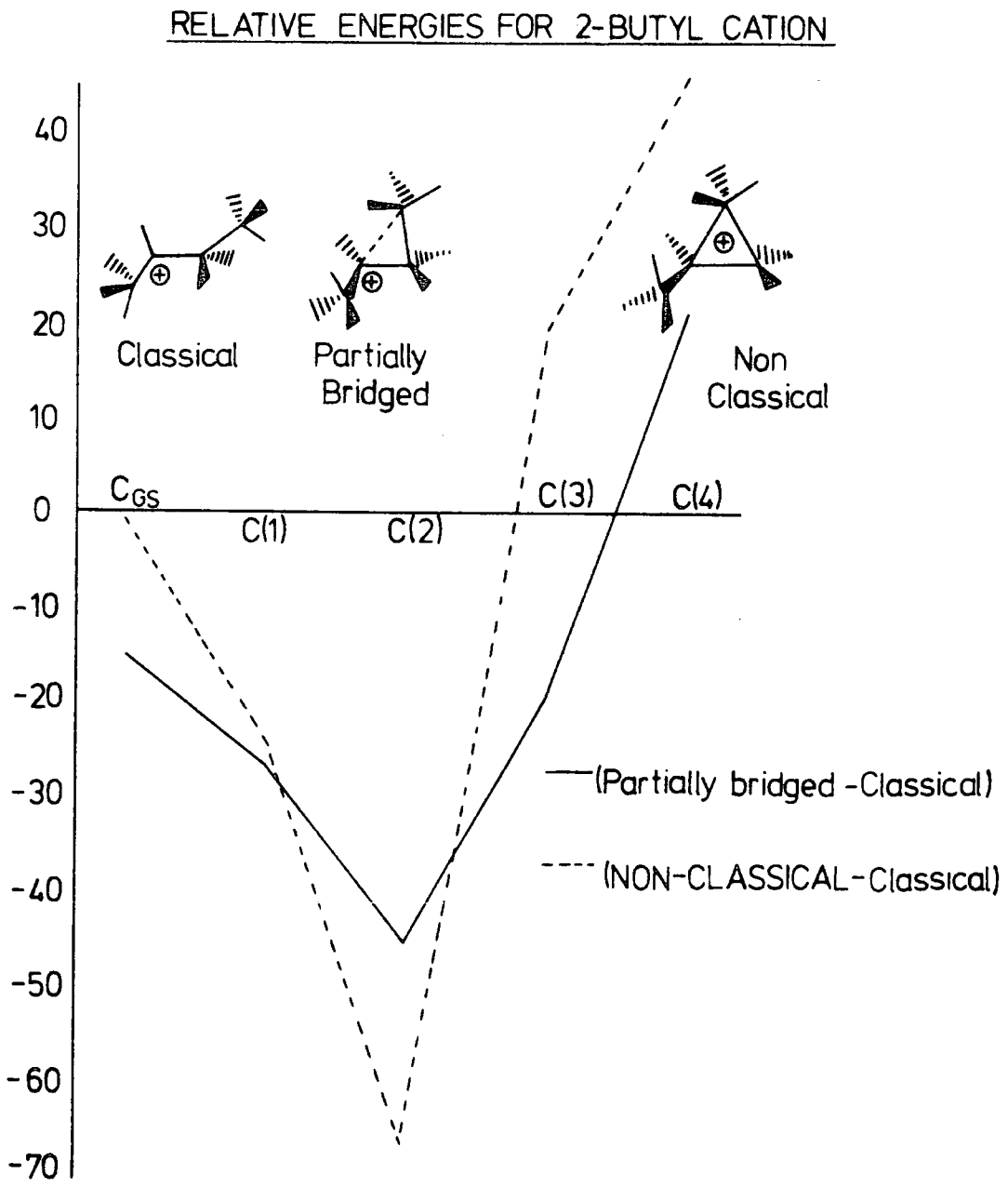

Figure 5.8 Relative energy differences as a function of hole state location for the 2-butyl cation models

bridging group is enhanced such that for the core ionised species, the fully bridged non-classical structure is stabilised by ∿70 K cal mol^{-1} compared to the classical ion. In contrast, creation of a core hole on the methyl bridging group carbon C(4) destabilises the fully bridged structure by ∿40 K cal mol^{-1}, as does the positioning of a core hole at C(3), by ∿20 K cal mol^{-1}. A core hole located at C(2) also stabilises the partially bridged isomer relative to the extended chain cation but by a lesser amount than noted above (∿40 K cal mol^{-1}), however, the destabilisation noted upon core ionisation of the bridging methyl carbon C(4) is also substantially less (∿20 K cal mol^{-1}) and this therefore provides evidence for the existence of a degree of C-C hyperconjugation in this form. Perhaps the most significant difference between the relative stabilities of the partially bridged and fully bridged non-classical isomers as a function of core hole location, is seen upon creation of a core hole at C(3). Whereas it was noted that a destabilisation of ∿20 K cal mol^{-1} is evident in the case of the latter, an equivalent stabilisation is observed for the partially bridged form relative to the classical isomer. Comparisons of the relative energies for the two non-classical forms are therefore clearly drawn from what is essentially the differences of the two lines in Figure 5.8, and it is interesting to note that only in the instance of core ionisation at C(2) is there a tendency towards greater stabilisation of the fully bridged ion.

From the results of the above analysis and their comparison with those for the 2-norbornyl cation, and indeed

earlier results reported for the cyclopentyl cation it is clear that binding energies for the classical and non-classical species would be expected to be of a distinctive nature. The ΔSCF computed core binding energies and relaxation energies for the classical, partially bridged and fully bridged, methyl substituted corner protonated cyclopropane structures for the 2-butyl cation are included in Table 5.5.

Table 5.5.

ΔSCF Core Binding Energies and Relaxation Energies (eV) for the 2-butyl cation

ΔSCF Method STO-4.31G

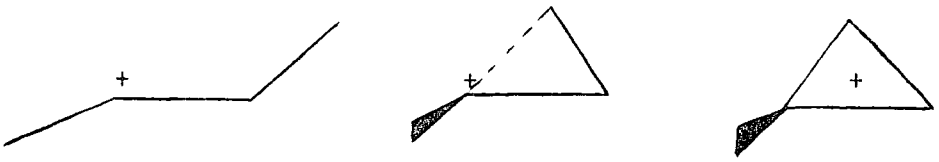

Hole State	B.E.	R.E.	B.E.	R.E.	B.E.	R.E.
C(1)*	300.6	11.3	300.1	11.4	299.6	11.5
C(2)*	304.6	11.1	303.2	11.6	301.7	11.9
C(3)*	300.6	11.7	300.4	11.7	301.5	11.9
C(4)*	298.5	11.6	300.1	11.9	300.6	11.9

The spans in binding energies for the models studied are 6.1 eV, 3.1 eV and 2.1 eV respectively and are distinctively different regarding classical and non-classical forms. The overall span for the relaxation energies is 0.8 eV and hence differences contribute significantly to shifts in binding energy, showing the danger of using Koopmans' Theorem, as was apparent in earlier discussions of the cyclopentyl cation.

Thus in going from the classical ion to the fully bridged structure there is a decrease in core binding energy values for C(1), which for the latter and partially bridged species become controlling factors for their respective spans, and this is accompanied by a slight increase in relaxation energy. This may be qualitatively understood from a simple electronegativity standpoint since in the classical 2-butyl cation, stabilisation of the positive charge at C(2), is largely dependent upon the distortion of the charge cloud at C(1) allowing only limited reorganisation upon core ionisation at the latter and hence a lower relaxation energy. In the partially bridged configuration, increased interaction between the bridging methyl carbon C(4) and C(2) diminishes the degree of distortion necessary at C(1) and hence, in part, decreases the core electron binding energy observed at the latter due to increased relaxation effects. The binding energy at C(1) attains its lowest value when there is maximum interaction of C(2) with the bridging methyl group, thus delocalising the positive charge and allowing greater polarisability of the C(1) charge cloud, and an increased ability for reorganisation.

The above discussion is perhaps best illustrated in the data pertaining to core ionisation of C(2) for which the shifts in binding energy between configurations are most significant (as would be expected from the relative energies of the hole states). Relaxation effects again increase with increasing C-C hyperconjugation, the manifestation of this result being that in the classical ion, the localisation of the positive

charge substantially contracts the electronic distribution about C(2) and hence further relaxation accompanying core ionisation is negligible.

Distortions of the charge clouds at C(3) and C(4) are more complex since there exists an internal interaction and also both are interactive in stabilising the positive charge at C(2). Therefore it would be unlikely that upon core ionisation at these centres, simple trends between core binding energy and relaxation effects would be shown and this is evident in Table 5.5. The distinctive nature of the predicted C_{1s} core level spectra for the configurations studied, is clearly shown in Figure 5.9.

In summary, therefore, computations at the STO-4.31G level suggest that 2-butyl cation may well prefer a partially bridged structure and it is interesting to note that this presents an organic analogy to the current emphasis on gradations in degree of bridging between two centres which is a feature of recent discussions of bridge bonded carbonyl groups in inorganic chemistry.[271] The core hole state computations show that in principle E.S.C.A. should provide a fast time scale probe for the structure of 2-butyl cation, since the computed spectra are so characteristic of a given structure.

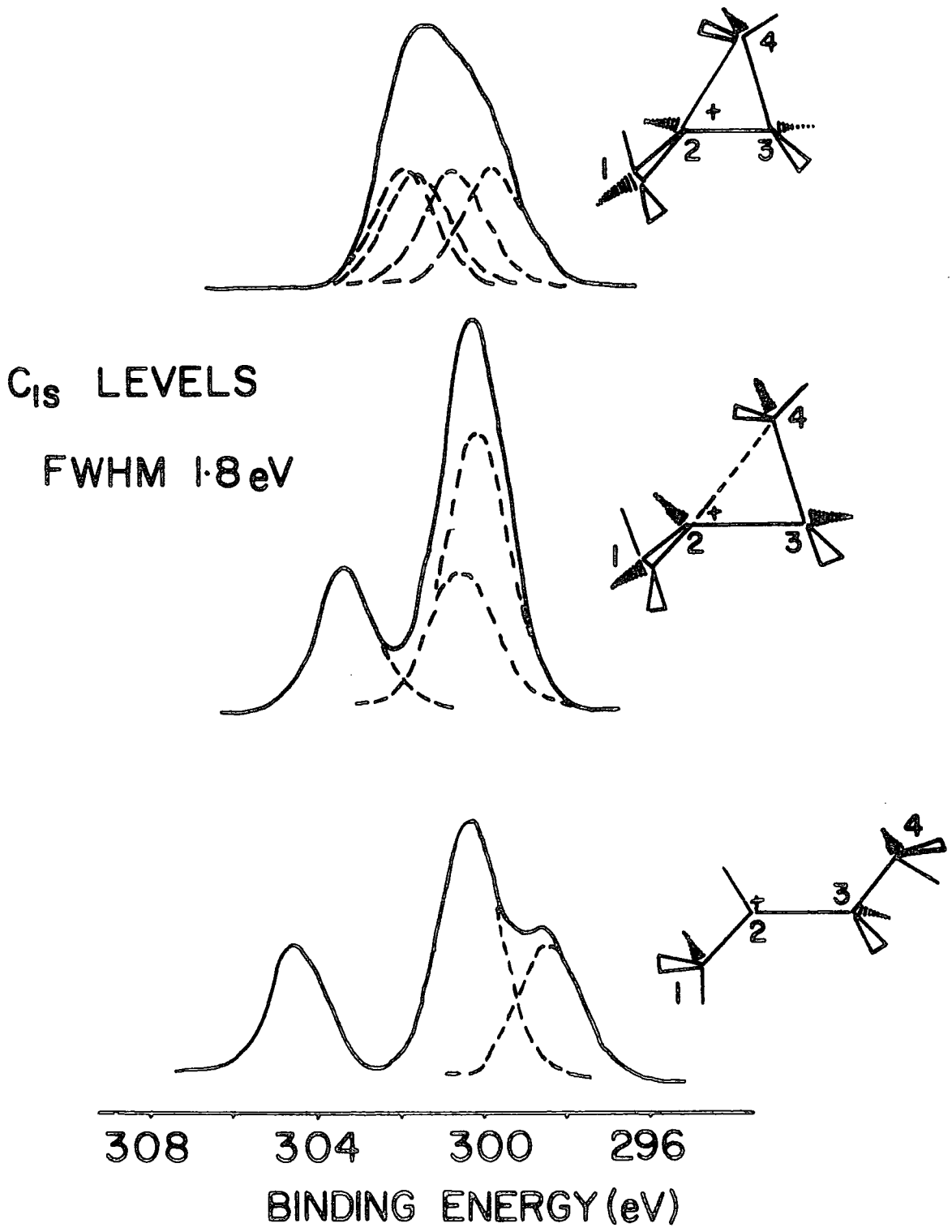

Figure 5.9 ΔSCF computed Core level Spectra for Classical and Non-classical, 2-butyl cation species

CHAPTER SIX

SATELLITE STRUCTURE ACCOMPANYING CORE IONISATION IN THE ISOMERIC HYDROCARBONS AND BENZOQUINONES

Non-empirical LCAO MO SCF computations have been carried out on the ground and localised core hole states of tetrahedrane and cyclobutadiene over a range of geometries available in the literature, and the experimentally determined structures for ortho- and para-benzoquinone. The object of such a study was to investigate the suitability of E.S.C.A. as a technique for distinguishing between structurally related, isomeric systems of appreciable energy difference. Differences in energy are found to be considderably magnified in the core-hole state manifold and this is shown to be distinctive in the structural determination for the C_4H_4 isomers. Whilst shifts in binding energy are found to be closely similar for both pairs of isomers, the shake-up transitions accompanying core ionisation are clearly characteristic of structural type.

6.1 Introduction

In the discussions of the previous chapters, the wide range of information levels available from a single E.S.C.A. experiment have been presented. However, emphasis has been placed upon the importance of the primary sources of information, namely absolute binding energies, relative peak intensities and internal binding energy shifts, and their dependence upon relaxation phenomena. Although the interpretation of satellite structure accompanying core ionisation, as described in Section 2.2.3, may be regarded as a secondary level of information, the distinctive nature of the inform-

ation derived from such a study is clear in the results previously presented relating to the investigation of keto-enol tautomerism in dicarbonyl systems (Chapter Four).

The interrogation of details of structure and bonding in solely hydrocarbon based systems by E.S.C.A. is not generally a straightforward process.[273-275] Indeed for a given hydrocarbon system with inequivalent carbon atom environments, the shift in binding energy is often so small that there are even ambiguities in assignments derived from line-shape analysis. Thus, in the particular case of neopentane, correlation of binding energies with model systems led Thomas and co-workers[273,274] to correctly assign the higher binding energy component to the carbons of the methyl groups; however the first attempt at interpreting the data theoretically, indicated that the overall line-shape could be equally well-fitted with the alternative assignment, of the methyl groups at lower binding energy.[275]

That such a situation might arise, is readily understood from the discussions of the previous chapters, since it has been shown (c.f. Chapter Three) that the binding energies of core electrons are subtly dependent upon substitution patterns. and that a significant proportion of differences in relative binding energies for a given core level can arise from differences in relaxation energies accompanying core-ionisation. Gas phase studies by Siegbahn *et al*[276] encompassing the range of linear alkanes from methane to tridecane have demonstrated that due to the similarity in valence electronic environment about any given carbon atom, the total shift range is compressed into a

narrow region of ∿0.6 eV. on the binding energy scale. A comparison of these results with those from a theoretical study by Clark and Cromarty[277] covering both linear and branched alkanes up to C_6, has shown that the factors which determine both absolute and relative binding energies are indeed short-range in nature and that these shifts are largely due to changes in relaxation energy across the series. The experimental investigation also included high resolution shake-up spectra for methane, ethane and propane the results of which are displayed in Table 6.1.

Table 6.1

Excitation energies for the C_{1s} shake-up in methane, ethane and propane.[277] (eV).

	Peak			
Molecule	1	2	3	4
Methane	∿15.0	19.2	22.7	26.5
Ethane	14.7	18.5	22.5	26.5
Propane	∿15.0	17.9	21.5	26.3

All of the spectra exhibited broad structures at approximately 15, 22 and 26 eV, but also a clearly distinguishable narrower line at ∿19 eV from the main line. From Table 6.1, it is apparent that as the number of carbon atoms in the molecule increases then the shake-up transition energy for the peak designated 2 in the spectra, decreases systematically. These results suggest that since the C_{1s} levels exhibit binding energies which are closely similar, then the main differences which can be observed are then due to low energy shake-up satellites.

As noted in Section 2.2.3, for solids the investigation of shake-up and shake-off states is complicated by the presence of the general inelastic tail, which provides a broad energy distribution, usually peaking at ~20 eV from the main photoionisation peaks and in the above study this phenomena was observed at higher pressures. Therefore, only in systems where relatively high-intensity, low-energy shake-up peaks are evident can the information derived from this source be conveniently exploited. Fortunately such conditions are generally satisfied in the core ionisation studies of polymer systems which contain either unsaturated backbones, or pendant groups, since low energy $\pi \rightarrow \pi^*$ shake-up transitions are possible. Thus, as shown in Figure 6.1, although the major photoionisation peaks for the C_{1s} levels of polystyrene and polyethylene are similar, the spectra are clearly distinguishable on the basis of the well-defined satellite structure evident in the former. The nature of such transitions has been determined in a study of the para-substituted polystyrenes.[242] The substituents varied from strong π-electron donors to π-electron acceptors, in the series X = NH_2, OCH_3, Br, and Cl, and it was observed that the centroids for the satellite structures increased in energy separation as did the intensity within the given series, relative to the main photoionisation peaks. The satellite structure for each substituted system was resolved into two components ($b_{1\pi} \rightarrow b_{1\pi^*}$ and $a_{1\pi} \rightarrow b_{1\pi^*}$) and comparison with calculations on the related para-substituted toluene systems showed that while the intensity for the former transition remained constant for π electron-donating substituents, the latter decreased in intensity, consistent with the experimental data, thereby assigning the nature of the transitions.

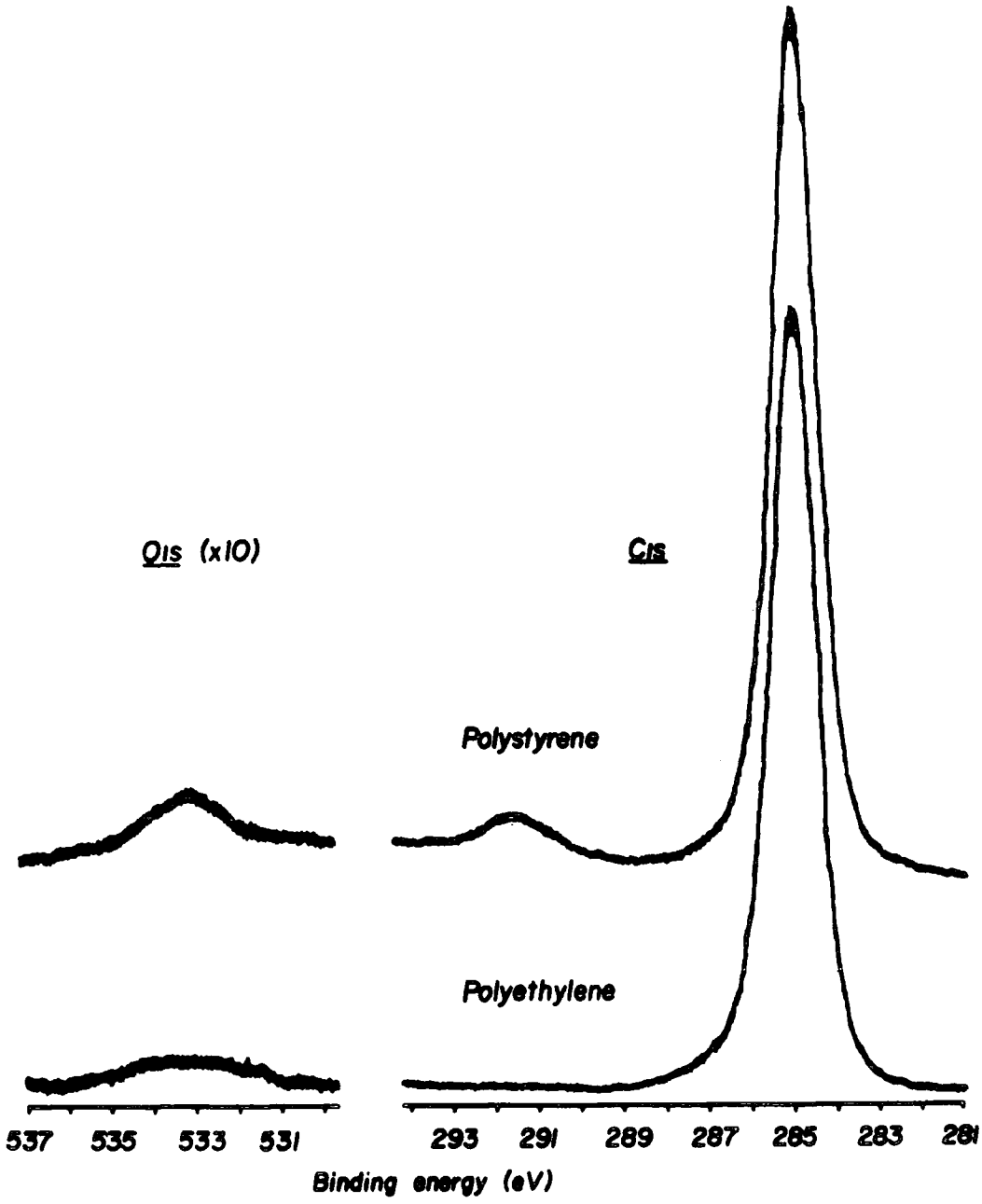

Figure 6.1 A comparison of the C_{1s} spectra for polystyrene and polyethylene

In particular cases, the investigation of such satellites can prove rewarding.[239-242] From Figure 6.1 it is clear that information on co-polymer compositions in styrene-alkane systems is possible by reference to the distinctive $\pi \rightarrow \pi^*$ shake-up structure accompanying core ionisation.

Oxidation of the polystyrene system was previously referred to in Chapter Three, and it has been suggested that information concerning the unsaturated centres in the polymer can be derived by monitoring the shake-up intensity[191] (Figure 6.2).

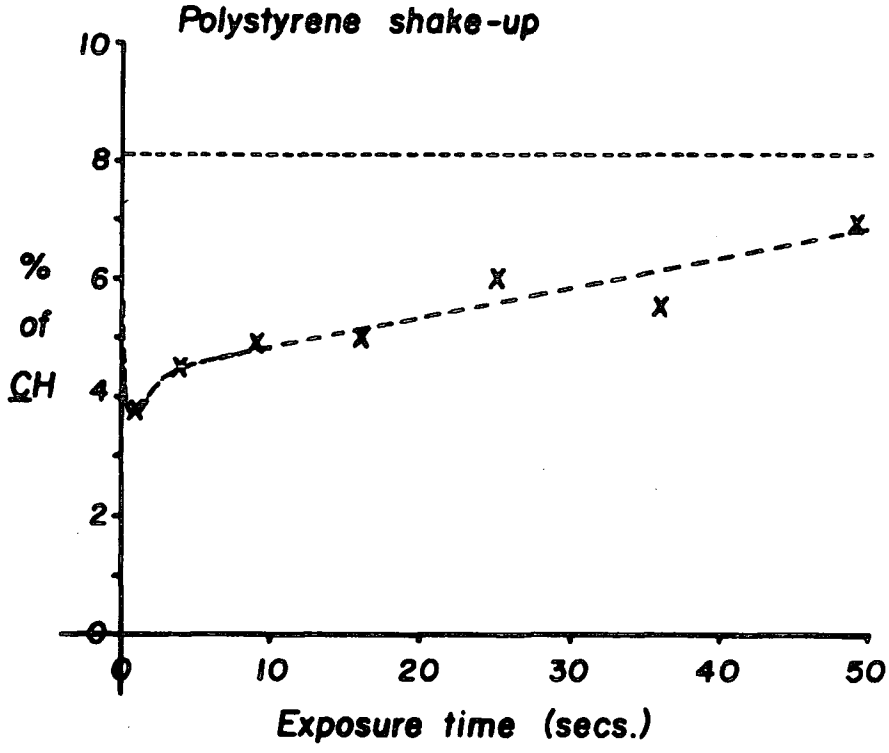

Figure 6.2 Shake-up intensity relative to CH (carbon not attached to oxygen) intensity in polystyrene as a function of exposure time to an oxygen plasma.

The intensity of such structure is greatly reduced in the first second of reaction due to loss of unsaturation and substituent effects consequent upon replacing ring hydrogen by an oxygen-containing functionality. This loss occurs rapidly to a definite depth of the sample, and it is noted that the apparent slight increase in the shake-up intensity,

with respect to CH, most probably arises from the increase in interchain distance in the surface regions, consequent upon the introduction of oxygen functionalities. Clearly, this would reduce the number density of carbon atoms in the surface and decrease the total C_{1s} intensity. Because the signal due to carbon atoms not attached to oxygen reduces in intensity as the reaction proceeds, the shake-up intensity in relation to this not surprisingly increases.

The study of the isomeric carbocation structures in the previous chapter illustrates the considerable capability provided by E.S.C.A. in studying weak interactions, which are clearly enhanced in going from the ground to the core hole state manifold. However much less emphasis has been placed to date on the investigation of the core level spectra of isomeric systems separated by appreciable energy barriers.

A study of the isomeric 5 and 6 aza-uracils[278] has shown that the short-range nature of the interactions which dominate E.S.C.A. chemical shifts, may be turned to particular advantage, since the distinctive nature of the substituent effects on the core levels C_{1s} and N_{1s}, allow ready identification of a particular structure, and show the two to be linkage isomers. It is clear from the dicarbonyl studies (Chapter Four) that shake-up satellite structure may be characteristic of a given structural type, and its importance as a means of distinguishing between systems of similar composition is evident in the previous discussion. Investigations have therefore been made concerning isomeric, CH and CHO, containing systems, which on the basis of these previous discussions may be considered as constituting the case in which the configurations are separated by an appreciable energy

difference; but their composition is such that the factors determining shifts in binding energy are so short range as to render such shifts negligible.

6.2 A Theoretical Investigation of the Ground and Core Ionised States of Tetrahedrane and Cyclobutadiene

The considerable current interest in the electronic structures and relative energies for the isomeric C_4H_4 systems represented by tetrahedrane and cyclobutadiene has therefore prompted the investigation of the core level and low lying shake-up states of these molecules to ascertain the potential of E.S.C.A. as a diagnostic tool for these systems.

Early theoretical studies[279] at a non-empirical level have indicated the inherently greater stability of the cyclobutadiene ring system in its rectangular ground state, however the computations also suggested that tetrahedrane might well lie in a local minimum with an appreciable activation barrier being involved for the conversion to cyclobutadiene. The elegant synthesis of tetra tertiary butyltetrahedrane as a stable white solid, recently reported by Maier and co-workers,[280] and the consequent rationalisation of the large barrier to interconversion to the thermodynamically more stable cyclobutadiene isomer in terms of the "corset effect" has promoted a series of theoretical[281-287] and experimental studies.[288] The focus of attention in these studies has primarily been on the relative energies and ground state geometries for these systems and possible routes for their interconversion. Thus, Dewar *et al*[281] using the MINDO/3 method. showed that the lowest energy path

for the rearrangement to the cyclobutadiene system needed an activation energy of ∿41 K cal mol^{-1}. Being symmetry forbidden, the study concluded that the reaction coordinate passed through three different conformers of the bicyclobutyl diradical. In an MNDO study,[282] comparison with the analogous tetra-tertiary butyltetrahedrane rearrangement predicted energy differences for the tetrahedrane-cyclobutadiene systems and their corresponding tetra-tertiary butyl-derivatives of 45.9 and 6.7 K cal mol^{-1} respectively, indicating the extra stability of the tetrahedral system upon replacement of the four hydrogen atoms. The MNDO-CI activation energy for rearrangement of the parent system was, at this level, calculated to be 15.2 K cal mol^{-1}.

More recent calculations by Kollmar,[283] with the inclusion of polarisation functions and estimates of correlation energy, gave a value of ∿30 K cal mol^{-1} for the activation energy and predicted a stabilisation of the cyclobutadiene system by ∿29 K cal mol^{-1}. Indeed, since the first non-empirical calculation on the tetrahedrane system, by Buenker and Peyerimhoff[279] which predicted a destabilisation of ∿70 K cal mol^{-1}, each subsequent calculation has been indicative of the inherent stability of the tetrahedral moiety.

Whilst the experimental and theoretical studies have considered some aspects of the low lying valence ionised states, for both tetrahedrane and cyclobutadiene, as will be discussed in due course, there have been no previous studies of the core hole state manifold, either theoretical or experimental. The focus of attention in this part of the chapter will therefore be as follows:

(i) the computed ΔSCF core binding energies and relax-

ation energies for the C_{1s} core levels of both tetrahedrane and cyclobutadiene for a variety of geometries, which have previously been reported for these systems:

(ii) the computed relative energies of both the ground and core hole states as a function of geometry;

(iii) the investigation of low lying shake-up satellites accompanying core ionisation in these systems.

Some consideration has also been given to the highest valence ionised states for the two isomers.

6.2.1 Computational Details

The geometries used in this study are a selection of those optimised at various levels of sophistication for both tetrahedrane and cyclobutadiene, and quoted in the literature. In the case of tetrahedrane, those chosen were as follows: the Gaussian 4.31G optimised geometry obtained by Schulman and Venanzi[284] giving CC and CH bond lengths of 1.482Å and 1.054Å respectively within a T_d symmetry; and also that determined by Kollmar[283] at the SCF level using a double zeta Gaussian basis set with the inclusion of polarisation functions (CC 1.46Å, CH 1.064Å) again within the T_d symmetry. For cyclobutadiene, a geometry described by Kollmar[283] was again used, determined at the same level and basis set as used for the tetrahedrane calculations, and giving C=C 1.313Å, C-C 1.572Å and C-H 1.073Å. These values are comparable with those pertaining to the STO-3G optimised geometry of Pople and Hehre.[285] A geometry taken from the definitive study by

Jafri and Newton[286] was also employed. This study predicted that the rectangular singlet should be the ground state at the 2-configuration SCF and CI levels, with bond lengths C=C 1.334Å, C-C 1.564Å and C-H 1.075Å. Geometries for both systems were optimised within the multi-variational scheme contained in the semi-empirical MNDO program, and gave values of C-C 1.52Å, C-H 1.063Å; and C=C 1.357Å, C-C 1.534Å; C-H 1.071Å; respectively in agreement with those determined by Schweig and Thiel.[282]

Ab initio calculations were carried out on the ground and core hole states of the above structures, again using the ATMOL 3 suite of programs. Two basis sets were used in each case, both the STO-4.31G, with best atom exponents, as previously outlined (Section 1.7.5) and the Dunning (4s3p/2s) contraction of the Huzinaga (9s5p/4s) primitive Gaussian set. Core binding energies and relaxation energies were calculated in the manner previously described and valence ionised states have also been investigated by direct ΔSCF computations.

6.2.2 Results and Discussion

(a) Ground States

The relative energies for the various ground state geometries included in this work are displayed in Table (6.2) and are presented relative to the most stable structures calculated for cyclobutadiene within each basis set, at the SCF level.

For cyclobutadiene, the lowest energy for both basis sets corresponds to the geometry determined by Jafri and Newton.[286] The computations indicate however that distortions

Table 6.2

Relative energies (K cal mol^{-1}) for the tetrahedrane and cyclobutadiene models studied

	TETRAHEDRANE			CYCLOBUTADIENE			
	MNDO (Opt.)	Ref.283	Ref.284		MNDO (Opt.)	Ref.283	Ref.286
C-C (Å)	1.520	1.460	1.482	C-C (Å)	1.534	1.572	1.564
C-H (Å)	1.063	1.064	1.054	C=C (Å)	1.357	1.313	1.334
				C-H (Å)	1.071	1.073	1.075
METHOD							
STO-4.31G	35.6	40.3	37.1		1.7	2.0	0.0
Dunning (4s3p/2s)	43.5	44.6	42.3		2.4	0.1	0.0

involving predominantly the carbon-carbon double bonds must be relatively inexpensive energetically, since both basis sets predict that the potential energy surface is rather flat about the Jafri and Newton geometry. For tetrahedrane, the results are somewhat more basis set dependent. Thus the lowest absolute energy is predicted to be for the MNDO optimised geometry when the STO-4.31G basis set is used, however, employing the Dunning (4s3p/2s) contraction for the computations is indicative of stabilisation for a structure exhibiting parameters equal to those determined by Schulman and Venanzi[284] (see Table 6.2). While differing with one another, these calculations give good agreement with values determined by Kollmar[283] at equivalent degrees of accuracy. Thus in a minimal basis set SCF geometry optimisation a value for the CC bondlength of 1.523Å was obtained, and using a double zeta SCF level of calculation, CC 1.492Å. It is therefore equally consistent that at both levels, the geometry shown to be most stable by Kollmar, is in the present study predicted to be the least stable, since as noted above polarisation functions were included in the basis set previously employed.

The computed energy differences between the optimum values for cyclobutadiene and tetrahedrane over the range of geometries considered are 35.6 K cal mol^{-1} and 42.3 K cal mol^{-1}, for the STO-4.31G and Dunning (4s3p/2s) basis sets respectively. These may be compared with the MNDO (opt.) value of 45.9 K cal mol^{-1} and previous *ab initio* computed values[279,285,28] of 70, 31.4 and 29 K cal mol^{-1}.

(b) Core Hole States

A re-occurring theme in the previous chapters has been the enhancement of weak interactions in going from the ground state to the core hole state species. It is therefore of interest to consider the relative energies of the localised core hole states for tetrahedrane and cyclobutadiene within the models considered. The relevant data are displayed in Figure 6.3, where for comparison purposes, data are also included for the ground states.

In Figure 6.3, A, B, C and D represent the geometries taken, within each system, and relate to the determinations by Schulman and Venanzi, Kollmar, Jafri and Newton, and optimisation within the MNDO subroutine respectively. The parameters for each are readily observed in Table 6.2. The ground state data are presented relative to the optimum absolute energy values for cyclobutadiene within the confines of each basis set (in both cases corresponding to the Jafri and Newton geometry as previously noted). The C_{1s} core hole state data are presented relative to the absolute energy values for the corresponding core ionisation in these systems. In Figure 6.3, a positive gradient represents a relative destabilisation of the core ionisation process for a given structure, whilst a negative gradient is therefore indicative of a stabilisation relative to the core ionisation process of the lowest energy, cyclobutadiene system calculated for the ground state within each basis set. It is therefore clear from Figure 6.3, that creation of a core hole magnifies the differences in energy between the two structures, since the tetrahedral moiety shows a relative destabilisation in energy upon core ionisation, and the computed energy

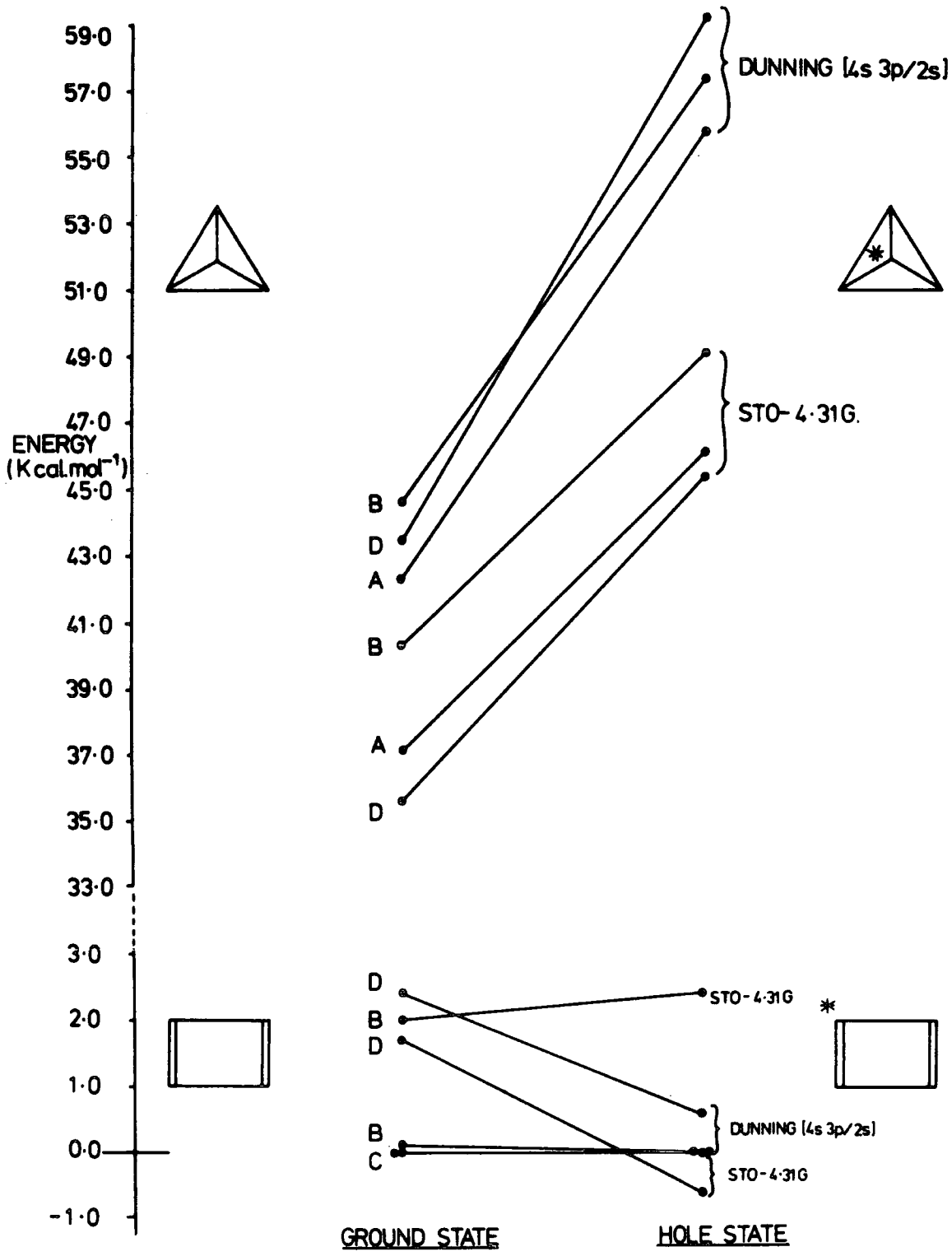

Figure 6.3 Relative energies for tetrahedrane and cyclobutadiene

differences for the hole state data of 55.8 K cal mol^{-1} and 44.8 K cal mol^{-1} for calculations performed with the Dunning and STO-4.31G basis sets respectively, are ∿30% larger than for those of the ground state systems. Part, at least, of this increased energy difference arises from the somewhat larger relaxation energy for the conjugated system, as is apparent in Table 6.3.

In an absolute sense, the tetrahedrane structures found to be most stable in the core hole state manifold are equivalent to those determined using either of the two basis sets in the groundstate. However, for cyclobutadiene, whilst agreement is found for the structures lowest in energy, in both the ground state and the core hole state, from calculations at the Dunning level, the STO-4.31G basis set favours the stability of the MNDO (opt.) geometry (D) in the hole state, in preference to that determined by Jafri and Newton (C) which is the most stable on an absolute scale in the ground state. It is interesting to note, that the MNDO (opt.) geometry is also favoured in a relative sense when the relative stabilisation for the core ionisation processes of the cyclobutadiene structures are compared at the Dunning level. These results compare well with a further series of calculations by Kollmar[283] which included estimates of correlation energy. In a study at the double zeta level with estimates of correlation energy included, the following parameters were obtained (C-C 1.627, C=C 1.357). The inclusion of polarisation functions also, produced the following (C-C 1.571, C=C 1.336). A comparison of the results from the above studies, with those due to Kollmar, serves to indicate that the most favourable ground state structure for cyclobutadiene is most probably a

rationale between the MNDO (opt.) and, Jafri and Newton, geometries.

An equivalent study may be made for the tetrahedrane system, although in this case, it is only in a relative sense. From Figure 6.3, it is clear that the results from both the Dunning and STO-4.31G calculations show a relative stabilisation for the geometry determined by the Kollmar study (B), which in both cases was found to be the least stable in the ground state. Confirmation of this assignment is again provided by further calculations, including estimates of correlation, as performed by Kollmar.[283]

The core binding and relaxation energy data displayed in Table 6.3 indicate that the computed absolute binding energies show only a small dependence on the assumed structure. Thus with a given basis set, the binding energies and relaxation energies for the three structures considered for cyclobutadiene and tetrahedrane give essentially the same results, and it is convenient to display the data as in Figure 6.4. The tendency for the STO-4.31G basis set to overestimate absolute binding energies as a result of an underestimation of relaxation energies is clearly evident when comparison is made with the data calculated at the Dunning level. However it is apparent that the shifts in binding energy derived from the two distinct sets of data are in very good agreement. Thus, a shift of $\sim$0.6 eV is predicted between the core levels of cyclobutadiene and tetrahedrane, and on the basis of previous studies outlined earlier, this difference is surprisingly large. The data in Figure 6.4 reveal that irrespective of the extra lowering in energy arising from the relaxation

Table 6.3

ΔSCF Binding and Relaxation Energies (eV) for Tetrahedrane and Cyclobutadiene

	TETRAHEDRANE			CYCLOBUTADIENE		
	ΔSCF BE (RE)			ΔSCF BE (RE)		
	MNDO (Opt.)	Ref. 283	Ref. 284	MNDO (Opt.)	Ref. 283	Ref. 286
STO-4.31G	294.1 (12.2)	294.0 (12.0)	294.0 (12.1)	293.5 (12.4)	293.6 (12.3)	293.6 (12.3)
Dunning (4s3p/2s)	291.7 (14.9)	291.6 (14.7)	291.6 (14.8)	291.0 (15.3)	291.0 (15.1)	291.0 (15.2)

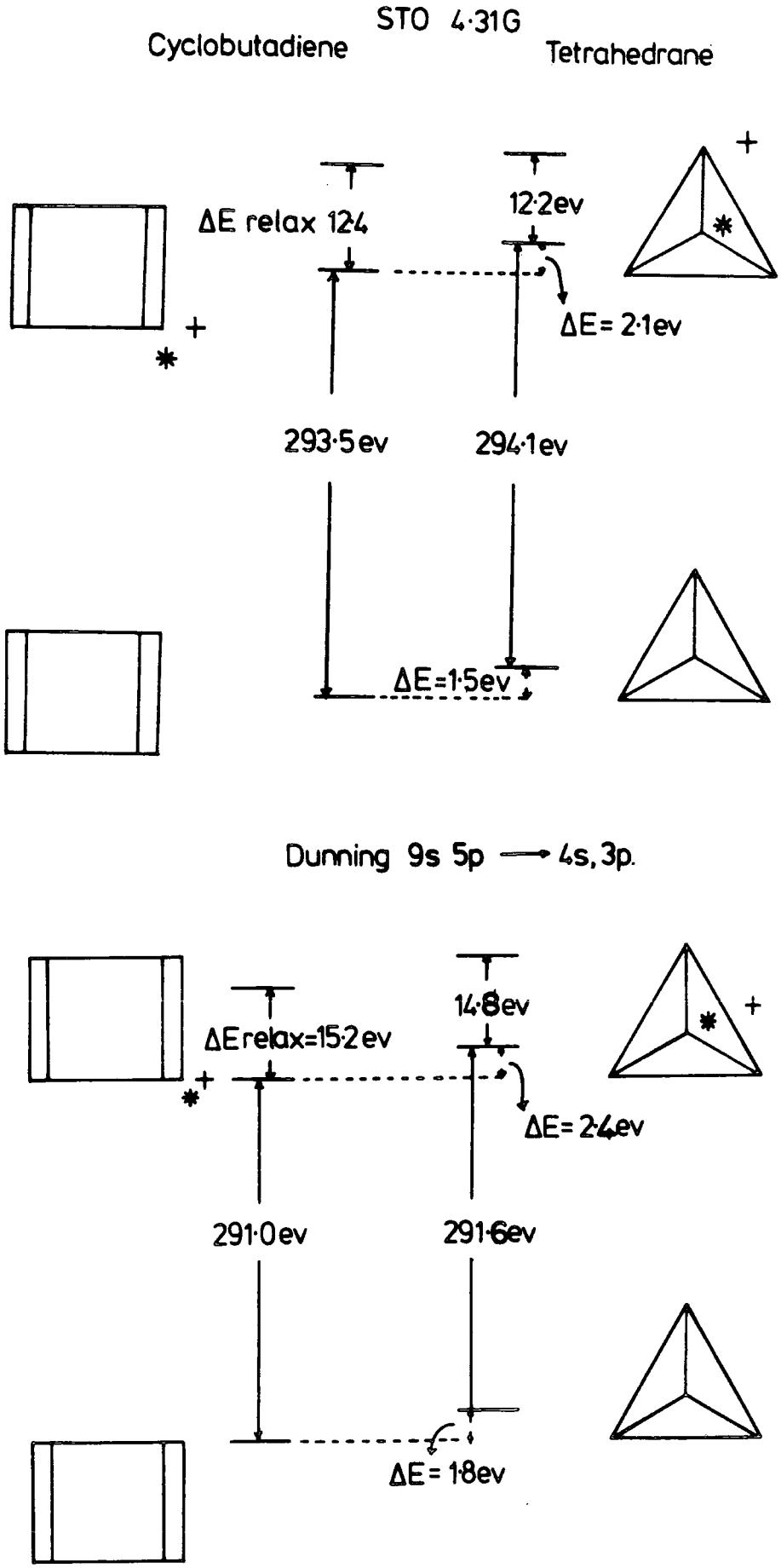

Figure 6.4 A comparison of the binding energies and relaxation energies as a function of basis set

process, the conjugated system is better able to stabilise a localised core hole.

(c) Valence Ionised States

Heilbronner *et al*[288] have recorded the He(1α) photoelectron spectra for both tetra-tertiary-butyl-tetrahedrane and tetra-tertiary-butylcyclobutadiene, and note that from an analysis of alkyl-substituted systems, substitution of the four hydrogen atoms in the parent compound by four tertiary butyl-groups is estimated to lead to a reduction of the ionisation energy for the former by approximately 1.4 - 1.7 eV. Comparison with a similar study for the cyclobutadiene system concluded that ionisation from the b_{3g} orbital of the latter should be at considerably lower energy ($\sim$1.6 eV) than for the corresponding orbital of tetrahedrane (1e). The actual values noted are 8.3 ± 0.2 eV and 9.5 ± 0.2eV respectively, which are essentially in agreement with results evident in the geometrical studies referenced in this chapter,[284,286-288] and the MNDO studies (8.4 eV and 9.8 eV), if Koopmans Theorem is assumed valid. The theoretical studies also confirm the assignment of the highest three orbitals in cyclobutadiene as $b_{3g}(\pi)$ HOMO, b_{3u} (σ) and b_{2u} (π), and it is therefore difficult to assess whether or not this agreement for the ionisation potentials is merely fortuitous or due to a convolution of the two prime factors neglected in the theoretical estimates, namely relaxation and correlation effects. To investigate this further, the relevant valence ionised states for tetrahedrane and cyclobutadiene have been studied.

It was evident, from the Koopmans' values, ΔSCF ionisation potentials and computed relaxation energy data, that the results obtained were again in good agreement between the assumed structures, however as in the case of the core level data, these were characteristic of the basis set used in the calculations. The ionisation potentials, Koopmans' values and relaxation energies are displayed in Table 6.4.

Table 6.4

Ionisation Potentials and Relaxation Energies (eV)

		ΔSCF	KOOPMANS	R.E.
Tetrahedrane				
STO-4.31G	$1e$	7.8	8.7	0.9
	$3t_2$		14.3	
Dunning (4s3p/2s)	$1e$	8.3	9.3	1.0
	$3t_2$		14.9	
Cyclobutadiene				
STO-4.31G	b_{3g}	6.3	7.1	0.8
	b_{3u}		11.9	
Dunning (4s3p/2s)	b_{3g}	6.8	7.6	0.8
	b_{3u}		12.5	

It is evident from the data in Table 6.4 that the difference in ionisation potentials between the cyclobutadiene and tetrahedrane systems is well described for both basis sets, within the ΔSCF method (shift 1.5 eV), however, it is also clear that the relaxation energy differences play a negligible role in determining the relative ionisation potentials, and it may therefore be inferred that correlation energy differences must also be quite small.

For the sake of completeness and to aid the discussion presented in the next section, the Koopmans' values representing the orbital energies and assignments for the two highest occupied levels in both systems are also included in Table 6.4. The ordering for the cyclobutadiene molecular orbitals has already been described and that for the lower ionisation potentials in tetrahedrane is as follows: $1e \equiv$ HOMO, $3t_2$ and $3a_1$.

(d) Shake-Up

From an experimental standpoint, the importance of satellite structure as a means of identification, and its assignment as arising from $\pi \rightarrow \pi^*$ transitions, with appreciable intensity, has been discussed earlier in this chapter. As has also been noted, it is clear from the distinctive nature of the theoretical data relating to such satellites in the dicarbonyl systems and their good agreement with experiment, (Chapter Four), that the transition energies and intensities, for HOMO -LUMO shake-up transitions accompanying core ionisation may be semi-quantitatively described within the sudden approximation (c.f. Section 2.2.3). The transition energies and intensities for the HOMO-LUMO transitions in the tetrahedrane and cyclobutadiene systems, over the range of geometries studied, have therefore been computed from the relevant ground and core hole state eigenvectors and eigenvalues for the C_{1s} levels, and the data are displayed in Table 6.5.

Table 6.5

$\pi \rightarrow \pi^*$ Shake-up, Energy transitions (eV) and Intensities (%) for tetrahedrane and cyclobutadiene

	TETRAHEDRANE ($1e \rightarrow 4t_2$)						CYCLOBUTADIENE ($b_{3g} \rightarrow b_{1g}$) and ($b_{3g} \rightarrow a_{1u}$)					
	ΔE (eV) Intensity						ΔE (eV) Intensity					
METHOD	MNDO (Opt.)		Ref. 283		Ref. 284		MNDO (Opt.)		Ref. 283		Ref. 286	
STO-4.31G	9.5	1%	9.6	2%	9.7	1%	1.9	6%	2.8	6%	2.5	7%
							7.2	1%	7.9	1%	7.6	1%
Dunning (4s3p/2s)	10.1	1%	10.2	2%	9.9	1%	2.0	9%	2.7	5%	2.4	6%
							7.5	1%	7.6	1%	7.3	1%

It is clear from Table 6.5, that for both levels of calculation, there is good agreement between both computed intensities and transition energies for each system. The computations predict the shake-up spectra to be clearly distinguishable in that for each tetrahedral moiety, only one transition is expected ($1e \rightarrow 4t_2$), within the energy range 0-10 eV, whilst for the cyclobutadiene structures, two transitions are evident. The differences in transition energies and intensities for these peaks are appreciable, rendering them distinctive. The centroid, for that in the vicinity of the main photoionisation peak is predicted to be shifted by 2.3 ± 0.4 eV and is the more intense ($b_{3g} \rightarrow b_{1g}$), whilst that at lower energy has transition energy 7.5 ± 0.4 eV ($b_{3g} \rightarrow a_{1u}$) and is comparable in intensity to the shake-up structure expected for the tetrahedrane system.

On the basis of the earlier discussion concerning the alkanes, the shift in C_{1s} binding energies between the tetrahedrane and cyclobutadiene systems ($\sim$0.6 eV) calculated from the core hole state data in Section 6.2.2(b), is comparatively large, although the significance of a shift of this size in an actual spectrum is difficult to assess. However, from the computed core level and shake-up spectra (Figure 6.5) it is clear that this is of no consequence, since these are readily distinguishable by consideration of the satellite structure. It is clear from this study of the isomeric C_4H_4 systems that E.S.C.A. might indeed be a useful tool for distinguishing between structurally related hydrocarbons, and it is of interest to extend this study to isomeric C,H,O. containing species.

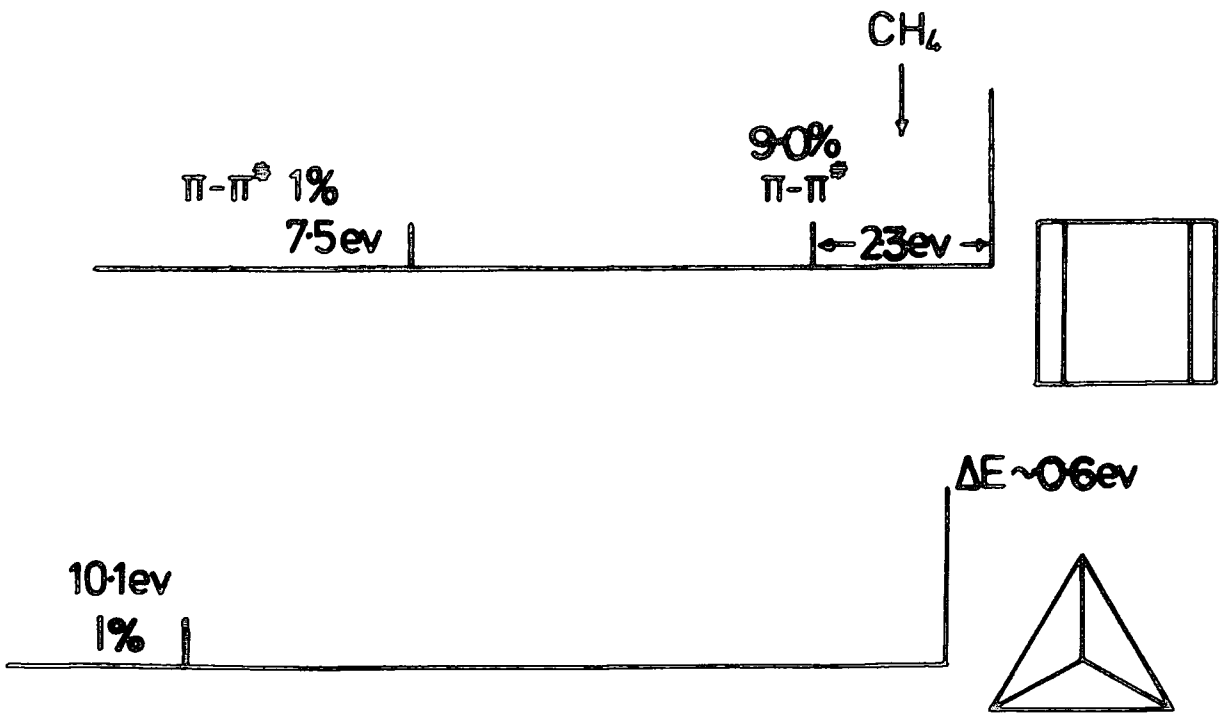

Figure 6.5 Comparison of the C_{1s} core level spectra for tetrahedrane and cyclobutadiene.

6.3 A Theoretical Investigation of the Ground and Core Ionised States of 2,5-Cyclohexadiene-1,4-Dione and 3,5-Cyclohexadiene-1,2,-Dione

The isomeric benzoquinones are particularly appropriate to this study, since they are sufficiently small to be amenable to non-empirical investigation, and are representative of the large class of quinones, which act as retarders and inhibitors in free radical polymerisations, depending upon their redox potential.[193] Indeed quinones of high redox potential, such as 2,5,7,10-tetrachlorodiphenoquinone, copolymerise with styrene to high-molecular-weight products. Since these do not polymerise with acrylonitrile or with

vinyl acetate, it is presumed that copolymerisation with styrene proceeds via a charge transfer complex.

p-Benzoquinone is itself, an effective inhibitor for free-radical polymerisations. Thus in industry, hydroquinone is often added to monomers, although it acts as neither inhibitor or retarding agent, and if oxygen is present in the system then it is oxidised to quinone. In the particular case of peroxide initiated reactions, hydroquinone acts in two ways: directly as a reducing agent for the initiation; and indirectly (as benzoquinone) as an inhibitor. Hydroquinone in this case is therefore a stabiliser.

Current interest in the benzoquinone isomers has concerned the assignments of the bands in the lower energy regions of the photoelectron spectra. Whilst a vast body of literature[289-300] is available for the p-benzoquinone structure, only recently has attention been directed towards the o-benzoquinone isomer.[301-303] A number of qualitatively similar photoelectron spectra have been reported for p-benzoquinone, and these have been interpreted using both semi-empirical[291-297] and *ab initio* methods.[298-299] Common to all of these studies is the assignment of the four lowest energy ionisations, in the region 10-12 eV, as arising from two π-type molecular orbitals and two from the oxygen lone-pairs, however, the debate concerning their ordering continues.

Schang and co-workers[302] have recently made the first attempt at assigning the bands in the previously published photoelectron spectrum for o-benzoquinone, using the MINDO/3 method. Whilst in the lower energy region, these are again seen as arising from two π-type orbitals and the lone-pairs

of the oxygens, a more recent semi-empirical study by Hilal[303] again disputes the ordering of the assignments.

Despite the vast number of investigations concerning the valence levels of these isomeric species, only a single study has appeared in the literature concerning the core levels of either. The E.S.C.A. spectrum for the C_{1s} levels of p-benzoquinone has been reported by Ohta and co-workers,[304] and although this is qualitatively similar to that which would be expected on the basis of the discussions in Chapter Three, the deconvolution is interesting since it bears no relation to the trends in relative binding energies mentioned earlier. The O_{1s} levels are described, but the actual spectrum is not included, however, an attempt has been made to qualify the binding energy assignments for both the C_{1s} and O_{1s} levels using the CNDO method and charge potential type calculations, assuming Koopmans' Theorem. Clearly, relaxation effects are not, therefore explicitly considered and the merits of such a study have been outlined previously (c.f. Chapters Three and Four.

With this introduction, the following points of interest may be addressed:

(i) the relative energies for the ground state structures of o- and p-benzoquinones studied, and the nature of the higher occupied molecular orbitals as compared to previous studies;

(ii) the computed ΔSCF core binding energies and relaxation energies for the C_{1s} and O_{1s} core levels and for p-benzoquinone, a comparison with the experimental data;

(iii) the investigation of the low lying shake-up satellites accompanying C_{1s} and O_{1s} core ionisation in the o-benzoquinone and p-benzoquinone systems.

6.3.1 Computational Details

In this instance, investigation of a range of geometries was unnecessary, since experimentally determined structures were available. That for p-benzoquinone was taken from an electron diffraction study by Hagen and Hedberg[305] whilst the ortho-configuration was determined from Cu-K_α diffractometry data in a study by Macdonald and Trotter.[306]

The *ab initio* computations were performed in the manner described in Section 6.2.1, however only the STO-4.31G basis set was adopted since as shown in the earlier discussions of this chapter and in particular, Chapter Four, shifts in binding energy and the transition energies and intensities, computed for satellite structure arising from $\pi \rightarrow \pi^*$ transitions, are well described at this level.

6.3.2 Results and Discussion

(a) Ground States

The total energies relating to the experimental geometries for each isomer are displayed in Table 6.6. At this level, the para-substituted structure is found to be more stable than the ortho-isomer by $\sim$39.7 K cal mol^{-1}. Assuming the above geometries, this value is confirmed in

Table 6.6 Total energies (a.u.) for the benzoquinone isomers studied

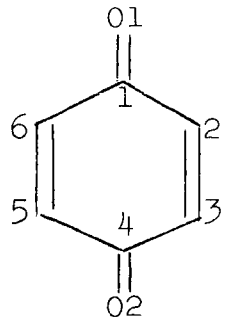

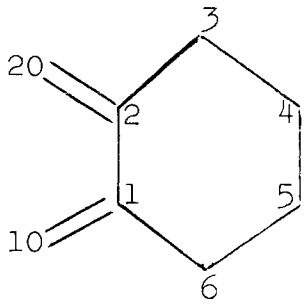

C=O	1.225Å	C=O	1.220Å
C=C	1.344Å	C=C	1.341Å
C-C	1.481Å	=C-C=	1.454Å
C-H	1.089Å	=C-C	1.469Å
		C-C	1.552Å
		C-H	0.95Å
Total Energies (a.u.)	-377.2467		-377.1835

MNDO semi-empirical calculations ($\sim$38.4 K cal mol^{-1}), however, whilst it is well known[307] that the para-isomer is more stable than the o-benzoquinone a full geometry optimisation at this level reduces this difference in energy to $\sim$0.1 K cal mol^{-1}. In this respect, it is of interest that for p-benzoquinone the optimised geometry is in good agreement with that determined from the electron diffraction data, however, a distorted planar structure is predicted for the ortho-substituted isomer, contrary to the slightly non-planar, boat configuration determined experimentally by Macdonald and Trotter. Although Schang *et al*[302] note that the geometry obtained from MINDO/3 calculations differs only slightly from the diffractometry data, an overestimation of the bondlengths is generally apparent from the MNDO study.

As previously mentioned, current interest in the benzoquinone isomers has centred upon the nature and ordering of the higher occupied molecular orbitals in the ground state. For p-benzoquinone, concensus of opinion is that the first two bands in the photoelectron spectrum arise as a result of ionisation from two lone-pair n (b_{3g} and b_{2u}) and two π (b_{3u} and b_{1g}) orbitals, however, various permutations have been suggested as to their assignment.

The HeI photoelectron spectra of p-benzoquinone and many of its derivatives have been reported by several workers.[289-292] The assignment of the first UPS band as being due to the two n ionisation events as proposed by Turner *et al.*[289] has been supported in subsequent studies by Schweig and co-workers,[293] Dougherty and McGlynn,[294] and in recent work by Asbrink *et al.*[295] at a semi-empirical level. Kobayashi[292] has reported spectra for p-benzoquinone, toluquinone and 2,5-dimethyl-1,4-benzoquinone. A comparison of these and CNDO/2 calculations gives the ordering $b_{3g}>b_{3u}>b_{2u}>b_{1g}$ in terms of decreasing molecular orbital energy, in agreement with extended Huckel calculations by Cowan and co-workers.[291] This assignment is also supported by recent investigations using the multiple scattering $X\alpha$ method and Bloor *et al*[296] also note that changes in geometry and/or the oxygen parameters within the CNDO/S approach allows the ordering of the four highest molecular orbitals to be altered at will.

Brundle and co-workers[290] in an investigation of the "perfluoro effect" tentatively suggested yet another assignment ($b_{2u}>b_{3u}>b_{1g}>b_{3g}$) and this was favoured in the CNDO/S study of Bigelow[297] although the energies of the higher three orbitals were found to be closely similar. Indeed both

ab initio studies to date,[298,299] predict the b_{3u} π-type molecular orbital to be the HOMO in agreement with the absorption spectroscopic work of Tromsdorff.[300] Dougherty and McGlynn have suggested that this may be an artefact of the geometry assumed, since that due to Trotter[308] differs significantly from the more recent electron diffraction data. However, the present non-empirical study has employed the; structure due to Hagen and Hedberg[305] and renders an ordering in agreement with that found by Jonkman *et al.*[299] ($b_{3u} > b_{1g} > b_{2u} > b_{3g}$). As noted previously, geometry optimisation within the MNDO subroutine gives parameters in good agreement with the above structure, and as in the work by Bigelow,[297] the two higher orbital energies are similar, and assigned as b_{2u} and b_{3u}.

Following the reported photoelectron spectrum of o-benzoquinone by Koenig *et al*[301] the first attempt at the band assignment by Schang and co-workers[302] from MINDO/3 calculations predicted the ordering $a_1(n) > a_2(\pi) > b_2(n) > b_1(\pi)$. This is disputed by Hilal[303] who again from a semi-empirical study predicts $a_1(n) > b_2(n) > a_2(\pi) > b_1(\pi)$. The non-empirical study presented here suggests that the HOMO is of π-type, with the ordering $a_2(\pi) > a_1(n) > b_1(\pi) > b_2(n)$ in terms of decreasing orbital energies.

(b) Core Hole States

The discussions of Chapter Three clearly show that the binding energies of core electrons are subtly dependent upon substitution patterns, and that a significant proportion of the differences in relative binding energies for a given core level can arise from differences in relax-

ation energies accompanying core ionisation. On this basis, Figure 3.4, which showed the trends in binding energy for the C_{1s} and O_{1s} core levels for a range of carbon/oxygen systems, is indicative of the similarity expected in the C_{1s} and O_{1s} core level spectra for the particular case of the isomeric benzoquinones. Although it is clear that the shifts in binding energy for the various oxygen-core levels span a much smaller range than those for carbon, both o-benzoquinone and p-benzoquinone if studied as thin films would be expected to show a single O_{1s} ionisation at $\sim$532.8 eV. Also, from a consideration of the above the C_{1s} core level spectrum for p-benzoquinone might be expected to exhibit two peaks. That from the carbonyl carbon, at higher binding energy should be shifted by $\sim$3 eV from that due to the other carbons which in the solid state would be expected to be 285.0 eV.
Regarding the peak due to the four remaining carbon atoms in the hexadiene ring, this ought to be of twice the intensity of the above component, with shift between them only slightly diminished from the 3 eV noted previously, since the secondary effect for oxygen as a substituent is shown to be small (0.3 ± 0.1 eV).

In this respect, it is reasonable to suppose that the C_{1s} spectrum for o-benzoquinone will also consist of two components, comprising of an ionisation from the carbonyl carbon core levels and from the small nature of the secondary effect due to oxygen, again only one from the remaining carbons of tha hexadiene ring.

Of the two isomers, an E.S.C.A. spectrum for the C_{1s} levels of p-benzoquinone only, has been reported and the

binding energy for the single ionisation observed in the O_{1s} spectrum is stated as being 530.8 eV.[304] The C_{1s} envelope is resolved into three components (FWHM ~2.0 eV) centred at 283.4 eV, 284.3 eV and 286.0 eV, and those at lowest and highest binding energy (1:2 intensity ratio) are assigned to the carbonyl and remaining hexadiene carbon atoms respectively with the central feature arising from hydrocarbon contamination. It is clear, that even without a detailed analysis of the p-benzoquinone isomer, the observed shift between the carbonyl component and that arising from the hydrocarbon contamination (often used as a means of reference c.f. Section 2.4) is inconsistent with the above discussion. Also, whilst from the discussion for acetylacetone (Chapter Four) and that presented earlier for cyclobutadiene ionisation from an olefinic type carbon may well produce an asymmetry of the component due to the hydrocarbon, to the low binding energy side, however a value of ~1 eV seems comparatively large.

The O_{1s} spectra for both ortho- and para-benzoquinone computed at the STO-4.31G level are in good agreement with one another, and with the knowledge that shifts are well reproduced at this level, correcting the calculated binding energies to the solid phase, shows excellent agreement with the expected carbonyl O_{1s} value noted above. In the case of p-benzoquinone, the experimental O_{1s} value would therefore seem to be underestimated by ~2 eV. The computed C_{1s}

Table 6.7

C_{1s} and O_{1s} Absolute and Relative binding energies (solid phase) for the ortho- and para-isomers of benzoquinone

	Absolute B.E. (eV)					Relative B.E. (eV)		
	Para-			Ortho-		Para-		Ortho-
Hole State	ΔSCF	Expt.	Expt.[a]	ΔSCF	ΔSCF	Expt.	Expt.[a]	ΔSCF
O(1)*	532.6	533.1	530.8	532.9	-2.4	-1.9	-4.2	-2.1
O(2)*	532.6	533.1	530.8	532.9	-2.4	-1.9	-4.2	-2.1
C(1)*	287.9	288.3	286.0	287.8	2.9	3.3	1.0	2.8
C(2)*	285.3	285.7	283.4	287.8	0.3	0.7	-1.6	2.8
C(3)*	285.3	285.7	283.4	284.7	0.3	0.7	-1.6	-0.3
C(4)*	287.9	288.3	286.0	285.2	2.9	3.3	1.0	0.2
C(5)*	285.3	285.7	283.4	285.2	0.3	0.7	-1.6	0.2
C(6)*	285.3	285.7	283.4	284.7	0.3	0.7	-1.6	-0.3

(a) Ref. 304

O_{1s} Referenced to H_2O Expt. 535.0 C_{1s} Referenced to CH_4 Expt. 285.0

core level spectrum for p-benzoquinone is also of the form noted above with a shift in binding energy between the two components of 2.6 eV. Again, it is clear from Table 6.7 that the experimental values[a] are underestimated by some 2 eV. however the measured shift between these components is noted to be 2.6 eV as was found in the non-empirical calculations. Ohta and co-workers note however that the C_{1s} spectra are time dependent and it is clear that hydrocarbon contamination is a problem in completing an assignment.

With this in mind an independent study has been made of the core level spectra of p-benzoquinone studied as a thin film and the data are displayed in Figure 6.6. The O_{1s} levels consist of a single peak centred at 533.1 eV in excellent agreement with the computed value thus indicating that Ohta et al's data is almost certainly incorrectly referenced. A low intensity shake-up component is evident at 4 eV to higher binding energy in tolerable agreement with the theory, (see subsequent Section).

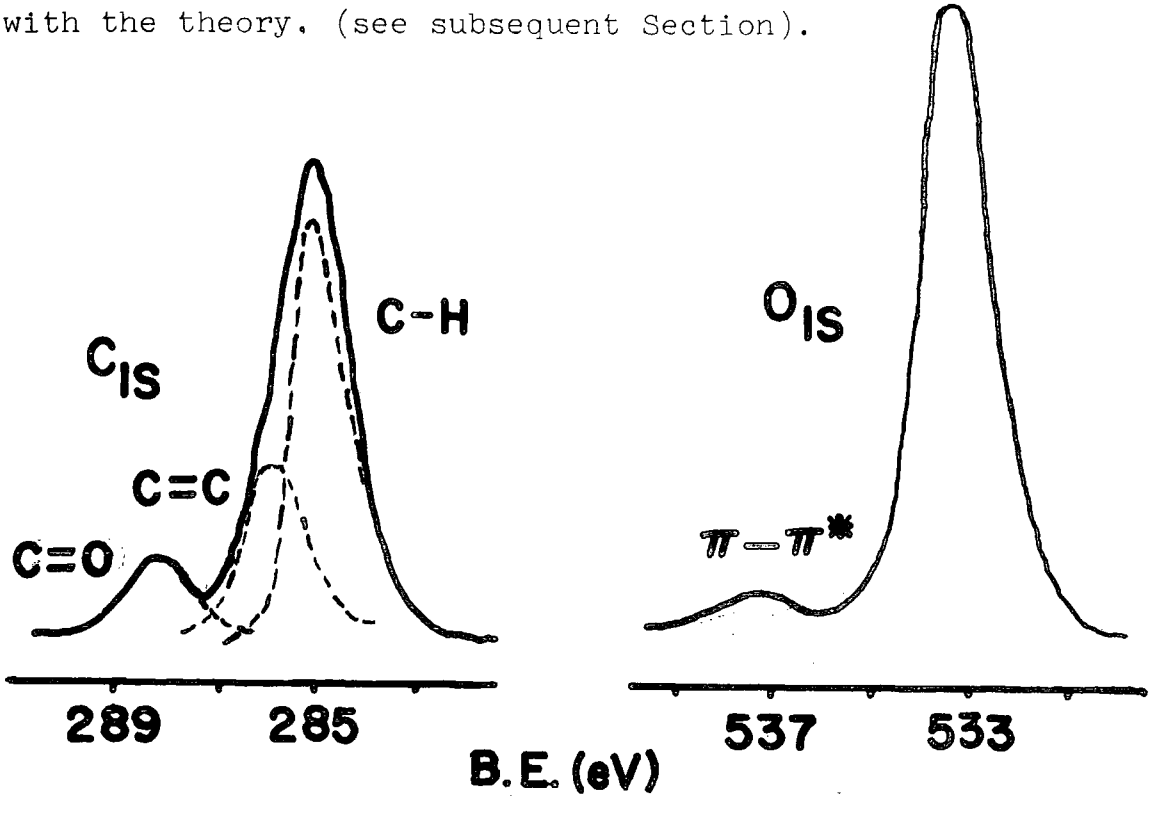

Figure 6.6 C_{1s} and O_{1s} spectra for p-benzoquinone

Turning to the computed spectra for o-benzoquinone, whilst it is clear that the O_{1s} spectrum is in good agreement with that for p-benzoquinone and hence the trends established in Figure 3.4, the C_{1s} envelope is predicted to arise from three components. The binding energy computed for the carbonyl component corresponds to that observed in the para-isomer, however a comparatively large internal shift in binding energy (0.5 eV) is apparent between the components corresponding to ionisation of the hexadiene ring. This shift is clearly not as a result of the small secondary effect arising from the oxygen substituent, since it is the carbon atoms adjacent to the carbonyl groups which exhibit the lower binding energy. A consideration of the relaxation energies accompanying core ionisation (Table 6.8) shows that this observation is largely due to a difference in relaxation effects.

Table 6.8

Relaxation energies for o-benzoquinone and p-benzoquinone (eV)

Hole State	o-benzoquinone	p-benzoquinone
O(1)*	18.6	18.7
O(2)*	18.6	18.7
C(1)*	11.4	11.5
C(2)*	11.4	12.2
C(3)*	12.3	12.2
C(4)*	12.0	11.5
C(5)*	12.0	12.2
C(6)*	12.3	12.2

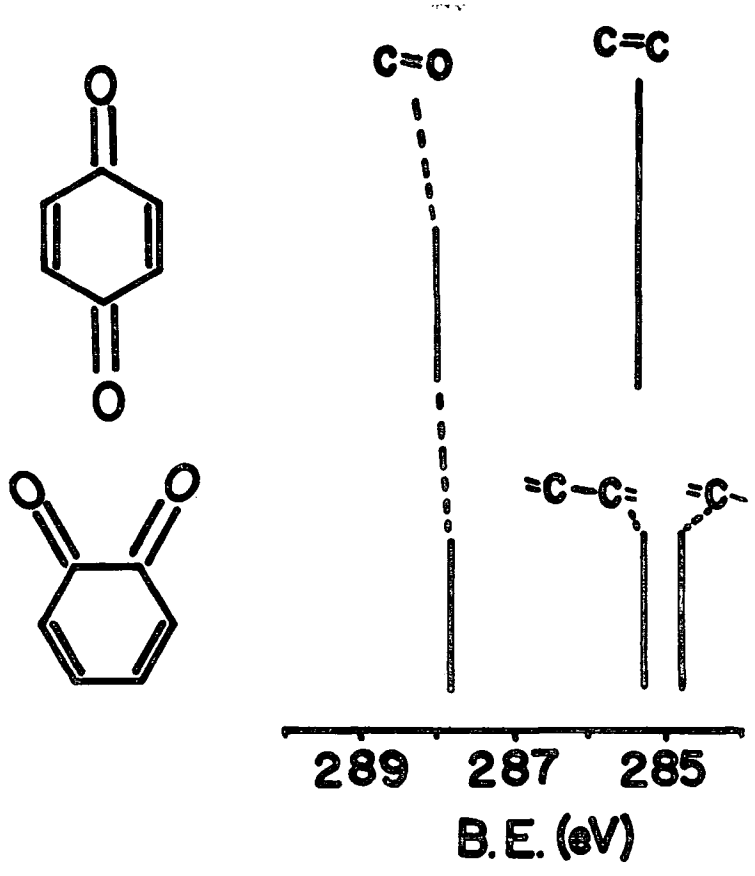

Figure 6.7 Comparison of the computed C_{1s} Spectra for the ortho- and para-isomers

Comparison of the two computed spectra (Figure 6.7) shows that the differences in binding energy evident for o-benzoquinone are not so significant as to render the overall lineshapes distinctive. To this end it is advantageous to consider the predicted satellite structure in the C_{1s} and O_{1s} spectra for both isomers.

(c) Shake-up

In the C_{1s} spectrum reported by Ohta and co-workers, there is no evidence of satellite structure to the high binding energy side of the main photoionisation peaks. It

is noted however that both the C_{1s} and O_{1s} core level spectra for hydroquinone and tetrachlorohydroquinone exhibit shake-up satellites, and in the C_{1s} spectrum of the former, a broad band spanning ~5 eV is evident at a separation of 6-7 eV from the main peak arising from ionisation of the four equivalent carbon atoms in the hexadiene ring. An interesting point deriving from this is that in each case the C_{1s} profiles are resolved into two components of intensity ratio 1:2. Unless this is fortuitous, this situation would normally pertain to the case where shake-up structure is absent since as was noted in the dicarbonyl studies of Chapter Four, the appearance of such structure detracts from the intensity of the relevant component.

Once again, invoking the sudden approximation allows the intensities and transition energies for the satellite structure to be computed in the manner described for tetrahedrane and cyclobutadiene. For the isomeric benzoquinones however significant intensities were not only noted for the HOMO-LUMO $\pi \rightarrow \pi^*$ transitions, but also for the various permutations arising from two lower-lying π-type molecular orbitals and their unoccupied π^*-type counterparts. These are recorded in Table 6.9 (p-benzoquinone) and Table 6.10 (o-benzoquinone).

As shown in Table 6.9 for the O_{1s} spectrum of p-benzoquinone, three $\pi \rightarrow \pi^*$ transitions are predicted, and each is expected to be clearly distinguishable due to their appreciable energy separations. As might be expected, that arising between the HOMO and LUMO is of greatest intensity (9.3%) with transition energy ~4 eV from the major component. Of

Table 6.9

Shake-up intensities (%) and transition energies (eV) for p-benzoquinone

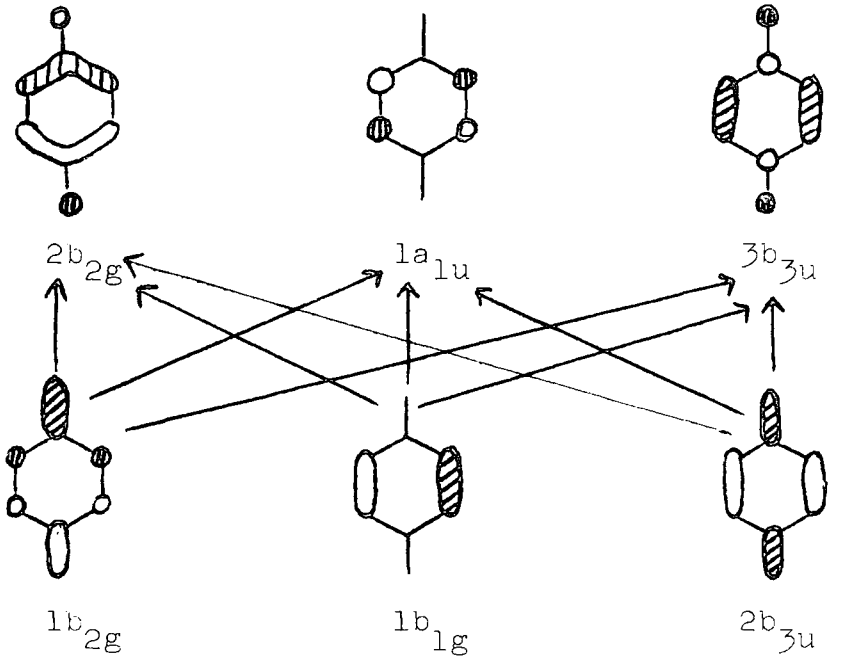

	HOLE STATE					
	O(1) O(2)		C(1) C(4)		C(2)C(3)C(5)C(6)	
Transition	%	ΔE	%	ΔE	%	ΔE
$1b_{2g} \longrightarrow 2b_{2g}$	0.0	0.0	2.0	8.3	2.1	8.7
$1b_{2g} \longrightarrow 1a_{1u}$	0.0	0.0	0.0	0.0	0.0	0.0
$1b_{2g} \longrightarrow 3b_{3u}$	1.1	13.7	0.5	8.6	0.0	0.0
$1b_{1g} \longrightarrow 2b_{2g}$	0.0	0.0	0.0	0.0	0.6	5.3
$1b_{1g} \longrightarrow 1a_{1u}$	0.0	0.0	0.0	0.0	0.0	0.0
$1b_{1g} \longrightarrow 3b_{3u}$	0.0	0.0	0.0	0.0	0.0	0.0
$2b_{3u} \longrightarrow 2b_{2g}$	9.3	4.2	0.5	4.1	1.6	4.6
$2b_{3u} \longrightarrow 1a_{1u}$	0.0	0.0	0.0	0.0	0.0	0.0
$2b_{3u} \longrightarrow 3b_{3u}$	3.5	9.5	0.5	8.6	1.7	10.3

the eight transitions predicted to be present in the C_{1s} spectrum, a consideration of their transition energies suggests that possibly only five may be readily observed at shifts of ∿5, 7, 8.5, 10 and 11 eV from the higher intensity component of the main photoionisation profile.

The total intensity of the satellite structure corresponding to the carbonyl component is computed to be ∿3.5%, whilst that relating to core ionisation of the carbon atoms in the hexadiene ring is ∿6%. This therefore suggests that in the particular case of p-benzoquinone there would be some justification in deconvolution of the C_{1s} spectrum as two components of intensity ratio 1:2.

From Table 6.10 it is clear that the satellite structure expected in the C_{1s} and O_{1s} spectra for o-benzoquinone is more complex than that predicted in the case of p-benzoquinone. Ten transitions are expected to contribute to the C_{1s} spectrum, although the energy shifts suggest that only seven will appear distinctive (∿4, 6.5, 8, 10, 11.5, 13 and 14 eV from the component at lowest binding energy). A particular feature which distinguishes between the two C_{1s} spectra is the high intensity of the HOMO-LUMO transition accompanying core ionisation at C(3),C(6) in o-benzoquinone (∿8%).

The two isomers are perhaps more readily identified by the nature of the satellite structure in their O_{1s} spectra. Whilst only three contributions are clearly evident for p-benzoquinone, six transitions are expected for the ortho-isomer although the transition energies suggest that only five may be readily detected. Once again, the HOMO-LUMO transition is of greatest intensity (∿11% at ΔE ∿3 eV),

Table 6.10

Shake-up intensities (%) and transition energies (eV) for o-benzoquinone

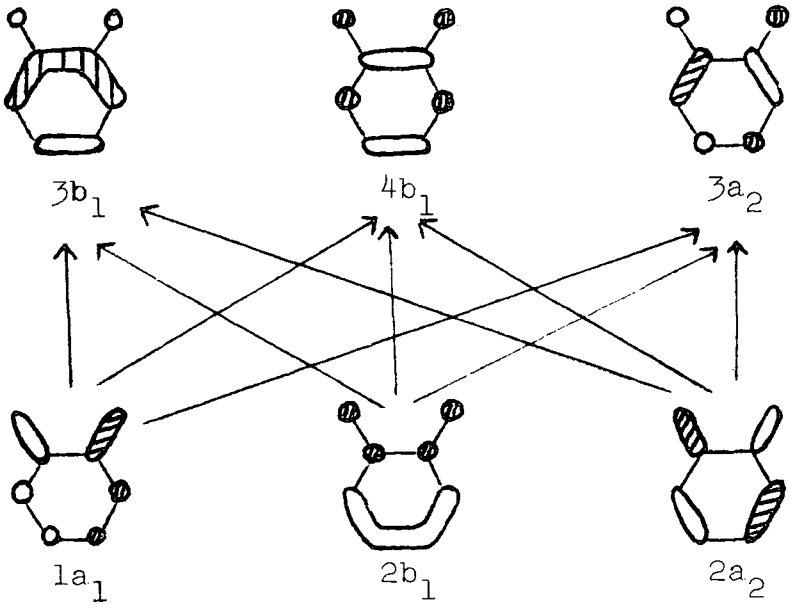

HOLE STATE

	O(1)	O(2)	C(1)	C(2)	C(3)	C(6)	C(4)	C(5)
Transition	%	ΔE	%	ΔE	%	ΔE	%	ΔE
$1a_1 \longrightarrow 3b_1$	2.4	7.2	0.9	7.2	0.0	0.0	1.6	7.7
$1a_1 \longrightarrow 4b_1$	0.0	0.0	0.0	0.0	0.0	0.0	0.9	12.9
$1a_1 \longrightarrow 3a_2$	1.4	11.8	1.8	11.1	0.0	0.0	0.6	11.8
$2b_1 \longrightarrow 3b_1$	0.0	0.0	0.0	0.0	0.0	0.0	1.9	6.5
$2b_1 \longrightarrow 4b_1$	0.0	0.0	0.0	0.0	0.0	0.0	0.0	0.0
$2b_1 \longrightarrow 3a_2$	1.1	10.7	0.0	0.0	0.0	0.0	0.0	0.0
$2a_2 \longrightarrow 3b_1$	10.7	2.9	0.0	0.0	7.7	3.6	1.2	3.5
$2a_2 \longrightarrow 4b_1$	9.5	8.6	0.0	0.0	1.1	7.6	0.0	0.0
$2a_2 \longrightarrow 3a_2$	2.0	7.6	0.0	0.0	0.0	0.0	0.6	7.6

however a second transition arising from the HOMO, of almost equivalent intensity (∿10%), and appreciable energy shift (ΔE ∿8.5 eV). as shown in Figure 6.8 confirms the distinctive nature of the O_{1s} spectra for the ortho- and para-isomers.

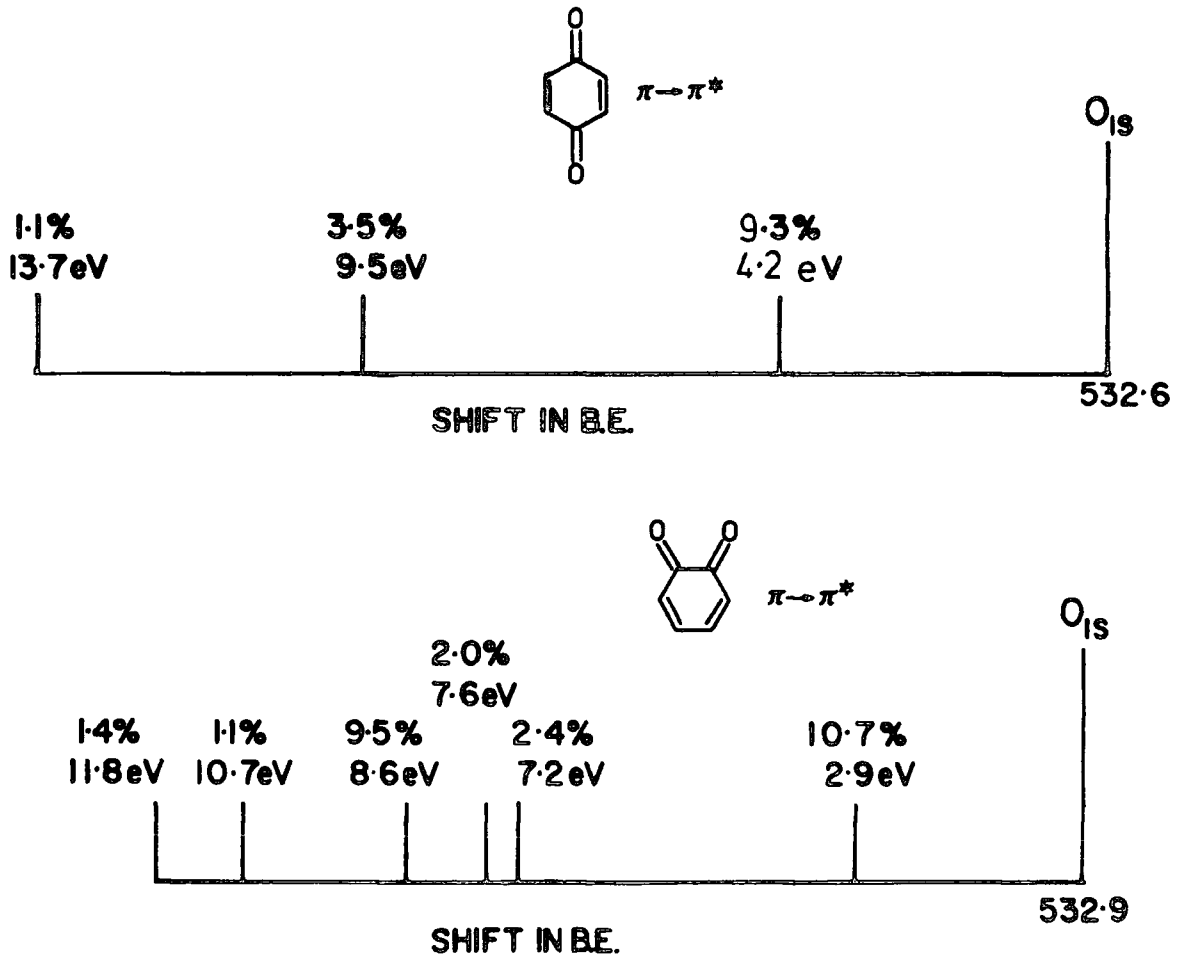

Figure 6.8 A Comparison of the Computed O_{1s} Spectra for p-benzoquinone and o-benzoquinone

Whilst Chapters Three, Four and Five clearly demonstrate the importance of absolute and relative binding energies as the primary source of information from the E.S.C.A. experiment, largely due to their dependence upon substitution patterns and the manner in which weak interactions of the ground state are enhanced in the core hole state manifold, the distinctive nature of the satellite structure accompanying

core ionisation was noted in the studies of the di-carbonyl species. The above discussion clearly shows that in certain cases, where the factors determining shifts in binding energy are particularly short range in nature (e.g. polymer systems exhibiting unsaturated backbones or pendant phenyl groups) then it may be advantageous to focus attention upon the $\pi \rightarrow \pi^*$ shake-up structure, since the energy of such transitions is sufficiently low as to render them unobscured by inelastic scattering evident in the solid phase.

APPENDIX

APPENDIX

LECTURES AND SEMINARS ATTENDED DURING THE PERIOD 1978-81

15 September 1978

Professor W. Siebert (University of Marburg, West Germany), "Boron Heterocycles as Ligands in Transition Metal Chemistry".

22 September 1978

Professor T. Fehlner (University of Notre Dame, U.S.A.), "Ferraboranes: Syntheses and Photochemistry".

12 December 1978

Professor C.J.M. Stirling (University of Bangor), 'Parting is Such Sweet Sorrow' - the Leaving Group in Organic Reactions.

14 February 1979

Professor B. Dunnell (University of British Columbia) "The Application of N.M.R. to the Study of Motions in Molecules".

16 February 1979

Dr. J. Tomkinson (Institute of Laue-Langevin. Grenoble), "Properties of Adsorbed Species".

4 March 1979

Dr. J.C. Walton (University of St. Andrews). "Pentadienyl Radicals".

20 March 1979

Dr. A. Reiser (Kodak Ltd.), "Polymer Photography and Mechanism of Cross-Link Formation in Solid Polymer".

25 March 1979

Dr. S. Larsson (University of Uppsala), "Some Aspects of Photoionisation Phenomena in Inorganic Systems".

25 April 1979

Dr. C.R. Patrick (University of Birmingham). "Chlorofluorocarbons and Stratospheric Ozone: An Appraisal of the Environmental Problem".

1 May 1979

Dr. G. Wyman (European Research Office. U.S. Army). "Excited State Chemistry in Indigoid Dyes".

2 May 1979

Dr. J.D. Hobson (University of Birmingham), "Nitrogen-centred Reactive Intermediates".

8 May 1979

Professor A. Schmidpeter (Institute of Inorganic Chemistry. University of Munich), "Five-membered Phosphorus Heterocycles Containing Dicoordinate Phosphorus".

9 May 1979

Dr. A.J. Kirby (University of Cambridge), "Structure and Reactivity in Intramolecular and Enzymic Catalysis".

9 May 1979

Professor G. Maier (Lahn-Giessen), "Tetra-tert-butyltetrahedrane".

10 May 1979

Professor G. Allen, F.R.S. (Science Research Council). "Neutron Scattering Studies of Polymers".

16 May 1979

Dr. J.F. Nixon (University of Sussex), "Spectroscopic Studies on Phosphines and their Coordination Complexes".

23 May 1979

Dr. B. Wakefield (University of Salford), "Electron Transfer in Reactions of Metals and Organometallic Compounds with Polychloropyridine Derivatives".

13 June 1979

Dr. G. Heath (University of Edinburgh) "Putting electrochemistry into Mothballs - (Redox Processes of metal Porphyrins and Phthalocynanines".

14 June 1979

Professor I. Ugi (University of Munich), "Synthetic Uses of Super Nucleophiles".

20 June 1979

Professor J.D. Corbett (Iowa State University, Ames, Iowa, U.S.A.). "Zintl Ions: Synthesis and Structure of Homo-polyatomic Anions of the Post-Transition Elements".

27 June 1979

Dr. H. Fuess (University of Frankfurt), "Study of Electron Distribution in Crystalline Solids by X-ray and Neutron Diffraction".

21 November 1979

Dr. J. Müller (University of Bergen), "Photochemical Reactions of Ammonia".

28 November 1979

Dr. B. Cox (University of Stirling). "Macrobicyclic Cryptate Complexes, Dynamics and Selectivity".

5 December 1979

Dr. G.C. Eastmond (University of Liverpool). "Synthesis and Properties of Some Multicomponent Polymers".

12 December 1979

Dr. C.I. Ratcliffe (University of London), "Rotor Motions in Solids".

19 December 1979

Dr. K.E. Newman (University of Lausanne), "High Pressure Multinuclear NMR in the Elucidation of the Mechanisms of Fast, Simple Inorganic Reactions".

30 January 1980

Dr. M.J. Barrow (University of Edinburgh) "The Structures of some Simple Inorganic Compounds of Silicon and Germanium - Pointers to Structural Trends in Group IV".

6 February 1980

Dr. J.M.E. Quirke (University of Durham), "Degradation of Chlorophyll-a in Sediments".

23 April 1980

B. Grierson B.Sc., (University of Durham), "Halogen Radiopharmaceuticals".

14 May 1980

Dr. R. Hutton (Waters Associates, U.S.A.), "Recent Developments in Multi-milligram and Multi- gram Scale Preparative High Performance Liquid Chromatography".

21 May 1980

Dr. T.W. Bentley (University of Swansea), "Medium and Structural Effects in Solvolytic Reactions".

7 October 1980

Professor T. Tehlner. "Metalloboranes Cages or Coordination Compounds?"

16 October 1980

Dr. D. Maas (Salford University) "Reactions a Go-Go".

30 October 1980

Professor N.Grassie, (Glasgow University), "Inflammability Hazards in Commercial Polymers".

6 November 1980

Professor A.G. Sykes (Newcastle University), "Metallo-proteins: An Inorganic Chemists Approach".

12 November 1980

Dr. M. Gerloch (University of Cambridge), "Magnetochemistry is about Chemistry".

13 November 1980

Professor N.N. Greenwood (Leeds University), "Metall-borane Chemistry".

19 November 1980

Dr. T. Gilchrist (University of Liverpool) "Nitroso-olefins as Synthetic Intermediates".

4 December 1980

Reverend R. Lancaster "Fireworks".

18 December 1980

Dr. R. Evans (University of Brisbane, Australia), "Some Recent Communications to the Editor of the Australian Journal of Failed Chemistry".

22 January 1981

Professor E. Dawes (Hull University), "Magic and Mystery through the Ages".

29 January 1981

Mr. H. Maclean, (I.C.I. Ltd.), "Managing in the Chemical Industry in the 1980's".

5 February 1981

Professor F. Stone (Bristol University), "Chemistry of Carbon to Metal Triple Bonds".

18 February 1981

Professor S. Kettle (University of East Anglia), "Variations in the Molecular Dance at the Crystal Ball".

25 February 1981

Dr. K. Bowden (University of Essex), "The Transmission of Polar Effects of Substituents".

11 March 1981

Dr. J.F. Stoddart (I.C.I. Ltd.), "Stereochemical Principles in the Design and Function of Synthetic Molecular Receptors".

17 March 1981

Professor W. Jencks (Brandeis University, Massachusetts), "When is an Intermediate not an Intermediate?".

7 May 1981

Professor M. Gordon (Essex University), "Do Scientists Have to Count?".

10 June 1981

Dr. J. Rose (I.C.I. Plastics), New Engineering Plastics.

CONFERENCES ATTENDED DURING THE PERIOD 1978-1981

Summer School on Topics in Theoretical Organic Chemistry (18 - 30 June 1979), Gargnano-Brescia Italy.

Royal Institute of Chemistry/Chemical Society Annual Congress, April 1980, Durham.

Polymer Characterisation Symposium, July 1981, Durham.

REFERENCES

1. Eyring, H., Walter, J. and Kimball, G.E., "Quantum Chemistry", J. Wiley & Sons, (14th Edition, 1967)

2. Pilar, F.L., "Elementary Quantum Chemistry", McGraw-Hill (1968).

3. Richards, W.G. and Horsley, J.A., "*Ab Initio* Molecular Orbital Calculations for Chemists", Clarendon (1970).

4. Schaefer, H.F. III, "The Electronic Structure of Atoms and Molecules", Addison-Wesley (1972).

5. McWeeny, R., "Quantum Mechanics: Principles and Formalism" Pergamon (1972).

6. Cook, D.B., "*Ab Initio* Valence Calculation in Chemistry" Butterworths (1974).

7. Csizmadia, I.G., "Theory and Practice of MO Calculations on Organic Molecules", Elsevier (1976).

8. Hurley, A.C., "Introduction to the Electron Theory of Small Molecules", Academic Press (1976).

9. McWeeny, R., and Sutcliffe, B.T., "Methods of Molecular Quantum Mechanics", Academic Press (Revised Edition 1976)

10. Schaefer, H.F. III, "Methods of Electronic Structure Theory" Vol. III, Plenum Press (1977).

11. Born, M. and Oppenheimer, J., Ann.Physik, 84, 457 (1927).

12. Discussed in, e.g. Longuet-Higgins, Adv. in Spectroscopy, 2, 429, (Interscience 1962).

13. Jahn, H.A. and Teller, E. Proc.Roy.Soc.(London) A161, 200 (1937).

14. Kotani, M, Amemiya, A., Ishiguro, E. and Kimura, T., "Table of Molecular Integrals", Maruzen Co. Ltd., Tokyo (1955).

15. Eckart, C.E., Phys.Rev., 36, 878 (1930).

16. Goddard, W.A. III, J.Am.Chem.Soc. 94, 793, (1972).

17. Fock, V., Z.Physik, 61, 126 (1930).

18. Slater, J.C., Phys.Rev. 35, 210 (1930).

19. Roothaan, C.C.J., Rev.Mod.Phys. 23, 69 (1951).

20. (a) Löwdin, P.O., J.Chem.Phys. 18, 365 (1950).
(b) Löwdin, P.O., in "Advances in Quantum Chemistry", 5, 185 (1970).

21. Discussion of other methods for Matrix Diagonalisation (e.g. LU, QR and Givens-Householder) are given in "Mathematical Methods for Digital Computers II", ed. A.Ralston and H.S. Wilf, (Wiley 1967).

22. Roothaan, C.C.J., Rev.Mod.Phys. 32, 179 (1960).

23. Pople, J.A., and Nesbet, R.K., J.Chem.Phys. 22, 571 (1954).

24. Freeman A.J., and Watson, R.E., in "Magnetism" ed. by G.T. Rado and H. Suhl (Academic Press 1965).

25. Useful methods are those due to R.K. Nesbet, J.Math.Phys. 2, 701 (1961) and P.O. Löwdin, Rev.Mod.Phys. 32, 328 (1960), 36, 966 (1964).

26. Löwdin, P.O., Advan.Chem.Phys. 2, 207 (1959).

27. Clark, D.T., Ann.Reports (B) of the Chemical Society, p.40 (1972).

28. Hehre, W.J., Ditchfield, R., Radom, L. and Pople, J.A., J.Am.Chem.Soc. 92, 4796 (1970).

29. Cade, P.E., Sales, K.D. and Wahl, A.C., J.Chem.Phys. 44, 1973 (1966).

30. MacDonald, J.K.L., Phys.Rev. 43, 830, (1933).

31. Nesbet, R.K., J.Chem.Phys. 43, 311 (1965).

32. Shavitt, I., J.Comput,Phys. 6, 124 (1970).

33. This topic is discussed in many standard texts, e.g. G. Hertzberg, "Spectra of Diatomic Molecules" Van Nostrand (1950).

34. Slater, J.C., Phys.Rev. 34, 1293 (1929).

35. Desclaux, J.P., At.Data.Nucl.Data Tables, 12, 311 (1973).

36. Huang, K-N,Aoyagi, M., Chen, M.H. and Crasemann, B., At.Data.Nucl.Data Tables, 18, 243 (1976).

37. Mulliken, R.S., J.Chem.Phys. 23, 1833, 1841 (1955).

38. Slater, J.C., Phys.Rev. 36, 57 (1930).

39. Boys, S.F., Proc.Roy.Soc. (London), A200, 542 (1950).

40. Shavitt, I., Methods.Comp.Phys., 2, 1 (1963).

41. Preuss, H., Z.Naturforsch, 11, 823 (1956).

42. Whitten, J.L., J.Chem.Phys. 44, 359 (1966).

43. Clementi, E. and Raimondi, D.L., J.Chem.Phys. 38, 2686 (1963).

44. Clementi, E., Raimondi, D.L. and Reinhardt, W.P., J.Chem. Phys. 47, 1300 (1967).

45. Foster, J.M. and Boys, S.F., Rev.Mod.Phys. 32, 303 (1960).

46. Hehre, W.J., Stewart, R.F., Pople, J.A., J.Chem.Phys. 51-2657 (1969).

47. Hehre, W.J., Ditchfield, R., Stewart, R.F. and Pople, J.A., J.Chem.Phys. 52, 2769 (1970).

48. (a) Ditchfield, R., Hehre, W.J. and Pople, J.A., J.Chem.Phys. 54, 724 (1971).

(b) Hehre, W.J., and Pople, J.A., J.Chem.Phys. 56 4233 (1972).

(c) Hehre, W.J., and Lathan, W.A., J.Chem.Phys. 56. 5255 (1972).

49. Nesbet, R.K., J.Chem.Phys., 40, 3619 (1964).

50. Hariharan, P.C., and Pople, J.A., Chem.Phys.Lett, 16, 217 (1972).

51. (a) McLean, A.D. and Yoshimine, M., Tables of Linear Molecule Wave Functions, A Supplement to IBM,J.Res. Develop. 12, 206 (1968).

(b) Roos, B. and Siegbahn, P., Theoret.Chim.Acta 17, 199 (1970).

(c) Rothenberg, S. and Schaefer, H.F., J.Chem.Phys. 54, 2765 (1971).

(d) Dunning, T.H., J.Chem.Phys. 55, 3958 (1971).

52. (a) Clementi, E., J.Chem.Phys. 40, 1944 (1964).

(b) Clementi, E., Matcha, R. and Veillard, A., J.Chem. Phys. 47, 1865 (1967).

53. Huzinaga, S. and Arnau, C., J.Chem.Phys. 53, 451 (1970).

54. (a) Huzinaga,S., J.Chem.Phys. 42, 1293 (1965).

(b) Veillard, A., Theoret.Chim.Acta. 12, 405 (1968).

(c) Whitman, D.R. and Hornback, C.J., J.Chem.Phys. 50, 398 (1968).

(d) Huzinaga, S. and Sakai, Y., J.Chem.Phys. 51, 1371 (1969)

(e) Wachters, A.J.H., J.Chem.Phys. 52, 1033 (1970).

55. Dunning, T.H., J.Chem.Phys. 53, 2823 (1970).

56. (a) Whitten, J.L., J.Chem.Phys. 44, 359 (1966).

(b) Clementi, E. and Davis, D.R., J.Comput.Phys. 2, 223 (1967).

57. All Enquiries and General Correspondence should be directed to:
Quantum Chemistry Program Exchange,
Chemistry Department, Room 204,
Indiana University, Bloomington,
Indiana (47401).

58. McLean, A.D., Proc.Conf.Potential Energy Surfaces in Chemistry, (1970), p. 87, IBM Research Laboratory, San Jose, California 95114.

59. Hehre, W.J., Lathan, W.A., Ditchfield, R., Newton, M.D. and Pople, J.A., Q.C.P.E. 236.

60. Clementi, E., and Mehl, J., "IBM. System/360 IBMOL 5 Program. Quantum Mechanical Concepts and Algorithms", IBM. Research Laboratory, San Jose, California 95114 (1971).

61. Almöf, U., USIP Technical Report No. 7209, Stockholm.

62. Neumann, D.B., Basch, H., Kurnegay, R.L., Snyder, L.C., Moskowitz, J.W., Hornback, C. and Liebmann, S.P., Q.C.P.E. 199.

63. Saunders, V.R., Guest, M.F., Atlas Computing Division, Rutherford Laboratory, Chilton, Didcot, Oxon Oxll OQX.

64. Saunders, V.R., "An Introduction to Molecular Integral Evaluation" in Computational Techniques in Quantum Chemistry and Molecular Physics". ed. G.H.F. Dierckson, B.T. Sutcliffe, A. Veillard and D. Reidel (1975).

65. Shavitt, I., and Karplus, M., J.Chem.Phys. 43, 398 (1965).

66. Veillard, A., "The Logic of SCF Procedures" in "Computational Techniques in Quantum Chemistry and Molecular Physics", ed. G.H.F. Dierckson, B.T. Sutcliffe, A. Veillard D. Reidel.

67. Saunders, V.R. and Hillier, I.H., Int.J.Quant.Chem. 7, 699 (1973).

68. Hillier, I.H., Saunders, V.R., Proc.Roy.Soc.(London), A320, 161 (197o).

69. Guest, M.F. and Saunders, V.R., Mol.Phys. 28, 819 (1974).

70. Siegbahn, K., Nordling, C., Fahlman, A., Nordberg, R., Hamrin, K., Hedman, J., Johansson, G., Bergmark, T., Karlsson, S.E., Lindgren, I. and Lindberg. B., "E.S.C.A.: Atomic, Molecular and Solid State Structure studied by means of Electron Spectroscopy" Almquist and Wiksells Uppsala (1967).

71. Siegbahn, K. Nordling, C., Johansson, G., Hedman, J., Heden, P.F., Hamrin, K., Gelius, U., Bergmark, T., Werme, L.D., Manne, R. and Baer, Y., "E.S.C.A. Applied to Free Molecules" North-Holland (1969).

72. Shirley, D.A., "Photo Electron Spectroscopy: Proceeding of an International Conference at Asilomar", North-Holland (1972).

73. Dekeyser, W., *et al*, "Electron Emission Spectroscopy" D. Riedel (1973).

74. Caudano, R., and Verbist, J., "Electron Spectroscopy - Progress in Research and Applications", Elsevier (1974)

75. Carlson, T.A.,"Photoelectron and Auger Spectroscopy", Plenum (1975).

76. Briggs, D., "Handbook of X-ray and Ultraviolet Photoelectron Spectroscopy", Heyden and Sons, London (1977).

77. Brundle, C.R., and Baker, A.D.,"Electron Spectroscopy, Volume I:"Theory, Techniques and Applications", Academic Press (1977).

78. Fadley, C.S., "Theoretical Aspects of X-ray Photoelectron Spectroscopy", in Ref. 73 (1973).

79. Shirley, D.A., Adv.Chem.Phys., 23, 85 (1973).

80. Basch, H., J.Electron Spectrosc. Rel.Phenom. 5, 463 (1974).

81. Schwartz, M.E., "Electron Spectroscopy" in "Modern Theoretical Chemistry, Volume 4", ed. H.F. Schaefer, Plenum (1977).

82. Schwartz, M.E., Int.Rev.Sci., Theoret.Chem.Phys.Chem.Ser.2, 1, 189 (1975).

83. Einstein, A., Ann.Phys. 17, 132 (1905).

84. Robinson, H. and Rawlinson, W.F., Phil.Mag.28, 277 (1914).

85. Robinson, H., Proc.Roy.Soc., A, 104, 455 (1923).

86. Robinson, H., Phil.Mag. 50, 241 (1925).

87. De Broglie, M., Compt.Rend., 172, 274 (1921).

88. Jenkin, J.G., Leckey, R.C.G. and Liesengang, J., J.Electron Spectrosc. Rel.Phenom, 12, 1 (1977).

89. Cederbaum, L.S. and Domcke, W., J.Electron Spectrosc.Rel. Phenom. 13, 161 (1978).

90. Snyder, L.C., J.Chem.Phys. 55, 95 (1971).

91. Gelius, U. and Siegbahn, K., Faraday Disc., 54, 257 (1972).

92. Adams, D.B. and Clark, D.T., Theoret.Chim.Acta, 31 171 (1973)

93. Guest, M.F., Hillier, I.H., Saunders, V.R. and Wood, M.H., Proc.Roy.Soc. A333, 201 (1973).

94. Clark, D.T., Cromarty, B.J. and Sgamellotti, A., Chem. Phys.Lett. 51, 356 (1977).

95. Clark, D.T., Cromarty, B.J. and Sgamellotti, A., J.Chem.Soc. Faraday Trans. 2, 74, 1046 (1978).

96. Clark, D.T., Cromarty, B.J. and Sgamellotti, A., J.Electron Spectrosc.Rel.Phenom. 13, 85 (1978).

97. Clark, D.T., Cromarty, B.J., and Sgamellotti, A., J.Electron Spectrosc. Rel.Phenom. 14, 175 (1978).

98. Clark, D.T., Cromarty, B.J., Sgamellotti, A. and Guest, M.F., J.Electron Spectrosc. Rel.Phenom. 17, 237 (1979).

99. Åberg, T., Phys.Rev. 156, 35 (1967).

100. Krause, M.O., Carlson, T.A. and Dismukes, R.D., Phys.Rev. 170, 37 (1968).

101. Martin, R.L. and Shirley, D.A., "Many Electron Theory of Photoemission" in Ref. 77.

102. Manne, R. and Åberg, T., Chem.Phys.Lett. 7, 282 (1970).

103. Hedin, L. and Lundqvist, S., in "Solid State Physics" 23, 1 Ed. E. Ehrenreich, F. Seitz and H. Turnbull, Academic Press, New York (1969).

104. Sunjic, M. Sokcevic, D. and Lucas, C., J.Electron Spectrosc., and Rel. Phenom, 5, 963 (1974).

105. Sandstrom, A.E. in "Handbook of Physics", Vol.XXX "X-Rays" 164 Ed. S.F. Flugge, Springer-Verlag (1957).

106. Castle, J.E. and West, R.H., J.Electron Spectrosc. Rel. Phenom. 16, 195 (1979).

107. Grant, J.T. and Hooker, M.P., J.Electron Spectrosc. Rel.Phenom. 9, 93 (1976).

108. Ombach, E. Fuggle, J.C. and Menzel, D., J.Electron Spectrosc. Rel. Phenom, 10, 15 (1977).

109. Rye, R.R., Houston, J.E., Jennison, D.R., Madey, T.E. and Holloway, P.H., Ind.Eng.Chem.Prod.Res.Dev. 18, 2 (1979).

110. Jennison, D.R., Chem.Phys.Lett. 69, 435 (1980).

111. Asaad, W.N. and Burhop, E.H.S., Proc.Phys.Soc. (London) 72, 369 (1958).

112. Shirley, D.A., Phys.Rev. A7, 1520 (1973).

113. Henke, B.L., Advan.X-Ray Anal. 13, 1 (1969).

114. Wagner, C.D., Faraday Disc.Chem.Soc. 60, 306 (1975).

115. Barrie, A. in Ref. 76 p. 79 (1976).

116. Siegbahn, K., Hammond, D., Fellner-Feldegg, H. and Barnett, E.F., Science 176, 245 (1972).

117. Purcell, E.M., Phys.Rev. 54, 818 (1938).

118. Cross, Y.M. and Castle, J.E., J.Electron Spectrosc. Rel.Phenom. 22, 53 (1980).

119. Kratos Ltd., Operator's Handbook ES200 Spectrometer.

120. Sokolowski, E., Arkiv,Fysik, 15, 1 (1959).

121. Nordling, C., Arkiv,Fysik, 15, 397 (1959).

122. Johansson, G., Hedman, J. Berndtsson, A., Klasson, M. and Nilsson, R., J.Electron Spectrosc. Rel.Phenom. 2, 295 (1973).

123. Ascarelli, P. and Missoni, G., J.Electron Spectrosc. Rel.Phenom. 5, 417 (1974).

124. Clark, D.T., "Chemical Aspects of E.S.C.A." in Ref.73 373 (1973).

125. Clark, D.T., Thomas, H.R., Dilks, A. and Shuttleworth, D., J.Electron Spectrosc. Rel.Phenom. 10(4), 455, (1977).

126. Clark, D.T. and Thomas, H.R., J.Polym.Sci.Polym.Chem.Edn. 14, 1671 (1976).

127. Clark, D.T., Cromarty, B.J. and Dilks, A., J.Polym.Sci. Polym.Chem.Edn. 16, 3173 (1978).

128. Mills, B.E., Martin, R.L. and Shirley, D.A., J.Am.Chem.Soc. 98(9), 2380 (1976).

129. Jolly, W.L. and Schaaf, T.F., J.Am.Chem.Soc. 98(11) 3178 (1976).

130. Clark, D.T. and Dilks, A., J.Polym.Sci.Polym.Chem.Edn. 17, 957 (1979).

131. Parrat, L.G., Rev.Mod.Phys. 31, 616 (1959).

132. Geise, A.T. and French, C.S., Appl.Spectrosc. 9, 78 (1955).

133. Vanderbuilt, J.M. and Henrich, C., Appl.Spectrosc. 7, 171 (1953).

134. Gunders, E. and Kaplam, B., J.Opt.Soc.Amer.55, 1094 (1965).

135. Ebel, H. and Gurker, M., J.Electron Spectrosc. Rel.Phenom. 5, 799 (1974).

136. Wertheim, G.K., J.Electron Spectrosc. Rel.Phenom, 6, 239, (1975).

137. Van Vleck, J.H., Phys.Rev.Lett. 45, 405 (1934).

138. Fadley, C.S. in Ref. 72 page 781, *et seq*. (1972).

139. Carver, J.C., Carlson, T.A., Cain, L.C. and Schweitzer, G.K., in "Electron Spectroscopy" 803, Ed. D.A.Shirley, North-Holland, Amsterdam (1972).

140. cf. Atkins, P.W., "Molecular Quantum Mechanis" O.U.P. London (1970).

141. cf. Cotton, F.A. and Wilkinson, G., "Advanced Inorganic Chemistry", Wiley, New York (1972).

142. Novakov, T. and Hollander, J.M., Bull.Amer.Phys.Soc. 14, 524 (1969).

143. Novakov, T. and Hollander, J.M., Phys.Rev.Lett. 21, 1133 (1968).

144. Wertheim, G.K., "Mossbauer Effect: Principles and Applications", Academic Press, New York (1964).

145. Bancroft, G.M., Adams, I., Lampe, H. and Sham, T.K., Chem.Phys.Lett. 32, 173 (1975).

146. Gupta, R.D. and Sen, S.K., Phys.Rev.Lett. 28, 1311 (1972).

147. Martin, R.L. and Shirley, D.A., J.Chem.Phys. 64, 3685 (1976).

148. Wertheim, G.K. and Rosencwaig, A., Phys.Rev.Lett. 26. 1179 (1971).

149. Koopmans, T.A. Physica, 1, 104 (1933).

150. Richards, W.G., J.Mass.Spectrom. Ion.Phys. 2, 419 (1969).

151. Bagus, P.S., Phys.Rev. 139, A619 (1965).

152. Brundle, C.R., Robin, M. and Basch, H., J.Chem.Phys. 53, 2196 (1970).

153. Bagus, P.S. and Schaefer, H.F. III, J.Chem.Phys. 56, 224 (1972).

154. Murrell, J.N. and Ralston, B.J., J.Chem.Soc. Faraday Trans.II 68, 1393 (1972).

155. Aarons, L.J., Guest, M.F. and Hillier, I.H., J.Chem.Soc. Faraday Trans.II, 68, 1866 (1972).

156. Siegbahn, H., UUIP-891 (1975).

157. Turner, D.W., Baker, C., Baker, A.D. and Brundle, C.R., "Molecular Photoelectron Spectroscopy", Wiley-Interscience (1970).

158. Eland, J.H.D., "Photoelectron Spectroscopy", Butterworths (1974).

159. Gelius, U., Basilier, E., Svensson, S., Bergmark, T., and Siegbahn, K., J.Electron Spectrosc.Rel.Phenom. 2, 405 (1974).

160. McGuire, E., Phys.Rev. 185, 1 (1969).

161. Hertzberg, G., "Molecular Spectra and Molecular Structure Volume III" Van Nostrand (1966).

162. Franck, J., Trans.Faraday Soc. 21, 536 (1926).

163. Condon, E.U., Phys.Rev. 28, 1182 (1926).

164. Condon, E.U., Phys.Rev. 32, 858 (1928).

165. Ansbacher, F., Z. Naturforsch, 14a, 889 (1959).

166. Meyer, W., J.Chem.Phys. 58, 1017 (1973).

167. Gelius, U., Svensson, S., Siegbahn, H. Basilier, E., Faxalv, Å. and Siegbahn, K., Chem.Phys.Lett. 28, 1 (1974).

168. Corvilan-Berger, S., and Verhnegen, G., Chem.Phys.Lett. 50, 468 (1977).

169. Fadley, C.S., Hagstrom, S.B.M., Klein, M.P. and Shirley, D.A. J.Chem.Phys. 48, 3779 (1968).

170. Clementi,Eand Popkie, H., J.Am.Chem.Soc. 94, 4057 (1972).

171. Bagus, P., Phys.Rev. 139. A619 (1965).

172. Jolly, W.L. and Hendrickson, D.N., J.Am.Chem.Soc. 92, 1863 (1970).

173. McWeeny, R., and Velenik, A.A., Mol.Phys. 24, 1421 (1972).

174. Clark, D.T. and Muller, J., Theoret.Chim.Acta. 41, 193 (1976)

175. Clark, D.T., Scanlan, I.W., and Muller, J., Theoret.Chim. Acta. 35, 341 (1974).

176. Schwartz, M.E., Chem.Phys.Lett. 5, 50 (1970).

177. Rohmer, M.M. and Veillard, A., J.Chem.Soc.D. 250 (1973).

178. Meyer, W., "Configuration Expansion by Means of Pseudo-Natural Orbitals", pp. 413 in Ref. 10 (1977).

179. (a) Goscinski, O., Pickup, B.T., and Purvis, G., Chem. Phys.Lett. 22, 167 (1973).

(b) Goscinski, O., Howat, G. and Åberg, T., J.Phys.B. 8, 11 (1975).

(c) Goscinski, O., Hehenberger, M., Roos, B. and Siegbahn, P., Chem.Phys.Lett. 33, 427 (1975).

180. (a) Rowe, D.J., Rev.Mod.Phys. 40, 163 (1968).

(b) Rowe, D.J., Phys.Rev. 175, 1283 (1968).

181. (a) Simons,,J., and Smith, W.D., J.Chem.Phys. 58, 4899 (1973).

(b) Simons, J., Chem.Phys. Lett. 25, 122 (1974).

(c) Chen, T.T., Smith, W.D., and Simons, J., J.Chem.Phys. 61, 2670 (1974).

182. Slater, J.C., Adv. Quantum,Chem. 6, 1 (1972).

183. (a) Chong, D.P., Herring, F.G., McWilliams, D., J.Chem.Phys. 61, 78 (1974).

(b) Chong, D.P., Herring, F.G., McWilliams, D., *ibid* 61, 958 (1974).

183. (c) Chong, D.P., Herring, F.G., and McWilliams. D., Chem.Phys.Lett. 25, 568 (1974).

(d) Chong, D.P., Herring, F.G., and McWilliams, D., J.Chem.Phys. 61, 3567 (1974).

(e) Chong, D.P., Herring, F.G., and McWilliams, D., J.Electron Spectrosc. Rel.Phenom. 7, 445 (1975).

184. (a) Hubač, I., Kvasnička, V., and Holubec, A., Chem.Phys.Lett. 23, 381 (1973).

(b) Kvasnička, V., Hubač, I., J.Chem.Phys. 60, 4483 (1974).

(c) Biscupič, S., Valko, L. and Kvasnička, V., Theoret. Chim.Acta. 38, 149 (1975).

185. Csanak, Gy., Taylor, H.S. and Yaris, R., Adv. At. Mol. Phys. 7, 287 (1971).

186. Linderberg, J. and Ohrn, Y., "Propagators in Quantum Chemistry", Academic Press (1973).

187. Cederbaum, L.S., Hohlneicher, G. and von Neisson, W., Chem.Phys.Lett. 18, 503 (1973).

188. Fuggle, J.C. Fabian, D.J., and Watson, L.M., J.Electron Spectrosc. Rel. Phenom. 9, 99 (1976).

189. Helmer, J.C. and Weichert, N.H., Appl.Phys.Lett. 13, 266 (196

190. Clark, D.T., in "Characterisation of Polymers by Means of Photon, Ion and Electron Probes", A.C.S. Symposium Series, Ed. H.R.Thomas and D.W. Dwight 1980 in press.

191. Clark, D.T., Dilks, A. and Shuttleworth, D., in "Polymer Surfaces", p. 185 ed. D.T. Clark and W.J. Feast, Wiley (1978).

192. c.f. references 127, 190-192 and A.A. Bakke, H-W.Chen and W.L. Jolly, J.Electron Spectrosc. Re-.Phenom. 20, 333 (1980).

193. Clark, D.T. in "Polymer Surfaces", 309, ed. D.T. Clark and W.J. Feast, Wiley (1978).

194. Willis, H.A. and Zichy, V.J.I. in ref. 193, p.287.

195. Clark, D.T., Feast, W.J., Musgrave. W.K.R. and Ritchie, I., J.Polym.Sci.Polym.Chem.Ed. 12, 1049 (1974).

196. Elias, H.G., "Macromolecules 2. Synthesis and Materials", Wiley, London (1977).

197. Priebe, E., Simak, P. and Stange, K., Kunstoffe 62:2, 105 (1972).

198. Clark, D.T. and Stephenson, P.J., Propellants and Explosives, Proceedings of the Nitrocellulose Conference, Waltham Abbey 1980, Ed. T.J. Lewis, Plenum Press.

199. Clark, D.T. and Muller, J., Chem.Phys.Lett. 23, 429 (1977).

200. Harding. L.B. and Goddard, W.A. III, J.Am.Chem.Soc. 100, 7180 (1978).

201. Gillies, C.W. and Kuczkowski, R.L., J.Am.Chem.Soc. 94, 6337 (1972).

202. Thomas, L.F., Sherrard, E.I. and Sheridan, J., Trans. Farad.Soc. 51, 619 (1955).

203. Kessler, M., Ring, H., Trambarulo, R. and Gordy, W., Phys.Rev. 79, 54 (1950).

204. Nishikawa, T. Itoh, T. and Shimoda, K., J.Chem.Phys. 23, 1735 (1955).

205. Brockway, L.O. and Jenkins. H.O., J.Am.Chem.Soc. 58, 2036 (1936).

206. Cox, A.P. and Waring, S., J.C.S. Faraday II, 68, 1060 (1972).

207. Brockway, L.O., Beach, J.Y. and Pauling, L., J.Am.Chem.Soc. 57, 2693 (1935).

208. Rogowski, F., Ber. 75, 244 (1942).

209. Brockway, L.O. and Pauling, L., J.Am.Chem.Soc. 59, 13 (1937).

210. Kimura, M. and Aoki, M., Bull.Chem.Soc. Japan, 26, 429 (1953).

211. Boersch, H., Sitzung Sber.Akad.Wiss.Wien.144, 1 (1935).

212. Mills, I. and Thompson, H.W., Trans.Farad.Soc. 50, 1270 (1954).

213. Tyler, J.K., Thomas, L.F. and Sheridan, J. Proc.Chem.Soc. 155 (1959).

214. Dewar, M.J.S. and Thiel, W., J.Am.Chem.Soc. 99, 4899 (1977).

215. Program MNDO by W. Thiel; Fachbereich Physikalische Chemie Der Philipps-Universitaet, D-3550 Marburg, West Germany.

216. Dilks, A., J.Polym.Sci.Polym.Chem. Ed. in press.

217. Barber, M. and Clark, D.T., J.Chem.Soc.D, 1, 22 (1970).

218. Clark, D.T., Peeling, J. and Colling, L., Biochemica Et. Biophysica Acta, 453, 533 (1976).

219. Clark, D.T., Kilcast, D. and Adams, D.B., Discuss Faraday Soc. 54, 182 (1972).

220. c.f. Olah, G.A., Mateescu, G.D. and Riemenschneider, J.L., J.Am.Chem.Soc. 94, 2529 (1972).

221. Clark, D.T., Scanlan, I.W. and Muller, J., Theor.Chim.Acta, 35, 341 (1974).

222. Clark, D.T. and Muller, J., Chem.Phys,Lett. 30, 394 (1975).

223. Clark, D.T. and Muller, J., Theor.Chim.Acta, 41, 193 (1976).

224. Clark, D.T. in Progress in Theoretical Organic Chemistry, Vol.2. Elsevier, Amsterdam (1977).

225. Clark, D.T. and Cromarty, B.J., in *ibid.*

226. Clark, D.T., and Cromarty, B.J., Theor.Chim.Acta. 44, 181 (1977).

227. Brown, R.S., J.Am.Chem.Soc. 99:16, 5497 (1977).

228. Brown, R.S., Tse, A., Wakashima, T. and Haddon, R.C., J.Am.Chem.Soc. 101:12, 3158 (1979).

229. Maksic, Z.B., Rupnik, K. and Eckert-Maksic, M., J.Electron Spectrosc. Relat. Phenom. 16, 371 (1979).

230. Karlstrom, G., Wennerstrom, H., Jonsson, B., Forsen, S., Almlof, J. and Roos, B., J.Am.Chem.Soc. 97:15, 4188 (1975).

231. Lowrey, A.H., George, C., d'Antonio, P. and Karle, J., J.Am.Chem.Soc. 93, 7399 (1971).

232. Gordon, M.S. and Koob, R.D., J.Am.Chem.Soc., 95, 5863 (1973).

233. Catalan, J., Yanez, M. and Fernandez-Alonso, J.I., J.Am.Chem.Soc. 100:22, 6917 (1978).

234. Egan, W., Gunnarsson, G., Bull, T.E. and Forsen, S., J.Am.Chem.Soc. 99:14, 4568 (1977).

235. Schuster, P., Chem.Phys.Lett. 3, 433 (1969).

236. Thomas. T.D., J.Chem.Phys. 53, 1744 (1970).

237. Gelius, U., J.Electron Spectrosc. Rel.Phenom, 5, 985 (1974).

238. Clark, D.T. and Colling, L. Nouveau Journal de Chemie 2:3, 225 (1978).

239. Clark, D.T., Adams, D.B., Scanlan, I.W. and Woolsey, I.S., Chem.Phys.Lett. 25, 263 (1974).

240. Clark, D.T., Dilks, A., Peeling, J. and Thomas, H.R., Discuss Faraday Soc. 60, 183 (1975).

241. Clark, D.T., Adams, D.B., J.Electron Spectrosc. Rel.Phenom. 7(5), 401 (1975).

242. Clark, D.T., and Dilks, A., J.Polym.Sci.,Polym.Chem.Ed. 15, 15 (1977).

243. Buss, V., von R. Schleyer, P., Allen, L.C., "The Electronic Structure and Stereochemistry of Carbonium Ions" in "Topics in Stereochemistry, Vol.7", Ed. N.L. Allinger, El.Eliel, 253 (1973).

244. Lathan, W.A., Curtiss, L.A., Hehre, W.J., Lisle, J.B. and Pople, J.A., Prog.Phys.Org.Chem. 11, 175 (1974).

245. Pople, J.A., J.Mass Spectrom.Ion.Phys. 19, 89 (1976).

246. Hehre, W.J., "Carbonium Ions: Structural and Energetic Investigations" in"Modern Theoretical Chemistry, Vol.4" ed. H.F. Schaefer III, Plenum (1977).

247. (a) Jorgensen, W.L., J.Am.Chem.Soc. 99 4272 (1977).
(b) Jorgensen, W.L., and Munroe, J.E., Tet.Lett. 6, 581 (1977).

248. Ed. by G.A. Olah, P. von R. Schleyer, "Carbonium Ions, Vol.I-V", Wiley-Interscience (1968-1976).

249. Olah, G.A,, J.Am.Chem.Soc. 94, 808 (1974).

250. Kramer, G.M., Adv.Phys.Org.Chem.11, 177 (1975).

251. Brown, H.C., Tetrahedron 32, 179 (1976).

252. Olah, G.A., Acct.Chem.Res. 9, 41 (1976).

253. Brown, H.C, with comments by P. von R. Schleyer; "The Non-Classical Ion Problem", Plenum (1977).

254. Olah, G.A., Mateescu, G.D. Wilson, L.A. and Gross, M.H., J.Am.Chem.Soc. 92, 7231 (1970).

255. Lischka, H. and Kohler, H-J, J.Am.Chem.Soc. 100:17, 5297 (1978).

256. Clark, D.T. and Lilley, C.M.J., Chem.Comm. 549 (1970).

257. Clark, D.T., Cromarty, B.J. and Colling, L., J.Chem.Soc. Chem.Comm. 276, (1977).

258. Olah, G.A., Demember, J.R., Lui, C.Y. and White, A.M., J.Am.Chem.Soc. 91, 3958 (1969) and Refs. Therein.

259. Dewar, M.J.S., Haddon, R.C., Komornicki, A. and Rzepa, H., J.Am.Chem.Soc. 99:2, 377 (1977).

260. Clark, D.T., Cromarty, B.J. and Colling, L. J.Am.Chem.Soc. 99, 8120 (1977).

261. Franke, W., Schwarz, H., Thies, H., Chandrasekhar, J., P. von R. Schleyer, Hehre, W.J., Saunders, M. and Walker, G., Angew.Chem.Int.Ed. Engl. 19, 485 (1980).

262. Saunders, M., Hagen, E.L., Rosenfeld, J., J.Am.Chem.Soc., 90, 6882 (1968).

263. (a) Olah, G.A., Baker, E.B., Evans, J.C., Tolgyesi, W.S., McIntyre, J.S., and Bastien, I.J., J.Am.Chem.Soc., 86, 1360 (1964).

(b) Olah, G.A. and Lukas, J., *ibid* 89, 2227 (1967).

(c) Olah, G.A., Sommer, J. and Namanworth, E., *ibid*, 89, 3576 (1967).

264. Saunders, M., Vogel, P. Hagen, E.L. and Rosenfeld, J., Accts.Chem.Res. 6, 53 (1973).

265. (a) Radom, L., Pople, J.A., Buss, V. and P. von R. Schleyer, J.Am.Chem.Soc. 93, 1813 (1971).

(b) Radom, L., Pople, J.A. and P.von R. Schleyer, *ibid*, 94, 5935 (1972).

265. (c) Hariharan, P.C., Radom, L., Pople, J.A. and P. von R. Schleyer, *ibid*. 96, 599 (1974).

266. Olah, G.A. and Donovan, D.J., J.Am.Chem.Soc. 99, 5026 (1977)

267. Kohler, H-J, and Lischka, H., J.Am.Chem.Soc. 101, 3479 (1979)

268. Myhre, P.C. and Yannoni, C.S., J.Am.Chem.Soc. 103, 230 (1981)

269. Saunders, M. and Kates, M.R., J.Am.Chem.Soc. 100, 7082 (1978)

270. P. von R. Schleyer and Chandrasekhar, J., J.Org.Chem., 46, 227 (1981).

271. Wade, K. in Transition Metal Clusters, Ed. B.F.G. Johnson, Wiley, (1980).

272. Clark, D.T. and Cromarty, B.J., "Some Theoretical Aspects of Core Ionisation in Carbocations" in "Progress in Theoretical Organic Chemistry, Vol.II", ed. I.G. Cxizmadia, Elsevier, p.447 (1977).

273. Thomas, T.D., J.Chem.Phys. 52, 1373 (1970).

274. Davis, D.W., Hollander, J.M., Shirley, D.A. and Thomas, T.D. J.Chem.Phys. 52, 3295 (1970).

275. Adams, D.B., J.Electron Spectrosc.Rel.Phenom. 9, 251 (1976).

276. Pireaux, J.J., Svensson, S., Basilier, E. Malmquist, P-Å., Gelius, U., Caudano, R., and Siegbahn, K., Phys.Rev. A14, 2126 (1976).

277. Clark, D.T. and Cromarty, B.J., Chem.Phys.Lett. 49, 137 (1977

278. Clark, D.T. "E.S.C.A. applied to Organic and Polymeric Systems" in ref. 76.

279. Buenker, R.J. and Peyerimhoff, S.D., J.Am.Chem.Soc. 91, 4342 (1969).

280 Maier, G., Pfriem, S., Schafer, U. and Matusch, R., Angew.Chem. 90, 552 (1978).

281. Bingham, R.C., Carrion, F., Dewar, M.J.S., and Kollmar, H., to be published.

282. Schweig, A. and Thiel, W., J.Am.Chem.Soc. 101, 4742 (1979).

283. Kollmar, H., J.Am.Chem.Soc. 102, 2617 (1980).

284. Schulman, J.M. and Venanzi, T.J., J.Am.Chem.Soc. 96, 4739 (1974).

285. Hehre, W.J., and Pople, J.A., J.Am.Chem.Soc. 97, 6941 (1975)

286. Jafri, J.A. and Newton, M.D., J.Am.Chem.Soc. 100, 5012 (1978

287. Baird, N.C. and Dewar, M.J.S., J.Am.Chem.Soc. 89, 3966 (1967

288. Heilbronner, E., Jones, T.B., Krebs, A., Maier, G., Malsch, K-D, Pocklington, J. and Schmelzer, A., J.Am.Chem.Soc. 102, 564, (1980)

289. Turner, D.W., Baker, C., Baker, A.D. and Brundle, C.R., in Ref. 157.

290. Brundle, C.R., Robin, M.B., and Kuebler, N.A., J.Am.Chem. Soc. 94, 1466 (1972).

291. Cowan, D.O., Gleiter, R., Hashmall, J.A., Heilbronner, E. and Hornung, V., Angew Chem.Int.Ed. Engl. 10, 401 (1971

292. Kobayashi, T., J.Electron Spectrosc. Rel.Phenom. 7, 349 (197

293. Lauer, G., Schafer, W. and Schweig, A., Chem.Phys. Lett. 33, 312 (1975).

294. Dougherty, D. and McGlynn, S.P., J.Am.Chem.Soc. 99, 3234 (19

295. Åsbrink, L., Bieri, G., Fridh, C., Lindholm, E. and Chong, D.P., Chem.Phys. 43, 189 (1979).

296. Bloor, J.E., Paysen, R.A., and Sherrod, R.E., Chem. Phys.Lett. 60, 476 (1979).

297. Bigelow, R.W., J.Chem.Phys. 68, 5086 (1978).

298. Wood, M.H., Theoret. Chim.Acta. 36, 345 (1975).

299. Jonkman, H.T. van der Velde, G.A., and Nieuwport, W.C. in: Quantum Chemistry - the State of the Art, Proceedings of S.R.C. Atlas Symposium No. 4, p.243 (1974).

300. Tromsdorff, H.P., J.Chem.Phys. 56, 5358 (1972).

301. Koenig, T., Smith, M. and Snell, W., J.Am.Chem.Soc. 99, 6663 (1977).

302. Schang,P., Gleiter, R., and Rieker, A., Ber.Bunsenges, Phys. Chem., 82, 629 (1978).

303. Hilal, R., Int.J.Quant,Chem. 15, 37 (1979).

304. Ohta, T.,Yamada, M. and Kuroda, H., Bull.Chem.Soc. Japan, 47, 1158 (1974).

305. Hagen, K. and Hedberg, K., J.Chem.Phys. 59, 158 (1973).

306. MacDonald, A.L., and Trotter, J., J.C.S. Perkin II, 476 (1973).

307. c.f. T. Laird in "Comprehensive Organic Chemistry" Vol. 1, p.1213 Ed. J.F. Stoddart, Pergamon (1979).
J.M. Bruce in "Rodd's Chemistry of Carbon Compounds" Vol.IIIB, Ed. S. Coffey, Elsevier (1974).

308. Trotter, J., Acta Crystallogr. 13, 86 (1960).